Robust and Optimal Control for Disturbed Population Dynamics

Submitted by Stephanie Jane Lloyd to the University of Exeter as a thesis for the degree of Doctor of Philosophy in Mathematics in November 2015.

I certify that all material in this thesis which is not own work has been identified and that no material has previously been submitted and approved for the award of a degree by this or any other University.

Signature: .....

Acknowledgements

I would like to thank my supervisors Stuart Townley and Markus Mueller. I am extremely grateful for their continued help and patience over the last three years, without their support this submission would not have been possible.

Also thank you to my family, David, Isobel, Catherine and Imogen for helping me to stay motivated after particularly difficult days.

Abstract

We use control theory to explore management of populations affected by disturbances and uncertainty. We consider five related topics. Chapter 2 uses linear programming to find optimal translocation strategies between wild and captive populations. To allow comparison of the solutions we classify the optimal strategy depending on which stage classes are kept in captivity. We find depending on species, that different stages are targeted when the resource available is limited. In Chapter 3 we use linear programming to create management strategies for an invading population affected by disturbance. For a sinusoidal disturbance, the final population with control is bounded between a transfer function approximation and a feedback control solution. Then we assume worst case disturbance, which creates a 2-player game. In this linear programming context, minimax$\geq$maximin. Chapter 4 considers a 2-player linear-quadratic problem and introduces the use of disturbance attenuation into ecology. Disturbance attenuation shows how a disturbance is amplified or attenuated by the system. In Chapter 5 we consider an invading population, and we explore the effect that stochasticity has on the relationship between Allee effect and population inertia needed for successful invasion. We find that for small population densities, then demographic stochasticity dramatically reduces the likelihood of invasion and survival of the resident.

Contents

List of Figures

List of Tables

Chapter 1

Introduction

The overarching aim of this thesis is to explore the use of control theory tools in managing populations subject to disturbances and uncertainty. The motivation for this work is two-fold. First, the thesis seeks to extend recent work by Hastings et al. ([53], [14]) on using optimal control to manage invasive species, by including disturbances. Second, the research builds on the work of Townley and Hodgson ([129], [130], [121]) which focuses on using control and systems theory to model and analyse population dynamics. Figure 1.1 depicts a general framework for management of an uncertain and disturbed population. Consider a population model which may have an element of stochasticity or variability, demonstrated by the red process in Figure 1.1. The green process represents a control or management strategy acting on the population. The disturbance may act on the population or on the management strategy — these are captured by d_1 and d_2 in Figure 1.1. The role that each of these processes play in the system and how they can be modelled is described in Section 1.1.

1.1 Components in a general model

This section describes the elements required for the general model depicted in Figure 1.1, namely:

- Population model;
- Uncertainty;
- Disturbance;
- Management/control.

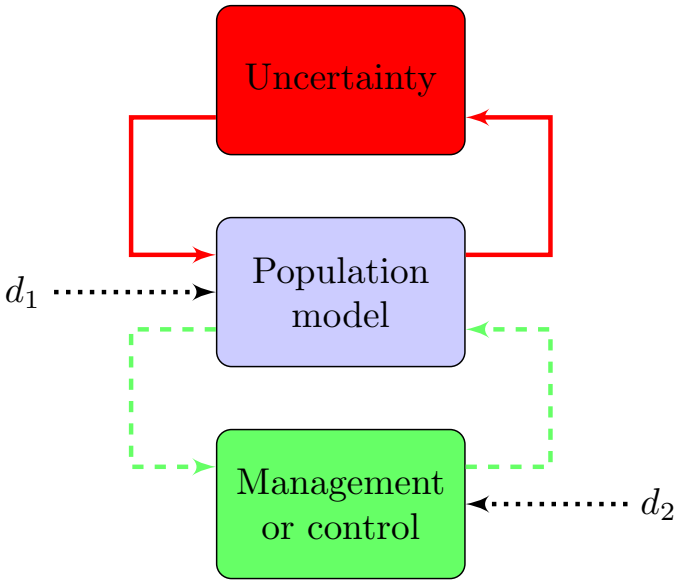

Figure 1.1: Generalised population model with control or management, disturbance and uncertainty.

1.1.1 The population model

There are many different types of structured population models. The models are determined by whether they consider a population in discrete or continuous time and whether the states of the system are discrete or continuous. These types are summarised in Table 1.1 [23].

Matrix population models

One of the simplest ways to model a discrete-time, stage structured model is to use matrix projection models which date back to the 1940's [23]. These models use a matrix, referred to as a population projection matrix (PPM), which contains the vital rates of the population. The stage structured population and vital rates can be visualised

	Discrete-state	Continuous-state
Discrete-time	Matrix population models	Integrodifference equations
Continuous-time	Delay-differential equations	Partial differential equations

Table 1.1: Types of structured population models

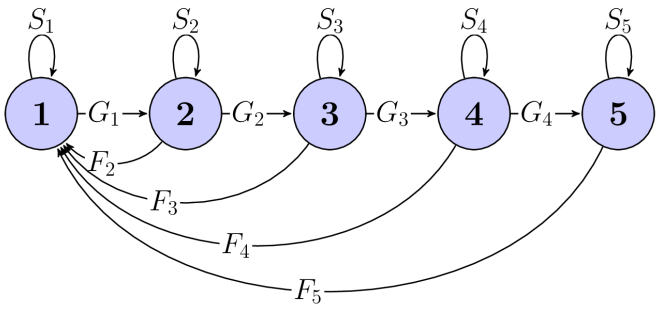

Figure 1.2: Life cycle diagram for 5 stage structured population

using a life-cycle graph, as illustrated for a 5 stage population in Figure 1.2. The corresponding population projection matrix (PPM) for the life cycle graph shown in Figure 1.2, is

$$A = \begin{pmatrix} S_1 & F_2 & F_3 & F_4 & F_5 \\ G_1 & S_2 & 0 & 0 & 0 \\ 0 & G_2 & S_3 & 0 & 0 \\ 0 & 0 & G_3 & S_4 & 0 \\ 0 & 0 & 0 & G_4 & S_5 \end{pmatrix}.$$

The top row $(F_2, \ldots, F_5)$ includes the fecundity (reproductive rate) of each stage class. The diagonal $(S_1, \ldots, S_5)$ contains the survival rates of each of the stages, and the sub-diagonal $(G_1, \ldots, G_4)$ consists of the growth rates of each stage into the next stage class. For an age-structured model, where the age is taken to be a discrete variable and the population is grouped by age with progression from one age class to the next occurring at each time step, then $S_1, S_2, \ldots, S_n = 0$. In this case the PPM is known as a Leslie matrix. The more generalised matrix A contains survival rates which allows an individual to remain in the same class and therefore would be used for a stage structured population, where stage maybe be determined by species size or developmental stage [23]. A simple population model using a PPM is given by

$$n(t+1) = An(t), \tag{1.1}$$

where $n(t)$ is a vector containing the population abundances in each stage at time t, and A is a PPM.

Integrodifference equations

Integrodifference equations (IDE's), also know as integral projection models, create models with discrete-time and continuous state space. Briggs et al. [17] describe a general overview of integral projection models and in particular draw comparisons between integral and matrix projection models. If the state is continuous then equation (1.1) becomes

$$n(y, t+1) = \int_{m_s}^{M_s} k(x, y) n(x, t)\, dx,$$

where m_s and M_s is the minimum and maximum size of the individuals, so that an individuals stage x belongs to the interval $[m_s M_s]$. The kernel $k(x, y)$ captures how individuals in stage x at time t contribute stage y at time $t+1$. This is analogous to the PPM, A, in equation (1.1) [17].

Integrodifference equations can also be used to add spatial dynamics to a temporally discrete model ([69],[51]). For this type of model there are two main components to the integrodifference equation. The difference equation which models the growth and interactions at a particular time step, and a redistribution kernel which determines the dispersal of the population at any given time step [93]. The dispersal is characterised by a probability distribution and the kernel is integrated to calculate the total dispersal of the population. As discussed in [68], a general single population IDE can be written as

$$N_{t+1}(x) = \int_{\omega} k(x, y) f(N_t(y))\, dy,$$

where $N_t(x)$ is the population at location x, at time t. The function f models the discrete-time growth of the population at any location. Finally, $k(x, y)$ describes the dispersal of N from y, which means that $k(x, y)dy$ is the probability that an individual disperses from on interval of length dy around y to the same size interval around x. Notice that as $k(x, y)dy$ is a probability, all the entries must be non-negative and $\int k(x, y)\, dy = 1$.

Delay-differential equations

Delay-differential equations (DDE's) are used for populations where individuals can be separated into discrete states and time is continuous. The use of delay-differential equations in modelling populations is discussed in [70]. Solving DDE's is more complex than solving differential equations without time delays. However for many situations the addition of a time delay produces a substantially more realistic model. An example of this is deforestation, where for each species there is a time lag before a tree reaches maturity [70]. A general time-delay differential equation is given in [70]. Let $x(t)$ be the population at time t then the time-delay differential equation can be written as

$$\frac{\mathrm{d}}{\mathrm{d}t}x(t) = f(t, x_t),$$

where $x_t = \{x(\tau) : \tau \leq t\}$, and f is a function. This creates a model which is continuous in time, and the rate of change of the population at time t may explicitly depend on the population at any previous time step. It is well known that if a potentially stabilizing feedback acts with a time delay then it will have a destabilising effect on the system [11], and therefore a considerable about of research has been done into the stability of these systems, for example [11] and [46]. Aiello et al. [2] use delay-differential equations for a single population with two stages, which represent immature and mature. The time delay used is constant and captures the time from birth to maturity. Then they show there is a globally asymptotically stable equilibrium and furthermore non oscillatory solutions exist. Examples of other uses of delay-differential equations in ecology are given in [90], [13].

Differential equations

In 1939 Lotka [78] created a well known integral equation which given the birth rate and an initial population can be used to predict the population size at subsequent time steps. There are several forms of this equation which are used throughout ecology, for example [141], [35] and [37]. These include the Lotka-Volterra equations which are differential equations used for predator-prey systems, and are given by [125]

$$\dot{x} = x(a - by), \qquad \dot{y} = y(-c + dx)$$

where x and y are the prey and predator population, respectively, and a, b, c and d are scalars. If the initial population of both populations are non-zero these coupled differential equations give rise to cyclical solutions, as an increase in prey leads to the predator population increasing but a larger predator population results in a decrease in the prey population.

Partial differential equations are also useful in ecology to model populations where the dispersal is assumed to be Brownian random motion. This leads to a population model given by

$$\frac{\partial u(x,y,t)}{\partial t} = D\left(\frac{\partial^2 u}{\partial x^2} + \frac{\partial^2 u}{\partial y^2}\right)$$

where D captures the dispersal rate and $u(x,y,t)$ is the population density at (x,y) location at time t [59]. Similar dispersal models are included in [3] and [19].

Population projection for PPMs

Matrix population models play a key role in the rest of thesis and so we spend some time describing some of their key features. For a matrix model, given that the stage (or age) structured population is known, then the PPM can be used to project forward in time the population size and stage structure. For a known population size and distribution the population at the next time step is calculated using equation (1.1). There are two main factors to consider when examining the growth or decline of a population:

- Firstly, the asymptotic behaviour which describes the long term growth or decline of the population.
- Secondly, the transient dynamics which determines how the population behaves in the short term.

Determining the asymptotic behaviour

Assuming that $A \in \mathbf{R}^{n\times n}$ is non-negative and regular ($A^k > 0$ for some k), sometimes called primitive, matrix then the Perron-Frobenius Theorem [23] states that:

- There is a eigenvalue, λ_{max}, of A that is real and positive, with positive left and right eigenvectors.
- Any other eigenvalue, λ, is such that $|\lambda| < \lambda_{max}$.
- The eigenvalue λ_{max} is simple.

The growth from one stage to the next must be non-negative, the survival which gives the proportion of the population remaining in the same stage class must also be non-negative and finally the number of stage 1 that each stage produces must also be non-negative, therefore PPM's must be non-negative matrices. In general PPM's are also regular matrices, so the Perron-Frobenius Theorem gives that the dominant eigenvalue is real and positive. The dominant eigenvalue of a PPM, A, denoted $\lambda_{max}(A)$, dictates the asymptotic behaviour of the population. The discrete-time population model, given by equation (1.1), gives that

$$n(t) = A^t n_0$$

where n_0 is the initial structured population. Therefore, if the dominant eigenvalue of A, $\lambda_{max}(A)$, is greater than one then asymptotically the population increases, whereas if the dominant eigenvalue, $\lambda_{max}(A)$, is less than one then the population decreases and tends to 0, and finally if $\lambda_{max}(A) = 1$ then the population density remains asymptotically unchanged.

The Perron-Frobenius Theorem also states that the left and right eigenvectors corresponding to the dominant eigenvalue are positive. This is important because n_0 can be written as a combination of the right eigenvectors such that

$$n(t) = A^t n_0 = \sum_i \alpha_i A^t w_i \approx \alpha_1 \lambda_{max}^t w_1,$$

where w_i are the right eigenvectors, α_i are scalar constants and w_1 is the right eigenvector corresponding to the dominant eigenvalue [67]. So this shows that for large enough t the population stage structure tends towards w_1, and therefore the right eigenvector w_1

corresponding to the dominant eigenvalue, λ_{max}, determines the stable stage structure of the population. This means that for any initial population and large enough t, the structure of population will be given by the stable stage structure.

The scalar constants α_i are dependent on the initial population such that

$$\alpha_i = \frac{v_i^T n_0}{v_i^T w_i},$$

where v_i is the left eigenvector corresponding to the i-th eigenvalue. As

$$\lim_{t\to\infty} \frac{n(t)}{\lambda_{max}^t} = \alpha_1 w_1$$

then the extent to which stage i affects the long-term population is given by the left eigenvector, v_1, corresponding to the dominant eigenvalue. This vector is known as the reproductive value ([67],[22]).

Transients for PPMs

Even for this simple PPM model there are many ways to measure the transient dynamics. As explained in [23], one way to measure transient dynamics is to calculate the damping ratio, which uses the eigenvalue of A with the second largest magnitude, denoted λ_2, to give that

$$\text{damping ratio} = \frac{\lambda_1(A)}{|\lambda_2(A)|}$$

The damping ratio gives a measure of how quickly the transient dynamics decays. The damping ratio does not depend on the population structure. However the transient dynamics may largely depend on the structure of the population, as illustrated in Figure 1.3. Therefore if the initial state of the population is known the population inertia [122] may be a more accurate measure of the transients. For a given initial population structure x_0, standardised so that $\|x_0\|_1 = 1$, the population inertia is given by

$$\frac{v^T \hat{x_0}}{v^T w},$$

Figure 1.3 shows the total population trajectory for three choices of initial conditions.

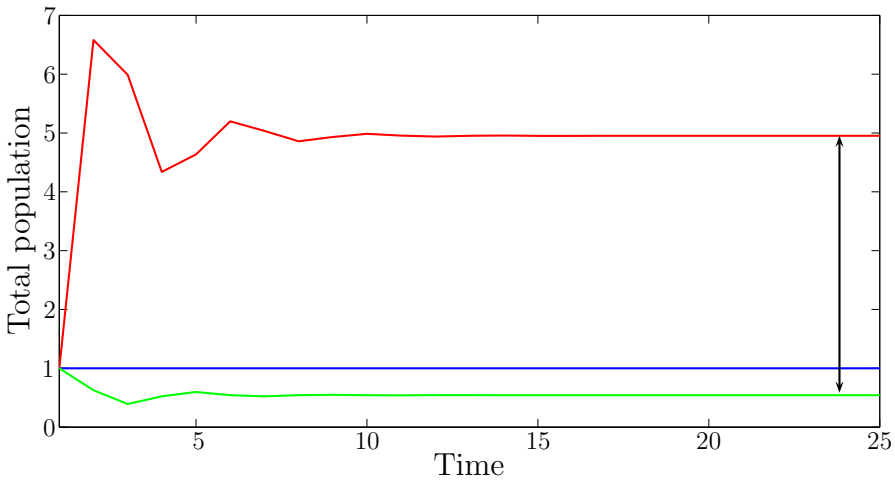

Figure 1.3: Illustration of transient dynamics of a populations with different initial distributions. The population inertia is given by the length of the arrow from the population density resulting from the stable stage structure, shown by the blue line, to the population density resulting from the initial condition.

The PPM is scaled such that the dominant eigenvalue is 1, which means that if the initial population is at stable stage structure, then the population does not change density. If the initial condition is not at stable stage structure then due to the transients the resulting long-term population density may be different. Given that the initial conditions for the transient dynamics in Figure 1.3 give the maximum and minimum amplification of the long-term population dynamics, then the population inertia must fall in the range denoted by the arrow. Other measures of transient dynamics include reactivity [122], momentum [49] and Kreiss bound [129].

1.1.2 Uncertainty

Uncertainty in models encompasses numerous aspects. In this thesis, uncertainty will mean deterministic perturbations or stochasticity which are illustrated by the red uncertainty process in Figure 1.1 or external disturbances which are demonstrated by d_1 and d_2 in Figure 1.1.

Deterministic perturbations

As the demography within a population may change, there has been much research devoted to analysing the effect of perturbations on matrix projection models. Two measures that can be calculated are the sensitivity and elasticity of the PPM ([23], [12], [24]). These give measures of how robust the matrix projection model is to perturbations in the transition rates, which therefore captures how much the model would be affected by stochasticity in the environment. For a given PPM ($A \in \mathbf{R}^{n\times n}$) with entries denoted a_{ij}, the sensitivity measures the effect that a change of transition rate (a_{ij}) has on the dominant eigenvalue of A. The result is a $n \times n$ sensitivity matrix, denoted by S. The corresponding elasticity matrix, E, measures the proportional response to a proportional perturbation. Therefore, the sensitivity and elasticity matrices are related and given by

$$S_{ij} = \left(\frac{\partial \lambda}{\partial a_{ij}}\right), \quad E_{ij} = \left(\frac{a_{ij}}{\lambda}\frac{\partial \lambda}{\partial a_{ij}}\right).$$

Caswell [24] explores the use of sensitivity and elasticity analysis for transient dynamics. He uses matrix calculus to give computationally simple results which can be applied to time-varying, stochastic, nonlinear and spatial models. However, it worth emphasising that sensitivity calculations are infinitesimal and only apply for "small enough" perturbations.

Transfer analysis is an alternative to sensitivity analysis and can be used to determine how the size of a "macroscopic" perturbation effects the dominant eigenvalues [58]. Hodgson and Townley [58] consider a system given by equation (1.1) and a perturbation of a single parameter in A. In this case, the PPM becomes

$$A + bpc$$

where A is the original PPM, p is the magnitude of the perturbation and b and c are vectors determining the parameter in A which is perturbed. In this case, the perturbed dominant eigenvalue λ_p of the perturbed matrix $A + pbc$ satisfies the equation

$$pc(\lambda_p I - A)^{-1} b = 1\,.$$

Hodgson et al. [57] extend this transfer function analysis to the case of perturbations affecting multiple transition rates and involving multiple parameters.

Stochasticity

The models discussed in Section 1.1.1 are deterministic as there is no randomness or variability included. Such deterministic models offer a good approximation, particularly when the population abundance is large. However in reality population dynamics are often stochastic, and this is especially likely when population abundance is low. Unlike for deterministic models where extinction is not possible, for stochastic models extinction is possible [72]. The risk of extinction clearly has a large impact on the population model and ecology and so modelling stochastic populations has attracted much attention in the last 20 years. Stochasticity can be included in population models in many ways. For example, patch-based models [104], individual based models [48] and stochastic matrix projection models [124]. Each of these stochastic models are described below.

The use of patch-based modelling for populations has increased since the 1970's. Patch-based models can form a middle ground between deterministic models and individual based models, as they can add stochasticity but by grouping the population they are less computationally intensive than individual based models. In ecology, patchiness may

occur both spatially or temporally in the structure or dynamics of the system [138]. Patch based models are often used to model spatially dependent populations, in particular for heterogeneous environments. Roff [104] considers twenty five sub-populations with different environments and connected by dispersal, and show that dispersal in a heterogeneous environment can increase population persistence by several orders of magnitude. Fahrig and Merriam [36] create a patch-based model with connected habitat patches for a white-footed mouse population. They find that the results from the patch-based model agree with field data, suggesting that patch-based models can be used as a realistic framework to approximate spatial population dynamics.

Individual based models (IBM's) have also been used in ecology since the 1970's [48]. The main motivation for IBM's is to create more realistic assumptions by accounting for individual variability which are not considered in deterministic models. As a result most IBM's are highly complex and require a considerable amount of data. Therefore, IBM's are particularly useful for small populations which have high levels of complexity in the population dynamics or in the spatially heterogeneous environment [74]. For example, [74] use an individual-based model to simulate the population dynamics of the red-cockaded woodpecker, and explore which parameters increase the stability of the endangered species. More recently, with the increase in computational power, IBM's have become more complex. For example, Castellani et al. [21] develops an individual-based eco-genetic model for salmon, which explores how the demography and genetics of an Atlantic salmon population changes throughout its life time. They find that this complex model accurately reproduces the characteristics of the Atlantic salmon population.

In Section 1.1.1 we outlined the simple matrix projection models. However the vital rates of the population may themselves be time dependent or vary between individuals. The resulting stochastic matrix models have attracted much attention in population ecology research. Sykes [124] introduces several ways in which stochasticity may be added to a system given by equation (1.1). The most realistic of these is to add randomness to the population projection matrix. Specifically, [124] suggests adding

stochasiticity to equation (1.1) to give a model of the form

$$n(t+1) = (A + \Delta_t)n(t),$$

where Δ_t is a matrix of random variables of the same dimension as A, such that the mean of Δ_t is 0. As the entries in Δ_t are both positive and negative then some restrictions on the entries of Δ_t are required to ensure that $(A + \Delta_t)$ remains a non-negative matrix. Nakaoka [92] reviews several studies which have used stochastic matrix models for different species. The population growth rates of the stochastic models were compared to the deterministic models and Nakaoka found that in each of the studies the stochastic growth rate was never greater than the deterministic growth rate which means if the stochasticity in the demography is ignored then the deterministic model may over predict the size of the population. Fieberg and Ellner [39] provides a review of the stochastic population projection models used, and illustrates the differences between these models. Depending on the structure of the PPM some vital rates can be particularly vulnerable to stochasticity, and therefore calculating their sensitivity is important.

Disturbances

Disturbance may act on a population in many different ways, for example migration, invasive species or a change to the habitat or environment. Typically population models consider a closed system. However un-modelled factors in surrounding areas are likely to have an impact on the population dynamics. The addition of disturbance in a population model allows the model to capture the effect that external un-modelled factors have on the population dynamics.

The importance of modelling disturbance is increasing, as due to human and environmental factors, the disturbances within most ecosystems are increasing. As climate change occurs both phenological and distribution shifts may occur within populations. For the species which the phenologies have changed, then 87% of these have changed in the way expected due to climate change, and out of 434 species 80% have experienced distribution shifts predicted by climate change [97]. This suggests that climate

change has already affected the life cycle and location of many species. It has been suggested by biologists that given the rate at which species are becoming extinct we are heading towards the Earth's sixth mass extinction, which is where the Earth loses more then three-quarters of its species in a short interval [7]. This is supported by [80] which states that 20-50% of the Earth's species may become extinct within the next decades. Recreational and industrial uses of countryside are rapidly increasing, for example housing, deforestation and farming. Between 33% and 50% of the land surface has been developed by human activity [134], from habitats such a forests and wetlands to agricultural and urban environments. Humanity also uses 54% of the geographically accessible run-off fresh water [99]. Furthermore, the increase in transport has allowed species to cross geographical barriers, which can increase the spread of invasive species [27]. Therefore, understanding the effect the disturbance has on the species is becoming increasingly important, and a method to quantify the effect of human disturbances is discussed in [45]. Seidl at al. [111] provide an overview of different approaches used for modelling five different types of natural forest disturbances. For each of these disturbances they discuss the susceptibility, occurrence and impact. [111] find that a large proportion of the literature uses statistical approaches. An example of this includes Russell et al. [108] which explores the affect that prescribed fire of ponderosa pine has on bird communities. Prescribed fires are managed fires which aim to reduce the frequency and severity of forest fires. [108] use a statistical approach to examine how bird populations changed on six study sites are prescribed fires. They found that after the fire several bark-insectivore species increased in density, whereas several foliage-insectivore and seed specialists decreases in density. DeAngelis et al. [33] also discuss several ecological models which they divide into groups depending on the spatial element of the model and the stability of the system. The majority of the models that [33] examine are differential models, and they discuss the limitations of each model. As every ecosystem is both temporally and spatially part of a larger system, then for every non-equilibrium system temporal and spatial scales can be found so that the system has an equilibrium. Therefore [33] conclude that "*scale is of paramount importance*" when considering stability of ecological models.

The increased spread of invasive species can lead to the extinction of native species. For 170 extinct species with known causes, then 54% included invasive species in the cause for extinction [29]. Not only can invasive species have large effects on the biodiversity, but then may also have huge economic consequences. For example, the Eurasian zebra mussel was spread to North America in the ballast water of ships and a report in 1993 predicted that over 10 years it will cost the economy about $3.1 billion in clearing intake pipes [133]. There are several ways an invasive species may affect the native species. These include rapid evolution of the native species, hybridization and behavioural shifts [89]. This illustrates the huge impact that disturbances from migration and invasive species can have on the population dynamics, and therefore the importance of attempting to capture the external factors in a population model. Olson [95] provides a review of the literature which examines the economic impact that invasive species have. They find there is a need further work, particularly in areas including uncertainty, prevention and spatial modelling. Molnar et al. [88] created a database including 329 invasive marine species. For each species this database contains information on the distribution, how it is introduced and the impact. They find that international shipping is a major source of invasive movement. This database could be used to find the most threatening invasive species and highlight the invasion pathways which have the largest impact on the spread of invasive species. Jimenez-Valverde et al. [62] discuss methods for creating risk maps, which summarise the suitability of a landscape for invasive species. Statistical and machine learning techniques are used, and they find that models should be careful not to over fit the training data. Creating maps for the spread of invasive species is important, and the use of remote sensing and GIS is discussed in [64]. Sutherst and Bourne [123] discuss the limitations of two statistical models in predicting the spread of invasion.

1.1.3 Management and control

There are many reasons why management of a population may be required, these include endangered species, migration, disease or invasive species. As habitats are hugely altered by human involvement, for example farming and deforestation, the need to protect endangered species increases. Much research has been done to find the manage-

ment strategies for many endangered species, including Red-Cockaded Woodpecker [60], Maui's dolphin [117], the Florida manatee [119] and Sumatran rhino [82]. For endangered species these management strategies can act in a range of ways as stated in [82]. If there only exist wild populations then examples include translocating individuals, raising the carrying capacity (e.g feeding), restricting dispersal, reducing morality (e.g vaccination) and restoring the habitat. If the population is restricted to captivity then captive breeding must be maintained for reintroduction or perpetual captivity. Finally, if the population is both captive and wild then the management must involve reintroduction of captive-reared individuals and continued capture of wild individuals. Similarly, extensive research has been carried out attempting to understand and predict invasive species. Invasive species can have a huge impact on biodiversity, which often if left unmanaged can cause irreversible change [53]. When an invasive species enters a new ecosystem it may alter the environment for some of the native species, thus the evolutionary pathway of the native species may change due to competition, niche displacement, hybridization and predation [89]. Research into managing invasive species is extensive and include [30] and [4].

There are different ways in which a management strategy can be calculated. The two main ways to find a management strategy are dynamic programming and a feedback controller. Dynamic programming uses optimisation algorithms to find the management strategy for a given cost function and constraints. The use of dynamic programming has become increasingly popular in ecology in the last 40 years, for example [71], [112] and [114]. The advantage of using dynamic programming is that other than the initial population no measurements are required. In contrast feedback control requires knowledge of the population to be managed. A type of feedback control is known as adaptive feedback control, where initially the control is unknown and changes depending on measurements. Using adaptive control in ecology has also been studied, particularly in systems where harvesting occurs, for example fisheries ([135], [136]). The pros and cons of using adaptive management are discussed in [85].

1.2 The contribution of the thesis and its relation to other work

The thesis considers the following strands of research:

1. Conservation by translocation (Chapter 2)
2. Management of disturbed and invasive species by linear programming approaches (Chapter 3)
3. Two-player quadratic game and disturbance attenuation for a disturbed population with management (Chapter 4)
4. The role of population inertia in stochastic models of invasion (Chapter 5)

The following discusses our contribution in the context of other work.

Conservation by translocation

As global extinction rates dramatically increase, much research has focused on predicting how the global diversity will change over the 21st century ([109], [98]). Conservation ecologists aim to prevent extinction, and often if it is not possible to protect the natural environment and so the only way to stop extinction is to use a captive breeding program [128]. Not only can captive breeding be extremely costly, but there are several potential complications. These include reduced genetic variation, issues with reintroduction and disease [118]. Reduced genetic variability can eventually lead to inbreeding which can cause extinction due to reduced reproduction and survival rates [41]. There are many reasons why reintroduction may fail. These include domestication and the habitat not being suitable if other population levels have not been maintained while the species has been in captivity. The reduced genetic variation in captivity can increase the susceptibility of the population to disease [94]. Furthermore, zoos do not focus on containing endangered species. Across 878 zoos, only 140 mammal and 33 bird species appear on the threatened species list, compared to 647 mammal and 1161 bird species which are listed as threatened [100]. As a result of these potential issues captive breeding programs in general are only used as a last resort to prevent extinction of endangered

species. The use of captive breeding is discussed in [9], which examines the use of reintroducing captive-born animals as a conservation strategy. Similarly, [113] explores how enriching the environment of captive individuals, can improve the success for reintroduction to the wild. Any captive breeding program must require translocation of individuals between the wild and captive populations. Tenhumberg et al. [128] uses stochastic dynamic programming to create optimal state-dependent strategies for the translocation between captive and wild populations. In particular [128] finds a robust rule of thumb which conservation biologists could use to minimise the probability of extinction. The rule of thumb suggests that when the wild population is less than 20 females, then the entire wild population should be kept in captivity and not released until the captive facilities are at least 85% full. This is illustrated using an Arabian oryx population. Lubow [79] also find the optimal translocation strategies for a stochastic population. The simulations by Lubow suggest that translocating between 1 and 6 individuals a year can increase the chance of persistence of the species. In Chapter 2 we use a linear programming framework to find an optimal translocation strategy between wild and captive populations. This framework is applied to a large range of species, so to allow comparison we create a method of classifying the optimal translocation strategy.

Management of disturbed and invasive species by linear programming approaches

As discussed in Section 1.1.3 there are many reasons why the management of a pest or invasive species may be required. In Section 1.1.2 we stated the devastating impact invasion can have on the environment and biodiversity. As a result several books have been written about the management of invasive species ([30], [20]). Also discussed in Section 1.1.3 there has been an increase in use of optimal control to create management strategies. For example, [137] use optimal control to find a management strategy for Gypsy moth using a biocontrol. When Gypsy moth populations are left uncontrolled then the population density undergoes large fluctuations, which can result in deforestation which is economically costly. Another example include [75] which compares economic cost of the optimal control and optimal prevention strategies for Zebra mussel in lakes which contain power plants. The detection of a invasive species

may be critical to the success of the eradication of the species, as an early detection will have a lower population density. Optimal control can been used to determine the amount of effort that should be focused on the detection of the invasive species [86]. Other examples of optimal control used in ecology with the aim to control invasive species include [50] and [126]. Linear programming has many uses and is often preferred for its simplicity compared to non-linear systems. Linear programming can be used when the density of the populations are sufficiently low [53], this means assuming an invader enters at small abundances then linear programming can be used to find the optimal control methods.

Hastings et al. in [53] use linear programming to control an invasive species, *Spartina alternifora*, by removal. Hastings et al. consider a stage structured model and find that the optimal removal strategy will target an individual stage at any time step. This is a consequence of using linear programming where the optimal solution generically occurs at the vertex of the constraint set. In Chapter 3 we expand the framework created by Hastings et al. in [53] by exploring the effect that disturbance may have on the population and removal strategy, in particular the worst case disturbance.

Two-player quadratic games and disturbance attenuation for a disturbed population with management

Unlike linear programming which has been widely used in ecology, linear-quadratic control has not been explored to the same extent. However, it has been used by Blackwood et al. [14] to find the optimal removal strategies for an invasive species, *Spartina alternifora*. Linear-quadratic control has been extensively studied in control theory and has many applications which include the standard regulator problem and tracking [5]. In control theory, a linear-quadratic control problem contains a linear control system and a quadratic cost function, which is dependent on the state and the control, then the cost minimised subject to the control system [5]. Blackwood et al. [14] motivate using a quadratic cost function because it is harder for pest managers to find, and hence remove, a larger proportion of the population. This is because once some individuals are removed it becomes harder to find, and remove, the rest of the individuals. They

use a linear discrete-time population model with a cost function which is quadratic in the population size and cost of removal. The optimal control is found using Riccati equations [65], which give an optimal solution for the removal strategy. The solution obtained from the Riccati equations is a feedback solution, which means that the optimal removal strategy depends explicitly on the size and structure of the population.

In recent years the study and use of linear-quadratic control has been superceded by the H^∞ paradigm. The applications of the H^∞ paradigm has rapidly increased since it was introduced in the 1980's by Zames [8]. H^∞ control considers the worst case situation for a linear system affected by additive disturbances. The H^∞ paradigm can be used to create a bound measuring the most a disturbance can be amplified by the system. There are a vast range of uses for H^∞ control, from oiling drilling process [139] to telecommunication satellites [42].

In Chapter 4 we add disturbance to the framework created in [14] to create a minimax problem, and explore the use of H^∞ theory to study the disturbance attenuation within the system. To the best of our knowledge the use of H^∞ paradigm in ecology has not been explored.

The addition of disturbance to a controlled population creates a two-player problem. A trade off occurs between the controller (player 1) and the disturbance (player 2), which means the problem can be thought of as a non-cooperative 2-player game. "*Game theory provides general mathematical techniques for analysing situations in which two or more individuals make decisions that will influence one another's welfare*"[91]. If there exists an strategy where for any player no derivation from this strategy is beneficial then this is known as a Nash equilibrium. A Nash equilibrium can formally be defined in the following way [43]. Consider a game with n players and let S_i denote the set of all strategies for player i, and $u_i(\sigma_i)$ be the payoff function evaluated at σ_i. Denote a strategy profile for player i to be σ_i and the strategy profile for all players except player i to be σ_{-i}. Then a strategy profile σ^* is a Nash equilibrium if for all players i

$$u_i(\sigma_i^*, \sigma_{-i}^*) \geq u_i(s_i, \sigma_{-i}^*) \quad \text{for all} \quad s_i \in S_i.$$

The role of population inertia in stochastic models of invasion

As discussed in Section 1.1.2 invasion can have a large impact on the dynamics of a population and may become extremely economically costly. Therefore, there is an increasing need to determine when invasion will occur. The invasion exponent was introduced about 20 years ago in [101] as a measure of whether invasion would occur. The invasion exponent calculates the rate at which a invasive population would grow given that it is introduced at low densities. The invasion exponent is often used to predict invasion ([1], [63]). Caswell and Takada [26] explore the elasticity of the invasion exponent for density-dependent models. They find that "*sensitivity analysis of the invasion exponent reveals important information about population density*"[26]. An Allee effect is when a growth rate of a sparse population increases non-linearly, and therefore as it can be assumed that introduced populations are small then Allee effects are often useful in invasion models [34]. Drake [34] creates a model for an invasive zooplankter and illustrates the importance of taking into account non-linear phenomena. Invasive species are often considered as a travelling wave as the invasive species spreads [52]. Therefore, the population models for an invasive species are often spatially dependent, for example [55]. Furthermore, stochastic spatial invasion attempts have been modelled in [76] and [77].

In [49] we create a discrete-time stage structured invasion model, with coupled resident-invader dynamics. The fecundity of the resident and invader populations are density dependent and the dynamics for the invader population contains an Allee effect. The addition of the Allee effect means that invasion can occur even though the invasion exponent would predict invasion to fail. For varying population projection matrices we find no correlation between the invasion exponent and the smallest Allee effect which allows invasion, implying that for this model the invasion exponent can not be used to predict invasion. However, there exists an inverse relationship between the population inertia and the minimum Allee effect required for invasion to occur. In Chapter 5 we explore the effect stochasticity has on the relationship, found in [49], between population inertia and Allee effect required for invasion.

Chapter 2

Linking Managed Conservation to Complex Demographies: A Linear Programming Approach

2.1 Introduction

As discussed in Chapter 1, the use of dynamic programming to create management or control strategies for ecological applications has greatly increased. Getz and Gutierrez [44], Shoemaker et al. [114] and Kennedy et al. [66] provide reviews of the earlier research. One of the key advantages of using dynamic programming is that it provides a middle ground between exhaustive simulations (which are very computationally intensive) and analytical models (which may be an over simplification). These control strategies can be useful for pest managers and conservation biologists. An example for creating control strategies required by pest managers is given by Bogich et al. [15], where the impact and control of gypsy moth is studied. There are many more examples [40] and [52] where management of invasive plants is determined using dynamic programming strategies. Dynamic programming can also be used to find conservation strategies for endangered populations. For example, Rout et al. [105] create translocation strategies for endangered marsupials, and Tenhumberg et al. [128] find a rule of thumb for translocation that can be used to minimise extinction.

Hastings et al. [52] use linear programming to find an optimal strategy to control an invasive plant, *Spartina alterniforna* in Willapa Bay. They divide the invasive species, *Spartina alterniforna*, into three stage classes; seedlings, isolated plants and meadows. A discrete-time model is used to find an optimal removal strategy that minimises the total population after 10 years, given that the resource available for removal is limited. They find that when the resource is limited, so the optimal control can not remove the whole population, then the optimal strategy focuses on individual stages. They also find that time-dependent control strategies are more effective and the stages with greatest reproductive value should be targeted first. We explore whether limited resource causes similar patterns in optimal translocation programmes.

A managed translocation programme is when the optimal strategy is able to move the population between a wild and a captive population. When the resource available is limited we expect a trade-off between the cost and maximising the population. We find that there are three essentially distinct strategies:

- *Zoo strategy* – individuals in all stages are captured initially and are only released when habitat conditions are improved [56].
- *Headstart strategy* – juveniles are reared through survival bottlenecks [54], [84].
- *Ark strategy* – individuals with high reproductivity are kept in captivity, and captive-born individuals are released into the wild [10].

For simplicity and to help illustrate our results we use population projection matrices (PPM's) [23], and linear programming [120] which is the simplest constrained optimization tool. Specifically, we assume that both wild and captive population dynamics can be described using linearised, discrete-time, stage structured projection models [23] with n distinct lifestages. These models are well-suited to handling demographic complexity. We focus on essential features involved in the design of captive rearing strategies:

- multi-dimensional stage structured models,
- costs attributed to capture, rearing and release,
- essential constraints imposed by targets,
- avoidance of extinction.

We create a managed translocation programme that increases the population growth. We set a time horizon T and assume that each captive individual has costs associated with capture and per-timestep rearing. A natural constraint on the strategy is that the wild population should not be exhausted during the translocation programme's time horizon. We consider a selection of PPM's with populations declining in the wild, then find the optimal strategy to maximise the population, at time T given that the resource is fixed. Next we classify each optimal strategy to explore the effect limited resource has on the strategy which maximises the final wild population.

Using our framework we also investigate whether captive rearing can promote growth even when both the wild and captive populations are in decline. Such interactions between two populations that are in decline are called sink-sink populations. Although the individual populations are declining, with movement it is possible for sink-sink populations to persist, as shown in [61] and [6].

The chapter is structured as follows. Section 2.2 outlines the model including the optimisation constraints. Then Section 2.3 explains the parameters to be defined and the implementation. The model and constraints are formulated into a linear programming problem in Section 2.4. Section 2.5 explains how we choose to classify the optimal strategies and Section 2.6 gives the results of both a meta analysis of 31 animal and 983 plants PPM's, and a number of illustrative case studies then discusses these results. Finally, Section 2.6.4 creates a simple example of a sink-sink population that grows with optimal translocation. Section 2.7 summaries our results.

2.2 The model

In our model we consider a managed translocation programme of a wild population which has long-term dynamics that asymptotically decline. The population is structured in multiple life stages, and the translocation programme involves the movement (capture and release) of individuals between the wild and captive populations in any stage class. The captive population is assumed to be 'better' than the wild population.

The specific meaning of 'better' is species-dependent and is determined by increasing the vital rates (Section 2.3) but in general the captive population will have an asymptotic growth rate greater than one. We calculate strategies to optimally manage the capture and release, and then create a method of classifying and comparing these optimal strategies.

We assume that we have linear, post-census models for both the wild and captive populations. Let $x(t) \in \mathbf{R}^n$ and $z(t) \in \mathbf{R}^n$ be the stage structure of the wild and captive populations, respectively, with n stages at the census time t. The wild PPM is denoted $A \in \mathbf{R}^{n\times n}$ whilst the captive PPM is $D \in \mathbf{R}^{n\times n}$. The stage structure of the captive individuals released into the wild at time t is $u(t) \in \mathbf{R}^n$, and $w(t) \in \mathbf{R}^n$ is the stage structure of wild individuals captured at time t and taken into captivity for rearing and breeding purposes. In Section 2.3 we discuss assumptions for $u(t)$ and $w(t)$ having different financial costs associated with them. The vector $x(t) - w(t) + u(t)$ is the stage structure of the wild population that has to survive to time $t+1$ under the transition dynamics of A, whilst $z(t) + w(t) - u(t)$ is the stage structure of the captive population that has to survive to time $t+1$ under that transition dynamics of D. Hence the model for the coupled wild and captive populations is given by

$$\begin{aligned} x(t+1) &= A(x(t) - w(t) + u(t)) \\ z(t+1) &= D(z(t) + w(t) - u(t))\,. \end{aligned} \tag{2.1}$$

Possible natural constraints on $u(t)$ and $w(t)$ are:

$$\|x(T)\|_1 \geq \|x_d\|_1 \quad \text{the total wild population exceeds the demand at time } t = T; \tag{2.2a}$$

$$w(t) \geq 0 \quad \text{non-negative capture in all stages;} \tag{2.2b}$$

$$u(t) \geq 0 \quad \text{non-negative release in all stages;} \tag{2.2c}$$

$$x(t) - w(t) + u(t) \geq w_0 \quad \text{wild population is above a stage structured } w_0; \tag{2.2d}$$

$$z(t) + w(t) - u(t) \geq 0 \quad \text{non-negative captive population in all stages}\,. \tag{2.2e}$$

The 1-norm, $\|\cdot\|_1$, used in constraint (2.2a) is given by

$$\|x\|_1 = \sum_{k=1}^{m} |x_k| \text{ where } x = [x_1, x_2, \ldots x_m].$$

Given these constraints there are two natural choices for objective functions:

- maximise the population given that the resource available is fixed;
- minimise the resource required to sustain the population.

These are clarified further in Section 2.4.

2.3 Defining the parameters

The solution will depend crucially upon several features of the problem. These features are design specifications for the optimally managed translocation programme and are treated as inputs to the problem.

The vital rates of the captive population: Given a PPM, A, for the wild population which is asymptotically declining, we created the captive PPM, D, such that the dominant eigenvalue of D is 1.15 ± 0.01. To do this the wild PPM, A, is scaled evenly such that the dominant eigenvalue is 1.15. The resulting matrix obtained from scaling A may have survival and growth rates in a stage class which sum to greater than one. If this occurs we fix these survival and growth rates in that particular stage so that they sum to one, such that the survival and growth rates are scaled evenly. Then the other entries in the PPM are scaled so that the eigenvalue is within 0.01 of 1.15. This creates a captive PPM, D, with a dominant eigenvalue of approximately 1.15 while ensuring that the sum of the survival and growth rates in any stage is not greater than one. We considered other options for creating D, for example for each species deciding if captivity would have greatest affect on fecundity, survival and growth and then only scaling these vital rates to create D. However, the method chosen in scaling the whole PPM is the most parsimonious (due to insufficient information it is infeasible to calculate bespoke choices of D).

Remark. *The dominant eigenvalue of D was chosen to be 1.15 as if the eigenvalue was smaller then for several of the PPM's, even with unlimited resource, it was not possible to sustain the population. This is because the wild population may have an eigenvalue much less than one and a proportion of the population must remain in the wild, so overall we can not conserve the population at the initial density. Also, if we chose the eigenvalue to be much larger than 1.15 then for several of the wild PPM's it is not possible to create a realistic D.*

Initial Population: The initial population is the initial state of the wild population, which we denote by $x_0 \in \mathbf{R}^n$. There are many possible choices for x_0 as it may be at stable stage structure with low density, or x_0 may reflect an unhealthy population which is biased towards certain stages with low reproduction or survival. We assume the initial stage, x_0, is at stable stage structure of the wild population, given by the right eigenvector of A corresponding to the dominant eigenvalue. The stable stage structure is scaled such that the total initial population is one, i.e. so $\|x_0\|_1 = 1$. It is assumed that the translocation programme starts at $t = 1$, so no individuals are in captivity at the initial time step, which means the initial captive population, denoted z_0, is a vector of zeros in $\mathbf{R}^n$.

Time frame: Let T denote the number of time steps the managed translocation programme will be in operation. For each species, T must be dependent on the number of stages and the survival rates within the PPM, as for a PPM with a larger number of stages it will take more time steps for an individual to grow from a baby to an adult and therefore more time steps in the translocation programme are required to exploit the population dynamics. To obtain a suitable T for each species with wild PPM, A, we calculate the life expectancy at birth as described by Caswell [25]. Following [25], first let U denote a matrix containing the entries of A but with zeros in the first row. This matrix gives the probability of visiting each of the stages after one time step. Therefore the expected number of visits to each stage over a life time is given by

$$N = (I - U)^{-1}.$$

As the stages are numbered such that birth occurs in stage 1, then the life expectancy at birth is

$$E = \mathbb{1}^T N e_1,$$

where $\mathbb{1} \in \mathbf{R}^n$ is a vector of ones and $e_1 \in \mathbf{R}^n$ is a vector of zeros with 1 in the first component. To allow time for the population dynamics to have an effect the number of time steps, T, is chosen such that $T \approx 4E$. Note, that T is an integer, whilst E is unlikely to be integer valued. Hence T is only approximately $4E$.

Remark. *Note that T measures the number of time steps and the length of the time steps will vary between species depending on the data collection, as time intervals within a PPM depend on the species and the number of stages. For example for a* Acyrthosiphon pisum *(Pea aphid) with 3 stages each time step is a day and $T = 8$, whereas for a* Ailuropoda melanoleuca *(Giant panda) with 18 stages the length of a time step is a year and $T = 72$.*

Conservation Target: We require that the wild population achieves a threshold at time T, which is denoted by x_d. Given that the wild population is asymptotically declining then a natural target is to sustain the wild population at the initial density and at stable stage structure. However, releasing the captive population may alter the wild population structure. Therefore the target population is relaxed slightly so that just the density of the wild population remains unchanged, i.e. $\|x_d\|_1 = \|x_0\|_1$.

Cost required for translocation programme: A translocation programme will carry significant costs. There will be one-off start-up costs and recurrent running costs. The running costs will include costs of capture and release, food and medical costs. So the running costs will increase as the captive population increases. As the start-up cost are independent of the capture and release strategy these costs are ignored and we only focus on the running costs, which are dependent on u and w. We focus on two primary costs needed to manage the translocation programme: the cost associated with rearing and looking after the captive individuals, and the separate cost associated with capturing wild individuals. It is reasonable to assume lower costs are needed to release captive individuals into the wild and accordingly we also ignore this cost. Hence, the

cost, denoted by J, is a function of $u(0), \ldots, u(T-1)$ and $w(0), \ldots, w(T-1)$. At low densities it makes sense to assume that the costs are linear in $u(t)$ and $w(t)$, so an appropriate cost function has the form

$$J(u, w) = \sum_{j=0}^{T-1} \|K_j(z(j) + w(j) - u(j))\|_1 + \sum_{j=0}^{T-1} \|L_j w(j)\|_1 \,, \tag{2.3}$$

where K_j and L_j are weighting matrices which can reflect both variability of cost required in different stage classes, which may also be time dependent. The first term in equation (2.3) reflects the cost of keeping the population in captivity and the second term is the cost required to capture the population.

Constraints on translocation programme: A managed translocation programme will not allow the entire population to be kept in captivity, and reduce the wild population to 0. Therefore, how much of the population can be taken into captivity is constrained by keeping the wild population above a threshold. We let the non-negative vector w_0 represent the smallest that the stage structured wild population can become. We assume that the wild population can not be removed to less than 1% of the original wild population, which means that $w_0 = 0.01x_0$.

2.4 Linear Programming problem

The constraints given by equations (2.2) hold at each time step. Therefore, to proceed we rewrite the dynamic equations (2.1), constraints (2.2) and resource (2.3) such that they include the constraints for all time steps $t = [1 \ldots T]$. First, let

$$U = \begin{pmatrix} u(0) \\ \vdots \\ u(T-1) \end{pmatrix} \quad \text{and} \quad W = \begin{pmatrix} w(0) \\ \vdots \\ w(T-1) \end{pmatrix}.$$

Then equation (2.1) implies that

$$x(T) = A^T x_0 + [A^T \, A^{T-1} \, \ldots \, A](U - W) = A^T x_0 + \mathcal{B}(U - W), \tag{2.4}$$

where

$$\mathcal{B} = [A^T \ A^{T-1} \ \dots \ A] \, .$$

Therefore, constraint (2.2a), i.e. that the final population reaches a demand threshold such that $\|x(T)\|_1 \geq \|x_d\|_1$, becomes

$$\mathbb{1}^T \mathcal{B}(U - W) \geq \mathbb{1}^T (x_d - A^T x_0). \tag{2.5}$$

The second and third constraints (2.2b) and (2.2c), i.e. that the capture and release must be non-negative, become

$$U \geq 0, \quad W \geq 0 \, . \tag{2.6}$$

Next, let

$$\mathcal{A} = \begin{pmatrix} I & 0 & 0 & \dots & 0 \\ A & \ddots & \ddots & \dots & 0 \\ \vdots & \ddots & \ddots & \ddots & \vdots \\ \vdots & \ddots & \dots & \ddots & 0 \\ A^{T-1} & \dots & \dots & A & I \end{pmatrix} \quad X_1 = \begin{pmatrix} x_0 \\ Ax_0 \\ \vdots \\ A^{T-2}x_0 \\ A^{T-1}x_0 \end{pmatrix}$$

and

$$\mathcal{D} = \begin{pmatrix} I & 0 & 0 & \dots & 0 \\ D & \ddots & \ddots & \dots & 0 \\ \vdots & \ddots & \ddots & \ddots & \vdots \\ \vdots & \ddots & \dots & \ddots & 0 \\ D^{T-1} & \dots & \dots & D & I \end{pmatrix} \quad Z_1 = \begin{pmatrix} z_0 \\ Dz_0 \\ \vdots \\ D^{T-2}z_0 \\ D^{T-1}z_0 \end{pmatrix} .$$

Then the constraint (2.2d), i.e. that the wild population is no less than w_0, becomes

$$-\mathcal{A}(U - W) \leq X_1 - w_0, \tag{2.7}$$

whilst the constraint (2.2e), i.e. that the captive population is non-negative, becomes

$$\mathcal{D}(U - W) \leq Z_1 \, . \tag{2.8}$$

Finally, we use equation (2.3) to write a constraint, such that the total cost at time T is constrained by the resource available, denoted by C_T. We assume that there is no weighting of the cost for different stages or times, so we take K_j and L_j to be the identity matrices. Therefore, the cost given by equation (2.3) can be written as

$$J(U, W) = \|(Z_1 + \mathcal{D}(W - U))\|_1 + \|W\|_1 .$$

Since the constraint (2.6) requires W to be non-negative, and (2.8) requires $Z_1 + \mathcal{D}(W - U)$ to be non-negative, we have that

$$\|(Z_1 + \mathcal{D}(W - U))\|_1 = \mathbb{1}^T(Z_1 + \mathcal{D}(W - U)) \quad \text{and} \quad \|W\|_1 = \mathbb{1}^T W .$$

Hence, the cost equation (2.3) can be rewritten as an affine linear function (in W and U)

$$J(U, W) = \mathbb{1}^T \left(\mathcal{D}(W - U) + W + Z_1\right).$$

Hence, the constraint that the cost be no greater than some specified positive resource, C_T, becomes the affine linear inequality:

$$\mathbb{1}^T \left(\mathcal{D}(W - U) + W\right) \leq C_T - \mathbb{1}^T Z_1, \tag{2.9}$$

where C_T is to be defined.

As discussed in Section 2.2 there are two optimisation problems to be considered. The following defines these problems and the corresponding objective function required for the optimisation, which we solve in Matlab using `Linprog`.

Problem 1: Maximise the terminal population with fixed resource:. In this problem we fix the available resource and maximise the wild population at time T. The constraints required for this problem are given by equations (2.6 - 2.9), and the objective is to maximise

$$\|x(T)\|_1 = \mathbb{1}^T x(T).$$

As $A^T x_0$ is a constant this is equivalent to maximising

$$\mathbb{1}^T (x(T) - A^T x_0).$$

Using equation (2.4), this is the same as minimising the linear objective function

$$\begin{aligned} &\min(\mathbb{1}^T \mathcal{B}(W-U)) \\ \text{subject to: } &U \geq 0,\ W \geq 0 \\ &-\mathcal{A}(U-W) \leq X_1 - w_0 \\ &\mathcal{D}(U-W) \leq Z_1 \\ &\mathbb{1}^T \left(\mathcal{D}(W-U) + W\right) \leq C_T - \mathbb{1}^T Z_1. \end{aligned}$$

Problem 2: Minimise the cost while maintaining the population: In this problem the goal is to minimise the cost required, while the total population at time T is maintained at $\|x_d\|_1$ or higher. Here the constraints needed are equations (2.5 – 2.8), and the objective function comes from equation (2.9), such that we minimise the linear function

$$\begin{aligned} &\min\left(\mathbb{1}^T \left(\mathcal{D}(W-U) + W\right)\right) \\ \text{subject to: } &\mathbb{1}^T \mathcal{B}(U-W) \geq \mathbb{1}^T (x_d - A^T x_0) \\ &U \geq 0,\ W \geq 0 \\ &-\mathcal{A}(U-W) \leq X_1 - w_0 \\ &\mathcal{D}(U-W) \leq Z_1. \end{aligned}$$

In this chapter we find the optimal translocation programme to maximise $\|x(T)\|_1$ for a large range of species given that the resource available is fixed. However, this fixed resource may vary between species and it is difficult to know a suitable estimate that is required to sustain the population. Therefore to overcome this problem of unknown resource, first for each species we considered Problem 2 to find the minimum resource required to maintain the population density for each species. Problem 1 is then solved for a range of multiples of this minimum resource. Having calculated these optimal strategies it is important to be able to compare them which we do by classifying the various optimal capture and release strategies, as described in the following section.

2.5 Classifying the optimal strategies

As discussed in Section 2.1 when a trade off between cost and targets occurs then the optimal strategy may focus on different stages. Therefore, we classify the optimal solutions into three different types which are labelled in the following way;

Headstart: The strategy focuses on helping the population through a bottleneck in survival of the population. To do this a particular stage with low survival and fecundity would be kept in captivity.

Ark: The optimal strategy increases population growth by prioritising the stages which have high reproductivity. Therefore these stages are kept in captivity and the offspring are released.

Zoo: This optimal strategy increases population and growth by removing as much of the whole population from the wild as possible at the first time step and keeping it in captivity until time T.

A zoo strategy focuses on keeping all the stages in captivity, whereas an ark or headstart strategy only keeps some of the stages in captivity. This means that a zoo strategy can be thought of as an 'intersection' of the ark and headstart strategies. Therefore, to classify the optimal strategy we calculate a measure of 'distance' between the optimal solution and an ark strategy and the 'distance' between the optimal solution and a headstart strategy.

The optimisation produces an optimal vector in $\mathbf{R}^{2nT}$ which contains the optimal removal and capture strategies for each of the n stages, for $t = [1, \ldots, T]$. For an optimal solution, first calculate the net movement in and out of captivity for each stage i and time t. This allows us to calculate the corresponding wild population $x(t)$ and captive population $z(t)$ at each time step, t. For each stage we compare the wild population given by the optimal strategy to the minimum allowed in the wild determined by w_0. The constraint that the wild population can not get below a threshold is given by $x(t) - w(t) + u(t) \geq w_0$ which means that

$$x(t+1) = A(x(t) - w(t) + u(t)) \geq Aw_0.$$

The 'perfect' ark and headstart strategies focus on keeping different stages in captivity. To determine if keeping a stage in captivity contributes to the ark or headstart we use the column sum of D, which captures how each stage class of the captive population contributes to the total size of the population at the next time step. We refer to the vector of column sums of D as the production rate. Let C be a vector containing the column sums of D then

$$Cx_0 = \|Dx_0\|_1,$$

which shows how the components of C contribute in one time-step to the total population. If the production rate in a stage is greater than one then it has a net contribution to the population size, and if the production rate in a stage is less than one then the stage causes the population density to decline.

Distance from being an ark: For the optimal solution to be an ark strategy the optimal strategy focuses on increasing the reproduction. Therefore, the wild population in the stages with production rate greater than one will have the smallest density possible for $t = 1 \ldots T-1$, as given by Aw_0. To calculate a measure of how 'ark-like' the optimal strategy is we use the following steps:

I For each stage i with production rate greater than or equal to one we create a vector in $\mathbf{R}^{T-1}$ given by $\mathcal{A} = \Big(Aw_0(i), \quad \ldots \quad , Aw_0(i)\Big)$, where $Aw_0(i)$ corresponds to the i-th component of Aw_0.

II Let $\tilde{x}_i \in \mathbf{R}^{n \times T-1}$ denote the wild population in the i-th stage given by the optimal translocation strategy, for $t = 1 \dots T-1$.

III Then for each stage i with production rate greater than or equal to one we calculate

$$\tilde{d}_i = \frac{\|\tilde{x}_i - \mathcal{A}\|_1}{\|\tilde{x}_i\|_1},$$

which gives a value in the interval $[0\,1]$ measuring the 'distance' between stage i of the optimal solution and a perfect ark strategy in stage i.

IV The overall distance between the optimal solution and the 'perfect' ark strategy is given by

$$\mathcal{K}_A = \sum_i \frac{\tilde{d}_i C_i}{\sum_j (C_j)}, \tag{2.10}$$

where C_i is the production rate for the i-th stage, and i and j both are summed over the stages with production rate greater than or equal to one. This weighted sum is used because when the resource is limited an 'ark-like' strategy will focus on the stages with highest production rate.

Distance from being an headstart: A strategy is classified as a headstart strategy if it removes individuals from the wild in stages with production rates less than one. This means that the wild population in the stages with production rate less than one would be as small as possible, as given by Aw_0. So in a similar way to calculating the distance to an ark we calculate $\tilde{d}_i$ for all the stages with production rate of less than one. Then we calculate the total 'distance' between the optimal strategy and a 'perfect' headstart strategy by using a different weighted sum given by

$$\mathcal{K}_H = \sum_i \frac{\tilde{d}_i \frac{1}{C_i}}{\sum_j \left(\frac{1}{C_j}\right)}, \tag{2.11}$$

where i and j are summed over the stages with production rate less than one. This weighted sum is used because a headstart strategy will focus on the stages with smallest production rate, and therefore we want the distance, $\tilde{d}_i$, in these stages to have a greater affect on $\mathcal{K}_H$.

Therefore, for a given optimal strategy we are able to classify it in terms of the two distances $\mathcal{K}_A$ and $\mathcal{K}_H$ which are in the interval [0 1]. The smaller the values of $\mathcal{K}_A$ or $\mathcal{K}_H$ the closer the optimal translocation strategy is to the 'perfect' ark or headstart strategy.

Distance from being a zoo: The distance to a 'perfect' ark strategy $\mathcal{K}_A$ has included all the stages with production rate greater than or equal to one, and $\mathcal{K}_H$ includes all the other stages with production rate less than one. Therefore when both of these values are small the optimal solution gives a wild population close to Aw_0 in all of the stages. This is classified as a zoo strategy, because as much as possible of the population is kept in captivity.

Example 1: Here we demonstrate the classification, for a simple example of an optimal translocation strategy, that is we derive the distance from ark and headstart strategies. An example wild PPM with 4 stages is given by

$$A = \begin{pmatrix} 0 & 0.1 & 5 & 10 \\ 0.5 & 0 & 0 & 0 \\ 0 & 0.1 & 0 & 0 \\ 0 & 0 & 0.1 & 0.1 \end{pmatrix}$$

which has dominant eigenvalue of 0.716. Scaling A by $\frac{1.15}{0.716}$ gives the corresponding captive PPM D with a dominant eigenvalue of 1.15 to be

$$D = \begin{pmatrix} 0 & 0.1606 & 8.0314 & 16.0627 \\ 0.8031 & 0 & 0 & 0 \\ 0 & 0.1606 & 0 & 0 \\ 0 & 0 & 0.1606 & 0.1606 \end{pmatrix}.$$

Calculating the stable stage structure of A gives that

$$x_0 = \begin{pmatrix} 0.552 \\ 0.385 \\ 0.053 \\ 0.008 \end{pmatrix}, \text{ and hence } w_0 = \begin{pmatrix} 0.0055 \\ 0.0039 \\ 0.0005 \\ 0.0001 \end{pmatrix} \text{ and } Aw_0 = \begin{pmatrix} 0.0038 \\ 0.0028 \\ 0.0004 \\ 0.0001 \end{pmatrix}.$$

For this example, let $T = 5$ then an example optimal translocation strategy gives the resulting wild population from $t = 0 \dots T-1$ to be

$$x_0 = \begin{pmatrix} 0.552 \\ 0.385 \\ 0.053 \\ 0.008 \end{pmatrix} \quad x_1 = \begin{pmatrix} 0.004 \\ 0.003 \\ 0.05 \\ 0.005 \end{pmatrix} \quad x_2 = \begin{pmatrix} 0.004 \\ 0.003 \\ 0.05 \\ 0.005 \end{pmatrix} \quad x_3 = \begin{pmatrix} 0.004 \\ 0.003 \\ 0.05 \\ 0.005 \end{pmatrix} \quad x_4 = \begin{pmatrix} 0.004 \\ 0.003 \\ 0.05 \\ 0.005 \end{pmatrix}.$$

Calculate distance to ark

In view of D we see that stages 3 and 4 have production rates greater than 1, so we calculate $\tilde{d}_3$ and $\tilde{d}_4$. For stage 3, step I gives that $\mathcal{A} = \begin{pmatrix} 0.0004 & 0.0004 & 0.0004 & 0.0004 \end{pmatrix}$, and II gives that $\tilde{x}_3 = \begin{pmatrix} 0.05 & 0.05 & 0.05 & 0.05 \end{pmatrix}$, then using the equation in step III gives that

$$\tilde{d}_3 = \frac{\| \begin{pmatrix} 0.05 & 0.05 & 0.05 & 0.05 \end{pmatrix} - \begin{pmatrix} 0.0004 & 0.0004 & 0.0004 & 0.0004 \end{pmatrix} \|_1}{\| \begin{pmatrix} 0.05 & 0.05 & 0.05 & 0.05 \end{pmatrix} \|_1} = 0.99,$$

and in a similar way for stage 4 $\tilde{d}_4 = 0.98$. Finally, step IV gives the total distance to an ark to be

$$\mathcal{K}_A = \frac{0.99 \times 8.19 + 0.98 \times 16.22}{8.19 + 16.22} = 0.983.$$

Calculate distance to headstart

D gives that stages 1 and 2 have production rate less than one, so in a similar way to above, to calculate the distance to headstart we calculate $\tilde{d}_1$ and $\tilde{d}_2$. For stage 1, step I gives that $\mathcal{A} = \begin{pmatrix} 0.0038 & 0.0038 & 0.0038 & 0.0038 \end{pmatrix}$, and II gives that $\tilde{x}_1 = \begin{pmatrix} 0.004 & 0.004 & 0.004 & 0.004 \end{pmatrix}$, then step III gives $\tilde{d}_1$ to be

$$\tilde{d}_1 = \frac{\| \begin{pmatrix} 0.004 & 0.004 & 0.004 & 0.004 \end{pmatrix} - \begin{pmatrix} 0.0038 & 0.0038 & 0.0038 & 0.0038 \end{pmatrix} \|_1}{\| \begin{pmatrix} 0.0064 & 0.004 & 0.004 & 0.004 \end{pmatrix} \|_1} = 0.05$$

and $\tilde{d}_2$ is calculated in a similar way to give $\tilde{d}_2 = 0.067$. Finally, step IV gives the total distance to headstart to be

$$\mathcal{K}_H = \frac{0.05 \times \frac{1}{0.8031} + 0.067 \times \frac{1}{0.3212}}{\frac{1}{0.8031} + \frac{1}{0.3212}} = 0.062.$$

In this simple example $\mathcal{K}_A = 0.983$ and $\mathcal{K}_H = 0.062$ and so the optimal solution is an almost 'perfect' headstart strategy, as it focuses on keeping stages with productive rate less than one in captivity.

2.6 Results

Having established a framework for calculating and classifying the optimal translocation strategy, we find the optimal strategy for a range of real PPM's given in two databases.

2.6.1 Data

We use two databases, one for animal PPM's and another for plant PPM's. The database we use for the animal PPM's contains 346 PPM's for 169 animals species. This database has been developed over the last decade started by Dave Hodgson, where data has been collected from publications. The PPM's we use from this database are in Appendix A1.

The second database we use for plants species is called COMPADRE III [83]. This database contains 5683 PPM's for plants. The collection of this data started over 25 years ago and formed COMPARDE I. Since 2011 the Max Planck Institute for Demographic Research has hosted COMPADRE III to create a single, comprehensive database of plant demographic data.

We require some restrictions to find the PPM's that we can use from the databases. First, as we are creating translocation strategies to amplify a population, we assume the wild population is in decline. Therefore we use only the species where the dominant eigenvalue of the wild PPM is less than one. Furthermore, for simplicity we require the

wild PPM to be primitive. A $n \times n$ dimensional matrix, A, is primitive if

$$A^{n^2-2n+2} > 0.$$

We attempt to find optimal solutions for all the PPM's in the two databases which satisfy these two criteria.

2.6.2 Meta analysis

In this Section we find the optimal strategies for a range of available resource, for the data discussed in Section 2.6.1. Then the optimal strategies are classified as explained in Section 2.5.

Before this, we first explore the choice of x_0, w_0 and T as described in Section 2.3. To do this we consider the PPM for a grey squirrel population and let w_0 be 0.01 or 0.25, T be $2 \times E$ or $4 \times E$ and x_0 either be at stable stage structure, denoted x^*, or the stable stage structure but with half the number of individuals in the adult stages, denoted $\hat{x}$. The optimal strategy is calculated and classified for 300 choices of resource for all combinations of these parameters, given in Figure 2.1. In Figure 2.1 it can be seen that although numerically the distance to ark and headstart strategies do depend on the choice of parameters, overall the type of strategy required to maximise the population at intermediate levels of resource are the same. Therefore we choose to fix the parameters as defined in Section 2.3.

Having justified our choice of parameters we now consider the animal database. We calculate the optimal strategy for 300 choices of resource, between the minimum resource required to solve Problem 2 and 30 times this minimum resource. Solutions to this problem exist for 31 of the species in the animal database. These solutions are classified by calculating $\mathcal{K}_A$ and $\mathcal{K}_H$ (equations (2.10) and (2.11)). First, in Figure 2.2 we plot 8 species to demonstrate the affect resource has on the classification of the optimal translocation strategy. We use coloured lines to distinguish between the species and dots which increase in size as the resource available increases. Although the optimal

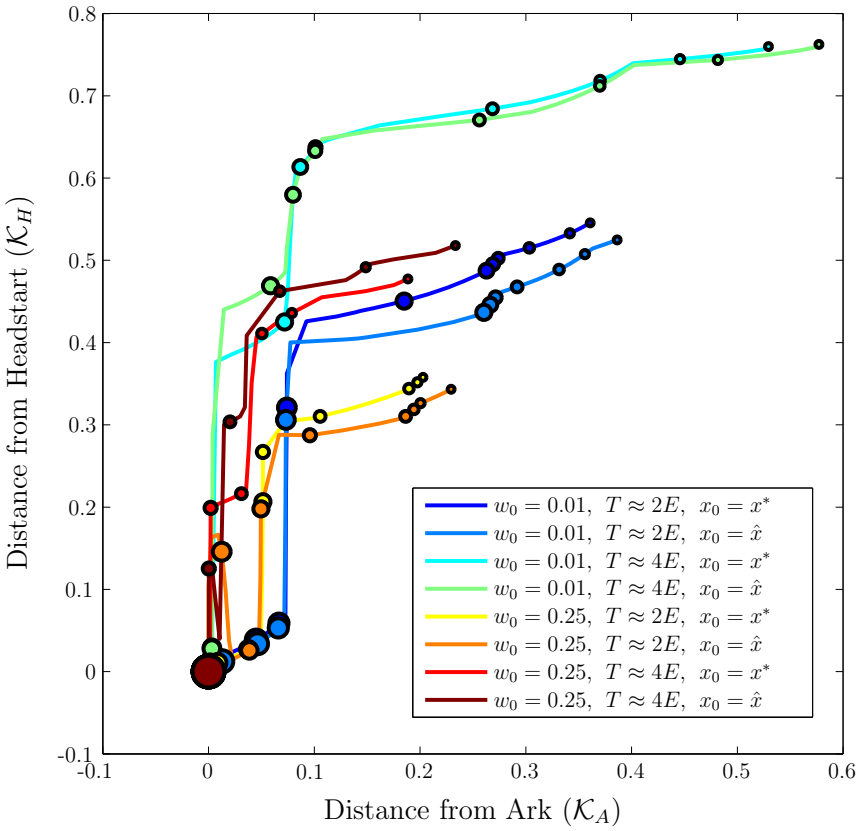

Figure 2.1: Classification of optimal strategy of grey squirrel, for 300 choices of resource and different choices of x_0, w_0 and T.

strategy is calculated for 300 choices of resource, in Figure 2.2 we use dots to represent magnitude of resource for 20 of the 300 choices. Secondly, having established the affect resource has, Figure 2.3 plots the classification of the optimal solution for the 31 species, for varying levels of resource.

Figure 2.2 shows that as the cost increases the strategies become closer to a zoo. This can be seen as for the 8 chosen species, the dots increase in size, and therefore value, as the classification of the optimal strategy gets closer to the origin. This is as expected because when the resource available is large enough, then the optimal strategy is able to keep the entire population in captivity from $t = 1$ to $t = T - 1$. Notice that the rate at which the size of the dots increases as the strategy changes varies between species. This means that for some species, increasing the resource available (which is always a multiple of the minimum resource) has a greater effect on the translocation strategy.

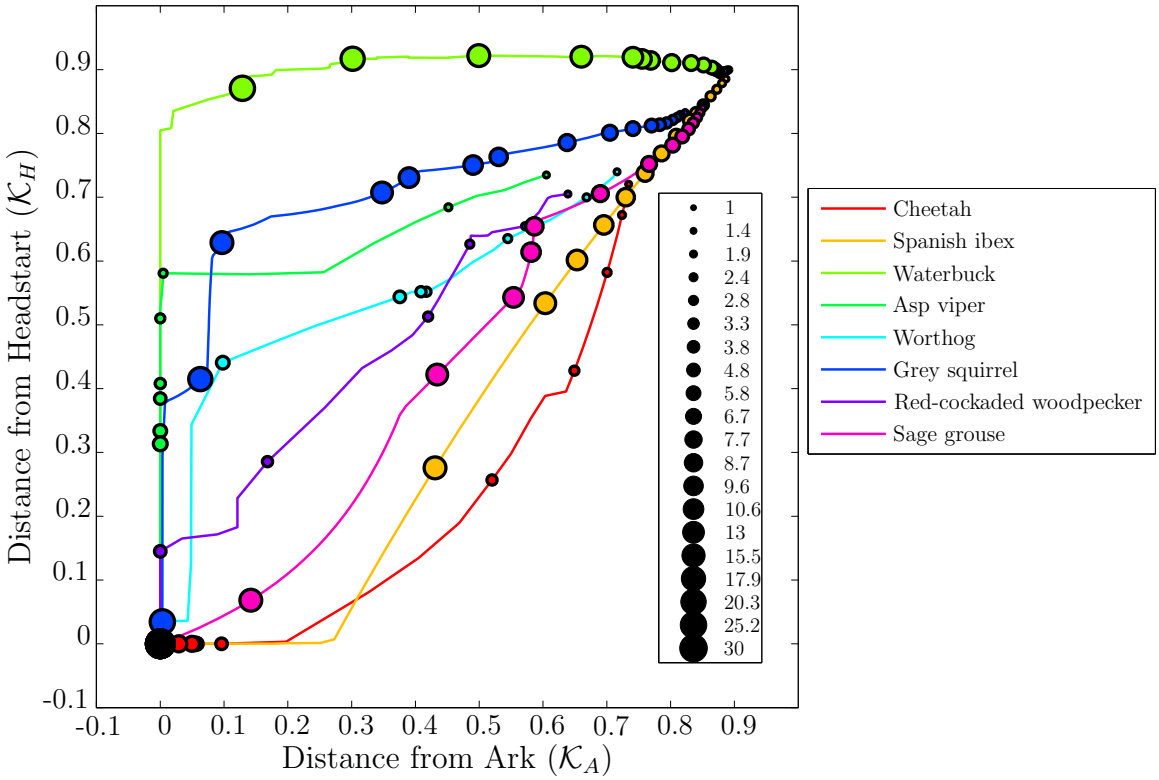

Figure 2.2: Classification of the optimal strategies (using equations (2.10) and (2.11)) for 8 species with 300 multiples of the minimum resource, with dots to represent the multiple of the minimum resource available.

At low levels of resource, most of the species are not close to being a headstart or an ark. This is because the optimal strategy associated with the minimum choice of resource is the optimal strategy which is able to sustain the total population density at time T. For most species this means little movement into captivity is required as the wild population is only declining slowly, and therefore little translocation is required to stabilise the population. However, for some species, the optimal strategy at minimum cost is closer to a 'perfect' zoo strategy, as indicated by the $\square$ in Figure 2.3. This means that for some species the optimal strategy associated with minimum cost must keep more of the population in captivity to sustain the population density. As the resource available increases a trade-off occurs between maximising the final population and the resource being limited. So the optimal strategy is able to keep particular stages in captivity, possibly to allow exploitation of the transient dynamics. Figure 2.3 shows that for about half the species there is an intermediate choice of resource such that the

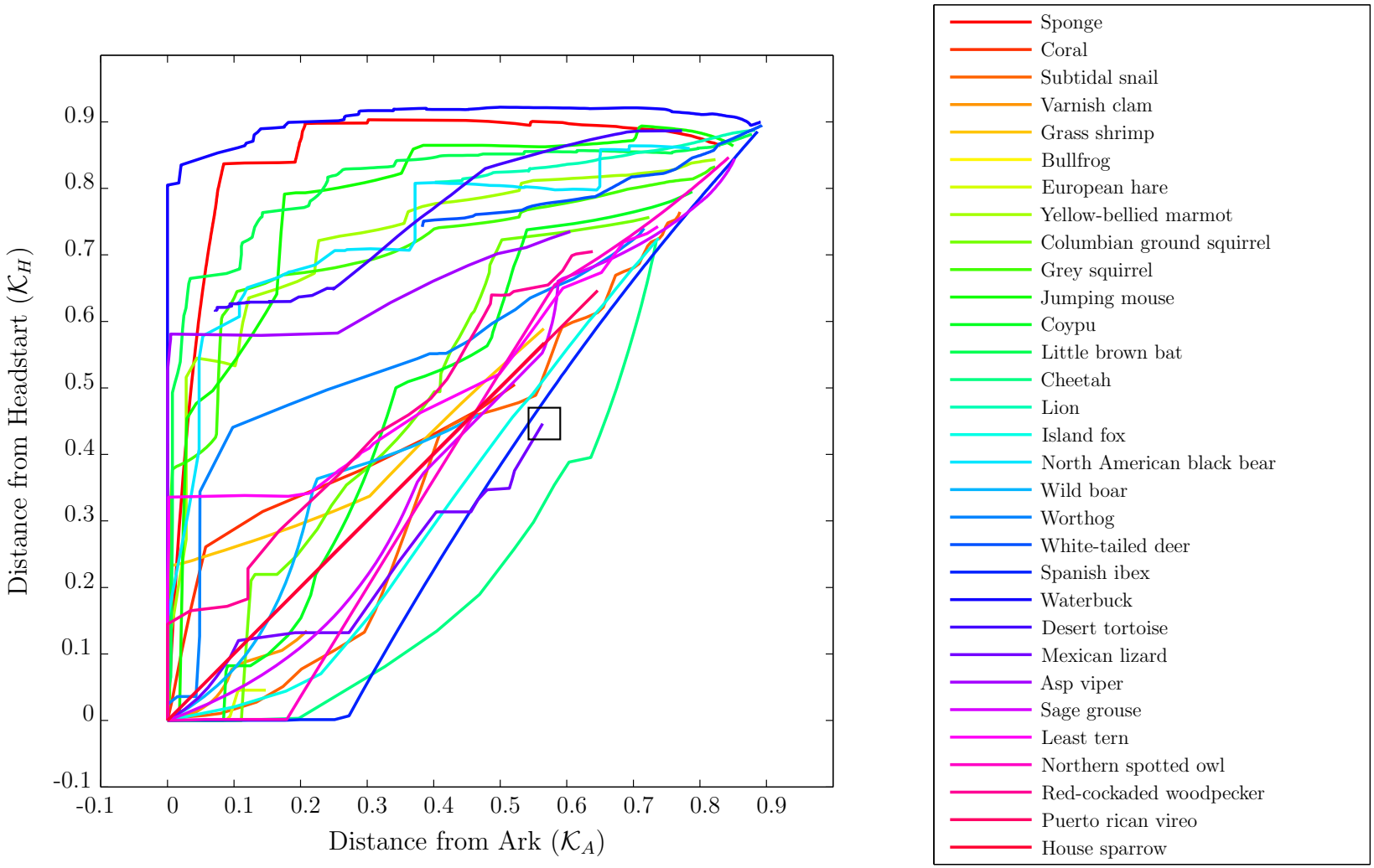

Figure 2.3: Classification of the optimal strategies (using equations (2.10) and (2.11)) for 31 species (shown by different coloured lines) for varying levels of resource.

optimal strategy is less than 0.1 from an ark and greater than 0.8 from a headstart. This means that when a trade off occurs for these species, the optimal strategy focuses on the stages with production rate greater than 1. As the resource increases further, then these optimal strategies also become closer to a headstart strategy, as the resource is large enough to keep the other stages in captivity and eventually with large enough resource we obtain a zoo strategy. Also, a lot of the species do not specifically target stages with high or low production rate. These strategies are illustrated in Figure 2.3, by the strategies which for all choices of resource are an equal distance between headstart and ark strategies.

Figure 2.3 shows for each species the classification of the optimal control strategy. However it is difficult to distinguish any pattern between species. So, Figure 2.4 shows the data used in Figure 2.3 with the species grouped by taxa. For the mammal taxa in Figure 2.4 no pattern can be seen in the classification of the optimal strategies. This is due to the huge range of diversity in this taxa (from little brown bat to lion). Although the majority of the species are mammals, Figure 2.4 does show that other taxonomic groups have general trends. The optimal strategies for the bird and arthropods species do not target any particular stage class, compared to the marine invertebrates and reptile species which for intermediate levels of resource tend to focus on increasing the reproduction by keeping the stages with production rate greater than 1 in captivity, representing ark strategies.

So far for each species we have explored how our classification of the optimal strategy changes with the resource available. Although the optimal strategy maximises $\|x(T)\|_1$, it does not give any information about the magnitude or structure of the resulting population, $x(T)$. We examine the fitness of the final wild population, $x(T)$, resulting from the optimal strategies for varying resource. Clearly the total size of the resulting wild population given by $\|x(T)\|_1$ is important, but the structure of the population also has a large impact on the fitness. For example, if the resulting wild population is predominately comprised of babies, then for most species it is fair to assume that once the control strategy ends at time T, the wild population would rapidly decrease. Therefore we calculated two measures of fitness, which are dependent and independent

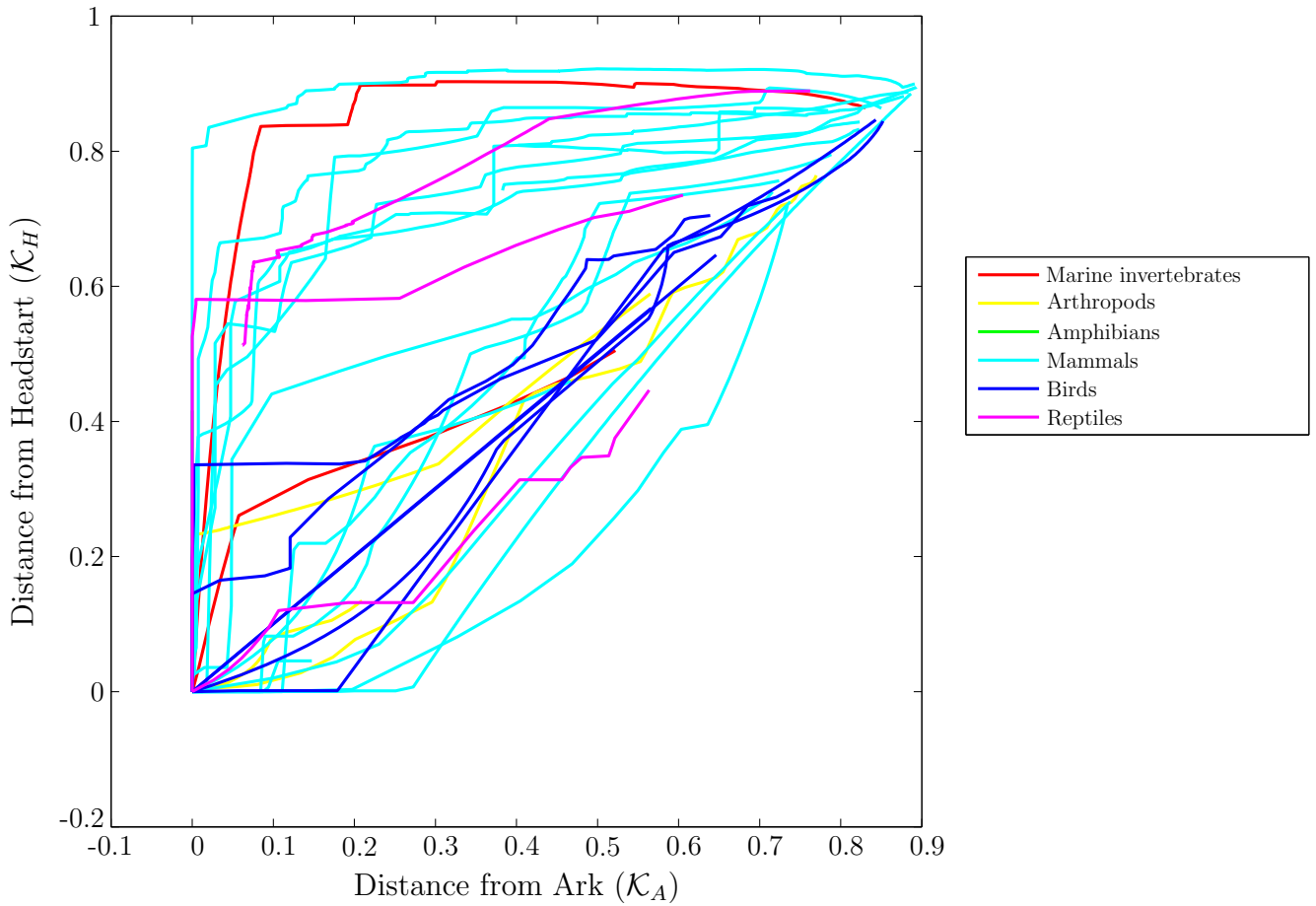

Figure 2.4: Classification of optimal strategies for 31 species with 300 choices of resource, grouped by taxa.

of the total wild population at the final time step, $\|x(T)\|_1$. As stated in Chapter 1 and [23] the reproductive value is given by the left eigenvector of the PPM, corresponding to the dominant eigenvalue. The reproductive value multiplied by the stage structure of the population gives a measure of total reproductivity from that stage structure. To calculate $\mathcal{F}_1$, we scale this measure of total reproductivity by $v'w$ and the total population density at time T, so that if the final wild population is at stable stage structure then the fitness given by $\mathcal{F}_1$ is 1. Notice, this is the same formula as the population inertia [122], which means it also gives a measure of the transients of the wild population at the final time step. The two measures of fitness are given by

$$\mathcal{F}_1 = \frac{v'x(T)}{v'w\|x(T)\|_1} \text{ and } \mathcal{F}_2 = \frac{v'x(T)}{v'w},$$

where v and w are left and right eigenvectors of A. As $\mathcal{F}_1$ is the reproductive value divided by the population size, $\|x(T)\|_1$, $\mathcal{F}_1$ creates a measure of fitness which is independent of the size of the wild population at time T.

For each species we calculate $\mathcal{F}_1$ and $\mathcal{F}_2$ for each choice of resource, then plot $\mathcal{F}_1$ and $\mathcal{F}_2$ against the available resource to get Figures 2.5 and 2.6, respectively. Figure 2.5 shows that for most species when the resource is high then the value of $\mathcal{F}_1$ is approximately 1. This means that in general when the resource is large enough so that the optimal strategy focuses on keeping all the stages in captivity, then the wild population, $x(T)$, at time T is close to stable stage structure. This is because the captive PPM, D, is created by scaling A, which means the captive population has the same (or similar) stable stage structure as the wild population. So when the majority of the population is kept in captivity and released at time $T-1$ then the stable stage structure remains unchanged. For several of the species, at intermediate levels of resource the fitness drops below 1. This is because the optimal strategy targets particular stages which, when released, changes the stable stage structure of the wild population, hence reducing the fitness.

Figure 2.6 shows the effect of resource on $\mathcal{F}_2$ for each species. It can be seen for most species that $\mathcal{F}_2$ increases linearly as the resource available increases, and then a threshold is reached where $\mathcal{F}_2$ can not increase any further. This is because, at this

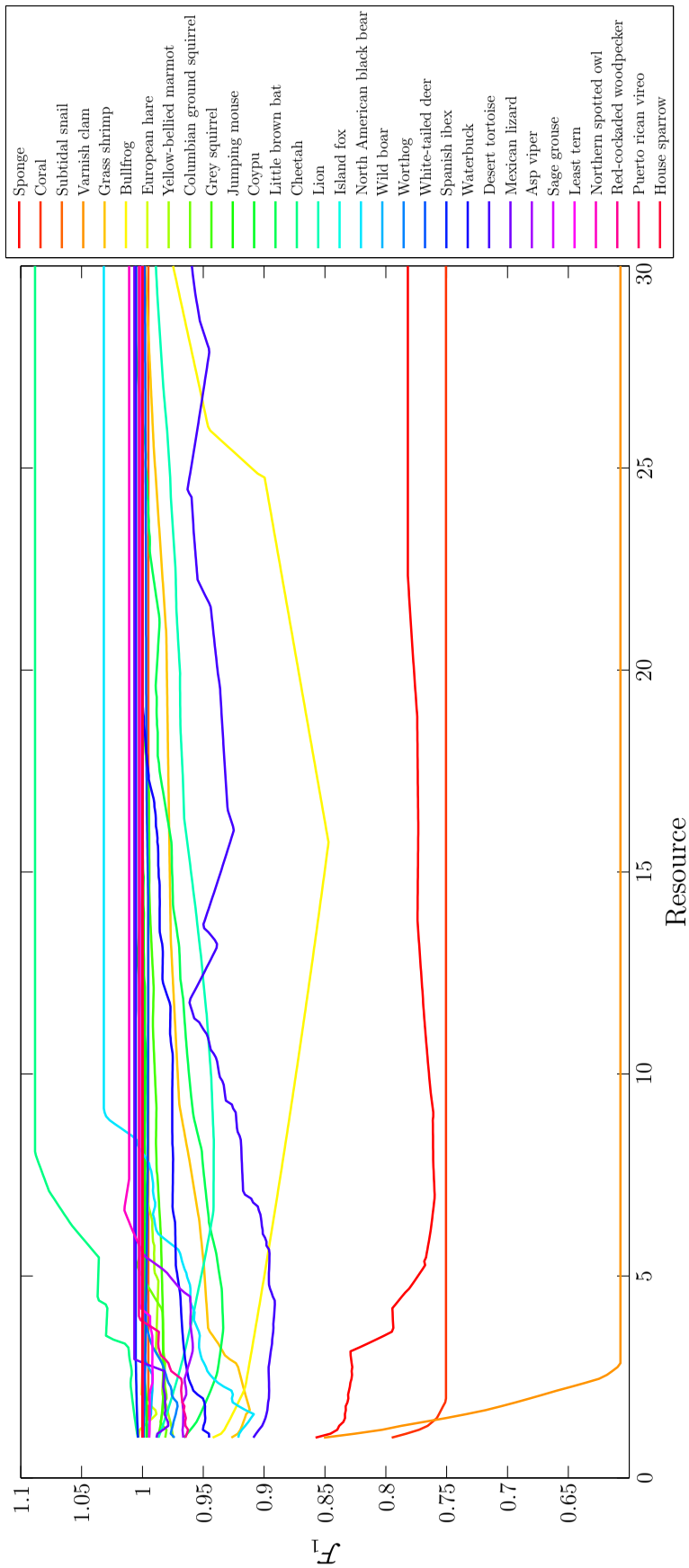

Figure 2.5: How resource affects 'fitness' of $x(T)$ for 31 species, independent of $\|x(T)\|_1$, given by $\mathcal{F}_1$.

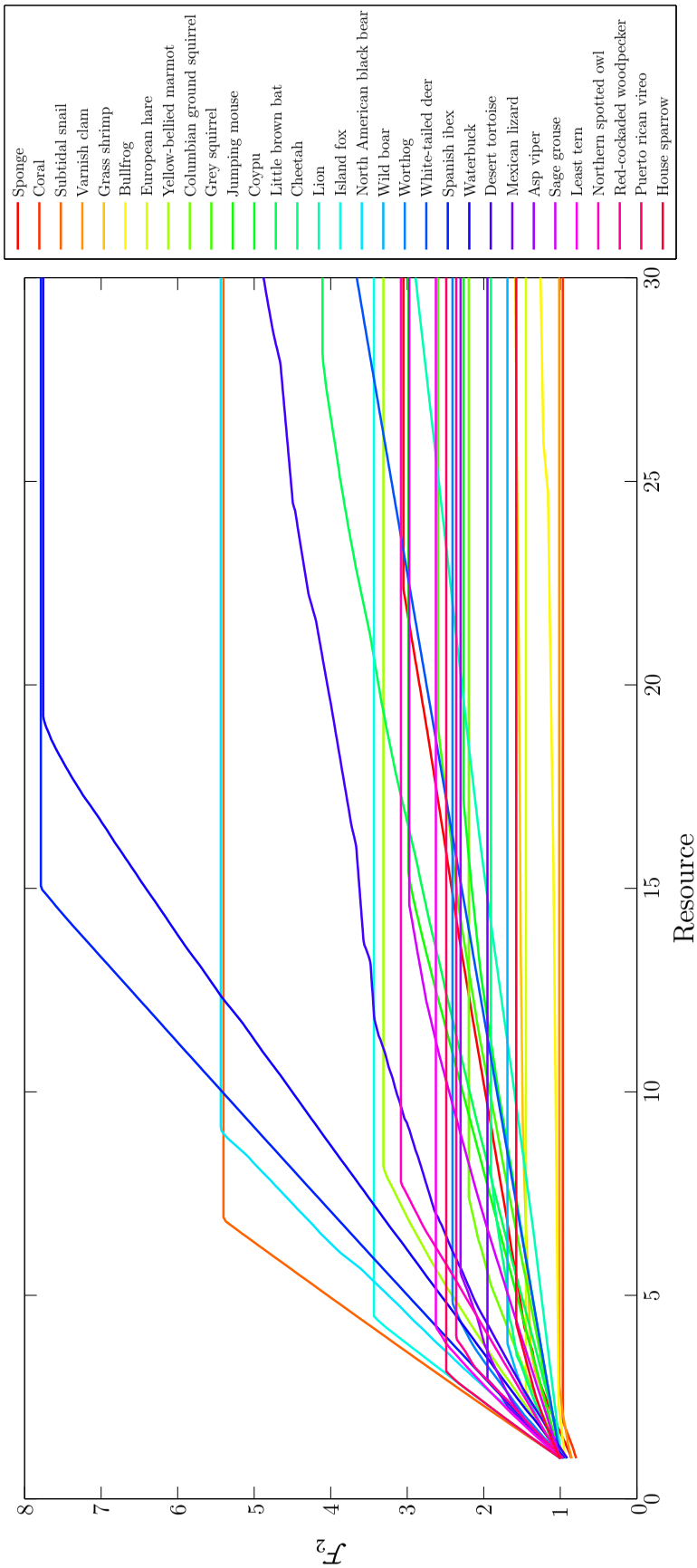

Figure 2.6: How resource affects 'fitness' of $x(T)$ for 31 species, dependent of $\|x(T)\|_1$, given by $\mathcal{F}_2$.

threshold of resource, the optimal strategy is a 'perfect' zoo strategy and therefore this is the maximum the final population can be and increasing the resource does not change the optimal strategy.

The translocation of plant species in captivity clearly presents different problems to captive animal populations. There are many ways to use in vitro conservation for plants [38]. These include botanical gardens, mircopropagation and vitro seed germination. Therefore, we consider the COMPADRE III database to find and classify the optimal strategies for the plant species, for varying levels of resource. There are 983 PPM's which have optimal control strategies. So to visualise the classification of these strategies we group the species by growth type to give Figure 2.7. Figure 2.7 shows that when the resource is limited the epiphytes, palms and succulents have a general trend to focus on keeping the stages with production rate greater than one in captivity. In contrast, the optimal strategies for the annual species focus on the stages evenly, as at intermediate levels of resource the optimal strategies are the same distance from being a headstart or an ark strategy.

The classification of the optimal strategies shown in Figure 2.7 show the classification for several different PPM's for the same species. Therefore, to check that the general trends shown in Figure 2.7 are not an artefact of having several of the same species we reduce the data to 122 PPM's with only one optimal strategy per species as shown in Figure 2.8. The PPM's for these 122 plant species are given in Appendix A2. Figure 2.8 shows the same general trends as Figure 2.7 and therefore the patterns seen in some growth types are not a result of having several optimal strategies for the same species.

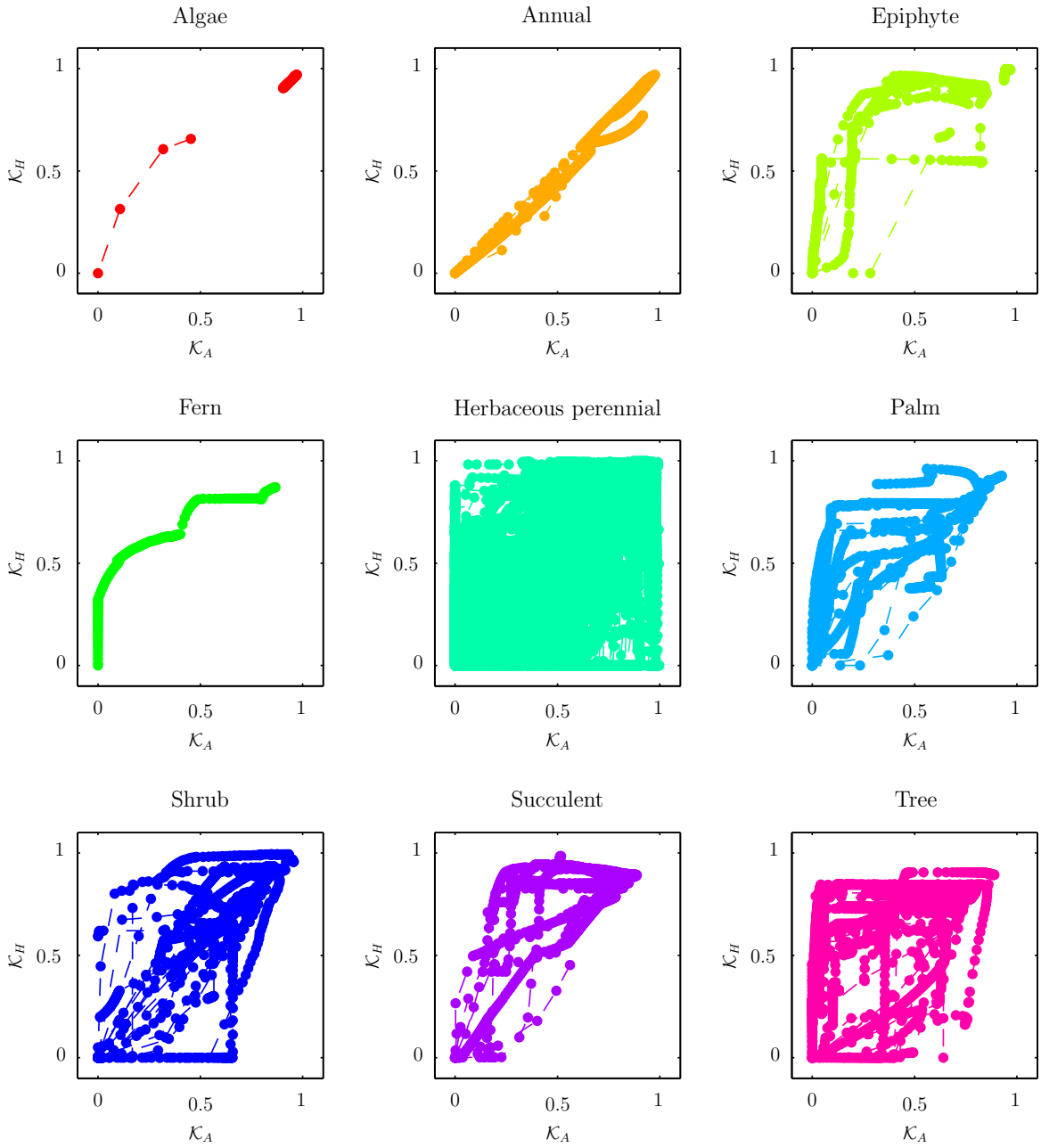

Figure 2.7: Classification of 983 optimal strategies for 300 multiples of minimum resource, sorted by growth type.

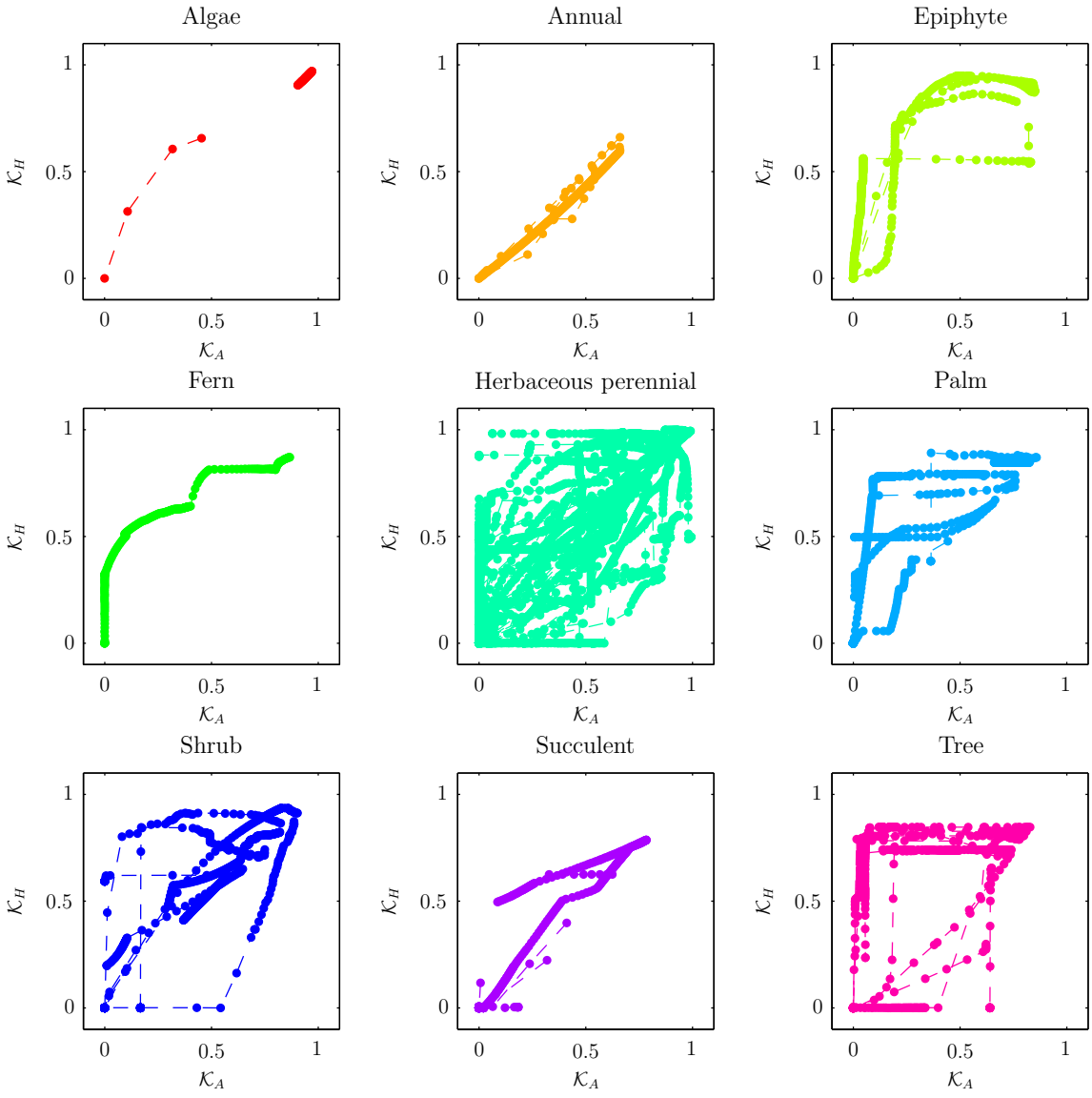

Figure 2.8: Classification of optimal strategies for 122 different species, for 300 levels of resource, grouped by growth type.

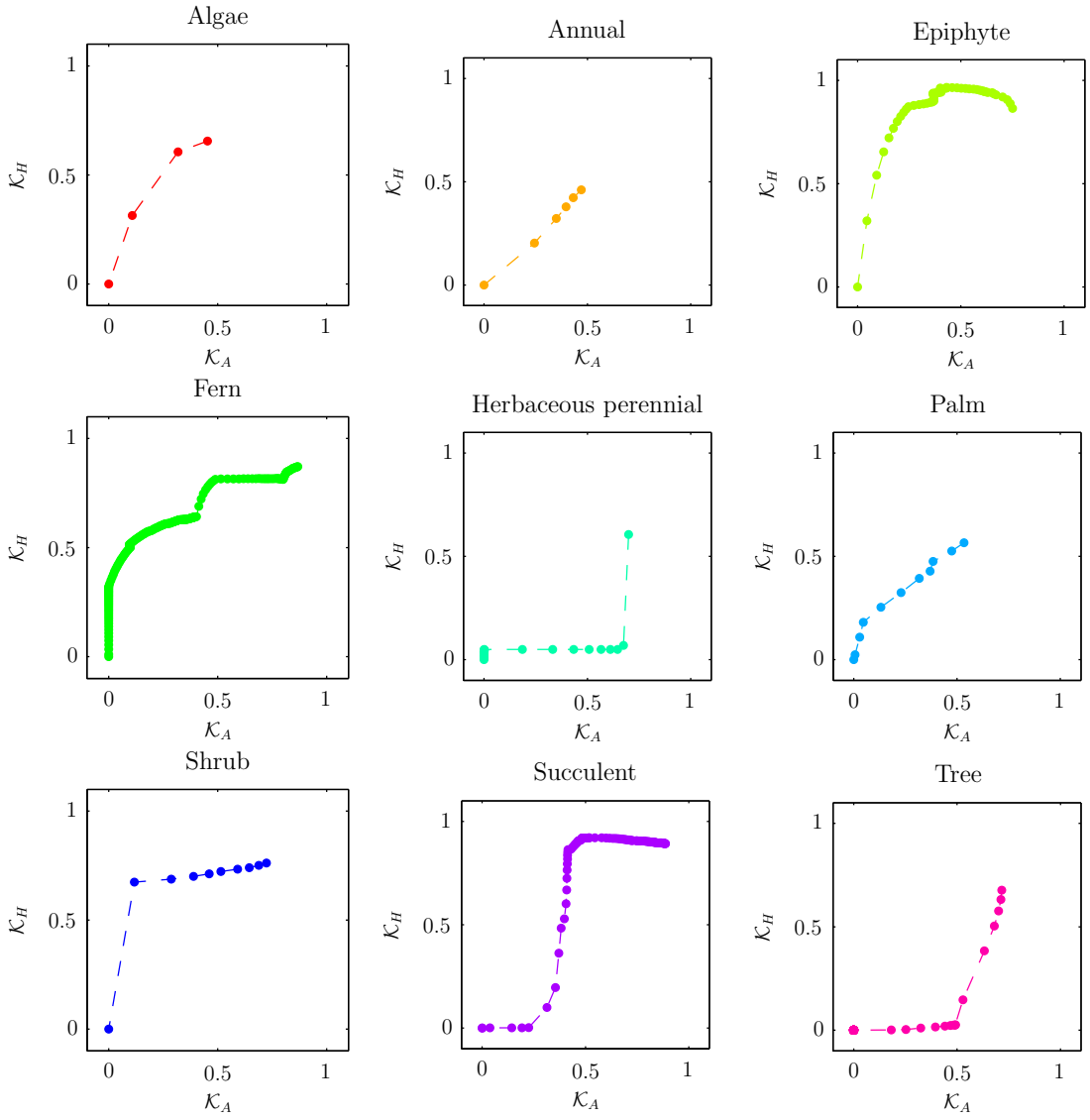

Figure 2.9: Classification of the optimal strategy for an example species for each of the 9 plant growth types, for 300 levels of resource.

Algae-*Laminaria digitata* $\begin{pmatrix} 0.34 & 0.34 & 0.255 & 0.06 & 0.024 \\ 0.12 & 0.25 & 0 & 0 & 0 \\ 0.004 & 0.22 & 0.44 & 0.33 & 0 \\ 0 & 0.056 & 0.22 & 0.44 & 0 \\ 0 & 0 & 0 & 0.11 & 0 \end{pmatrix}$	Annual-*Collinsia verna* $\begin{pmatrix} 0 & 0 & 0 & 4.3 & 4.3 & 4.3 & 4.3 \\ 0.15 & 0 & 0 & 0 & 0 & 0 & 0 \\ 0 & 0.19 & 0.09 & 0 & 0 & 0 & 0 \\ 0 & 0 & 0 & 0.5 & 0.5 & 0.5 & 0.5 \\ 0.0290 & 0 & 0 & 0 & 0 & 0 & 0 \\ 0 & 0.0145 & 0 & 0 & 0 & 0 & 0 \\ 0 & 0 & 0.0145 & 0 & 0 & 0 & 0 \end{pmatrix}$	Epiphyte-*Tillandsia macdougallii* $\begin{pmatrix} 0.15 & 0 & 0 & 0.06 & 0 & 0.19 \\ 0.46 & 0.36 & 0.05 & 0 & 0 & 0 \\ 0 & 0.32 & 0.064 & 0.09 & 0 & 0 \\ 0 & 0 & 0.12 & 0.67 & 0 & 0 \\ 0 & 0 & 0.01 & 0.03 & 0.14 & 0.13 \\ 0 & 0 & 0.003 & 0.03 & 0.6 & 0.68 \end{pmatrix}$
Fern-*Asplenium scolopendrium* $\begin{pmatrix} 0.29 & 0.03 & 0.054 & 3.12 & 0 \\ 0.4 & 0.43 & 0.11 & 0.12 & 0 \\ 0.011 & 0.02 & 0.27 & 0.42 & 0.07 \\ 0 & 0 & 0 & 0.35 & 0.73 \end{pmatrix}$	Herbaceous perennial-*Eryngium alpinum* $\begin{pmatrix} 0 & 0 & 0 & 1.1 \\ 0.22 & 0.7 & 0 & 0 \\ 0 & 0 & 0.78 & 0.86 \\ 0 & 0.19 & 0.08 & 0.07 \end{pmatrix}$	Palm-*Euterpe oleracea* $\begin{pmatrix} 0.44 & 0.17 & 0.34 & 0.58 & 0.9 & 1.62 \\ 0.05 & 0.4 & 0 & 0 & 0 & 0 \\ 0 & 0 & 0.3 & 0.52 & 0 & 0 \\ 0 & 0 & 0.02 & 0.5 & 0.45 & 0 \\ 0 & 0 & 0 & 0.03 & 0.45 & 0.89 \end{pmatrix}$
Shrub-*Purshia subintegra* $\begin{pmatrix} 0.06 & 0 & 0 & 0 & 0.49 \\ 0.002 & 0 & 0 & 0 & 1.5 \\ 0 & 0.06 & 0.36 & 0 & 0 \\ 0 & 0 & 0.04 & 0.86 & 0.2 \\ 0 & 0 & 0 & 0.09 & 0.78 \end{pmatrix}$	Succulent-*Mammillana pectinifera* $\begin{pmatrix} 0.25 & 0 & 0 & 1 & 3.97 \\ 0.05 & 0.16 & 0 & 0.21 & 0.82 \\ 0 & 0.04 & 0.53 & 0.07 & 0.06 \\ 0 & 0 & 0.085 & 0.67 & 0.18 \\ 0 & 0 & 0 & 0.06 & 0.41 \end{pmatrix}$	Tree-*Pinue lambertinana* $\begin{pmatrix} 0.82 & 0 & 0 & 0 & 1.45 \\ 0.04 & 0.84 & 0 & 0 & 0 \\ 0 & 0.11 & 0.91 & 0 & 0 \\ 0 & 0 & 0.06 & 0.82 & 0 \\ 0 & 0 & 0 & 0.05 & 0.94 \end{pmatrix}$

Table 2.1: The wild population PPM's corresponding to the examples shown in Figure 2.9

Having established the general trends for the different growth types next in Figure 2.9 we consider several examples to explore how the vital rates in the PPM affect the classification of the optimal strategy. First, if the rate of survival is particularly low, for example if very few seeds germinate, then placing the population in captivity will not be able to dramatically increase the survival. So, placing such stages with low survival in captivity has little affect on the population growth and therefore when the resource available for translocation is limited the optimal strategy focuses instead on placing the stages with high production rates in captivity. This means that at intermediate levels of resource the optimal strategy for populations with particularly low survival is classified as an ark strategy, as shown by the Shrub (*Purshia subintegra*) and Fern (*Asplerium scolopendrium*) examples. In contrast, when the survival rates are relatively high, then the captive population is able to slightly increase the survival and growth rates, so that in each stage they sum to approximately 1. Therefore, if the optimal translocation strategy moves the stages without reproduction into captivity then nearly 100% of the population is able to survive and then be released into the wild for reproduction. So, if the survival of non-reproductive stages is relatively high and the resource available is limited, then the optimal strategy will focus on stages which do not reproduce which results in an optimal translocation strategy which is classified as an headstart. Examples include Herbaceous perennial (*Eryngium alpinum*) and Tree (*Pinus lambertiana*). Figure 2.9 shows examples for Algae (*Laminaria digitata*), Annual (*Collinsia verna*) and Palm (*Euterpe oleracea*) for which the optimal translocation strategy at intermediate levels of resource does not target particular stages. Notice that the survival and growth rates in the corresponding PPM's (shown in Table 2.1) are moderate, which considering the previous examples is consistent with a optimal strategy which focuses on keeping the stages both with and without reproduction in captivity. Finally, at intermediate levels of resource the epiphyte (*Tillandsia macdougallii*) example in Figure 2.9, is classified as an ark strategy, although it is not clear why from studying the PPM in Table 2.1. This is perhaps because this is a high dimensional problem, with many factors in the PPM affecting whether a stage class should be kept in captivity.

2.6.3 Case studies

Section 2.6.2 focuses on the classification of the optimal strategy, and the fitness of the resulting wild population at time T. This section explores how the wild population changes in response to the optimal translocation strategy. To do this we examine the wild population for 3 different species and 8 choices of resource.

Firstly, Figure 2.10 shows the wild population of the *Vipera aspis* (Asp Viper) for 8 choices of resource. The Asp viper is a 5 stage structured model and the PPM is given in Appendix A1, where it can be seen that only the fifth stage has production rate greater than one. Figure 2.10 shows that when the resource available is large enough then the population is kept in captivity so the wild population is close to zero, at w_0 for $t = 1 \dots T-1$. Then the captive population is released at time T, so the wild population rapidly increases. For medium levels of available resource, stages 5 and 1 in particular are removed from the wild and placed in captivity. This means that when a trade-off occurs the optimal strategy focuses on increasing population reproduction by keeping as much of stage class 5 in captivity as possible. Then as the resource continues to increase the optimal strategy is able to keep stages 2, 3 and 4 in captivity thus increasing the survival. Therefore, the optimal strategy for the Asp Viper which focuses on increasing the reproduction when the resource is limited, is an ark strategy, which is consistent with the classification shown in Figure 2.3.

Secondly, the wild population of *Myocastus coypus* (Coypu) is shown in Figure 2.11 for 8 different levels of resource. As the resource available for the optimal strategy increases it can be seen that the wild population in all of the stages decreases. This means that the optimal strategy does not focus on keeping any particular stage in captivity. So for a Coypu population when a trade off occurs between resource and maximising the population the optimal strategy is part ark and part headstart. This is consistent with the classification in Figure 2.3.

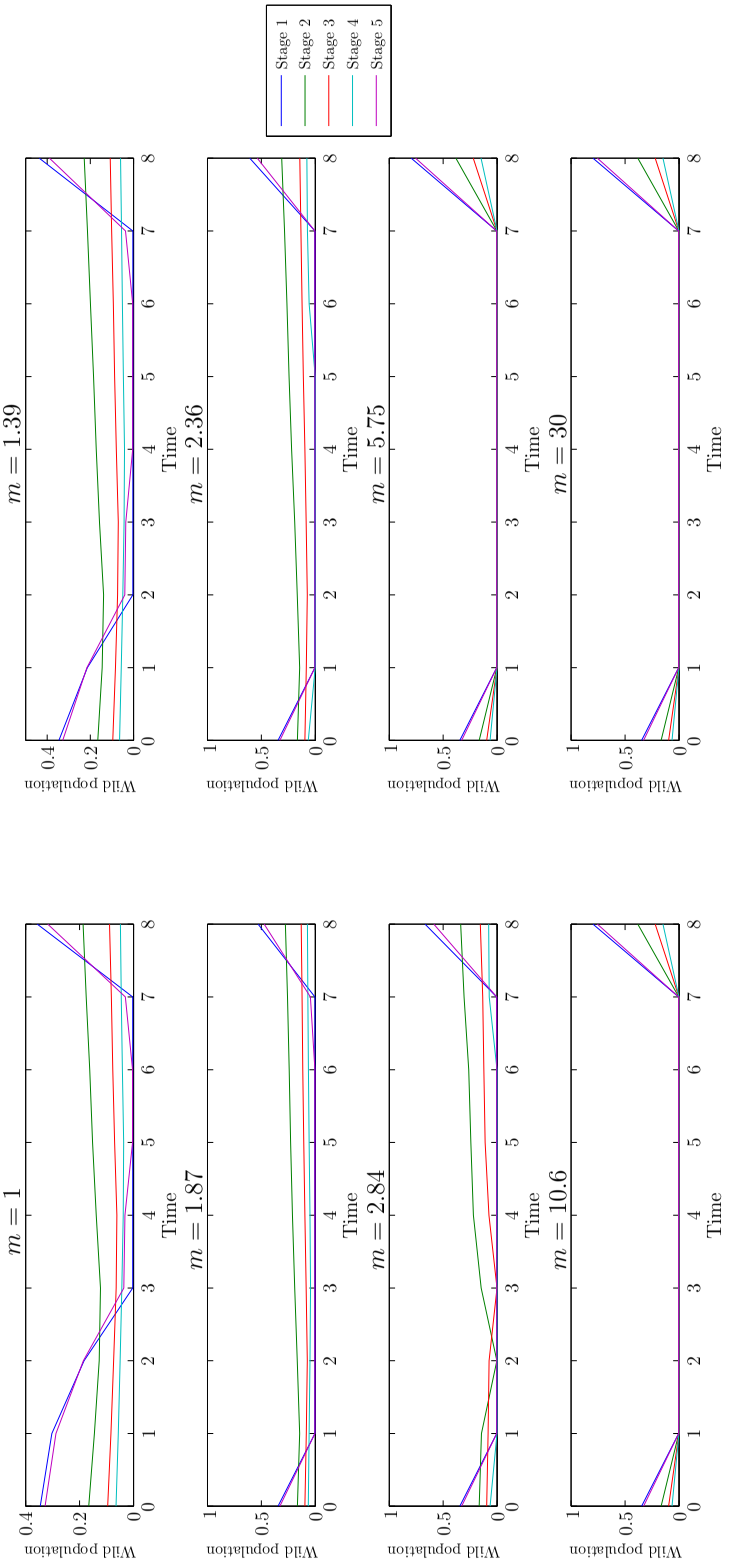

Figure 2.10: The wild population of *Asp viper* in each stage for 8 different levels of resource.

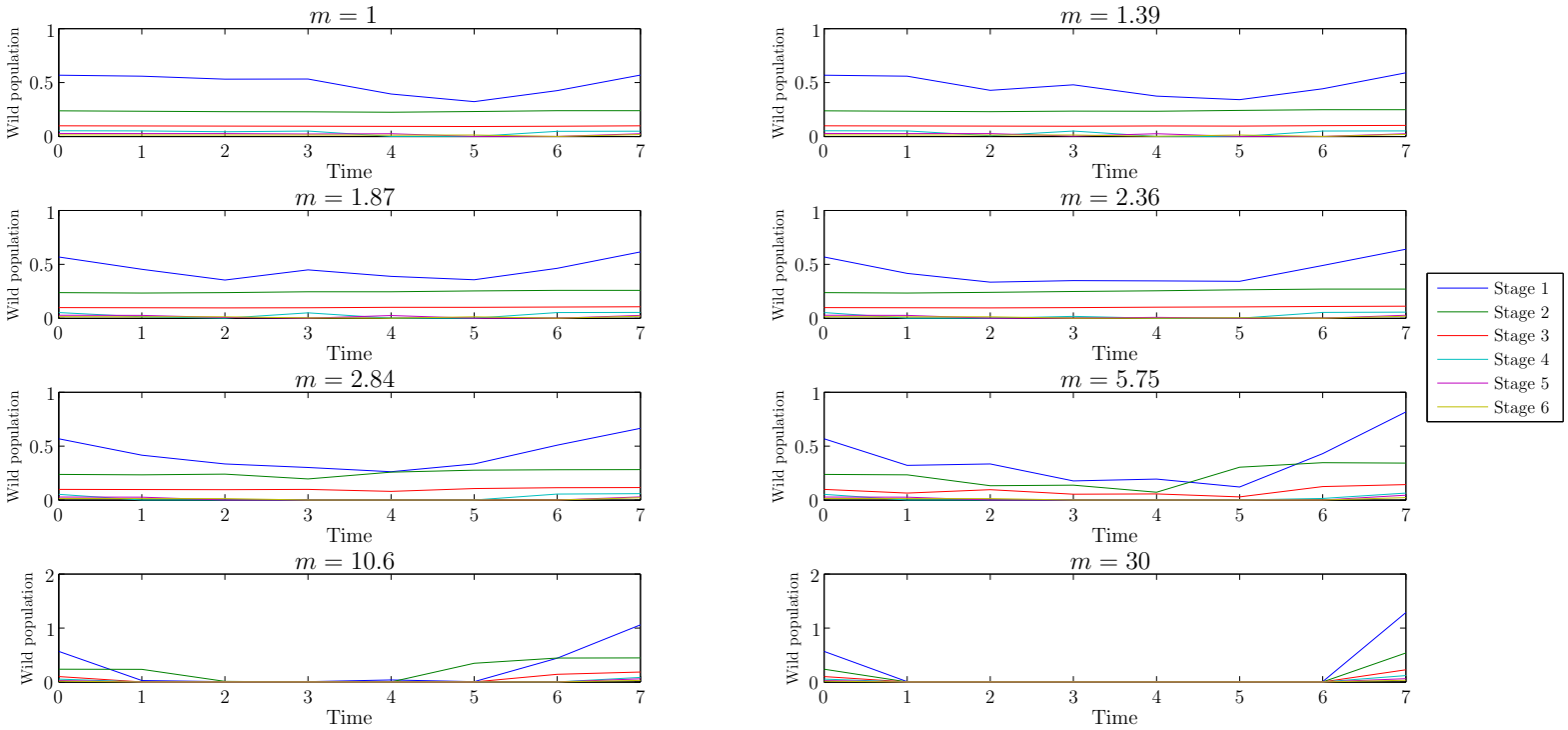

Figure 2.11: The wild population of *Coypu* in each stage for 8 different levels of resource.

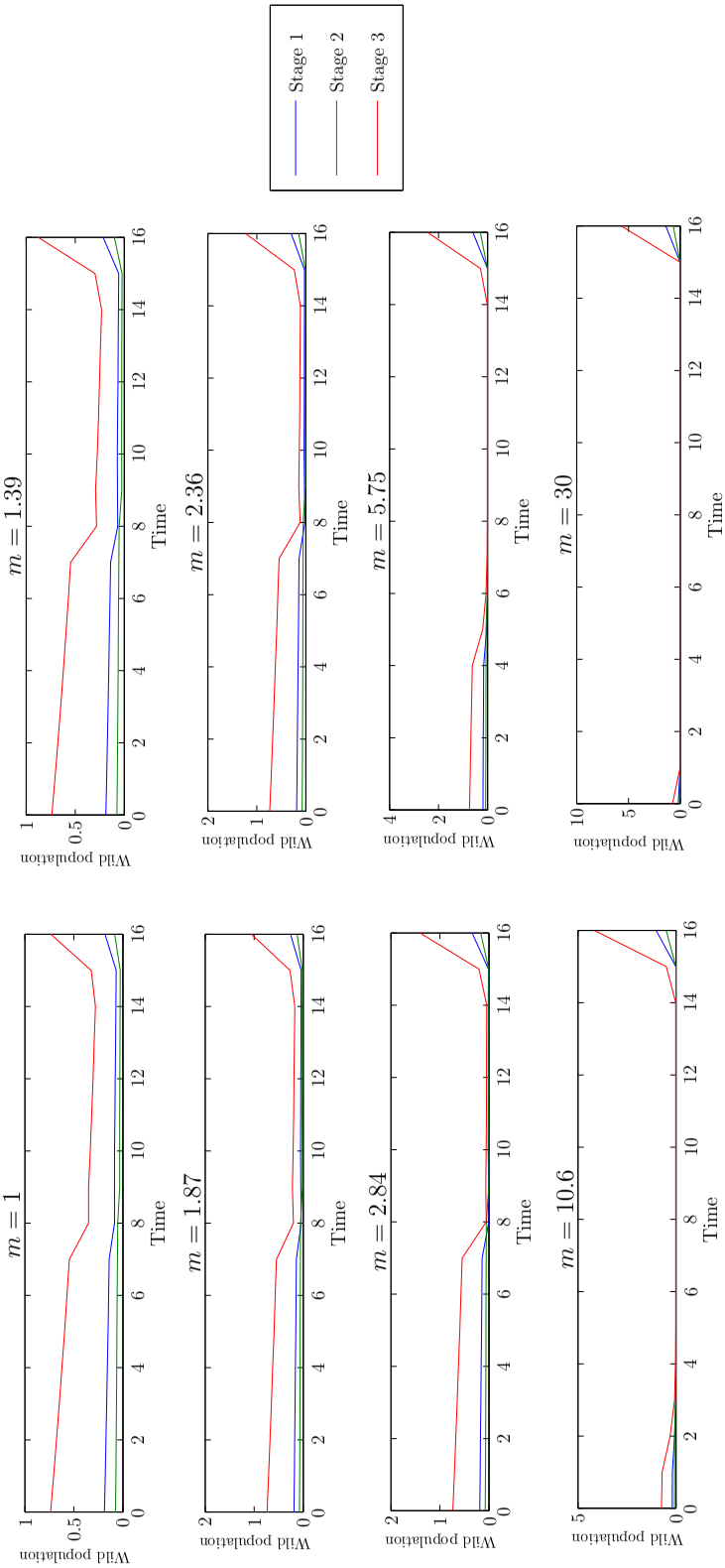

Figure 2.12: The wild population of *Spanish ibex* in each stage for 8 different levels of resource.

Finally, we consider the wild population of the *Capra pyrenaica* (Spanish ibex) for 8 choices of resource, in Figure 2.12. The PPM we use is for a 3 stage population and can be found in Appendix A1. It can be seen that only the third stage has production rate greater than one. Figure 2.12 shows that when the resource is high then, similar to the other examples, the optimal strategy keeps the wild population for $t = 1 \dots T-1$ as low as possible, which is the perfect zoo strategy. At medium levels of resource a trade-off occurs and the optimal strategy focuses on keeping stages 1 and 2 in captivity. This means that for medium levels of resource the strategy focuses on increasing the survival and is therefore a headstart strategy, which agrees with the classification seen in Figure 2.3.

2.6.4 Sink-sink population

In Sections 2.6.2 and 2.6.3 the captive population has been an increasing population and therefore if the resource is large enough then it is almost always possible to stablise the population. This section explores the possibility of being able to stablise a population with a decreasing captive population by utilizing transient dynamics. To be able to amplify a population using the transient dynamics then the population dynamics given by the two PPM's must be sufficiently different. If the two PPM's are very similar then no amount of translocation will allow growth of the total population, as moving between the populations won't change the dynamics.[1] Therefore, we can not calculate a captive PPM, D, in the same way as described in Section 2.2, so we use the COMPADRE III database to find two different PPM's for the same species in different locations. The species that we choose is *Tillandsia recurvata* [132] where the two PPMs are both in

[1]Note, that for asymptotic growth then the left eigenvectors of the two PPM's must be sufficiently different. Let M_1 and M_2 denote the two PPM's with dominant eigenvalue less than 1, and left eigenvectors v_1^T and v_2^T, respectively. Then for asymptotic growth we require $v_1^T M_2 \leq v_1^T$ and $v_2^T M_1 \leq v_2^T$.

decline, and are given by:

$$\mathcal{M}_1 = \begin{pmatrix} 0.56 & 0.1 & 0.09 & 0 \\ 0.23 & 0.69 & 0.31 & 0 \\ 0 & 0.21 & 0.55 & 0.22 \\ 0 & 0.02 & 0.1 & 0.56 \end{pmatrix}, \quad \mathcal{M}_2 = \begin{pmatrix} 0.64 & 0 & 0 & 0.11 \\ 0.21 & 0.42 & 0.19 & 0 \\ 0 & 0.42 & 0.63 & 0 \\ 0 & 0 & 0.19 & 0.96 \end{pmatrix}$$

with dominant eigenvalues $\lambda(\mathcal{M}_1) = 0.9665$ and $\lambda(\mathcal{M}_2) = 0.9985$, respectively.

We use our framework described in Section 2.2, which means that at $t = 0$ the entire population is in one location with the dynamics given by $\mathcal{M}_1$ or $\mathcal{M}_2$. This represents the "wild" population. Then the optimal strategy is able to move the population between the two locations, the original "wild" population and the other location which represents the "captive" population. The wild population is constrained such that in any stage class it is not smaller than w_0 which we choose to remain at 1% of x_0. The only parameter from the set up in Section 2.2 that we altered for the sink-sink model is the time that the optimal strategy runs for, which we choose to be $T \approx 10E$. Extending the time that the optimal strategy is calculated for gives the transient dynamics sufficient time to have an effect on the population dynamics.

So we need to decide which location represents the wild population, and firstly we choose M_1 as wild so $A = \mathcal{M}_1$ and M_2 as captive so $D = \mathcal{M}_2$. In this case the wild population is decreasing at a quicker rate than the captive population. Then we consider problem 1 where we maximise $\|x(T)\|_1$ given that the resource available is fixed. We choose the resource available to be 1000 times the minimum cost required to sustain the population, to simulate an unlimited resource, as it will not constrain the optimal strategy. Then the optimal control strategy gives the wild and captive population shown in Figure 2.13.

Figure 2.13 shows that although the individual dynamics of the wild and captive populations are declining, when a translocation strategy is able to move the population between the two dynamics it is possible to stabilise the population. This can be seen by calculating the wild population at time T and gives that $\|x(T)\|_1 \approx 1.15$, compared

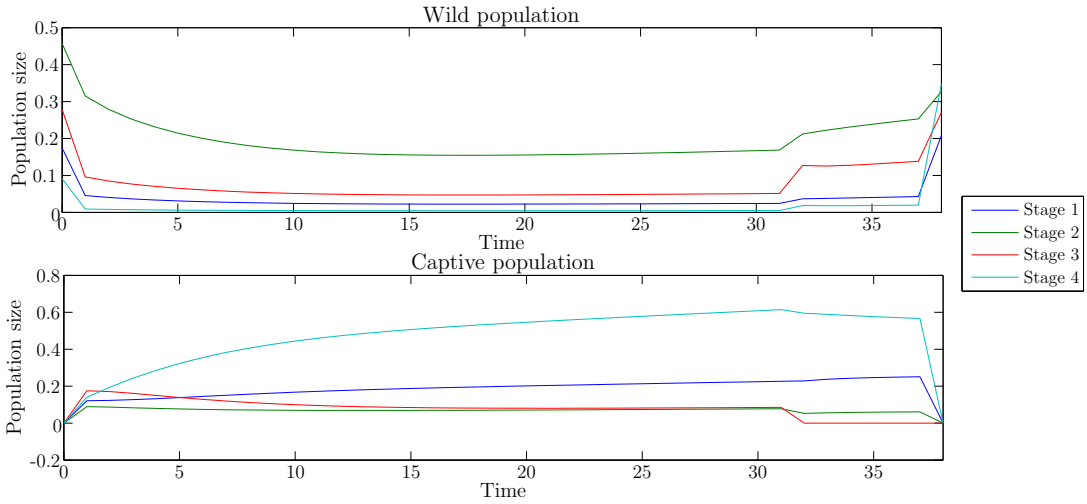

Figure 2.13: x and z populations for two declining PPM's where the optimisation maximises $\|x(T)\|_1$ given that the resource is 'unlimited'.

to $\|x_0\|_1 = 1$. Notice that the stage structure of the wild population at $t = 0$ and $t = T$ are substantially different. This is because the stable stage structure of the two PPM's are different, and therefore when the captive population is released the stage structure of the wild population is changed.

To analyse the optimal strategy that gives this resulting population we create two graphs. Firstly, Figure 2.14 which shows the net movement of each stage of the population from the wild to captivity at each time step. Secondly, Figure 2.15 shows the feedback strategy, which is the proportion of wild population which is moved into captivity at any given time. Figures 2.14 and 2.15 show that the optimal strategy removes stages 1, 3 and 4 from the wild and places them in captivity, once individuals in captivity reach the second stage class they are released into the wild. Figure 2.15 shows the feedback strategy, which is the proportion of the population available which is moved to and from captivity, it shows that nearly 100% of the wild population available in stage 1, 3 and 4 is moved into captivity. This suggests that in stages 1, 3 and 4 survival and reproduction of the captive population given by $\mathcal{M}_2$ is greater than those of the wild population given by $\mathcal{M}_1$. However, the survival and reproduction of stage class 2 is greater in the wild population. These observations are consistent with the vital rates in $\mathcal{M}_1$ and $\mathcal{M}_2$.

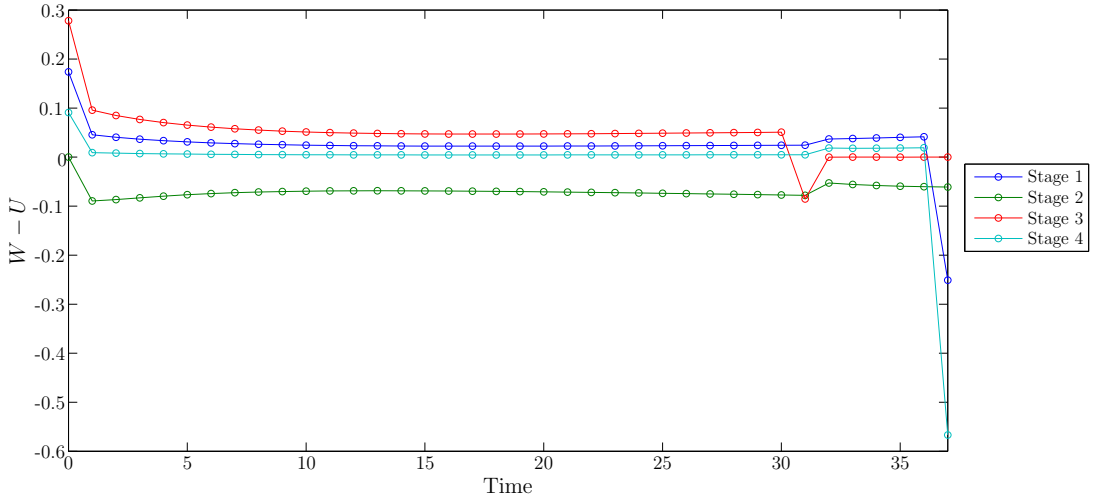

Figure 2.14: The net movement from x to z when the optimisation maximises $x(T)$ with 'unlimited' resource.

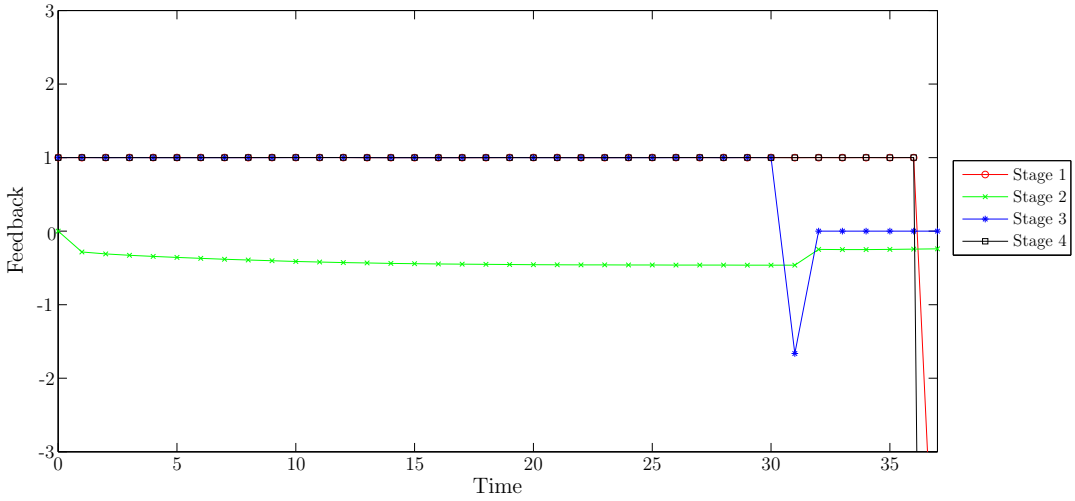

Figure 2.15: The feedback strategy, what proportion of the x population available was moved in each stage at any given time, when the optimisation maximises $x(T)$ with 'unlimited' resource.

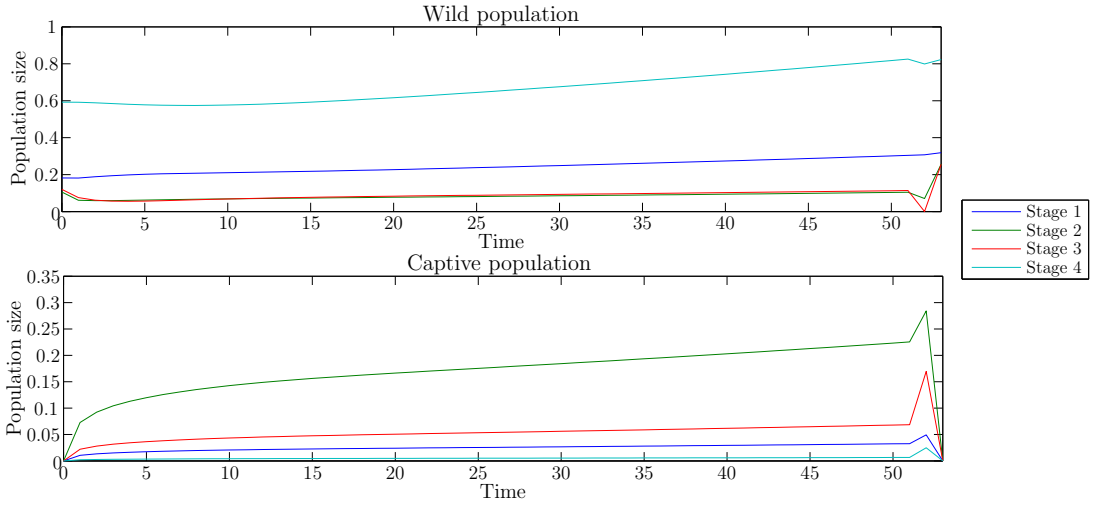

Figure 2.16: x and z populations for two declining PPM's where the optimisation maximises $\|x(T)\|_1$ given 'unlimited' resource.

Next, we consider the situation where the roles of the PPMs are reversed, such that $A = \mathcal{M}_2$ and $D = \mathcal{M}_1$. This means that A has dominant eigenvalue 0.9985, whilst the eigenvalue of D is 0.9665. So in the absence of translocation, the wild population is only declining at a slow rate, and the captive population is declining at a faster rate. Then we solve the same problem as described above by maximising $\|x(T)\|_1$ given that the resource is large enough that it does not constrain the optimal strategy, and $T \approx 10E$. Figure 2.16 shows the resulting wild and captive populations. As can be seen in Figure 2.16, it is possible to maintain this declining wild population by using a captive population which is declining at an even faster rate, in fact it shows that $\|x(T)\|_1 \approx 1.65$. As the original population was scaled such that $\|x_0\|_1 = 1$ then the wild population has been sustainably amplified. Finally, we plot the net movement and feedback for the optimal strategy in Figures 2.17 and 2.18. Unsurprisingly, the general trend of the translocation strategy is the opposite to that shown in Figures 2.14 and 2.15. This is because the optimal strategy now focuses on keeping stages 1, 3 and 4 in the wild and stage 2 in captivity, where the survival is greater.

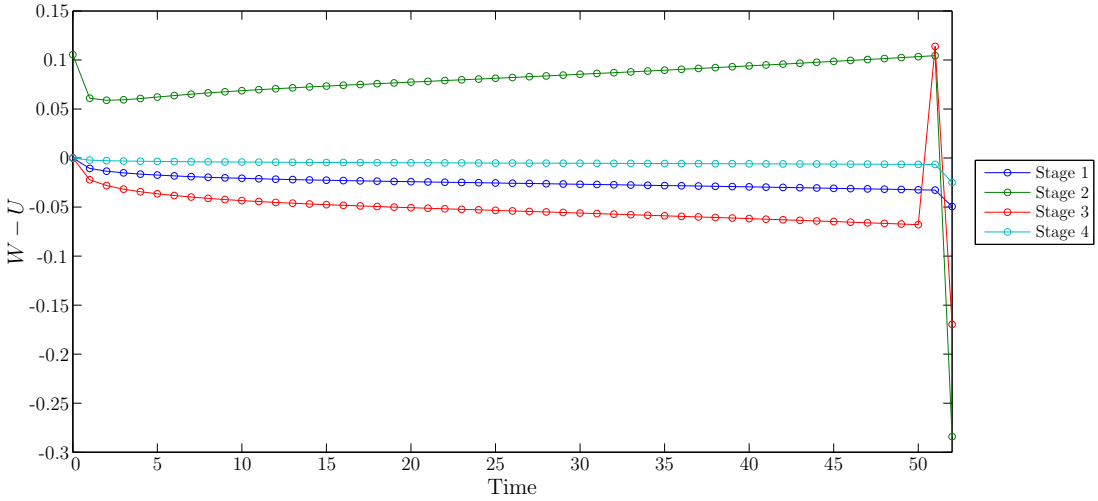

Figure 2.17: The net movement from x to z when the optimisation maximises $x(T)$ with 'unlimited' resource.

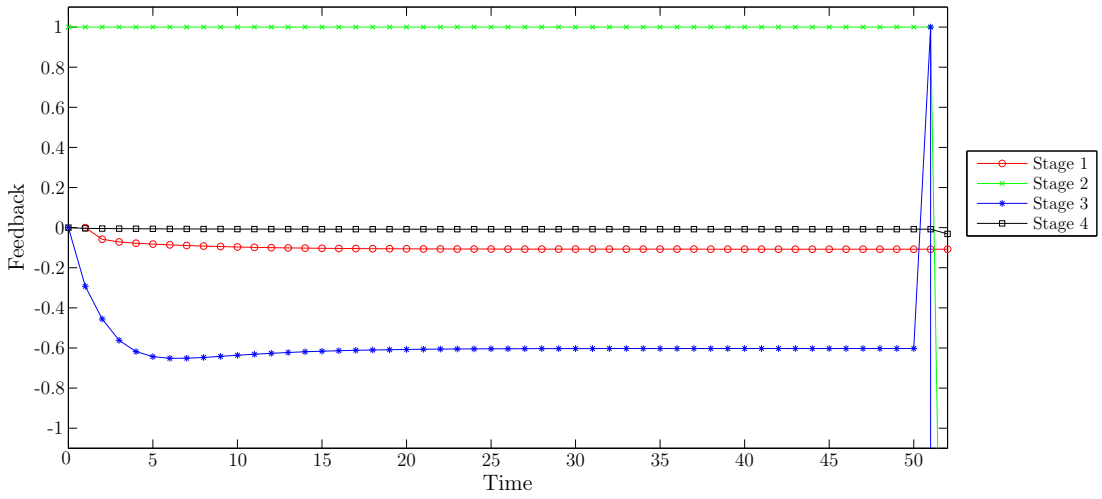

Figure 2.18: The feedback strategy, what proportion of the x population available was moved in each stage at any given time, when the optimisation maximises $x(T)$ with 'unlimited' resource.

2.7 Conclusion

We have used linear programming to find optimal translocation strategies to maximise a declining wild population, by being able to place some of the wild population in captivity. This optimal strategy was calculated for a range of available resource, and then the optimal strategy was classified depending on which stages were moved into captivity. We found optimal strategies for 31 animal PPM's and 983 plant PPM's. When the resource available is limited then a trade-off occurs between maximising the population and the cost this requires. When this trade-off occurs the optimal strategy for some species targets particular stages. This is similar to the results given by Hastings et al. [52], who find that when controlling the invasive weed *Spartina alternifora*, the optimal strategy targets particular stages.

To examine the 983 optimal strategies for the plants we grouped the species by growth type. This allowed us to find general trends in the optimal strategy for some growth types. For example, in general the optimal strategy for epiphyte's favour the stages with production rate greater than 1, whereas the optimal strategies for annuals do not favour any particular stage.

When the resource is limited and the optimal strategy targets particular stages this affects the fitness of $x(T)$. However, when the resource is higher and the optimal strategy is able to keep most of the population in captivity then the fitness of $x(T)$ remains unchanged, as the stable stage structure of captive and wild population is the same.

Finally, we explored a sink-sink population, and we found that using our framework we were able to stabilise two declining populations. This is possible because the optimal removal strategy can exploit the transient dynamics.

Chapter 3

Managing invasive species affected by disturbance: A linear programming approach

3.1 Background

As discussed in Chapters 1 and 2, there are many uses for dynamic programming in ecology. In particular dynamic programming can be used to create control or management strategies, either to help sustain an endangered population, as studied in Chapter 2, or to reduce an invading population.

Hastings et al. [53] use linear programming to find optimal control strategies for an invasive species, *Spartina alternifora*, in Willapa Bay. They use a discrete-time, three-stage structured model, where the population dynamics are given by

$$N_{t+1} = L(N_t - H_{t+1}). \tag{3.1}$$

Here L is a population projection matrix (PPM) containing the vital rates of *Spartina alternifora*, and at time t, N_t is the stage structured population whilst H_t is the optimal removal strategy to be found using linear programming. The linear programming problem is constrained such that:

- removal at time t in stage i is non-negative for all $t \in [1, \ldots, T]$ and $i \in [1, 2, 3]$;
- for any time t the removal strategy in stage i cannot remove more than is present;
- the resource available for removal at any time step T is limited.

Given these three constraints Hastings et al. [53] consider two objective functions to firstly, minimise the total population at a final time step T, given by $\|N_T\|_1$, and to secondly, minimise the total cost required to eradicate the invasive species by time T. They find that when the resource available is limited then the optimal control strategy, H, targets particular stages. They use a model where the invasive population at $t = 0$ is at low density, but the dominant eigenvalue of L is greater than one. In this case, a control strategy is needed to prevent the population increasing.

Motivated by the Hastings et al. study, we consider an invasive population that is subject to an external additive disturbance, for example due to immigration from a second remote population. We append the population projection matrix with an additional term to capture the disturbance. So in this case the model becomes

$$x_{t+1} = A(x_t - Bu_t + Dd_t), \tag{3.2}$$

where x_t is the stage structured population at time t, A is a PMM, u_t and d_t are the removal and disturbance at time t[1]. Notice that we have also introduced both stage structured management or control through the term Bu_t and stage structured disturbance through the term Dd_t. For example, $B = [0\ 1\ 0]^T$ will correspond to management (i.e. removal) of the invasive species in stage 2, whilst $D = [0\ 0\ 1]^T$ corresponds to immigration of the invasive species into stage 3. The aim of the management strategy is to find u which minimises the total population at time T in the face of a disturbance which maximises the population. This leads to problems of minimax or maximin type, which we will formulate later. But first, we emphasise that these minimax and maximin problems need not result in the same value of the objective, in this case population abundance at time T. To illustrate this we consider a simplified ecological example

[1]Note, this change of notation allows consistency with control notation.

where both removal and disturbance act at a single time step and calculate $\|x_T\|_1$. We use a 3-stage discrete-time population model given by equation (3.2), where

$$A = \begin{pmatrix} 0.5499 & 0.6221 & 0.4018 \\ 0.1450 & 0.3510 & 0.0760 \\ 0.8530 & 0.5132 & 0.2399 \end{pmatrix} \quad B = \begin{pmatrix} 0 \\ 0 \\ 1 \end{pmatrix} \quad \text{and} \quad D = \begin{pmatrix} 1 \\ 0 \\ 0 \end{pmatrix}.$$

Here we remove from stage class 3 and disturb into stage class 1. As both the disturbance and removal only act in a single time step, u_t and d_t are non-zero only at a single entry. We choose $T = 5$ and the initial population to be

$$x_0 = \begin{pmatrix} 0.1233 \\ 0.1839 \\ 0.2400 \end{pmatrix}.$$

Note that removal u is restricted such that it cannot remove more than the population in the third stage. We allow removal and disturbance to act in single time step, so $u = [u_0, u_1, \ldots u_4]$ and $d = [d_0, d_1, \ldots d_4]$ can take 5 possible values. Considering all possible choices of u and d, and calculating the corresponding $\|x_T\|_1$ gives

		Remove only at time				
		0	1	2	3	4
Disturb only at time	0	3.5019	2.6345	2.8033	2.9292	3.1186
	1	3.1367	3.1621	2.4381	2.5641	2.7534
	2	2.8270	2.8524	2.7988	2.2544	2.4438
	3	2.5403	2.5657	2.5121	2.5070	2.1570
	4	2.4093	2.4347	2.3811	2.3760	2.4047

Table 3.1: $\|x_T\|_1$ for each choice of h and d.

Firstly, the $\min_h(\max_d(\|x_T\|_1))$ problem is equivalent to a control manager modelling all possible removal strategies, u, given that the resource available for removal is limited. Assuming that the control manager knows the total disturbance is bounded then for each of these control strategies they could calculate the disturbance, d, which maximises $\|x_T(u, d)\|_1$. Then the control manager may want to prevent the worst case scenario, in

which case they pick the (u, d) pair which minimises $\|x_T(u, d)\|_1$. This is illustrated below where we calculate the $\min_u(\max_d(\|x_T\|_1))$ by maximising over d to give the coloured values in Table 3.2, then minimising over u gives that $\min_u(\max_d(\|x_T\|_1)) = 2.8033$.

		Remove only at time				
Disturb only at time		0	1	2	3	4
	0	3.5019	2.6345	**2.8033**	2.9292	3.1186
	1	3.1367	3.1621	2.4381	2.5641	2.7534
	2	2.8270	2.8524	2.7988	2.2544	2.4438
	3	2.5403	2.5657	2.5121	2.5070	2.1570
	4	2.4093	2.4347	2.3811	2.3760	2.4047

Table 3.2: $\min_u(\max_d(x_T))$ for all discrete choices of (u, d).

Secondly, the $\max_d(\min_u(\|x_T\|_1))$ problem is equivalent to the control manager considering all possible d and calculating the removal strategy, u, such that x_T is minimised. This will give a range of $\|x_T(h, d)\|_1$, the control manager then assumes the disturbance will maximise $\|x_T(u, d)\|_1$, and so chooses the corresponding u. Finally, the disturbance acts to maximise $\|x_T(u, d)\|_1$. Calculating the $\max_d(\min_u(\|x_T\|_1))$ by minimising over u to give the coloured cells in Table 3.3, then maximising these values over d gives $\max_d(\min_u(\|x_T\|_1)) = 2.645$.

		Remove only at time				
Disturb only at time		0	1	2	3	4
	0	3.5019	**2.6345**	2.8033	2.9292	3.1186
	1	3.1367	3.1621	2.4381	2.5641	2.7534
	2	2.8270	2.8524	2.7988	2.2544	2.4438
	3	2.5403	2.5657	2.5121	2.5070	2.1570
	4	2.4093	2.4347	2.3811	2.3760	2.4047

Table 3.3: $\max_d(\min_u(x_T))$ for all discrete choices of (u, d).

Therefore, it can be seen in this very simple ecological example that the maximin $\neq$ minimax. Furthermore, in general maximin $\leq$ minimax [87] which means that for a disturbed population with a optimal removal strategy a lower final population can be achieved if the worst disturbance is known and then the optimal removal strategy acts.

In this chapter we explore the use of linear programming in managing populations affected by additive disturbances. Firstly, we consider a sinusoidal disturbance, with fixed magnitude, to explore the simple effect of frequency dependent disturbance on the final population. Secondly, we study the $\max_d(\min_u(\|x_T\|_1))$ and $\min_u(\max_d(\|x_T\|_1))$ problems for a higher dimensional problem where the optimal solutions form a continuum. We find the worst case that $\|x_T\|_1$ could be, given that the disturbance can act before or after the optimal strategy is decided. This chapter is structured as follows, Section 3.2 states the population model and the linear programming constraints and objective function. Section 3.2 also gives the results for the different types of disturbance, then these results are discussed in Section 3.3. Finally, we summarise the results in Section 3.4.

3.2 Linear programming for a disturbed population

We use a framework similar to that established by Hastings et al. [53], but also include an additive disturbance. The discrete-time population model, equivalent to equation (3.2), is presented again for ease of reading:

$$x_{t+1} = A(x_t - Bu_t + Dd_t), \tag{3.3}$$

where $x_t \in \mathbf{R}^n$ is the stage structured population at time t, $u_t \in \mathbf{R}^n$ is the optimal control strategy to be found, $d_t \in \mathbf{R}^n$ is the stage structured disturbance at time t. As in the simple model given by equation (3.2), B and D determine the stages in which removal and disturbance act, respectively.

We aim to use linear programming to minimise the total population at time T, which is given by

$$\|x_{_T}\|_1 = \|A^T x_0 - \sum_{i=1}^{T} A^{T+1-i} B u_{i-1} + \sum_{i=1}^{T} A^{T+1-i} D d_{i-1}\|_1 \tag{3.4}$$

$$= \mathbb{1}\left(A^T x_0 - \sum_{i=1}^{T} A^{T+1-i} B u_{i-1} + \sum_{i=1}^{T} A^{T+1-i} D d_{i-1}\right). \tag{3.5}$$

Note that for a positive vector $\|\cdot\|_1$ is equivalent to multiplying by a vector of ones. First, we create the objective function and constraints for a given fixed d. For fixed d, $\mathbb{1}A^T x_0$ and $\mathbb{1}\sum_{i=1}^{T} A^{T+1-i} D d_{i-1}$ are constants. So our objective function for minimizing $\|x_{_T}\|_1$ becomes simply

$$\max_u \left(\mathbb{1}\sum_{i=1}^{T} A^{T+1-i} B u_{i-1}\right).$$

Note, as the removal term in equation (3.4) is negative then by changing the sign of this term the minimisation problem becomes a maximisation problem. The constraints imposed on this minimisation problem are similar to those used in [53]. However, with the addition of disturbance in our model the constraints depend on d, and can be formulated as follows.

(I) It is not possible to have a negative population, which means that the removal strategy is restricted by the size of the population in each stage. Clearly the size of the population given by equation (3.3) is dependent on the disturbance, therefore so is the constraint on the maximum that can be removed at any given time t. The population must be non-negative at each time step for all $t = [1...T]$, i.e. $x_{t+1} \geq 0$. As the population must also remain positive before the biology imposed by A then $x_t - Bu_t + Dd_t \geq 0$. Therefore for all $s = [1, \ldots, T]$ we require that

$$\sum_{t=1}^{s} A^{s-t} B u_{t-1} \leq A^{s-1} x_0 + \sum_{t=1}^{s} A^{s-t} D d_{t-1}. \tag{3.6}$$

(II) The removal strategy is also constrained by the resource available. In [53] the resource is constrained at each time step. However we use a different constraint such that the total resource spent on removal by time T is less than or equal to $C \times T$. Writing this constraint in terms of our parameters gives that

$$\sum_{i=1}^{T}\sum_{j=1}^{n} c_j u_{i-1} \leq C \times T. \tag{3.7}$$

where $c_1\ c_n \cdots c$ reflects different levels of resource required in each stage which we choose to be a vector of ones.

(III) The removal strategy must be non negative in each stage class for all time steps. Therefore the third constraint on the removal strategy is given by

$$u_{i-1} \geq 0 \tag{3.8}$$

for all $i \in [1, \ldots, T]$.

This objective function and constraints can be written in matrix from as follows. Let $\mathcal{A}_B = [A^T B\ A^{T-1}B \cdots AB]$ and

$$u = \begin{bmatrix} u_0 \\ u_1 \\ \vdots \\ u_{T-1} \end{bmatrix}.$$

Then the objective function with a fixed disturbance becomes

$$\max_u(\mathbb{1}\mathcal{A}_B u). \tag{3.9}$$

To rewrite the non-negative population constraint, given by equation (3.6), first define the matrices

$$\bar{\mathcal{B}} = \begin{pmatrix} B & 0 & \cdots & 0 \\ AB & B & \cdots & 0 \\ \vdots & \vdots & \ddots & \vdots \\ A^{T-1}B & A^{T-2}B & \cdots & B \end{pmatrix} \quad \mathcal{X} = \begin{pmatrix} x_0 \\ Lx_0 \\ \vdots \\ L^{T-1}x_0 \end{pmatrix}$$

and

$$\bar{\mathcal{D}} = \begin{pmatrix} D & 0 & \cdots & 0 \\ AD & D & \cdots & 0 \\ \vdots & \vdots & \ddots & \vdots \\ A^{T-1}D & A^{T-2}D & \cdots & D \end{pmatrix} \quad d = \begin{pmatrix} d_0 \\ d_1 \\ \vdots \\ d_{T-1} \end{pmatrix}.$$

Then the non-negative population constraint (3.6) can be written as

$$\bar{\mathcal{B}}u \leq \mathcal{X} + \bar{\mathcal{D}}d. \tag{3.10}$$

Now the constraint given in equation (3.7) that the total cost used for removal is bounded becomes

$$\mathbb{1}u \leq C \times T.$$

Finally, the constraint in equation (3.8), that the removal must be non-negative, becomes

$$u \geq 0.$$

Then for the parameters defined as follows and a fixed disturbance we consider the objective function given in equation (3.9), subject to constraints on removal (3.8), non-negative population (3.10) and resource (3.7). We choose two 4 stage structured models where the parameters in equation (3.3) are given by

$$A_1 = \begin{pmatrix} 0 & 0.75 & 6.36 & 15460 \\ 0.049 & 0 & 0 & 0 \\ 0 & 0.15 & 0 & 0 \\ 0 & 0 & 0.0053 & 0 \end{pmatrix} \text{ or } A_2 = \begin{pmatrix} 0.5675 & 1.1938 & 10.1202 & 8.5392 \\ 0.0779 & 0 & 0 & 0 \\ 0 & 0.2335 & 0 & 0 \\ 0 & 0 & 0.0084 & 0 \end{pmatrix}$$

$$\text{and } x_0 = \begin{pmatrix} 1 \\ 1 \\ 1 \\ 1 \end{pmatrix}.$$

Throughout this chapter $B \in \mathbf{R}^4$ and $D \in \mathbf{R}^4$ are vectors of zeros expect one in a single entry, and d_t is defined in the following sub-sections. As B and D only have one non-zero component the disturbance and removal acts in a single stage class, which simplifies the problem to a great extent. Note, the dominant eigenvalues of both A_1 and A_2 are equal to 0.9, so without disturbance the corresponding populations are decreasing. However with the addition of disturbance the population density may be increasing and therefore it is important to control the population.

Remark. *Hastings et al. [53] consider an invading population and therefore the dominant eigenvalue of their PPM is greater than one. As we are exploring the effect disturbances have on the population we do not want the population to grow asymptotically, as this behaviour may dominate the dynamics obscuring the effect of disturbance.*

3.2.1 Sinusoidal disturbance

First, consider a cyclical disturbance which could represent seasonal migration or fluctuations in a population. We choose the sinusoidal disturbance such that $d_t = \delta(1 + \sin(\theta t))$, where δ and θ determine the magnitude and frequency, respectively. We use $(1 + \sin(\theta t))$ so that the disturbance is cyclical but always positive, as we require the disturbance to be additive to ensure that population remains positive. Then for different choices of θ we use our linear programming framework to find the optimal strategy which minimises $\|x_T\|_1$. We choose θ such that for each choice of θ, $\sin(\theta T)$ has the same value, so that the disturbance at the final time step has the same effect on $\|x_T\|_1$. Therefore

$$\theta = \frac{(k + \frac{1}{4})\pi}{T}, \quad \text{where} \quad k = [1, \ldots, \frac{T}{2}].$$

So for each choice of θ, then $\sin(\theta T) = \sin((k + \frac{1}{4})\pi) = \sin(\frac{\pi}{4})$.

For a fixed sinusoidal disturbance, if the resource available for removal is very small then u_t must be very small for $t = [0, \ldots, T-1]$, and therefore the resulting population can be approximated by the system with no removal, so forms an upper bound on $\|x_T\|_1$. As the disturbance is sinusoidal, we can use the system's transfer function mapping $d \to x$ to approximate $\|x_T\|_1$, as discussed below in $\langle 1 \rangle$. Similarly, if the resource available for removal is large enough it will not constrain how much is removed at each time step. In this case, the optimal strategy will remove as much of the population as possible. This can be approximated by a feedback control, discussed below in $\langle 2 \rangle$, and forms a lower bound for the resulting $\|x_T\|_1$.

$\langle 1 \rangle$ ***Upper bound on*** $\|x_T\|_1$ ***using transfer functions***

As the disturbance is sinusoidal we can use transfer functions for the system given by equation (3.3) to approximate $\|x_T\|_1$ if no removal occurs. When there is no removal, then the model given by equation (3.3) becomes

$$x_{t+1} = L(x_t + Dd_t) \qquad \text{where} \qquad d_t = \delta(1 + \sin(\theta t)).$$

This means that

$$\begin{aligned}\|x_T\|_1 &= \mathbb{1}A^T x_0 + \delta \mathbb{1}A\sum_{j=0}^{T-1} A^j D + \delta \mathbb{1}A\sum_{j=0}^{T-1} A^{T-1-j} D\sin(\theta j).\\ &= \mathbb{1}A^T x_0 + \delta \mathbb{1}A\sum_{j=0}^{T-1} A^j D + \delta \mathbb{1}A \times \mathrm{Im}\left(\sum_{j=0}^{T-1} A^{T-1-j} D\mathrm{e}^{ij\theta}\right)\\ &= \mathbb{1}A^T x_0 + \delta \mathbb{1}A\sum_{j=0}^{T-1} A^j D + \delta \mathbb{1}A \times \mathrm{Im}\left(A^{T-1} D\sum_{j=0}^{T-1}[A^{-1} D\mathrm{e}^{i\theta}]^j\right).\end{aligned}$$

Using geometric progression then this becomes

$$\begin{aligned}\|x_T\|_1 &= \mathbb{1}A^T x_0 + \delta \mathbb{1}A(I-A^T)(I-A)^{-1}D\\ &\qquad + \delta \mathbb{1}A \times \mathrm{Im}\left(A^{T-1}D(I-A^{-T}\mathrm{e}^{iT\theta})(I-A^{-1}\mathrm{e}^{i\theta})^{-1}\right)\\ &= \mathbb{1}A^T x_0 + \delta \mathbb{1}A(I-A^T)(I-A)^{-1}D\\ &\qquad + \delta \mathbb{1}A \times \mathrm{Im}\left((A^T D - D\mathrm{e}^{iT\theta})(A-e^{i\theta}I)^{-1}\right)\\ &= \mathbb{1}A^T x_0 + \delta \mathbb{1}A(I-A^T)(I-A)^{-1}D\\ &\qquad + \delta \mathbb{1}A \times \mathrm{Im}\left((-A^T D + D\mathrm{e}^{iT\theta})(-A+e^{i\theta}I)^{-1}\right)\end{aligned}$$

Assuming that $T >> 1$, then as A is a decreasing matrix $A^T \to 0$ so

$$\|x_T\|_1 \approx \mathbb{1}A^T x_0 + \delta \mathbb{1}A(I-A)^{-1}D + \delta \mathbb{1}A \times \mathrm{Im}\left(D\mathrm{e}^{iT\theta}(-A+e^{i\theta}I)^{-1}\right).$$

Let $G(z) = \mathbb{1}A(zI-A)^{-1}D$ then

$$\|x_T\|_1 \approx \mathbb{1}A^T x_0 + \delta \mathbb{1}A(I-A)^{-1}D + \delta \times \mathrm{Im}(G(\mathrm{e}^{i\theta})\mathrm{e}^{iT\theta}),$$

so

$$\|x_T\|_1 \approx \mathbb{1}A^T x_0 + \delta \mathbb{1}A(I-A)^{-1}D + \delta|G(e^{i\theta})|\sin(\theta T + arg G(e^{i\theta})). \tag{3.11}$$

As this is an approximation of the population without any removal it forms an upper bound for $\|x_T\|_1$ with removal.

⟨2⟩***Lower bound on*** $\|x_T\|_1$ ***using feedback controller***

A lower bound for $\|x_T\|_1$ can be approximated by using a feedback controller. This means that each time step as much of the population as possible is removed. Assuming removal occurs in the j-th stage, then while ensuring the population remains positive the most the removal strategy can remove is

$$u_t = e_j x_t + e_j D d_t,$$

where $e_j \in \mathbf{R}^n$ is zeros except 1 in the j-th entry. This gives a similar optimal removal strategy as when the resource available is unlimited. Therefore using equation (3.2), as the disturbance is known, we use the feedback strategy to approximate $\|x_T\|_1$ when the resource is unlimited. This forms a lower bound for $\|x_T\|_1$.

We calculate the optimal removal strategy for 3 choices of resource, high and low to simulate unlimited resource and no removal, respectively. The third choice of resource is intermediate. For each choice of B and D, plotting $\|x_T\|_1$ resulting from the optimal removal strategy against θ, for the two PPMs (A_1 and A_2), gives Figures 3.1 and 3.2, respectively.

3.2.2 $\min_u(\max_d(\|x_T\|_1))$ and $\max_d(\min_u(\|x_T\|_1))$

In the previous section, we assumed a fixed sinusoidal disturbance. Such periodic disturbances could capture seasonal immigration. However, more realistically the disturbance itself would be unknown. One approach might be to assume a stochastic model for the unknown disturbance. In this case, population abundance is then a random variable influenced by the control, i.e. removal, term u_t. Minimising $\|x_T\|_1$ can then be formulated using stochastic dynamic programming (SDP), [112]. However, capturing constraints in SDP is challenging. An alternative is to assume a worst-case approach so that the disturbance term is acting to maximise $\|x_T\|_1$. This leads to an optimisation problem where the removal is trying to minimise $\|x_T\|_1$, whilst the disturbance is trying to maximise $\|x_T\|_1$. As discussed above, depending on whether

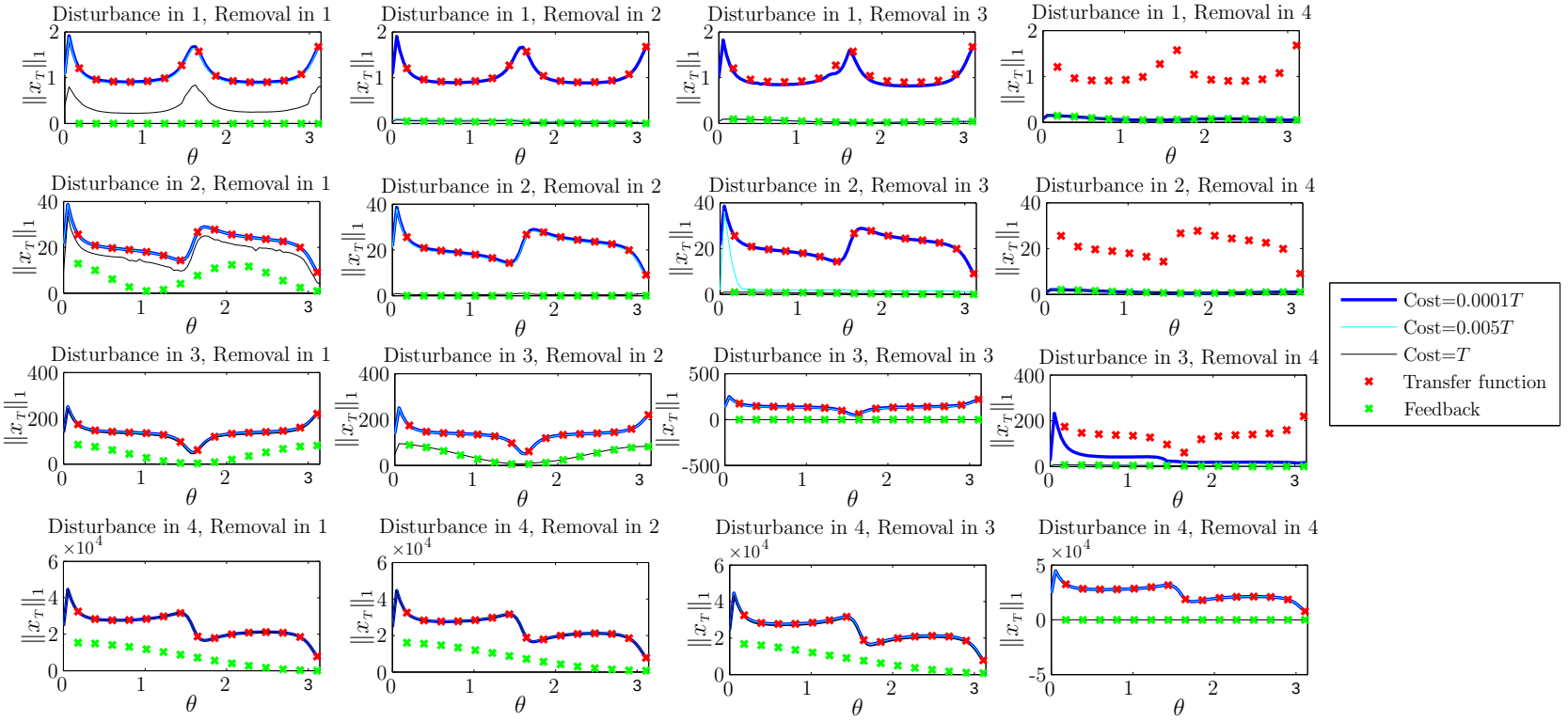

Figure 3.1: For A_1, the effect of sinusoidal disturbance with different θ on final population $\|x_T\|_1$ given that optimal removal strategy occurs.

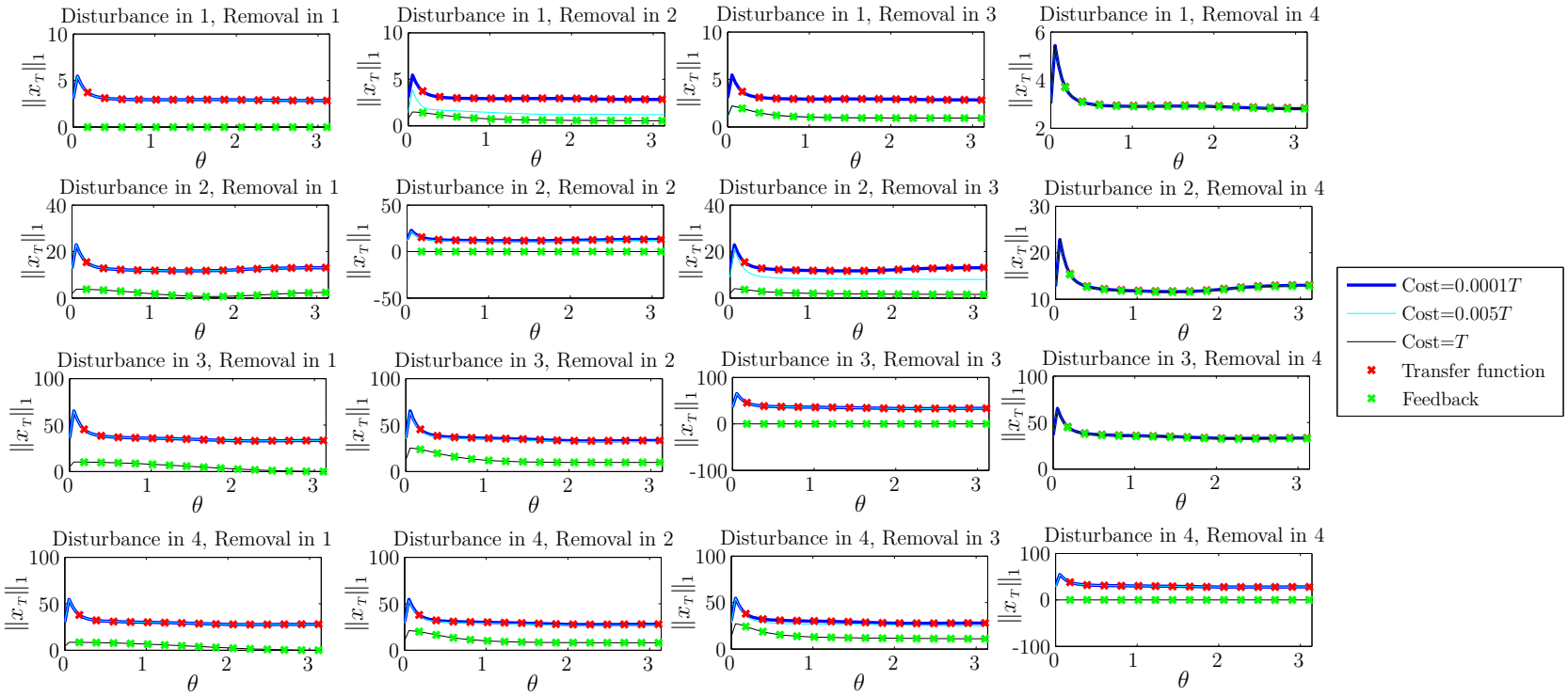

Figure 3.2: For A_2 the effect of sinusoidal disturbance with different θ on final population $\|x_T\|_1$ given that optimal removal strategy occurs.

the removal or disturbance the solutions may be different therefore we must consider the minimax and maximin problems separately.

To consider the minimax and maximin problems, in addition to the constraints given by equations (3.7), (3.10) and (3.8), two extra constraints are required for d. These constraints are such the disturbance in each stage and time step is non-negative so

$$d_i \geq 0, \tag{3.12}$$

for all $i \in [1 \dots T]$. Also, the total disturbance (e.g. a total source of migrants) from $t = 0$ to $t = T$ is bounded by a fixed constant, denoted Δ. That is

$$\|d\|_1 \leq \Delta. \tag{3.13}$$

First, we consider the $\max_d(\min_u(\|x_T\|_1))$ problem. As d is no longer fixed, the objective function must be dependent on d. Using the notation defined in Section 3.2 with the additional notation that

$$\mathcal{A}_D = [A^T D \; A^{T-1} D \cdots AD],$$

then equation (3.4) gives the objective function to be $-\mathcal{A}_B u + \mathcal{A}_D d$. We use `Linprog` to minimise over u, which creates a function ϕ_d of d, and can be written as

$$\phi_d = \begin{cases} \min_u \mathbb{1}(-\mathcal{A}_B u + \mathcal{A}_D d) \\ \text{subject to:} \quad \bar{\mathcal{B}} u \leq \mathcal{X} + \bar{\mathcal{D}} d \\ \qquad\qquad\quad \hat{c} u \leq C \times T \\ \qquad\qquad\quad h \geq 0. \end{cases}$$

We create ϕ_d as a function in Matlab with argument d. We then use `fmincon` to choose D to maximise ϕ_d

$$\begin{aligned} &\max_d(\phi_d) \\ \text{subject to:} \quad &0 \leq d \\ &[1 \; 1 \dots 1] d \leq \Delta. \end{aligned}$$

For $A = A_2$ and each choice of B and D, we calculate the $\max_d \min_u(\|x_T\|_1)$ for 4 choices of Δ and plot d, u and x_t to get Figures 3.3, 3.4, 3.5 and 3.6 for disturbance into stages 1, 2, 3 and 4, respectively.

Secondly, we explore the $\min_u(\max_d(\|x_T\|_1))$ problem, which can be written in the following way. First using `Linprog` we maximise over d to obtain a function of u, such that

$$\phi_u = \begin{cases} \max_d \mathbb{1}(-\mathcal{A}_B u + \mathcal{A}_D d) \\ \text{subject to:} \quad \bar{\mathcal{B}} u \leq \mathcal{X} + \bar{\mathcal{D}} d \\ \qquad\qquad\quad 0 \leq d \\ \qquad\qquad\quad [1\ 1 \ldots 1] d \leq \Delta. \end{cases}$$

Then we use `fmincon` to choose u to minimise ϕ_u subject to the constraints that the total cost of removal is limited and the removal is positive. This gives

$$\begin{aligned} &\min_u(\phi_u) \\ \text{subject to:} \quad &\hat{c}u \leq C \times T \\ &u \geq 0. \end{aligned}$$

Using $A = A_2$, for disturbance and removal into each stage class, all choices of B and D, the $\min_u(\max_d(\|x_T\|_1))$ problem with disturbance into stages 1, 2, 3 and 4 gives Figures 3.7, 3.8, 3.9 and 3.10, respectively. These figures show the disturbance d, removal u and total population x_t for 4 choices of Δ.

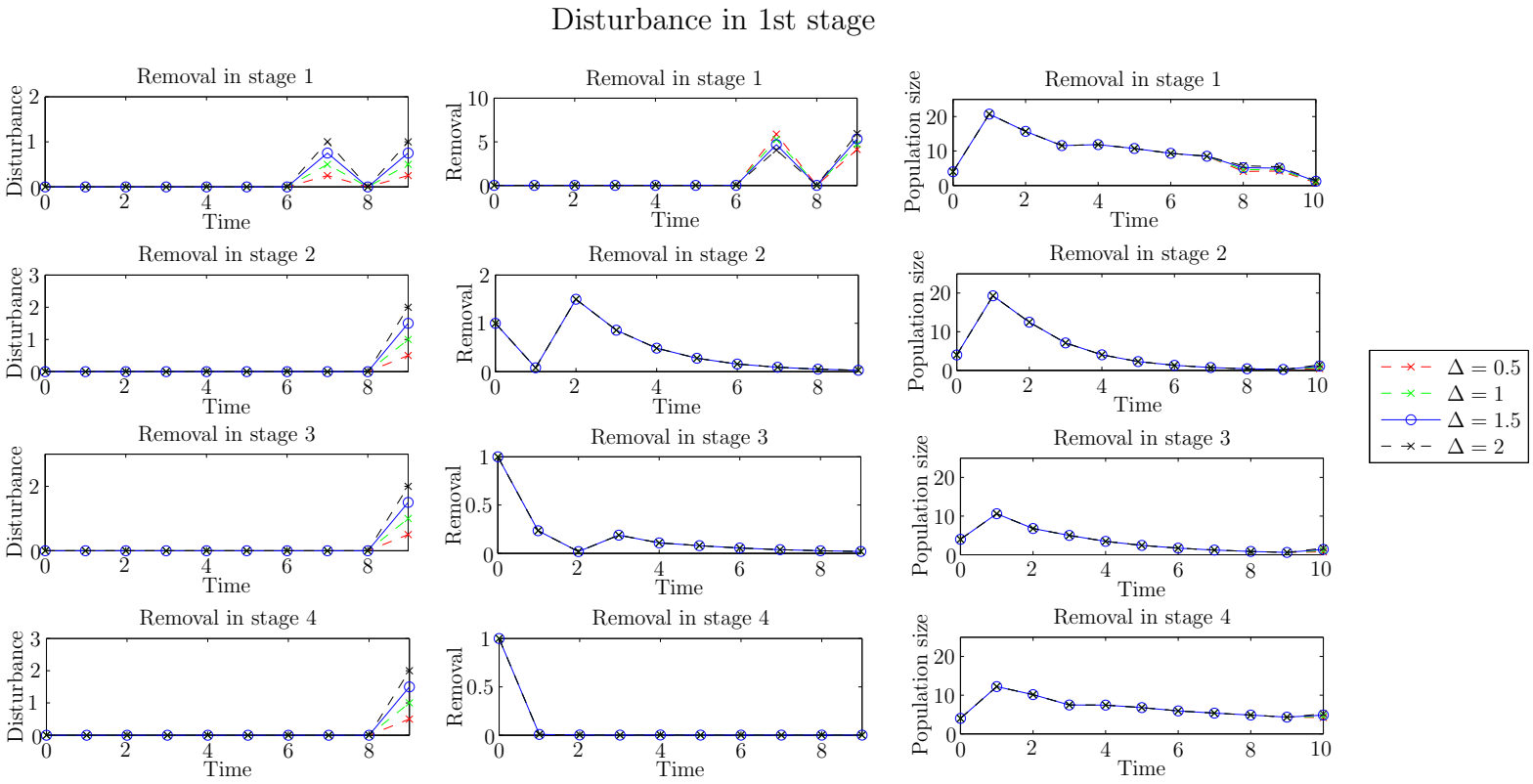

Figure 3.3: The disturbance, removal and resulting population for the $\max_d(\min_u(\|x_T\|_1))$ problem when disturbance acts in the first stage.

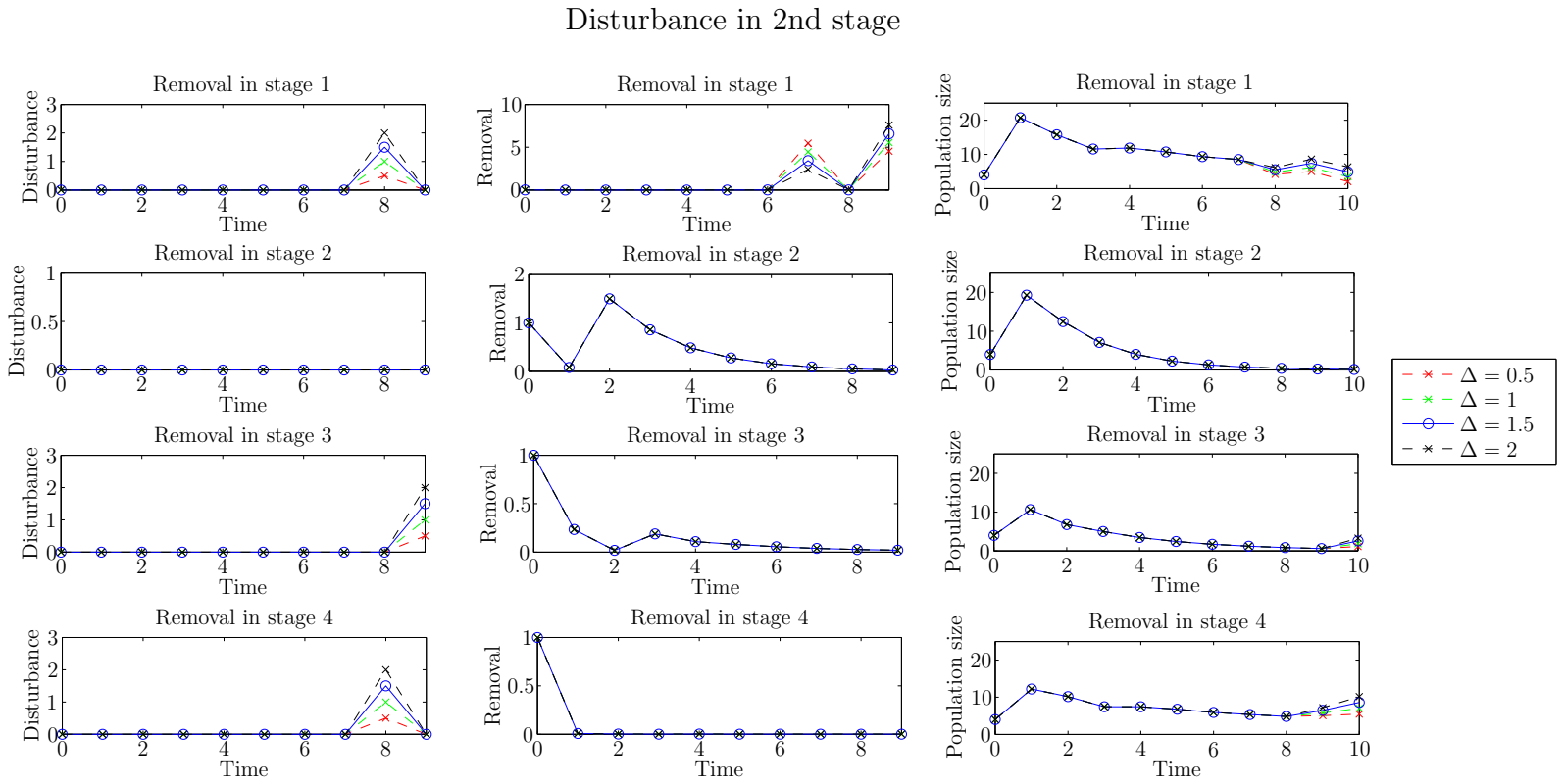

Figure 3.4: The disturbance, removal and resulting population for the $\max_d(\min_u(\|x_T\|_1))$ problem when disturbance acts in the second stage.

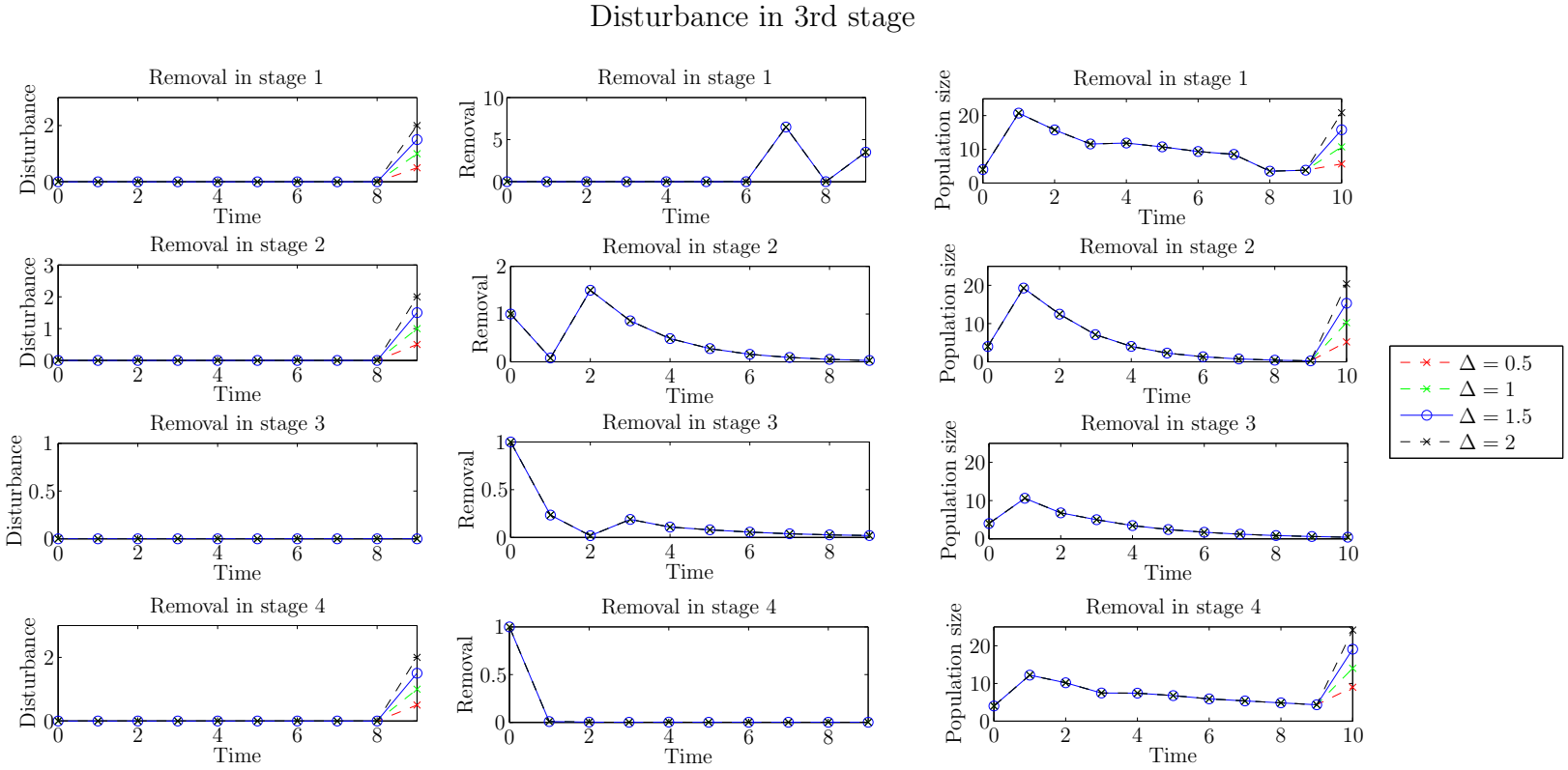

Figure 3.5: The disturbance, removal and resulting population for the $\max_d(\min_u(\|x_T\|_1))$ problem when disturbance acts in the third stage.

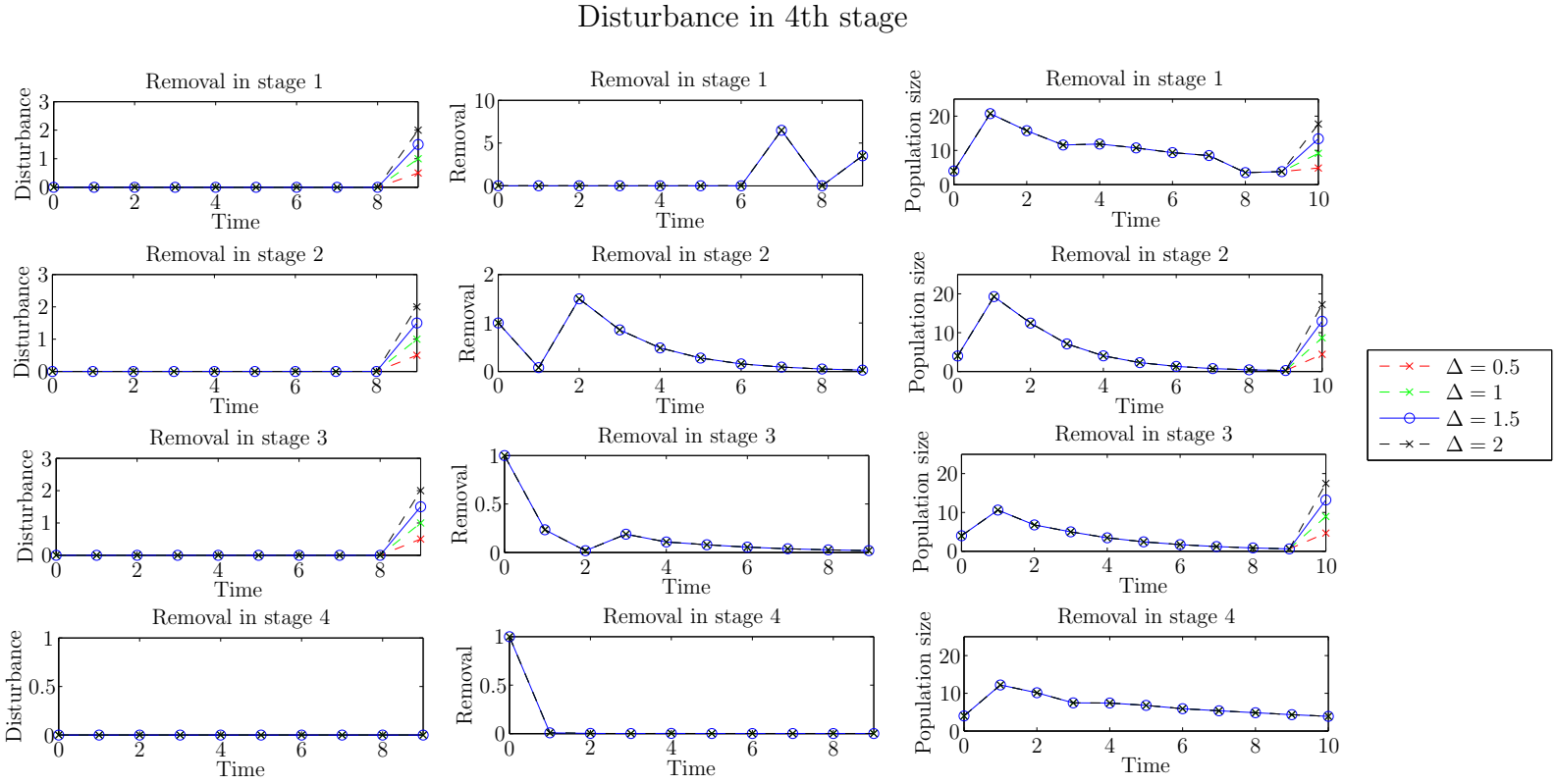

Figure 3.6: The disturbance, removal and resulting population for the $\max_d(\min_u(\|x_T\|_1))$ problem when disturbance acts in the fourth stage.

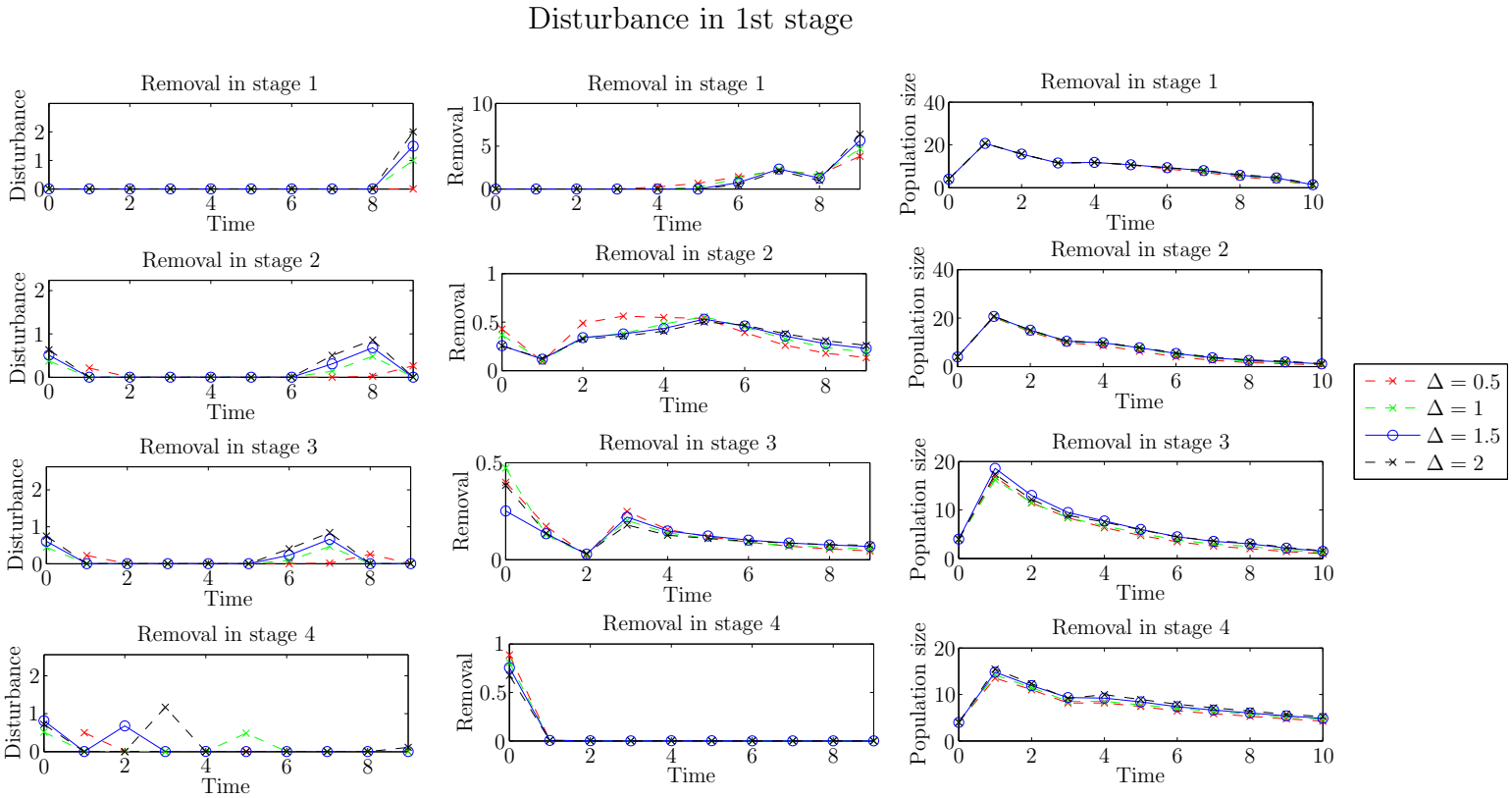

Figure 3.7: The disturbance, removal and resulting population for the $\min_u(\max_d(\|x_T\|_1))$ problem when disturbance acts in the first stage.

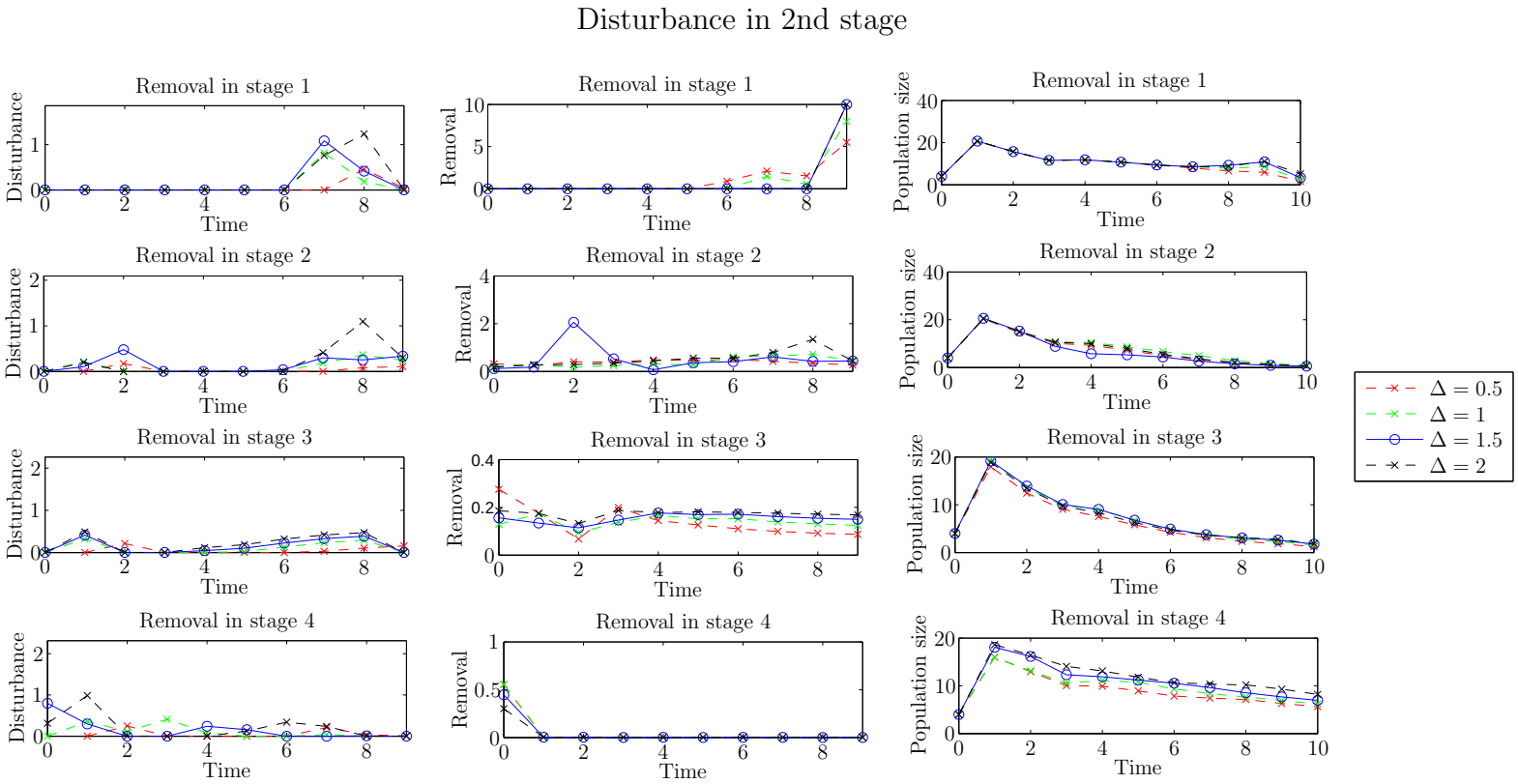

Figure 3.8: The disturbance, removal and resulting population for the $\min_u(\max_d(\|x_T\|_1))$ problem when disturbance acts in the second stage.

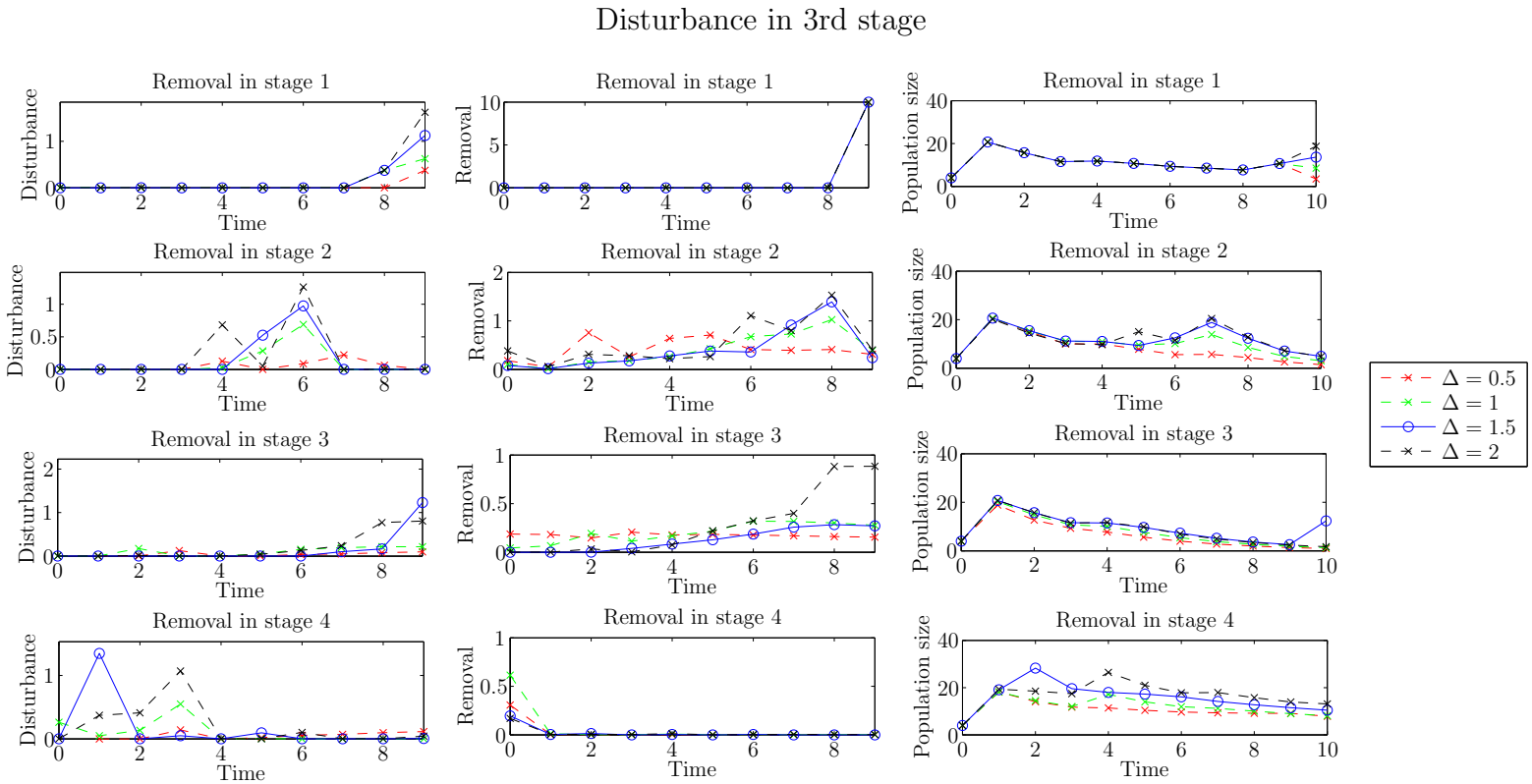

Figure 3.9: The disturbance, removal and resulting population for the $\min_u(\max_d(\|x_T\|_1))$ problem when disturbance acts in the third stage.

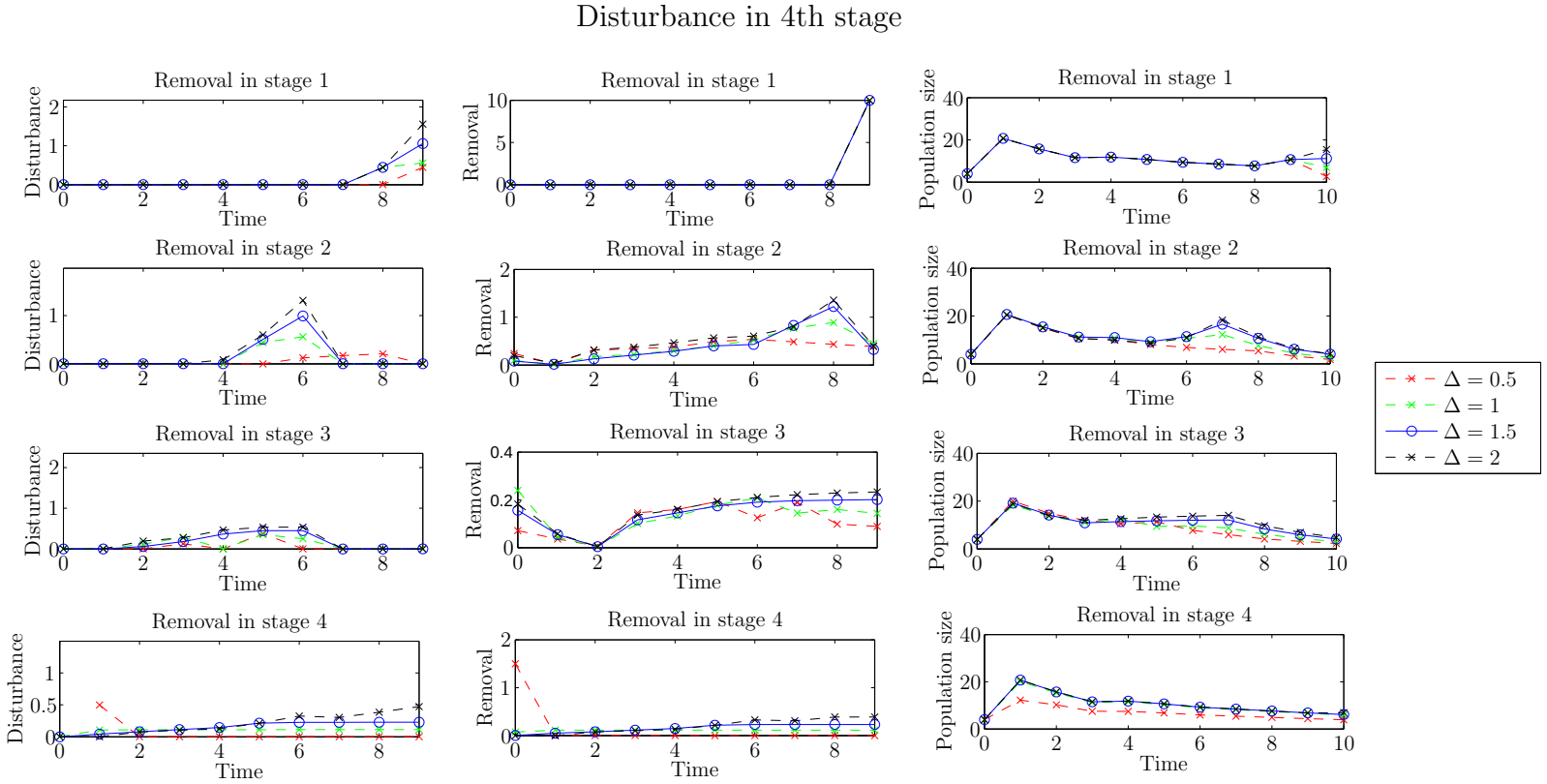

Figure 3.10: The disturbance, removal and resulting population for the $\min_u(\max_d(\|x_T\|_1))$ problem when disturbance acts in the fourth stage.

3.3 Discussion

3.3.1 Sinusoidal disturbance

We calculate the effect of sinusoidal disturbance on both A_1 and A_2 for each combination of B and D to illustrate different results. Figure 3.1 for A_1 shows that the stages in which the disturbance and removal act affects the frequency of disturbance which are amplified by the system the most. In Figure 3.1 it can be seen that for some choices of B and D, e.g. ($D = 3$, $B = 4$) and ($D = 2$, $B = 1$), the transfer function and feedback approximations do not approximate the high and low cost optimal strategies. This may be because the transfer function and feedback form approximations require that $T >> 1$, but we choose $T = 150$ to limit the size of the optimization problem.

In contrast Figure 3.2 for A_2 shows that for each combination of disturbance and removal in different stages, $\|x_T\|_1$ peaks at the same value of θ, where the frequency of the disturbance is very low. This means that the frequency of disturbance which is amplified by the system the most is the same for all choices of B and D. As shown in Figure 3.1 we would expect some particular frequencies of the sinusoidal disturbance to be amplified more by the system. Surprisingly for this example, the frequency of greatest amplification is independent of B and D. Figure 3.2 shows that for all choices of B and D, the transfer function given by equation (3.11) forms a close approximation to $\|x_T\|_1$ when the resource available for removal is low. Similarly, when the resource is high enough that the optimal strategy is able to remove the entire population in the corresponding stage class, then the $\|x_T\|_1$ is very closely approximated by the $\|x_T\|_1$ resulting from the feedback strategy. For some choices of B and D, for example $D = 2$ and $B = 3$, $\|x_T\|_1$ resulting from intermediate choice of resource can clearly be seen between the lower and upper bounds of $\|x_T\|_1$. When disturbance acts in the third and fourth stages the resulting $\|x_T\|_1$ is much larger for all choices of θ. This is because the fecundity in these stages are much larger, and so the disturbance is amplified more by the system.

3.3.2 $\max_d(\min_u(\|x_T)\|_1)$ problem

For a given disturbance d, we find the corresponding optimal removal strategy, u_d. Then we find the (u_d, d) pair such that $\|x_T\|_1$ is maximised. When the disturbance and removal act in the same stage, then the optimal strategy may remove what is added by disturbance, as illustrated by the disturbance and removal acting in the first stage in Figure 3.3. However, when disturbance and removal act in the same stage in Figures 3.4, 3.5 and 3.6, then the disturbance which maximises $\|x_T\|_1$ is 0 at all time steps. This is because for any choice of disturbance the optimal strategy can remove it, so that $\|x_T\|_1 = 0$. So, when we maximise $\|x_T\|_1$ over choices of d then each give the same result, and therefore the disturbance being 0 is itself a valid solution.

For all choices of D, examining the removal strategy from the second, third and fourth stages shows that the optimal removal strategy, u, removes the entire population in that stage class. The initial population is given by

$$x_0 = \begin{pmatrix} 1 \\ 1 \\ 1 \\ 1 \end{pmatrix},$$

which means that in each stage the most the optimal strategy can remove in the first time step is one.

- The removal strategy in the second stage then has a second peak at $t = 2$, when the babies produced by stages 3 and 4 reach the second stage.

- The removal strategy in the third stage has a second peak at $t = 3$, when the babies produced from the initial population reach the third stage class.

- The fourth stage has no such peak. A_2 shows that the growth into the fourth stage class is small, and therefore once the initial population in fourth stage is removed the population in the fourth stage remains very small so there is little to remove.

The disturbance in general acts in the final time step. This is because the population is decreasing ($\lambda(A_2) = 0.9$) and therefore if the disturbance is added at earlier time steps it is attenuated by the system. Also the disturbance has the greatest effect on $\|x_T\|_1$ if it acts when the removal strategy is not able to respond. In Figure 3.4 there are a couple of examples where the disturbance acts at $t = 8$ rather than $t = 9$, as the removal strategy cannot act to remove the disturbance but allows the population to grow when added to stage with high fecundity. Figure 3.5 shows that although the disturbance is added at $t = 9$, because it is added into the third stage with high fecundity it can have a large impact on x_{10}.

Notice that when removal occurs in the third and fourth stages, the peak in the population is not as large. This is because the removal strategy has removed the individuals with high reproductive value. However for removal in the fourth stage, although the initial transients are much smaller, the following $\|x_T\|_1$ is not as small as other stages as the survival into the fourth stage is so small that by removing the fourth stage it does not have a huge affect on the life cycle.

3.3.3 $\min_u(\max_d(\|x_T\|_1))$ problem

For a given removal strategy u, we find the corresponding worst case disturbance d_h that maximises $\|x_T\|_1$. Then we find the (u, d_u) pair such that $\|x_T\|_1$ is minimised. This means that the disturbance responds to the choice of control strategy u. In Figures 3.9 and 3.10 we see that when the disturbance and removal strategy occur in the same stage class it can be seen that disturbance replaces approximately what the removal strategy removes from the population.

Figures 3.9 and 3.10 also show that when the removal is in the second stage class, then the disturbance "acts" two time steps before the removal strategy. This is because in the $\min_u(\max_d(\|x_T\|_1))$ problem where u is already determined the constraint that the population is non-negative means that d is dependent on u. Therefore the choice of u forces d to act before the removal occurs, so that the population is large enough that the population in each stage remains non-negative when u occurs.

Figure 3.8 shows that when the disturbance acts in the second stage and the removal is in either the first or second stage class, then the disturbance maximises $\|x_T\|_1$ by acting at $t = 8$ and $t = 9$, respectively. This means that the population added by disturbance in the second stage class in able to grow into the third and fourth stage classes where fecundity is highest and therefore the disturbance has a greater affect on $\|x_T\|_1$.

3.4 Conclusion

In this chapter we have considered an invading population disturbed by migration. We use discrete-time population models with linear programming to explore various types of disturbance.

Firstly, we look at a population affected by a periodic disturbance. This creates a problem similar to [53] as the disturbance is fixed and so we minimise over u to find an optimal removal strategy. When the resource is low and therefore no removal occurs we find that the total final population can be approximated using the transfer function. Also, when the resource is high then the optimal control strategy can remove the whole population available and the resulting final population can be approximated using a feedback control.

Secondly, we explore when the disturbance is unknown, and we assume the worst case scenario, given that the disturbance is bounded. This creates minimax and maximin problems as we aim to minimise the total final population with respect to removal but maximise the effect of the disturbance. As illustrated with the simple ecological example in Section 3.1, the resulting final population from the minimax problem is not necessarily equal to the final population from the maximin problem, but necessarily $\text{maximin} \leq \text{minmax}$.

To solve the maximin and minimax problems we first use Matlab's `Linprog` where the constraints and the objective function are dependent on u and d, to create functions

of d and u respectively. We then used `fmincon` to maximise and minimise these functions over d and u, respectively. In the $\max_d(\min_u(\|x_T\|_1))$ problem d is not constrained by the choice of u, and therefore when we maximise over d the disturbance generally acts in the last time step, where the removal strategy is unable to respond. A secondary reason for why the disturbance acts in the last time step is because we have considered a decreasing population. If the population was increasing, so that $\lambda(A) > 1$, then the disturbance acts in the first time step so that it can be amplified by the system. The constraint (3.10) ensures that the population is non-negative, which for the $\min_u(\max_d(\|x_T\|_1))$ problem means that the constraint on d is dependent on u, as u can only remove what is present but d contributes to the size of the population. Therefore if u is chosen first then d may be forced to act before the removal u acts, so that the population remains non-negative. This is particularly clearly illustrated in Figures 3.9 and 3.10, when removal occurs in the second stage class.

Solving this problem is complicated by the fact that the minimax $\geq$ maximin. In a strategic game the players choices are made simultaneously and depend on the actions of the other players [96]. The steady state of a strategic game such that minimax = maximin, is known as a Nash equilibrium. We study the existence of a Nash equilibrium for a similar population model in Chapter 4.

Chapter 4

Minimax linear quadratic games and attenuation for managed and disturbed populations

4.1 Background

This chapter continues the theme of Chapter 3, studying a simple discrete-time population model with management and disturbance. In Chapter 3 we used a linear programming approach to explore optimal removal strategies when the population is subject to worst-case scenario disturbances. This linear programming approach gave rise to two different 2-player optimisation problems - a minimax problem where the disturbance "plays" first, and a maximin problem where the removal strategy "plays" first. Under the assumptions made in Chapter 3, the optimal strategies do not form a Nash equilibrium and there is no saddle point.

In this chapter we consider the minimax/maximin problem with a quadratic cost function by building on a existing model [14] with the addition of disturbance. The choice of quadratic cost is motivated by the approach of Blackwood et al. [14], where a quadratic cost is used to represent that it is harder for pest managers to find and remove a larger proportion of the population. [14] use a quadratic cost function to find an optimal removal strategy for controlling an invasive population of *Spartina alterniflora*. They

use a patch-based model which contains adult populations in each patch, which are connected by the dispersal of offspring. The model in [14] is given by

$$N_{t+1} = A_t N_t - B_t H_t \tag{4.1}$$

where A_t is a matrix containing the species vital rates within each patch and dispersal at time t, N_t is a vector containing the size of the population in each patch at time t, B_t is a diagonal matrix containing how effective the removal is in each patch and H_t is the amount removed in each patch at time t.

The quadratic cost function, used in [14], depends on the population size and the removal. The total cost at any time t is given by

$$C_t = N_t^T Q N_t + H_t^T S H_t, \tag{4.2}$$

where Q and S are diagonal matrices containing the relative ecological and economic costs of removal in each patch. The use of quadratic costs allows the control strategy H_t to be calculated in closed form using the Riccati equations, such that the total cost by time T is minimized subject to equation (4.1). Blackwood et al. [14] assume that $B_t = I$ and $A_t = A$ for all t, which means the removal is equally efficient in all patches and the vital rates and dispersal of the population are time invariant. They consider a model with 3 connected patches, and explore the total cost required for an optimal management strategy for different levels of connectivity, and find that as the number of connections between the patches decrease so the resulting C_T decreases. The use of Riccati equations is computationally fast, allowing the optimal management strategy to be easily calculated by solving a series of equations.

Greenman and Benton [47] explore the affect their system has on coloured noise. They consider several different models, where the amplitude of the noise is relatively small. Coloured noise refers to the power spectrum which captures the frequency of the noise, with red noise representing noise with high power at low frequencies and white noise having uniformly distributed power over the entire frequency spectrum. In particular

[47] examine the effect that coloured noise can have on increasing the risk of extinction. It has been suggested that red noise may increase the probability of extinction. The effect of red noise versus white noise on extinction is discussed in [103] and [110].

This chapter is structured as follows. First, Section 4.2 outlines the model and the relevant theory required for the dynamic linear quadratic game (DLQG) and the disturbance attenuation problem. In Section 4.3 we present the results for both the DLQG and disturbance attenuation problem. Then Section 4.4 discusses these results. Finally, Section 4.5 summarises the results we found.

4.2 The framework

The discrete-time, stage structured population with stage dependent removal and additive disturbance is given by

$$x_{t+1} = Ax_t + Bu_t + Dd_t, \tag{4.3}$$

where x_t is the stage structured population at time t, A is a PPM containing the population vital rates, u_t and d_t are the removal and disturbances at time t, and B and D are vectors determining in which stage classes the removal and disturbance act, respectively. Notice, that as u_t denotes the removal at time step t it must be negative.
As discussed in Section 4.1 the cost function used by Blackwood et al. [14] (equation (4.2)) is quadratic in the size of the population and the removal strategy at each time step t. Therefore, this cost function is convex in u which means that a unique minimum solution for the control strategy, u, exists. With the addition of disturbance, d, the cost function we use is dependent on the population size, the removal strategy u and the disturbance d, at each time step t. As we aim to maximise over d then we require that the cost function is concave in d, as well as remaining convex in u. Therefore, the cost function we use is given by

$$J_\gamma(u, d) = \sum_{t=1}^{T} (x_t^T Q x_t + \|u_t\|^2 - \gamma^2 \|d_t\|^2), \tag{4.4}$$

where γ is a parameter to be chosen to ensure that $J_\gamma(u,d)$ is concave in d. The cost function $J_\gamma(u,d)$ directly depends on u_t, but also indirectly on u_t via the x_t term. As both these terms are convex in u then $J_\gamma(u,d)$ is automatically convex in u. The cost function is also dependent on d directly, and indirectly in the x_t term. However, the indirect d term from x_t is convex in d whilst the direct term is concave. Therefore concavity in d is not guaranteed and we require a parameter γ, to ensure the cost function, $J_\gamma(u,d)$, will be concave in d. Q allows the stage classes to have different effects on the cost function. However, in this chapter we assume that each stage has the same effect on the cost and therefore Q is the identity. We aim to find the optimal removal strategy, u, which minimises $J_\gamma(u,d)$ given that the disturbance, d, maximises $J_\gamma(u,d)$. For γ large enough, optimal solutions for (u,d) form a saddle point, and we have a Nash equilibrium where

$$\min_u(\max_d(J_\gamma(u,d))) = \max_d(\min_u(J_\gamma(u,d))).$$

The following section states a constraint on γ for the existence of this saddle point solution, and describes how to calculate the optimal (u,d) pair when the saddle exists.

4.2.1 Dynamic Linear Quadratic Game

The following uses [107] and the discrete Maximum principle to outline the derivation of the discrete Riccati equations, which can be used to find solutions to the minimax problem. First, define the Hamiltonian function of our system to be

$$H_t = x_t^T Q x_t + u_t^T u_t - \gamma^2 d_t^T d_t + p_{t+1}^T((A-I)x_t + Bu_t + Dd_t), \tag{4.5}$$

then the Maximum principle states that the conditions for the minimax solutions are

$$\frac{\partial H_t}{\partial u_t} = 0, \quad \frac{\partial H_t}{\partial d_t} = 0, \quad \frac{\partial^2 H_t}{\partial u_t^2} > 0 \text{ and } \frac{\partial^2 H_t}{\partial d_t^2} < 0.$$

Therefore, using our Hamiltonian function we have

$$\frac{\partial H_t}{\partial u_t} = u_t + B^T p_{t+1} = 0 \text{ and } \frac{\partial H_t}{\partial d_t} = -\gamma^2 d_t + D^T p_{t+1} = 0, \tag{4.6}$$

which gives that at the minimax solution

$$u_t = -B_t^T p_{t+1} \text{ and } d_t = \frac{1}{\gamma^2} D^T p_{t+1}. \tag{4.7}$$

Using equation (4.3) then

$$x_{t+1} - x_t = (A - I)x_t + Bu_t + Dd_t. \tag{4.8}$$

Then substituting equations (4.7) into equation (4.8) gives that

$$x_{t+1} - x_t = (A - I)x_t - BB^T p_{t+1} + \frac{1}{\gamma^2} DD^T p_{t+1},$$

which rearranges to give that

$$x_{t+1} = Ax_t - BB^T p_{t+1} + \gamma^{-2} DD^T p_{t+1}, \tag{4.9}$$

and

$$x_t = A^{-1} x_{t+1} + A^{-1} BB^T p_{t+1} - \gamma^{-1} A^{-1} DD^T p_{t+1} \tag{4.10}$$

Also differentiating the Hamiltonian with respect to x_t gives

$$p_{t+1} - p_t = \frac{\partial H_t}{\partial x_t} = -Qx_t - (A - I)^T p_{t+1} \quad \text{so} \quad p_t = Qx_t + A^T p_{t+1}. \tag{4.11}$$

Substitute $t = T - 1$ into equations (4.10) and (4.11) to give

$$x_{T-1} = A^{-1} x_T + (A^{-1} BB^T - \gamma^{-2} A^{-1} DD^T) p_T$$

$$p_{T-1} = QA^{-1} x_T + (QA^{-1} BB^T - \gamma^{-2} QA^{-1} DD^T + A^T) p_T.$$

We choose the boundary condition of out Riccti equation such that $M_{T+1} = 0$ (see equation (4.16)), where T is the final time step. This boundary condition and our choice of cost function means that $P_T = 0$, which gives that

$$p_{T-1} = Qx_{T-1}. \tag{4.12}$$

Next, substitute $t = T - 2$ into equations (4.10) and (4.11) to get

$$x_{T-2} = A^{-1}x_{T-1} + (A^{-1}BB^T - \gamma^{-2}A^{-1}DD^T)p_{T-1}$$

$$p_{T-2} = QA^{-1}x_{T-1} + (QA^{-1}BB^T - \gamma^{-2}QA^{-1}DD^T + A^T)p_{T-1},$$

then rearranging using equation (4.12) gives that

$$p_{T-2} = (QA^{-1} + (QA^{-1}BB^T - \gamma^{-2}QA^{-1}DD^T + A^T)Q) \\ (A^{-1} + (A^{-1}BB^T - \gamma^{-2}A^{-1}DD^T)Q)^{-1}x_{T-2}.$$

Using proof by induction we can see that for any choice of t, p_t is linear in x_t and therefore we have that $p_t = M_t x_t$. Using equation (4.11) and that $p_t = M_t x_t$ then,

$$M_t x_t = Qx_t + A^T p_{t+1} = Qx_t + A^T M_{t+1}x_{t+1}. \tag{4.13}$$

Using that $p_t = M_t x_t$ and equation (4.11) then equation (4.9) becomes

$$x_{t+1} = Ax_t - BB^T M_{t+1}x_{t+1} + \gamma^{-2}DD^T M_{t+1}x_{t+1} \tag{4.14}$$

$$= (I + BB^T M_{t+1} - \gamma^{-2}DD^T M_{t+1})^{-1}Ax_t, \tag{4.15}$$

substituting this into equation (4.13) gives that

$$M_t x_t = Qx_t + A^T M_{t+1}(I + BB^T M_{t+1} - \gamma^{-2}DD^T M_{t+1})^{-1}Ax_t.$$

As $x_t \neq 0$ then we obtain the discrete-time Riccati equations given by

$$M_t = Q + A^T M_{t+1}(I + (BB^T - \gamma^{-2}DD^T)M_{t+1})^{-1}A. \tag{4.16}$$

Similar to in [14] we can assume that $M_{T+1} = 0$ because we consider a finite number of years T, where no removal or disturbance occurs at $T + 1$. Then using that $M_{T+1} = 0$ the Riccati equations can be solved backwards to give $M_T, M_{T-1} \dots M_0$. Theorem 1 describes the constraint on γ required, for the existence of a solution to equation (4.16), it is taken directly from [8].

Theorem 1. *For the two-person zero-sum*[1] *dynamic game with closed-loop perfect-state information pattern*[2] *and with fixed* $\gamma > 0$*:*

- *There exists a unique feedback saddle-point solution if*

$$\gamma^2 I - D^T M_{t+1} D > 0, \quad t \in [1, T], \tag{4.17}$$

where M_{t+1}*, for all* $t \in [1 \dots T]$*, is defined by equation* (4.16)

- *Under condition* (4.17)*, the matrices*

$$(I + (BB^T - \gamma^{-2} DD^T) M_{t+1})$$

are invertible, and the unique feedback saddle-point policies are

$$\tilde{u}_t^* = -B^T M_{t+1} (I + (BB^T - DD^T) M_{t+1})^{-1} A x_t, \quad t \in [1, T], \tag{4.18}$$

$$\tilde{d}_t^* = \gamma^{-2} D^T M_{t+1} (I + (BB^T - DD^T) M_{t+1})^{-1} A x_t, \quad t \in [1, T], \tag{4.19}$$

with corresponding unique state trajectory generated by the difference equation

$$x_{t+1}^* = (I + (BB^T - \gamma^{-2} DD^T) M_{t+1})^{-1} A x_t^*, \quad x_1^* = x_1,$$

and the saddle-point value is

$$J_\gamma^*(u, d) = x_1' M_1 x_1. \tag{4.20}$$

- *If the matrix* $\gamma^2 I - D^T M_{t+1} D$ *has a negative eigenvalue for some* $t \in [1, T]$*, then the game does not admit a saddle-point and its upper value becomes unbounded.*

The existence of the saddle point solution depends on finding γ large enough that condition (4.17) is satisfied. Therefore to find u and d, we must first find a γ that satisfies condition (4.17). The solutions for u and d, given by equations (4.18) and

[1] *Zero-sum*: the net worth of the system remains unchanged.

[2] *Closed-loop perfect state information pattern*: The control may depend on current and past values of the state such that $u_t = \mu_t(x_1, \dots, x_t)$ where $(\mu_1, \dots \mu_t)$ is the control policy.

(4.19), form a saddle point which means minimax = maximin. This saddle point solution is in contrast to solutions for u and d found using `Linprog` and `fmincon` in Chapter 3 where we showed that minimax $\geq$ maxmin.

4.2.2 Disturbance attenuation

Disturbance attenuation gives a measure of how a disturbance is amplified or attenuated by a system. As discussed in Section 4.1, Greenman and Benton [47] explore how a coloured noise disturbance can be affected by the system. In this chapter we study how a disturbance may be amplified by the system and how the effect of disturbance may be attenuated. The following presents the required framework.

The disturbance attenuation problem calculates a bound, denoted γ^*, such that the population and removal strategy is bounded by a multiple of the disturbance, that is

$$\sum_t \|x\|^2 + \sum_t \|u\|^2 \leq (\gamma^*)^2 \sum_t \|d\|^2. \tag{4.21}$$

An alternative bound for just the population size could be calculated by neglecting the $\|u\|^2$ term. However, in an ecological situation the removal strategy may be expensive, and therefore it is important to calculate the effect the disturbance has on both the population size and optimal removal strategy.

The following is adopted from [8]. To find this minimum level of attenuation, let γ be fixed so that equation (4.17) is satisfied, and let the corresponding controller and disturbance (given by equations (4.18) and (4.19)) be denoted by μ^γ and ν^γ, respectively. For a given control pair then equation (4.20) states that for all $x_1 \in \mathbf{R}^n$

$$J_\gamma(\mu^\gamma, \nu^\gamma) = x_1' M_1 x_1,$$

where M_1 is determined by the Riccati equation in equation (4.16). As the control and disturbance pair (μ^γ, ν^γ) are a minimax solution for the $\min_u(\max_d(J_\gamma(u, d)))$, then for

any choice of d in the set of possible disturbances

$$J_\gamma(\mu^\gamma, d) \leq J_\gamma(\mu^\gamma, \nu^\gamma) = x_1' M_1 x_1.$$

Next, define a second cost function, which is independent of d and therefore γ, to be given by

$$J(u) = J_\gamma(u, d) + \gamma^2 \sum_{t=1}^{T} \|d_t\|^2, \tag{4.22}$$

where $J_\gamma(u, d)$ is given by equation (4.4). Therefore letting $u = u^\gamma$, which is the optimal control strategy corresponding to a fixed γ which satisfies equation (4.17), then the second cost function in equation (4.22) becomes

$$J(\mu^\gamma) = J_\gamma(\mu^\gamma, d) + \gamma^2 \sum_{t=1}^{T} \|d_t\|^2.$$

Rewriting this equations using that $J_\gamma(\mu^\gamma, d) \leq x_1' M_1 x_1$ from equation (4.20) gives

$$J(\mu^\gamma) \leq x_1' M_1 x_1 + \gamma^2 \sum_{t=1}^{T} \|d_t\|^2.$$

The (μ^γ, ν^γ) pair are a feedback solution to the minimax problem valid for any choice of initial condition, x_1. Therefore, without loss of generality let $x_1 = 0$, which means that

$$J(\mu^\gamma) \leq \gamma^2 \sum_{t=1}^{T} \|d_t\|^2.$$

As defined by equations (4.4) and (4.22) then $J(\mu^\gamma) = \|x\|^2 + \|\mu^\gamma\|^2$, so

$$\sum_{t=1}^{T} \|x\|^2 + \sum_{t=1}^{T} \|\mu^\gamma\|^2 \leq \gamma^2 \sum_{t=1}^{T} \|d_t\|^2.$$

So we have shown that if γ satisfies condition (4.17) then it is a possible attenuation bound. Next we show that the attenuation bound is given by the smallest γ which satisfies condition (4.17).

Let

$$\hat{\gamma} := inf\{\gamma : \gamma \in \Gamma\} \text{ where } \Gamma := \{\gamma > 0 : (4.17) \text{ is statified}\}, \tag{4.23}$$

then as the definition the minimum attenuation is the smallest γ that satisfies equation (4.21) $\hat{\gamma}$ is a possible minimum attenuation bound. The following shows that if $\tilde{\tilde{\gamma}} < \hat{\gamma}$ then $\tilde{\tilde{\gamma}}$ can not satisfy equation (4.21). First suppose that $\tilde{\tilde{\gamma}}$ is the minimum level of attenuation then

$$\sum_t \|x_t\|^2 + \sum_t \|u_t\|^2 \leq \tilde{\tilde{\gamma}}^2 \sum_t \|d_t\|^2. \tag{4.24}$$

Therefore

$$\min_u \max_d J_{\tilde{\tilde{\gamma}}}(u, d) = \sum_t \|x_t\|^2 + \sum_t \|u_t\|^2 - \tilde{\tilde{\gamma}}^2 \sum_t \|d_t\|^2 \leq 0,$$

for all possible solutions of d. However, as stated in Theorem 1, because $\tilde{\tilde{\gamma}}$ does not satisfy the constraint (4.17) then the upper value of $\min_u \max_d J_{\tilde{\tilde{\gamma}}}(u, d)$ is unbounded, and therefore if $\tilde{\tilde{\gamma}} < \hat{\gamma}$ then equation (4.24) is impossible. This contradiction means that the attenuation bound can not be less than $\hat{\gamma}$, so the minimum attenuation (γ^*) is given by $\hat{\gamma}$.

Remark. *γ^* is the smallest value which satisfies*

$$\sum_t \|x\|^2 + \sum_t \|u\|^2 \leq (\gamma^*)^2 \sum_t \|d\|^2 \tag{4.25}$$

for all disturbances d and initial conditions x_0. So let $x_0 = 0$, which means that $u_0 = 0$ and let

$$d_t = \begin{cases} 1 & t = 0 \\ 0 & t > 0. \end{cases}$$

Then equation (4.25) *becomes*

$$\|D\|^2 = \|x_0 + Bu_0 + Dd_0\|^2 = \|x_1\|^2 \leq \sum_t \|x_t\|^2 + \sum_t \|u_t\|^2 \leq (\gamma^*)^2.$$

So $\gamma^* \geq \|D\|$.

4.3 Results

4.3.1 Dynamic Linear Quadratic Game

We use the backwards Riccati equation given by equation (4.16), to give the feedback solutions u and d for the minimax problem given by the cost function (4.4). We choose the parameters for the population model such that

$$A = \begin{pmatrix} 0.1330 & 0.2797 & 57.5922 & 2.3712 \\ 0.1826 & 0 & 0 & 0 \\ 0 & 0.0547 & 0 & 0 \\ 0 & 0 & 0.002 & 0 \end{pmatrix}, \tag{4.26}$$

where the dominant eigenvalue of A is 0.9. As in Chapter 3 we let the disturbance and removal act in a single stage class, so that both B and D are vectors of zeros and 1 in a single component. Using the remark in Section 4.2.2, then this choice of D means we find that γ^* is bounded from below by 1. We assume an initial population given by

$$x_0 = \begin{pmatrix} 1 \\ 1 \\ 1 \\ 1 \end{pmatrix}. \tag{4.27}$$

To be able to solve the Riccati equations we require the cost function (4.4), with the population model (4.3), to admit a saddle point solution. So, we choose a γ such that the condition (4.17) is satisfied. For each choice of B and D we obtain γ such that it is approximately $\hat{\gamma}$ (defined in equation (4.23)). If $\gamma \geq \hat{\gamma}$ then this would ensure that the minimax solution exists. Larger values of γ means that the disturbance has a larger contribution to the cost function, $J_\gamma(u, d)$, so we aim to choose a γ such that the disturbance does not dominate the cost function. Using $\hat{\gamma}$ and the Riccati equation (4.16) we calculate u and d, for each combination of B and D, similar to the computational analysis in Chapter 3. As u is negative, the removal at any time t is given by $-u_t$. Plotting the removal $(-u)$, disturbance (d) and the resulting population, x, gives Figures 4.1, 4.2, 4.3 and 4.4, for the disturbance in the first, second, third and fourth stage classes, respectively.

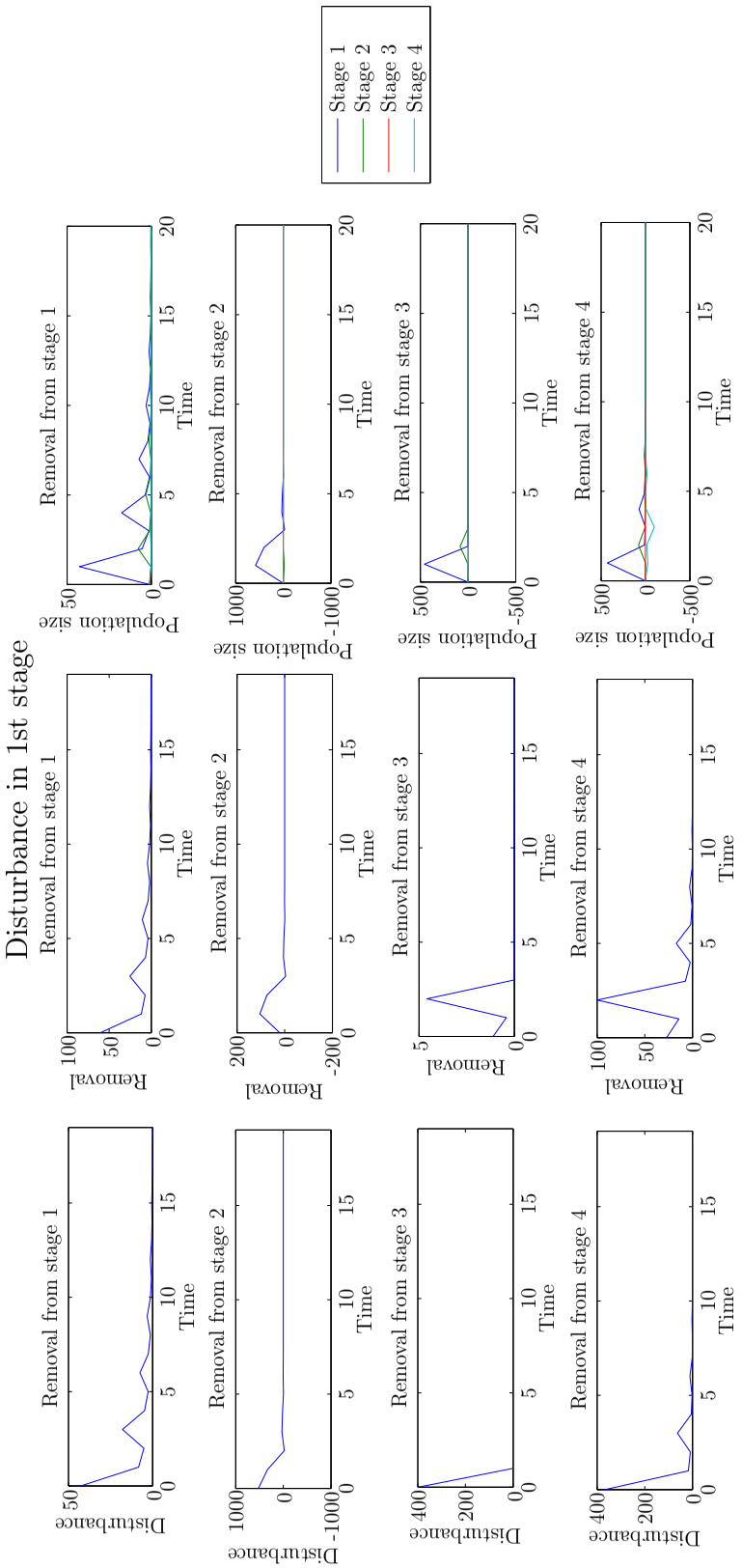

Figure 4.1: Disturbance into the 1st stage and removal from each stage, plots show corresponding d, $-u$ and x, calculated using Riccati equations (4.16).

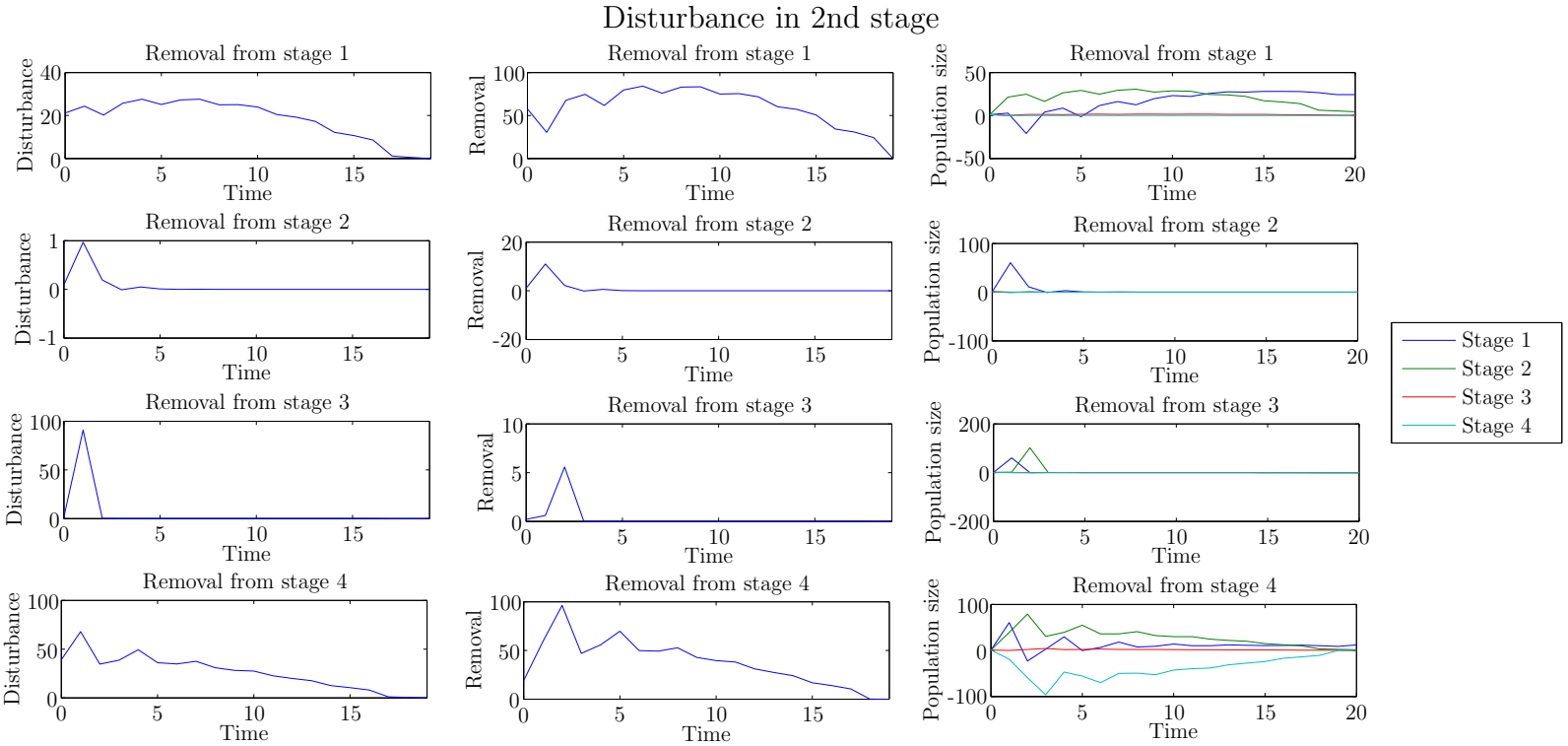

Figure 4.2: Disturbance into the 2nd stage and removal from each stage, plots show corresponding d, $-u$ and x, calculated using Riccati equations (4.16).

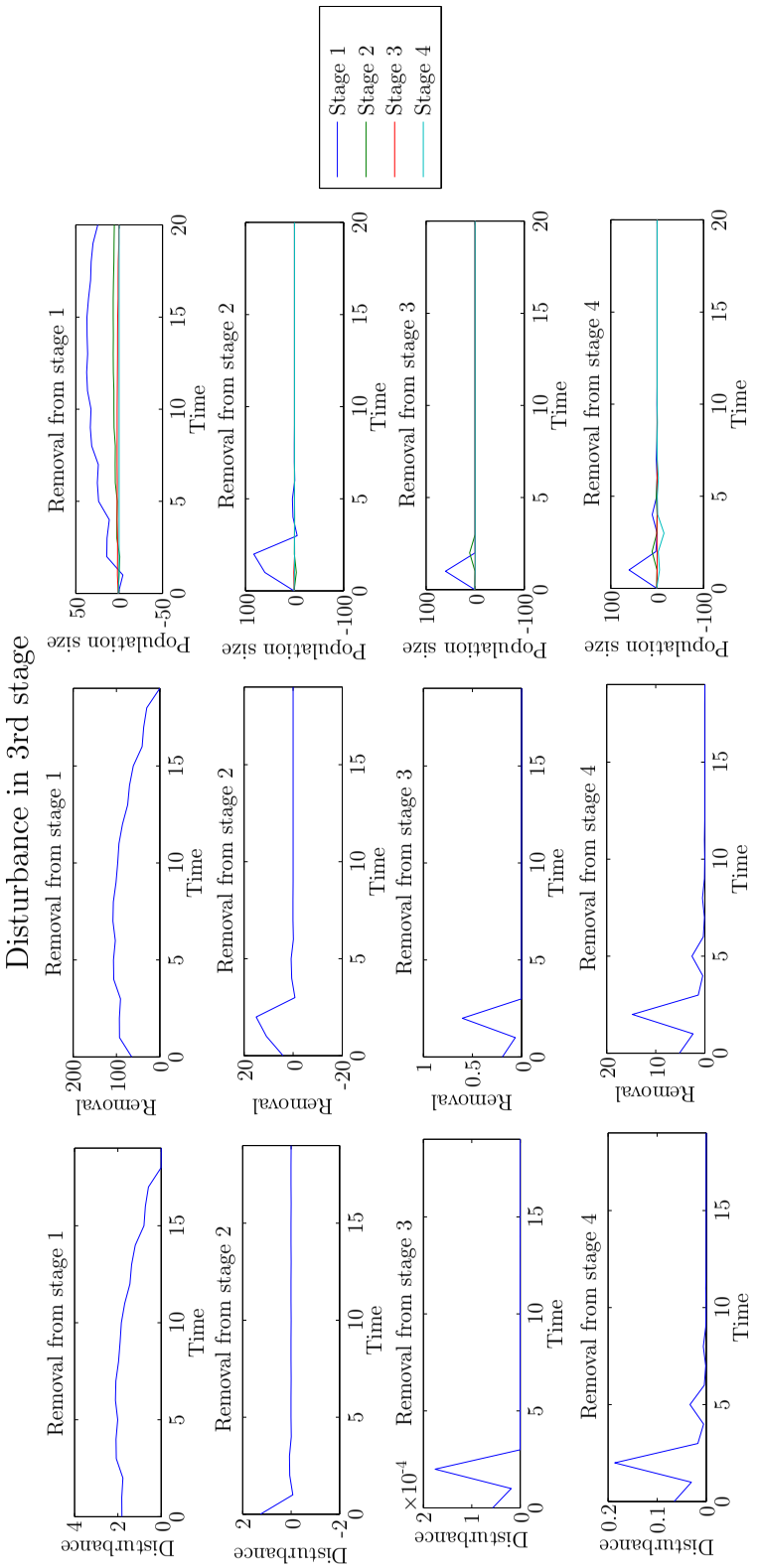

Figure 4.3: Disturbance into the 3rd stage and removal from each stage, plots show corresponding d, $-u$ and x, calculated using Riccati equations (4.16).

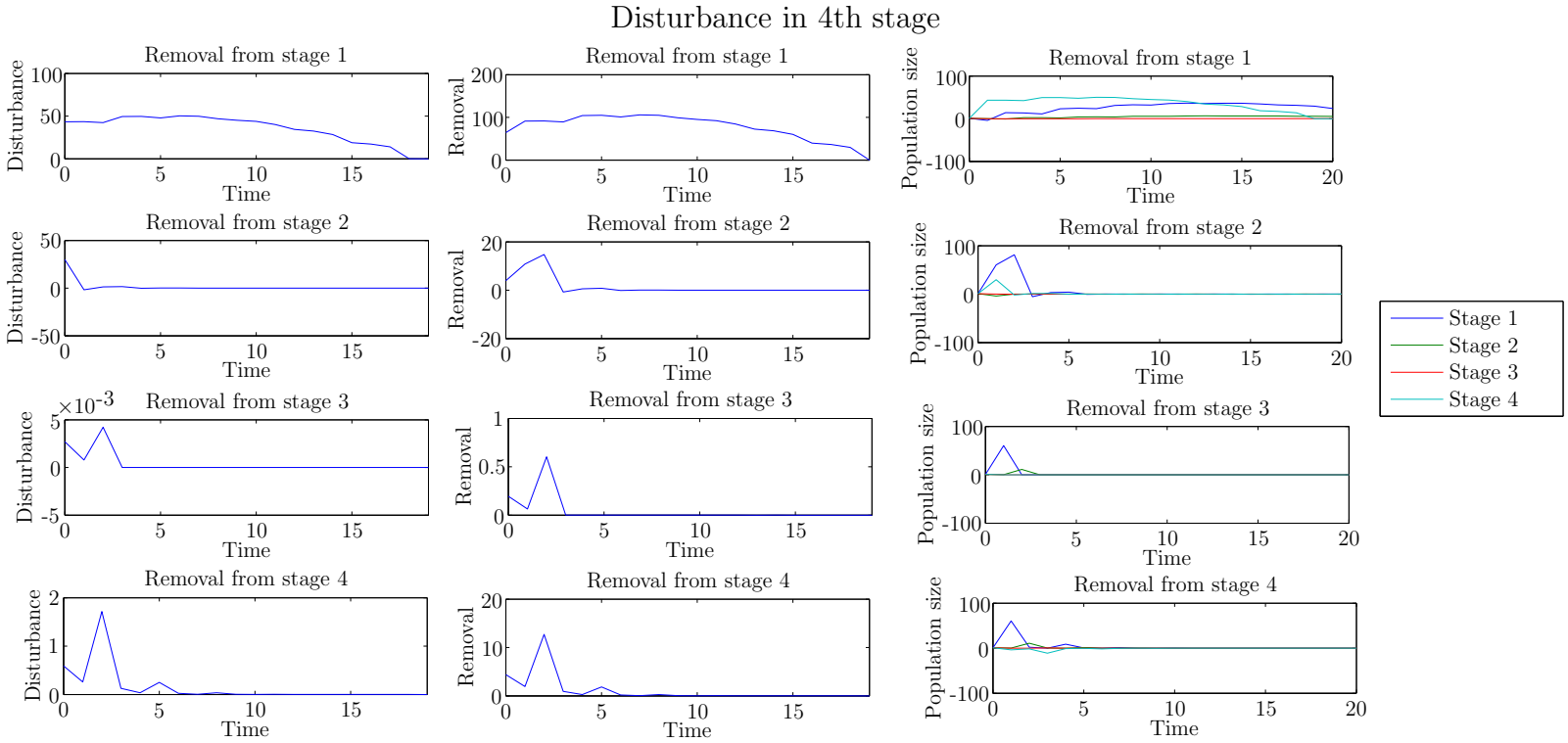

Figure 4.4: Disturbance into the 4th stage and removal from each stage, plots show corresponding d, $-u$ and x, calculated using Riccati equations (4.16).

4.3.2 Disturbance attenuation

As stated in Section 4.2.2 the minimum attenuation is to find the smallest γ^* such that

$$\sum_t \|x\|^2 + \sum_t \|u\|^2 \leq (\gamma^*)^2 \sum_t \|d\|^2.$$

In this section we consider the population model given by equation (4.3), and use the theory from Section 4.2.2 to calculate the minimum disturbance attenuation for a range of vital rates and PPM's.

Firstly, we consider a simple 3 stage structured PPM given by

$$A = \begin{pmatrix} M1 & M2 & M3 \\ G1 & 0 & 0 \\ 0 & G2 & S \end{pmatrix}.$$

Then we vary each vital rate while fixing the other parameters, to find the effect the vital rates have on the disturbance attenuation. As before we let the removal strategy and disturbance act in a single stage class, such that B and D are vectors of zeros other than 1 in a single component.

The minimum attenuation does not place a constraint on the non-negativity of the population. We could modify the cost function by penalising non-negative values so as to ensure non-negativity of the population, however the resulting problem would not be within the linear-quadratic framework we have created. Instead, we use a steady state gain calculation to approximate the achievable disturbance attenuation. The key result in summarised in the following proposition.

Proposition 1. *Let $u_t = -Fx_t$ for some fixed feedback matrix F. If $\lambda(A - BF) < 1$, then the "gain", i.e. smallest γ such*

$$\sum_{t=0}^{\infty} \|x_t\|^2 + \sum_{t=0}^{\infty} \|u_t\|^2 \leq (\gamma)^2 \sum_{t=0}^{\infty} \|d_t\|^2$$

is given by

$$\gamma = \max_{|z|=1} \left\| \begin{pmatrix} (F(zI-(A-BF))^{-1}D) \\ ((zI-(A-BF))^{-1}D) \end{pmatrix} \right\|. \tag{4.28}$$

If $A-BF$ is non-negative, then the maximum in equation (4.28) *is achieved at $z=1$ and*

$$\max_{|z|=1} \left\| \begin{pmatrix} (F(zI-(A-BF))^{-1}D) \\ ((zI-(A-BF))^{-1}D) \end{pmatrix} \right\| = \left\| \begin{pmatrix} (F(I-(A-BF))^{-1}D) \\ ((I-(A-BF))^{-1}D) \end{pmatrix} \right\|. \tag{4.29}$$

For a given F we use Proposition 1 to find

$$\gamma_{approx} = \left\| \begin{pmatrix} (F(I-(A-BF))^{-1}D) \\ ((I-(A-BF))^{-1}D) \end{pmatrix} \right\| \approx \gamma^*. \tag{4.30}$$

For simplicity we choose F such that it removes as much of the population as possible, without the population becoming negative. Therefore if removal is acting in the i-th stage we have that $F = A_i$, where A_i denotes the i-th row of A.

We calculate γ^* and γ_{approx} for all combinations of B and D and vary each vital rate while fixing the other parameters in A. To calculate the disturbance attenuation we require A to be stable, therefore as we vary the parameters in A we ensure that the dominant eigenvalue of A is less than 1. As we vary each of the parameters in A individually first fix all three of the fecundity rates (M_1, M_2, M_3) at 0.3 and the survival and growth rates (G_1, G_2, S) at 0.5. Then Figure 4.5 is created by varying M_1 from 0.1 to 0.65 and varying M_2 and M_3 individually from 0.1 to 1. Figure 4.6 is generated by individually vary G_1, G_2 and S between 0.01 and 0.8.

Secondly, we calculate the minimum attenuation γ^* for nine real 4-stage structured PPM's (found in Appendix A1), for all combinations of B and D. To calculate the attenuation we require that the PPM is stable, so we choose PPM's with dominant eigenvalue less than one. These results for the minimum attenuation are shown in Figure 4.7.

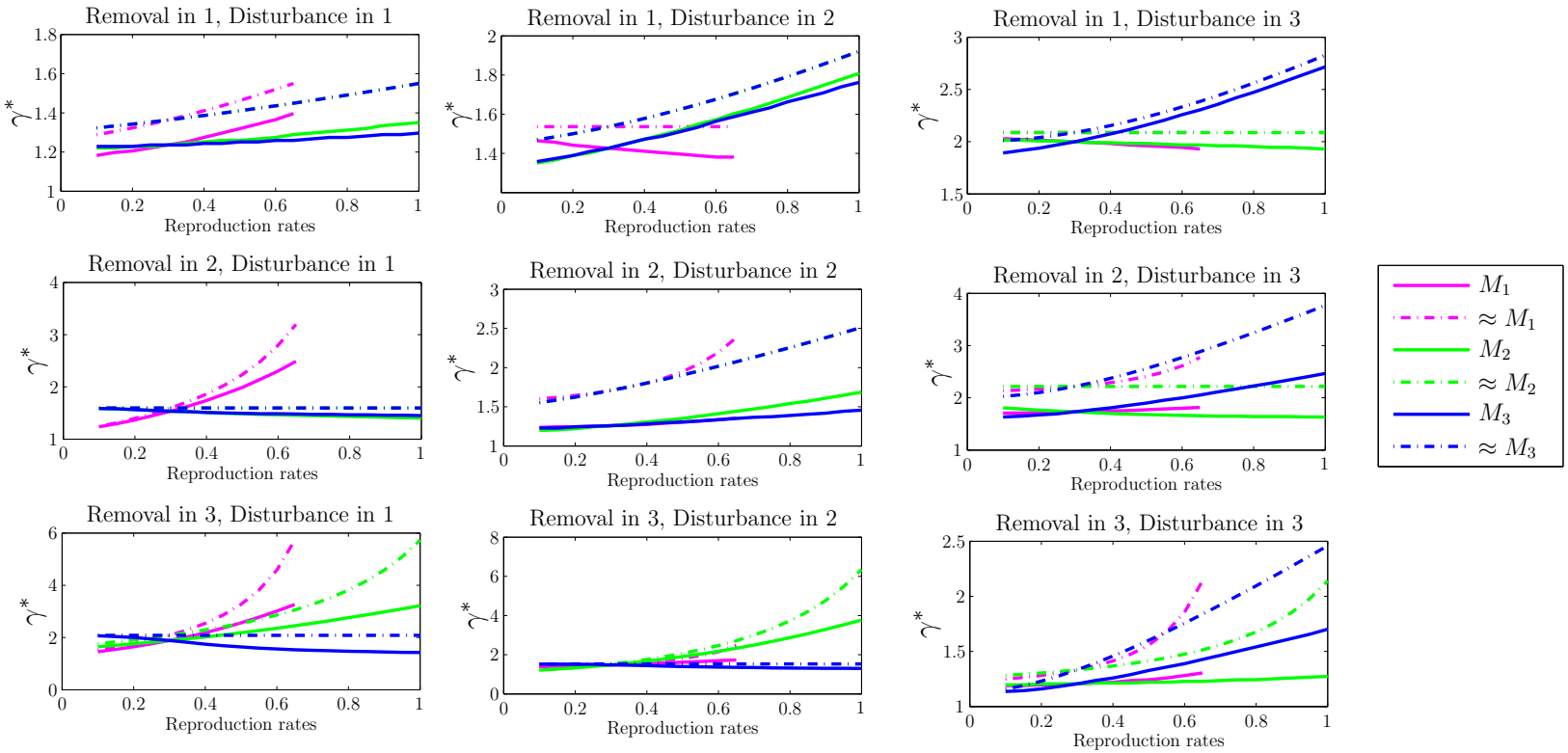

Figure 4.5: Effect of reproduction rate in each stage on minimum attenuation γ^* and γ_{approx}. The solid lines (denoted M_1, M_2 and M_3) give γ^* for varying the three fecundity rates, and the dashed lines (denoted $\approx M_1$, $\approx M_2$ and $\approx M_3$) shows γ_{approx} (equation (4.30)) for varying the three fecundity rates.

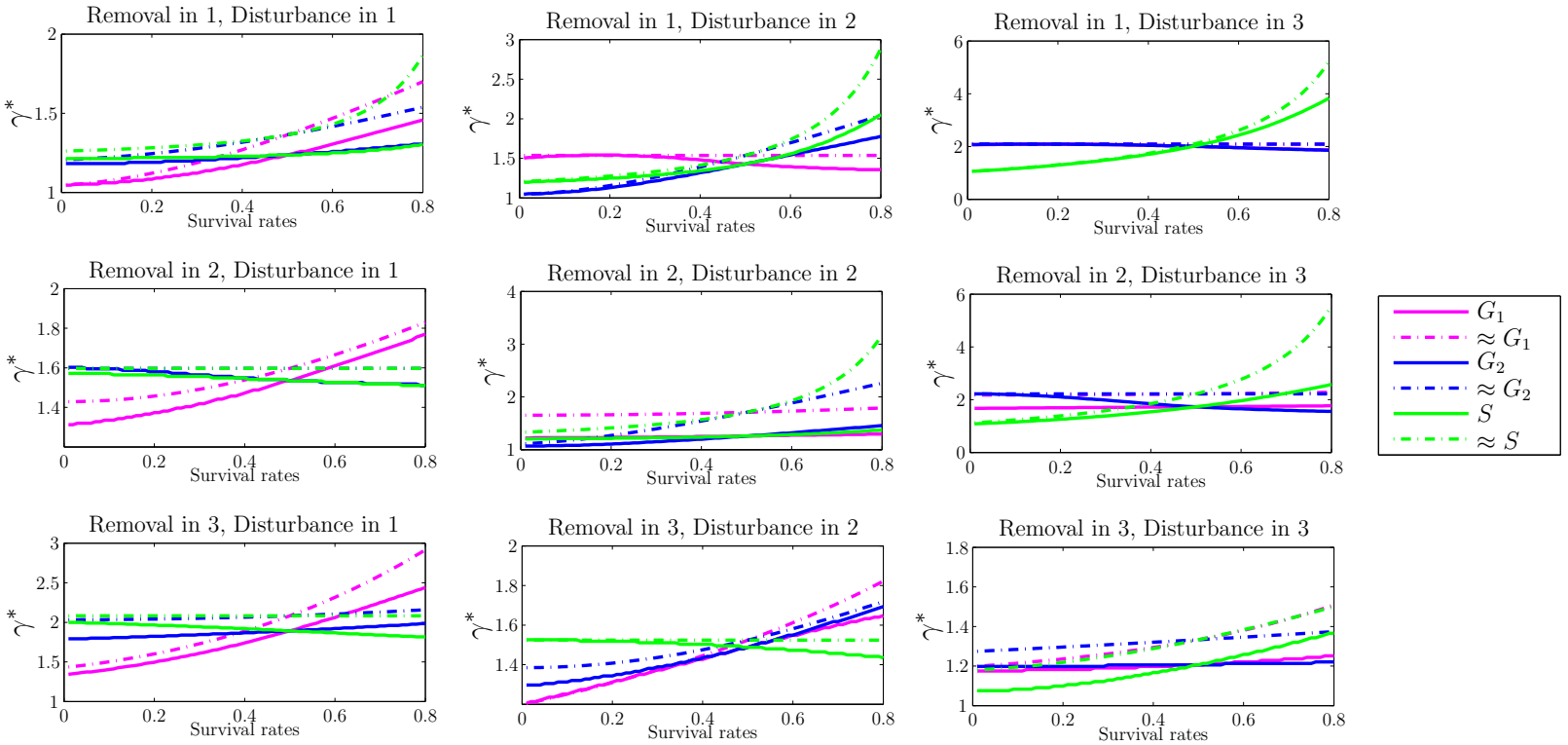

Figure 4.6: The effect of survival and growth rates on the minimum attenuation γ^* and γ_{approx}. The solid lines (denoted G_1, G_2 and S) give γ^* for varying survival and growth rates, and the dashed lines (denoted $\approx G_1$, $\approx G_2$ and $\approx S$) shows γ_{approx} (equation (4.30)) for varying survival and growth rates.

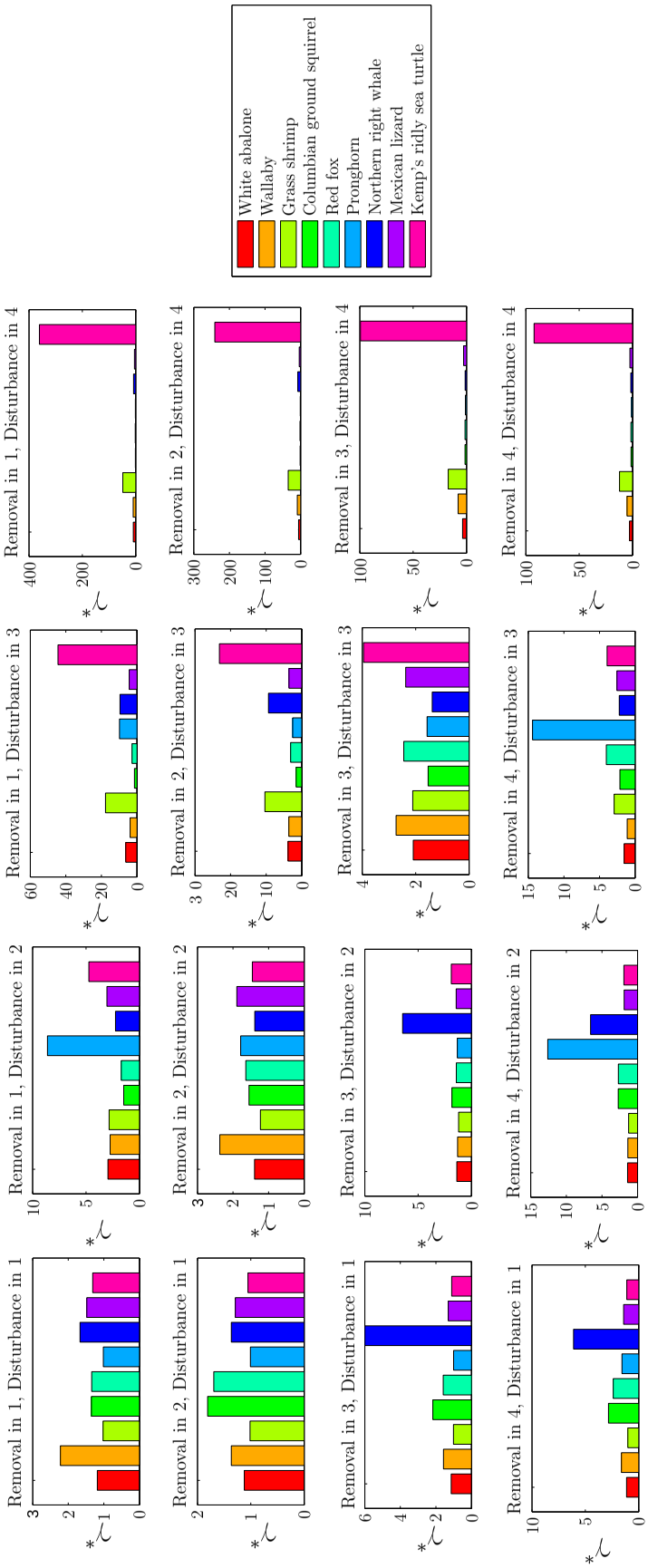

Figure 4.7: The minimum attenuation achieved for each choice of B and D for 9 real PPM's with 4 stages (see Appendix A1).

4.4 Discussion

4.4.1 Dynamic Linear Quadratic Game

As we chose $\gamma = \gamma^*$ such that constraint (4.17) holds, then as stated in Section 4.2.1 the optimal solution for u and d form a saddle-point. This means the solution is a Nash equilibrium solution such that

$$\max_d(\min_u(J_\gamma(u,d))) = \min_u(\max_d(J_\gamma(u,d))).$$

This is different to the results in Chapter 3, which use linear programming, where the optimal h and worst case d do not form a Nash equilibrium.

Unlike in the linear programming problem in Chapter 3, where the population is constrained to be non-negative, here we have not built constraints into the dynamic game. So using the Riccati equations to find the saddle-point solution for u and d does not constraint the population to be non-negative. Therefore, as can be seen in Figures 4.2 and 4.3 that the populations resulting from the control strategy, u, and disturbance, d, can become negative in some stages and at some time steps.

In general it can be seen that when $B = D$, the optimal removal strategy is able to remove what is added by disturbance. This is very similar to the results found in Chapter 3.

In Section 4.3.1 we used the minimum γ satisfying the constraint (4.17), which as explained in Section 4.2.2, is the solution to the minimum attenuation problem. These values of minimum attenuation for (4.3) are given in Table 4.1. As the attenuation problem allows negative populations, we calculate the disturbance attenuation given that the control strategy is constrained such that the population in each stage class is positive for all time steps. Whilst developing a dynamic game approach with non-negative constraints is beyond the scope of the thesis we can develop approximations which do account for non-negativity using the steady state gain, stated in Proposition 1. Here we outline two possible choices for F, which ensure non-negativity.

(Removal,Disturbance)	γ^*	γ_{opt}	γ_{sub}
(1,1)	1.1522	1.2689	1.2689
(1,2)	2.6259	3.5209	3.5742
(1,3)	43.1318	56.0592	57.6055
(1,4)	2.0376	2.5149	2.5735
(2,1)	1.1118	1.1724	1.1724
(2,2)	3.3448	4.1454	4.1454
(2,3)	61.6981	67.5363	67.5363
(2,4)	2.7297	2.9545	2.9545
(3,1)	1.0864	1.2459	1.2459
(3,2)	1.0529	1.1180	1.1180
(3,3)	58.5545	71.7658	71.7658
(3,4)	2.6097	3.1189	3.1189
(4,1)	1.1258	4.2238	4.2238
(4,2)	2.0170	14.7039	14.7039
(4,3)	58.7653	243.2699	243.2699
(4,4)	2.6160	10.0655	10.0655

Table 4.1: Disturbance attenuation for different removal strategies, with removal and disturbance in each stage class.

Firstly, consider the control strategy, used in Section 4.3.2, which removes as much as possible from any stage. So for a given $B_i = e_i$ let F be A_i, which denotes the i^{th} row of A. Then using that $F = A_i$ and equation (4.30) for γ_{approx} we calculate the minimum attenuation for each B_i and D_j, which we denote γ_{sub} (shown in Table 4.1).

Secondly, we calculate F which minimises γ_{approx} such that for any choice of B_i, F is constrained such that

$$[0, 0, ..., 0] \leq F \leq A_i$$

where A_i is the i^{th} row of A. For a given B_i and D_j having used `fmincon` to calculate F which minimises γ_{approx}, we use equation (4.30) to calculate the attenuation level corresponding to this optimal removal strategy, denoted γ_{opt} in Table 4.1. This gives the smallest possible γ which ensures non-negativity of the population.

Comparing the levels of attenuation shown in Table 4.1 for different choices of F, it can be seen, as expected, that γ^* forms a lower bound, for all combinations of B and D. Examining the difference between γ^* and γ_{opt} it can be seen that the relative difference

is much greater when removal occurs in the fourth stage class. Figures 4.1-4.4 show that for γ^*, the resulting population is more negative when removal occurs in the fourth stage class. This means that for our model and B_4, γ^* is a poor approximation of the attenuation which would be achievable if the control strategy was constrained to keeping a non-negative population in all stages. Interestingly, when the removal occurs in the first stage class then γ_{opt} may be smaller than γ_{sub}. This means that the minimum level of attenuation, with non-negative population, is not achieved by the removal strategy, u, removing the entire population available in all stages.

4.4.2 Disturbance attenuation

As discussed in Section 4.4.1 the minimum γ which satisfies the constraint (4.17) does not ensure that the resulting population is non-negative in each stage class. Therefore, in Figures 4.5 and 4.6 we compare the minimum attenuation, γ^*, with an approximation calculated using the steady state gain which ensures a non-negative population, although the removal strategy may not be optimal.

Figure 4.5 shows γ^* and γ_{approx} when varying the three reproductive rates, for each B_i and D_j. Notice that for all choice of B_i and D_j, the γ^* intersect at a reproductive rate of 0.3. This is due to the choice of the other reproductive rates at 0.3, and therefore each reproductive rate A is the same at 0.3, as $M_1 = M_2 = M_3 = 0.3$. As the fecundity rate increases, γ^* also increases. This is because with larger reproduction the amplification of any disturbance in the system will be greater. The increase in fecundity has the greatest effect on disturbance attenuation when removal acts in the third stage and disturbance acts in the second stage class. This is because if the second stage has higher fecundity and the disturbances acts in this stage, then the disturbance is amplified and produces a larger population in the first stage. However as the removal acts in the third stage class it is not able to remove the disturbance or the increasing population in the first stage class. For each choice of B_i and D_j, the approximate attenuation given by γ_{approx} forms an upper bound for γ^*. In general there is little difference between γ^* and γ_{approx}. However, the difference could be because γ^* allows a negative population or because γ_{approx} is not the optimal removal strategy.

Figure 4.6 shows γ^* and γ_{approx} for varying growth and survival rates in the simple 3-stage PPM. For each B_i and D_j, γ^* intersect when the growth or survival rate is 0.5. This is due to the choice of fixed parameters such that $G_1 = G_2 = S = 0.5$, and therefore at this choice of survival and growth rate the resulting PPM's are equal. In general as G_1, G_2 and S increase, γ^* also increases. This is unsurprising as increased survival means that any individuals added by disturbance remain in the population for more time steps. This increase in attenuation as survival increases is particularly prevalent when the removal is in the first stage and disturbance in the third stage class. This is because when disturbance occurs in the third stage with higher survival it remains in the third stage for longer, and removal in the first stage can not remove the disturbance. When removal is in the first stage and disturbance in the second stage then as G_1 increases then γ^* decreases slightly. Also, for removal in the third stage and disturbance in the second stage as S increases then γ^* decreases. This is likely to be because the attenuation allows a negative population. Similar to Figure 4.5, γ_{approx} forms a upper bound for γ^*. For the choices of B_i and D_j where γ^* has a decreasing relationship, as discussed above, then the corresponding approximation is constant for varying growth or survival rate. This means that in these cases γ_{approx} is independent of these parameters.

Figure 4.7 shows the minimum attenuation for nine real 4-stage structured PPM's, with removal and disturbance into each combination of stage classes. It can be seen that for some species, the stage class in which disturbance and removal occur has little effect on the disturbance attenuation, for example wood frog and wallaby. However, for some species, the stage class in which the disturbance acts has a significant affect on the disturbance attenuation. A couple of examples include:

- *Lepidochelys kempi* (Kemp's ridly sea turtle): For a disturbance acting in the fourth stage class, the disturbance attenuation is much larger than when it acts in the other stage classes, regardless of which stage the removal occurs. The PPM for the Kemp's ridly sea turtle, found in Appendix A1, shows that the fecundity rate in the fourth stage class is particularly high at ≈ 86, and the survival rate in the fourth stage class is also high at ≈ 0.82. This means that when disturbance acts on the fourth stage class, not only is the added population able to reproduce in the first time step but the majority of the individuals survive and are able to reproduce in following time steps, thus amplifying the population.

- *Antilocapra americana* (Pronghorn): The disturbance is amplified when disturbance enters in the third stage when removal acts in the fourth stage. As shown in Appendix A1, the PPM we use for Pronghorn only has reproduction in the third stage class. Therefore, when disturbance enters the population in the third stage class, and removal acts in the fourth stage, then the disturbance is amplified as the added population reproduces but removal in the fourth stage class would not have a large affect the population size.

4.5 Conclusion

In this chapter we have introduced the use of a 2-player game into ecology, which is a natural problem to solve as a Nash equilibrium exists. We used a discrete-time Riccati equation to find the solution to a 2-player game, with a quadratic cost function. The solution to the 2-player game forms a Nash equilibrium so that minimax = maximin. This is in contrast to the linear programming used in Chapter 3 which showed that the order in which the control and disturbance act affects the solutions, such that minimax $\geq$ maximin.

In particular, the solution to the disturbance attenuation problem is useful in ecology as it gives an upper bound on how disturbance is amplified in a system. However, the 2-player game does not prevent a negative population. So more work is required to create the theory which would ensure non-negativity. Creating this theory is beyond the scope of this thesis. As a compromise we calculate the attenuation for suboptimal removal strategies which satisfy the constraint that the population is non-negative. For most choices of parameters this suboptimal level of attenuation is close to the minimum attenuation given by the 2-player game, γ^*. This means that although γ^* does not necessarily satisfy the non-negativity constraint it can be used as a proxy to measure the amplification of the disturbance by the system. As can be seen in Table 4.1, for some choices of parameters, γ^* is not an accurate approximation. This is because the population becomes negative, reinforcing the need to create a framework which ensures the non-negativity constraint is satisfied.

As discussed in Section 4.1, Greenman and Benton [47] explore how the frequency of a disturbance changes within a system. If the power spectrum of a coloured noise disturbance is known then the framework created by the Riccati equations and H^∞ can be adapted and used to calculate the maximum attenuation of the coloured disturbance [140]. From this it would be possible to explore how the vital rates of a population would adapt if the population is continuously affected by coloured noise.

Chapter 5

Population inertia and invasion in stochastic models

5.1 Background

In this chapter we examine the effect stochasticity has on an invading population. In particular, we build on the work of Guiver et al. [49] by studying the relationship between population inertia and Allee effect for three models with varying levels of stochasticity.

What is invasion?

Invasion by a non-native species can have a huge effect on biodiversity. Therefore since the 1980's there has been a rapid increase in researching invasion biology. Publications include [81], [131] and [18] which concentrate on the impact of invasive species and whether management is required in different types of Nature Reserves, for example islands and tropical savannas.

Sometimes the effect of invasive species can be *"initially subtle and take a long time to be manifested"* [115]. However, waiting for an impact to occur before responding could have extreme consequences as it may be no longer possible to eradicate the invader. For example, invasive species are the sole cause of 20% of animal extinctions [29].

The definition of invasion is highly contested by ecologists. Indeed, there are many different terms used to describe an invasive species which include alien species, non-native, exotic and non-indigenous [106]. Larson et al. [73] state that *"most conservation biologists would agree that the spread of non-native species is undesirable and should be prevented whenever possible"*. However some ecologists, for example Davis et al. [32], state *"the practical value of the native-versus-alien species dichotomy in conservation is declining, and even becoming counterproductive."* Davis et al. define a species to be invasive or non-invasive depending on its negative impact on the environment instead of whether it is non-native of not. But it is difficult to determine whether a species is native or non-native and if it has a negative impact on the environment. Firstly, it is hard to define whether a species is native, because it depends when and how it was introduced into its current habitat. Many people believe a species is only non-native if it is introduced by humans, either intentionally or accidentally [102]. Chew and Hamilton [28] conclude that the *"categorical meaning and significance [of nativeness] both dissolve under scrutiny."* The authors continue: *"Biotic nativeness is theoretically weak and internally inconsistent, allowing familiar human desires and expectations to be misconstrued as essential belonging relationships between biota, places and eras. We believe much well-intended effort is wasted on research contrasting 'native' and 'alien' taxa"*. Therefore it is difficult to define if a species is native or non-native. Secondly, it is also difficult to establish whether a species has a negative impact on the environment. For example in Polynesia the rats on the islands are seen as both a source of food and a scourge [116].

Although, a clear definition of an invading population does not exist, it is undisputed that if a non-native species is having a negative impact on the environment or biodiversity then a strategy to manage the invader must be used. Therefore it is very important to be able to predict whether a population will 'invade'.

How to predict invasion?

A sensible starting point for invasion is to suppose a "resident" in equilibrium. So we start with a resident only model:

$$x(t+1) = F(x(t))x(t). \tag{5.1}$$

An equilibrium of equation (5.1), denoted x^*, is such that $x^* = F(x^*)x^*$. The linearisation around this equilibrium, denoted by A_R, is given by

$$A_R = \left.\frac{\partial(F(x)x)}{\partial x}\right|_{x=x*}.$$

In the context of invasion analysis it is reasonable to assume that x^* is stable in the absence of an invader. The equilibrium x^* is stable when the dominant eigenvalue of A_R is less than 1. Now to analyse invasion, we combine equation (5.1) with invasion dynamics to give a coupled resident-invader system of the form

$$\begin{pmatrix} x \\ z \end{pmatrix}(t+1) = \begin{pmatrix} F(x(t), z(t))x(t) \\ G(x(t), z(t))z(t) \end{pmatrix}, \tag{5.2}$$

where $x(t)$ and $z(t)$ are the resident and invader populations at time t, respectively, and F and G are non-negative functions of $x(t)$ and $z(t)$. Then the linearisation around the resident only equilibrium $x = x^*, z = 0$ in the coupled system (5.2) is given by

$$\left.\frac{\partial \begin{pmatrix} F \\ G \end{pmatrix}}{\partial \begin{pmatrix} x \\ z \end{pmatrix}}\right|_{(x*,0)} = \begin{bmatrix} \frac{\partial(F(x))}{\partial x} & \frac{\partial(F(x))}{\partial z} \\ \frac{\partial(G(z))}{\partial x} & \frac{\partial(G(z))}{\partial z} \end{bmatrix}_{(x^*,0)}.$$

Using the notation from the resident only population then we can define

$$\mathcal{M} = \begin{bmatrix} A_R & \mathcal{A} \\ 0 & A_I \end{bmatrix},$$

which is an upper triangular block matrix. As we have already assumed that $\lambda(A_R) < 1$,

$\mathcal{M}$ is stable if and only if $\lambda(A_I) < 1$, where $\lambda(A_I)$ denotes the dominant eigenvalue of A_I.

The so-called invasion exponent was introduced in [101], as the logarithm of the maximum eigenvalue of the linearisation $\mathcal{M}$ around the resident only equilibrium. The invasion exponent, $\bar{I}$, for the general resident-invader dynamical system is given by

$$\tilde{I} = \log(\lambda(A_I)) \quad \text{where} \quad A_I = \left.\frac{\partial(Gz)}{\partial z}\right|_{(x^*,0)}.$$

If the invasion exponent is positive then invasion is predicted to occur, and when it is negative then invasion should fail.

However, the initial conditions affect whether an invasion attempt will succeed. If the initial conditions are "close enough" to the resident only equilibrium and $\tilde{I} < 0$, then the population will tend towards the stable resident only equilibrium and the invasion attempt will fail. In this case the initial conditions are in the basin of attraction of the resident only equilibrium. In fact, it is the basin of attraction that determines whether invasion will occur rather than $\tilde{I}$. If the initial conditions are in the basin attraction of the resident only equilibrium then the invasion attempt will fail, whereas if the initial conditions are not in the basin of attraction then invasion may occur. So, ideally we would calculate the basin of attraction to determine the outcome of an invading population. However, such basin of attraction calculations are non-trivial, not least because this basin of attraction is a subset of $\mathbf{R}^{2n}$ where n is the number of stages in the population.

5.2 Preliminaries

In [49] we explore how reliable the invasion exponent (described in Section 5.1) is for predicting invasion. In [49] and throughout this chapter we use a coupled resident-invader model given by

$$x(t+1) = (G_R + \phi(N(t))df^T)x(t), \tag{5.3}$$

$$z(t+1) = (G_I + \phi(N(t))df^T + \alpha(N_z(t), s)bc^T)z(t), \tag{5.4}$$

where G_R, G_I are $n \times n$ non-negative matrices, b, c, d and f are non-negative, non-zero vectors of length n and α and ϕ are non-negative continuous functions. Here $N(t) = \|x(t)\|_1 + \|z(t)\|_1$ is the total population at time t, and $N_z(t) = \|z(t)\|_1$ is the total invader population at time t. The $\phi(N(t))df^T$ term represents density dependent fecundity for both the invader and resident population, whilst the density dependent function affecting the invader, $\alpha(N_z(t), s)bc^T$, acts as an Allee effect penalising the invader fitness for small invader populations. Taylor and Hastings [127] discuss the importance of using Allee effects when considering invasive species. An Allee effect is a density dependent function such that some aspect of the fitness decrease at low density. As invasion attempts often initially have a small population then the addition of an Allee effect can greatly affect the dynamics. In [49], ϕ is similar to a Beverton-Holt type function, as illustrated in Figure 5.1, and α is a function of Ricker type, as illustrated in Figure 5.2. Then if the model is given by equations (5.3) and (5.4) we find that invasion can occur even when the invasion exponent is negative. Moreover we find there is no relationship between the invasion exponent and the smallest Allee effect, s, required for invasion. Instead we find a link between successful invasion and

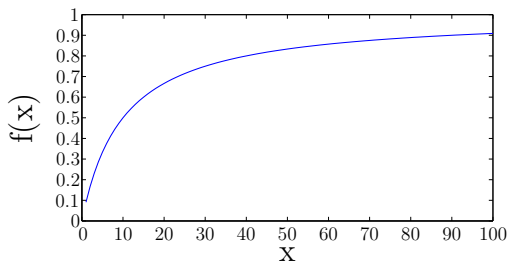

Figure 5.1: An example of Beverton-Holt function

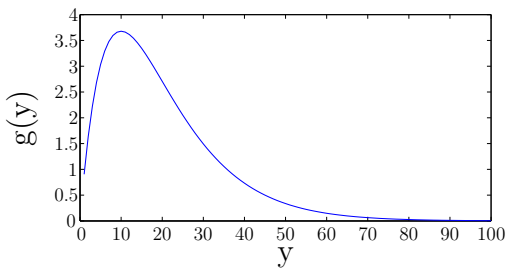

Figure 5.2: An example of Ricker function

the population inertia of the invasion attempt. Population inertia is used as measure of the transient dynamics. For a given PPM A_{inv} and a population structure given by z_0, population inertia is

$$\frac{v^T z_0}{v^T w},$$

where v^T and w are the left and right eigenvectors of A_{inv}, respectively, corresponding to the dominant eigenvalue of A_{inv}. In [49] and throughout this chapter we let A_{inv} be given by the linearisation of the invader population around the resident only equilibrium is given by

$$A_{inv} = G_I + \phi(0.1 \times p)df^T + \alpha(0)bc^T. \tag{5.5}$$

Remark. *Notice that the population inertia scales with $\|z_0\|_1$ and therefore to be able to compare the population inertia for two initial conditions, z_0 and y_0, when we calculate the population inertia we first scale the initial conditions such that $\|z_0\|_1 = \|y_0\|_1 = 1$.*

We find there is monotonic decreasing relationship between the population inertia and the minimum Allee effect, s, required for invasion to occur. An example of this general inverse relationship is shown in Figure 5.3. This decreasing relationship gives a lower bound for the combination of population inertia and Allee effect required for invasion, provided the initial density remains the same then for all choices of population inertia and Allee effect above this curve an invasion attempt would be successful. In this chapter we explore whether this inverse relationship between population inertia and Allee effect holds for a stochastic invasion model.

The results in [49] are for deterministic models with "infinite N". It is well known that finite models can give rise to substantially different results to those of infinite models. Boland et al. [16] and Dauxois et al. [31] explore the difference between the models by finding a finite correction term which when added to the finite population model gives the same results as the infinite model. Here we apply two ways to make the system given by equations (5.3), (5.4) into a finite population model. Firstly, the density dependent functions can be defined by finite approximations to the deterministic equations for ϕ and α. To create these finite approximations we use patch-based density dependent functions. Secondly, the survival, growth and fecundity rates can be made stochastic so that the entries of G_R, G_I and f are distributed around the values used in the deterministic model.

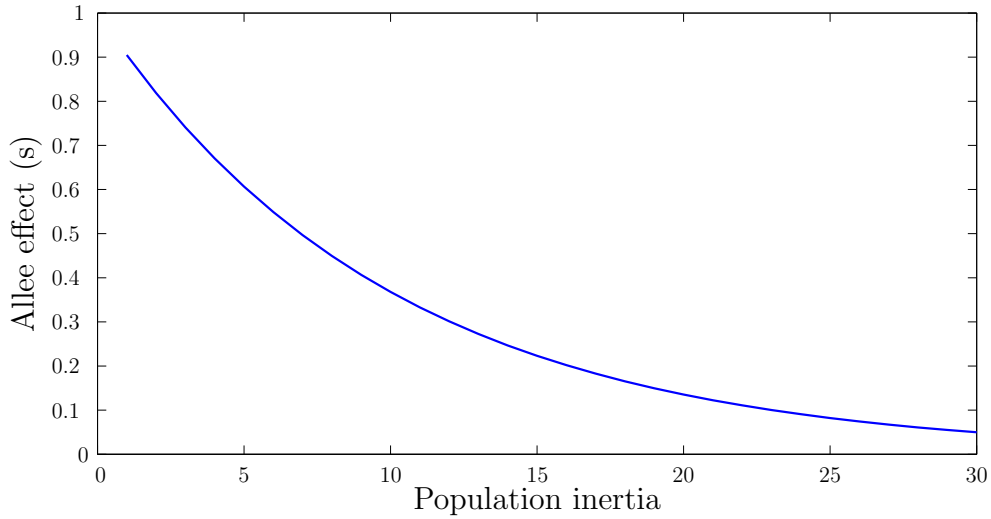

Figure 5.3: An example of the inverse relationship found in [49] between population inertia and minimum Allee effect required for invasion, above which invasion of the same initial density will succeed.

5.3 The inverse relationship between population inertia and invasion

In this chapter we investigate how having either a finite population or stochastic demography affects the likelihood of invasion, as indicated by population inertia. To do this we first define both the patch-based density dependent functions and stochastic demography in Section 5.3.1. Then we explore the effect of having a finite population on the relationship between population inertia and Allee effect. Section 5.3.2 gives the results for each of the three finite population models. Section 5.3.3 will discuss and compare the results.

5.3.1 Models

The deterministic model considers a discrete-time invading population, which is given by equations (5.3) and (5.4). We use a three stage structured model so that

$$G_R = \begin{pmatrix} 0 & 0 & 0 \\ 0.1 & 0 & 0 \\ 0 & 0.1 & 0.1 \end{pmatrix}, \quad G_I = \begin{pmatrix} 0 & 0 & 0 \\ 0 & 0 & 0 \\ 0 & 0.1 & 0.1 \end{pmatrix}, \quad d = \begin{pmatrix} 1 \\ 0 \\ 0 \end{pmatrix}, \quad b = \begin{pmatrix} 0 \\ 0.1 \\ 0 \end{pmatrix}, \tag{5.6}$$

$$f^T = [f_1\ f_2\ f_3] \quad \text{and} \quad c^T = [1\ 0\ 0],$$

where f is the fecundity vector and f_1, f_2 and f_3 are defined below. This section describes the framework and parameters needed to create the three models, these components of the model are;

- Creating the fecundity vector
- Initial conditions
- Invasion threshold
- Patch-based density dependent functions
- Demographic stochasticity.

Creating the fecundity vector

We assume that the matrices G_R and G_I are fixed, as given by equation (5.6). To create populations with a range of population inertias, different fecundity vectors f are generated. As only f changes, the stable stage structure remains the same. To see this, consider a model of the form

$$x(t+1) = (G_R + \phi(N(t))df^T)x(t),$$

where $x(t)$ is the population at time t, G_R is a matrix containing survival and growth rates, $b = [1\,0\ldots0]^T$ and f is a vector containing the fecundity rates. The equilibrium, denoted x^*, is given by

$$x^* = G_R x^* + \phi(N^*)df^T x^* = \phi(N^*)(I - G_R)^{-1}df^T x^*,$$

as $f^T x^*$ is a scalar the fecundity does not affect the structure of the equilibrium, x^*. As the effect of having a finite population is dependent on the size of the population we introduce a variable p, and we scale f so that the resident only equilibrium of the resident-invader system is dependent on p. We do this by scaling f such that

$$\phi(0.1 \times p)f^T(I - G_R)^{-1}d = 1,$$

then the total size of the population at the resident only equilibrium is $0.1 \times p$.

We are focusing on the case when the invasion exponent is negative. As described in Section 5.1 this means that according to [101] invasion should fail. We use the same framework as [49] to find a condition to generate the fecundity vectors f such that the invasion exponent is negative. Recall, the invasion exponent is the logarithm of the maximum eigenvalue of the linearisation. For this model, the eigenvalues of the linearisation are determined by the eigenvalue of A_{inv}, given in equation (5.5). We create the fecundity vectors f such that there is a range of population inertia and

$$0.94 < \lambda_{max}(G_I + \phi(0.1 \times p)df^T + \alpha(0)bc^T) < 0.96. \tag{5.7}$$

This constraint ensures that the maximum eigenvalue of the linearisation is less than 1, and so the invasion exponent, $\log(\lambda_{max}(A_{inv}))$, is guaranteed to be negative.

Initial conditions

We let the initial population of the resident be set at stable stage structure. This is scaled such that the total initial population of the resident is $\|x_0\|_1 = 0.1 \times p$, which by construction of the fecundity vector, is the population density at the resident only equilibrium. The initial density is dependent on the parameter p because in the finite models it is important to scale the size of the population. In the deterministic model the variables depend on p to allow a direct comparison between the models. There are many possibilities for specifying the initial population of the invader. To simplify the analysis, apart from when calculating the basins of attractions, the initial invader population is restricted to one stage class. First we choose z_0 to capture invasion only into the third stage with a given density $\|z_0\|_1 = 0.01 \times p$. Next, for each model, both the stage and density of the invader initial condition is varied, such that $z_0 = \delta e_i$ where $i = 1, 2, 3$ and for each i we consider four choices of δ. Finally, we calculate a small subset of the basin of attraction by varying the invader initial condition in the second and third stage.

Invasion threshold

A threshold is required to specify when the invader population is large enough to be deemed a successful invasion. After exhaustive simulations, this threshold is set at

$$N_z(600) > 0.25\|x_0\|_1,$$

that is if the density of the invader population at time $t = 600$ reaches a quarter of the total initial resident population. As the initial conditions are dependent on p this is equivalent to $N_z(600) > 0.025 \times p$. It was found that the population stabilises before 600 iteration steps are reached and therefore running the simulation for longer does not affect whether or not the threshold is reached.

It is also important to consider the survival of the resident population, as there may be equilibria with high densities of both populations or an equilibrium where both populations die out. The resident population is considered to have survived if at $t = 600$ the total resident population is over a quarter of the initial population. Analogous to the invader threshold, the resident threshold is given by

$$N_x(600) > 0.25\|x_0\|_1 = 0.025 \times p$$

where $N_x(t) = \|x(t)\|_1$ is the total resident population at time t.

Patch-based density dependent functions

As mentioned in Section 5.2, one way to develop a finite equivalent for the model given by equations (5.3) and (5.4), is to use finite approximations of the ϕ and α functions. In doing so, we create patch-based models that with large numbers of patches approximate accurately the deterministic ϕ and α functions. The patch-based models are defined in the following.

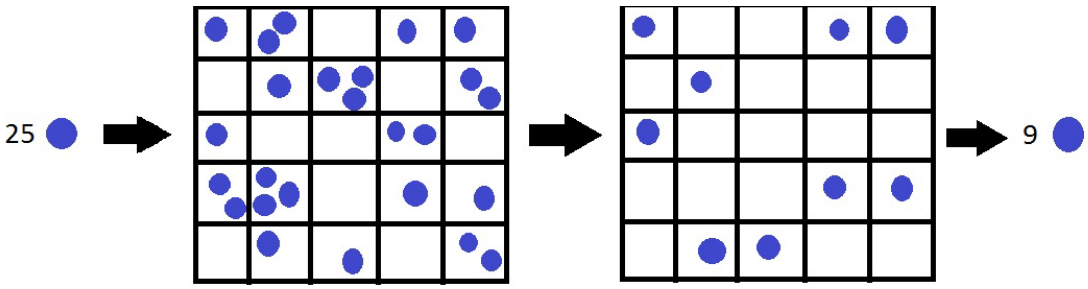

Figure 5.4: Illustration of scramble competition.

The ϕ function

In the experimental simulations that use patch-based density dependent functions, the approximate ϕ function is created by randomly distributing the population over p patches, where p is also used to create f and in the initial conditions. The whole population is "dropped" on a grid of patches. An individual survives and remains in a patch only if exactly one individual landed in the patch, as shown in Figure 5.4. We refer to this approximation method as "scramble". Then the resulting population is divided by the total population from the previous iteration step. So for the example in Figure 5.4 then $\phi(25) = \frac{9}{25}$. If the individuals are randomly dropped over the grid then the number of individuals in each patch form a Poisson distribution. Using the Poisson distribution to represent the number of individuals in each patch, then the scramble function can be approximated by

$$\phi(N(t)) = exp\left(-\frac{N(t)}{p}\right) \tag{5.8}$$

where $N(t)$ is the total population at time t and p is the number of patches. Figure 5.5 shows the ϕ function for different numbers of patches, by plotting $\phi(N(t))$ against $N(t)$. This shows that, as the number of patches increases, the patch-based function gives a better approximation of the deterministic function given by equation (5.8). Also, although the input values for ϕ are scaled by p this does not affect the output values. This means that although the population size will be scaled with p the density dependent effect on the fecundity will be the same.

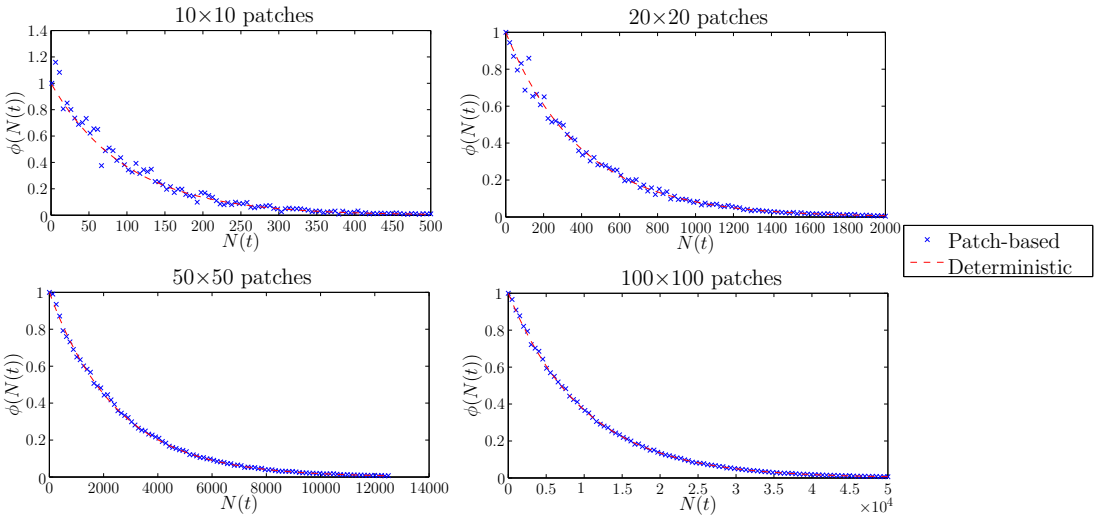

Figure 5.5: Comparing the patch-based ϕ function for 4 choices of p to the deterministic ϕ function given in equation (5.8).

The α function

The α function is created such that at low density the invader has a disadvantage, but if the invader population reaches a first threshold then the invader gains an advantage over the resident population, and when the invader population is much larger, above a second threshold, the invader has a disadvantage again. This means the function starts with values less than 1, increases to greater than 1 and then decreases to less than 1 again. To do this using a patch-based approximation, a function similar to scramble is used, where one individual survives in a patch if exactly three individuals land in the patch, as illustrated in Figure 5.6. The patch-based α function is given by

$$\alpha(N_z(t)) = 0.8 + s \times \frac{k}{\|N_z(t)\|_1},$$

where k is the output from the scramble and α is parametrised by s, which determines the magnitude of the Allee effect. Therefore, for the example shown in Figure 5.6 and assuming that $s = 3$, we obtain $\alpha(25) = 0.8 + 3 \times \frac{2}{25} = 1.04$. Requiring that exactly three individuals land in a patch means that at low input values the function does not increase too quickly. The α function is generated using scramble and is therefore dependent on the number of patches. For the initial conditions and ϕ function the number of patches is p. For $\alpha(N_z(t))$ we use a different number of patches given by $P = \frac{p}{25}$. This scaling of the number of patches means that the input value required for

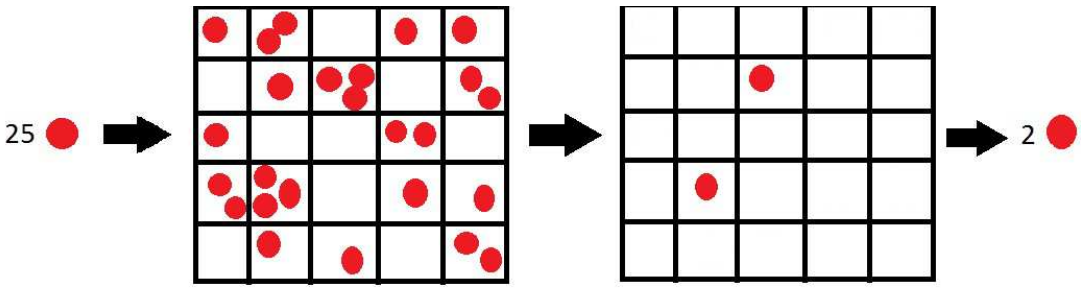

Figure 5.6: Illustration of patch-based competition required for α.

the function to get over 1 is much lower, so shifting the peak of the function. As with the ϕ function, assuming the population is dropped randomly over the patches, so the number of individuals in each patch form a Poisson distribution allows us to obtain the deterministic α function as

$$\alpha(N_z(t)) = 0.8 + s \times \left(\frac{P \times (\frac{N_z(t)}{P})^3}{6} \right) \times \frac{-exp(\frac{N_z(t)}{P})}{N_z(t)}, \tag{5.9}$$

where s determines the magnitude of the Allee effect.

Throughout this chapter we vary s to explore the affect the Allee effect has on invasion, therefore next we determine the largest s can be. As the growth rate from stage 1 to stage 2 can not be greater than 1, then $0.1 \times \alpha(N_z(t)) < 1$ which means a maximum s value can be found. To find the maximum s value we differentiate α with respect to $N_z(t)$, set this equation equal to 0 and solve for $N_z(t)$. This gives that α takes its maximum value when $N_z(t) = 2 \times P$. Substituting this value into $0.1 \times \alpha(N_z(t)) \leq 1$ gives that

$$0.1 \times \left(0.8 + s \left(\frac{P \times 2^3}{6} \times \frac{\exp(-2)}{2P} \right) \right) \leq 1.$$

Finally rearranging for s gives the maximum value which is independent of P, as

$$s \leq \frac{9.2 \times 6}{2^3 \exp(-2)} = 50.98.$$

The α function for different choices of P is plotted in Figure 5.7. This shows that as the number of patches increases, the difference between the patch-based approximation of α and the deterministic α given by equation (5.9) decreases.

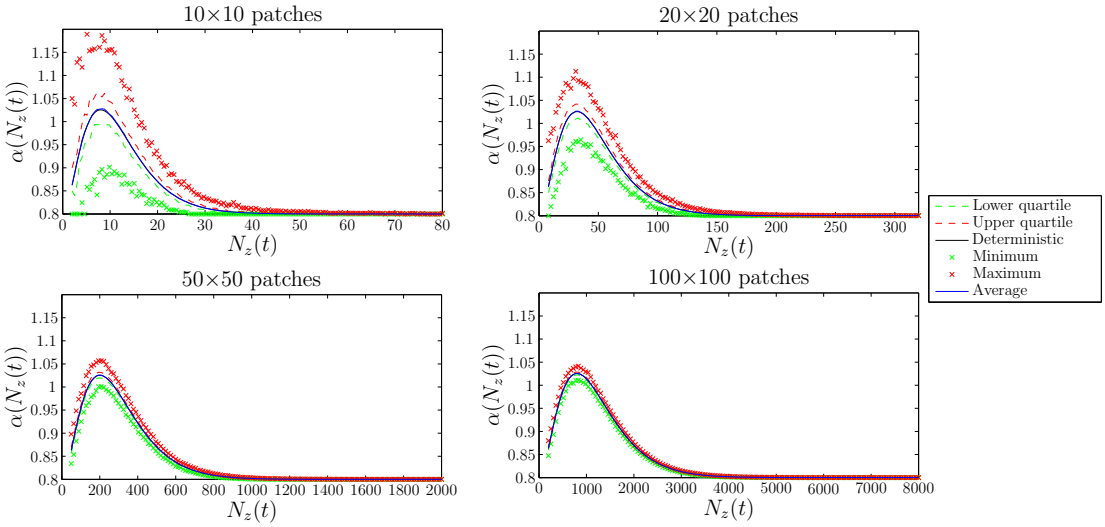

Figure 5.7: The maximum, minimum, average and quartile range for the patch-based α function and the deterministic α function given by equation (5.9) for four different P's with $s = 2.5$.

Demographically stochastic model

A second way to create a finite model is to allow stochastic vital rates as discussed in Chapter 1. The deterministic model assumes that all individuals behave the same. However in a real population for a given time, t, each individual behaves differently, which means that they have different survival, growth and fecundity. For example it is unlikely that every adult gives birth to exactly the same number of offspring during each time step. The values in a PPM are essential when considering deterministic population models. However when modelling a finite population the survival, growth and reproduction of each individual can vary. For each vital rate within a PPM, the real data which is collected forms a distribution around the mean vital rate. For the models which use stochastic demography, we use a Poisson distribution for the fecundity values, and the survival and growth rates of each individual are uniformly distributed around 0.1. The Poisson distribution and the uniform distribution require integer inputs and also output integers. This means that the initial conditions must be rounded. Rounding is also required when ϕ and α are used as the outputs are non integer valued.

Models	**Density-dependent functions (ϕ and α)**	**Population vital rates**
Deterministic case	Given by equations (5.8) and (5.9)	Fixed as given in equation (5.6)
Patch-based density dependent functions	Uses patch-based approximations illustrated in Figures 5.4 and 5.6	Fixed as given in equation (5.6)
Stochastic demography	Given by equations (5.8) and (5.9)	Poisson and uniformly distributed around values given in equation (5.6)
Patch-based density dependent functions and stochastic demography	Uses patch-based approximations illustrated in Figures 5.4 and 5.6	Poisson and uniformly distributed around values given in equation (5.6)

Table 5.1: The components used in each of our four models.

5.3.2 Results

This section explores the deterministic model and 3 finite N models. Table 5.1 shows the differences between the models. First, for each model we examine the relationship between population inertia and minimum Allee effect required for invasion as is discussed in Section 5.2. Second, we look at a small subset of the basins of attractions to see how they vary with maximum inertia, m, and Allee effect. We use maximum inertia rather than population inertia as a measure of transient dynamics, because population inertia is dependent on the initial conditions and within a basin of attraction the initial conditions vary, which means that population inertia cannot be used as a fixed measure of transients. The maximal inertia is given by

$$m = \frac{\|v\|_\infty}{v^T w}, \tag{5.10}$$

where v^T and w are the left and right eigenvectors of A_{inv} defined in Section 5.3.1. For our model the maximal inertia is bounded (see Appendix A3).

The experimental models do not give the same result for each simulation. This means that for a given population inertia, invasion does not occur at a certain Allee affect. Instead, we find the probability of invasion for a range of population inertia and Allee effect combinations. To calculate the probability of invasion for each combination we run 100 simulations and determine the proportion of successful invasions. The result is a colour-map of the likelihood of invasion, for a range of Allee effects and population inertia. The number of runs is chosen to be 100 as it was found that increasing the number of runs did not qualitatively change the results.

Deterministic case

As explained in Section 5.2, we found in [49] that there is a monotonic inverse relationship between the Allee effect required for invasion and the population inertia. As our model uses different ϕ and α functions to those in [49], we first recreate results similar to [49] by finding the minimum Allee effect required for invasion to occur for 12 different initial conditions, shown in Figure 5.8. This allows direct comparison between the infinite (deterministic) and finite models. Although the deterministic model given

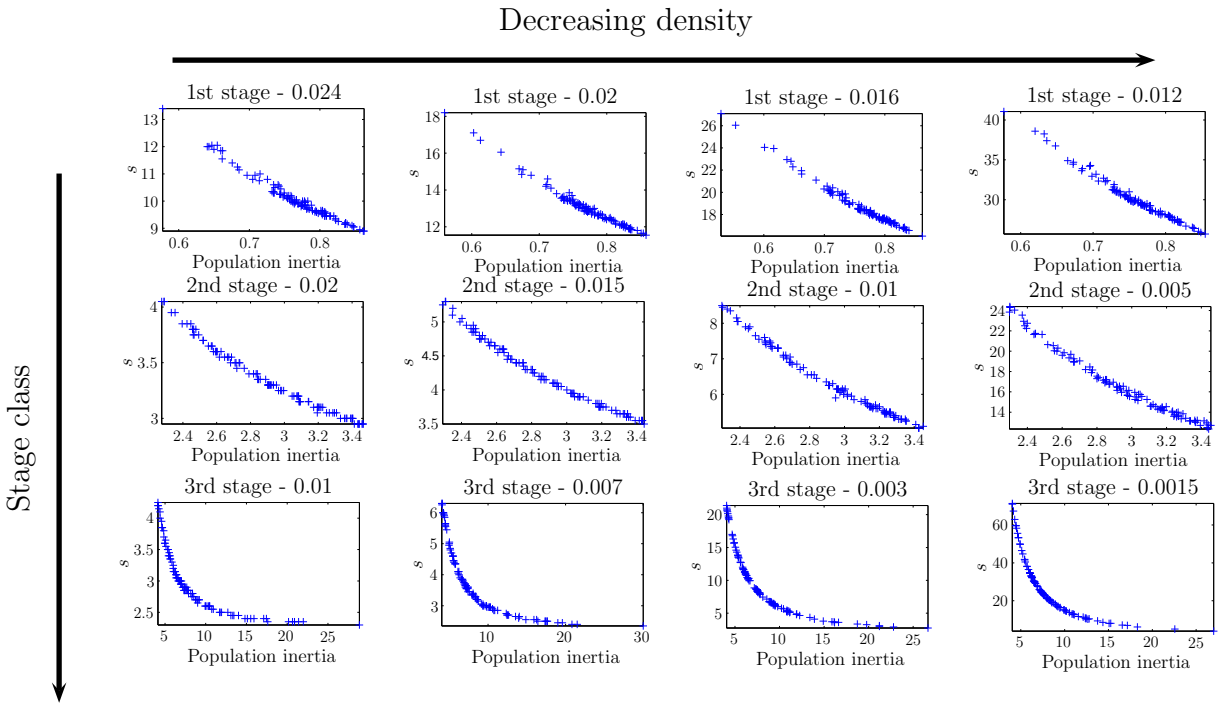

Figure 5.8: The effect of population inertia on the minimum s (determining the magnitude of the Allee effect) required for successful invasion for 12 different initial conditions of the invader. The values given in the title are scaled by p to give the initial condition in each stage class.

by equations (5.3) and (5.4) is not a finite model, the invasion threshold and the initial conditions depend on p. As we are using a deterministic model, for different values of p the population size and thresholds can be scaled by p to give the same results. Although the initial condition in Figure 5.8 are scaled by p, as the threshold for invasion is dependent on p, the Allee effect required for invasion is independent of p.

In Section 5.1 it was established that invasion fails when the initial conditions are in the basin of attraction of the resident only equilibrium. The basin of attraction for this model are 6 dimensional, and therefore difficult to calculate or visualise. So we look at a small subset by only varying two components of the initial conditions. The initial population of the resident remains at stable stage structure, and we choose to vary the second and third stage classes of the invader. We examine how this basin of attraction is affected by the Allee effect and maximum inertia. As population inertia is dependent on the initial conditions, which vary within the basin of attraction, we use maximum inertia defined by equation (5.10) as a measure of transients. Using simulations we compute the basin of attraction for 3 choices of maximum inertia and Allee effect, as shown in Figure 5.9.

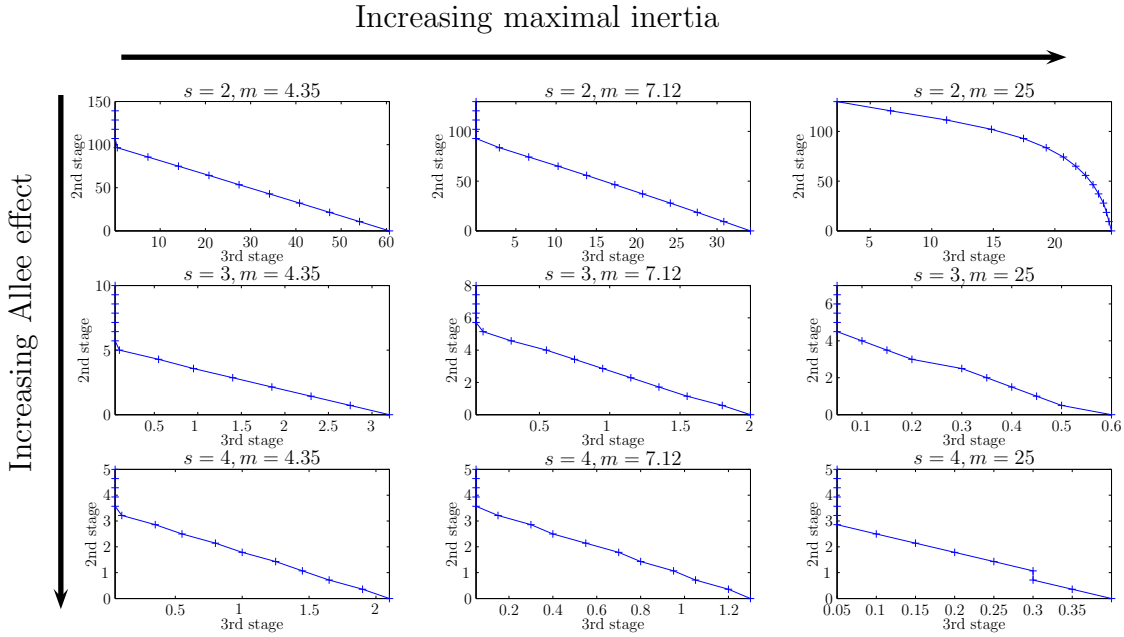

Figure 5.9: Varying the densities of the second and third stage of the invader initial condition to find the basin of attractions for 3 maximum inertia and 3 Allee effects in the deterministic model.

Patch based density dependent functions

Next we explore the effect a finite population has on the relationship between population inertia and the Allee effect required for invasion. To create a finite population model, we first use patch-based density dependent functions. The population now depends on the number of patches. Therefore, to examine the effect that p has, we choose the initial condition of the invader to be $0.01 \times p$ in the third stage class. Then calculating the probability of invasion for varying population inertia and Allee effect for 4 choices of p we obtain Figure 5.10. To allow comparison, the Allee effect required for invasion in the deterministic model is also shown by the white line. It is also important to consider the survival of the resident population. To do this we use the threshold given in Section 5.3.1 to find the probability that the resident survives for varying population inertia and Allee effect for the same 4 choices of p, to give Figure 5.11. We use a white line to represent the Allee effect where in the deterministic model the resident does not survive above the threshold.

At large numbers of patches the model with patch-based ϕ and α agrees perfectly with the deterministic model. However, when $p = 20 \times 20$ the models appear to give quite different results. So to allow direct comparison to Figure 5.8 we next consider 12 different initial conditions of the invader with $p = 20 \times 20$ to give Figure 5.12.

Finally, we calculate the basins of attraction for the model with patch-based ϕ and α for the same choice of maximum inertia and Allee effect as given in Figure 5.9. In the deterministic model, exactly one of the populations persist which means outside the basin of attraction of $(x^*, 0)$ the population will tend to $(0, z^*)$. However, as seen in Figures 5.10 and 5.11 this is not necessarily the case for the model with patch-based density dependent functions, as the $(0, 0)$ equilibrium is no longer necessarily unstable. Therefore, we calculate the probability of invasion for a range of initial conditions, which is equivalent to finding the basin of attraction of the combined equilibria $(0, 0)$ and $(x^*, 0)$, as we only care about the complement which is when invasion occurs. Choosing the number of patches to be $p = 20 \times 20$, we get Figure 5.13.

Stochastic demography

Recall, as discussed in Section 5.2 and shown in Figure 5.8, there is a monotonic decreasing relationship between population inertia and Allee effect. Next we examine if this relationship holds if stochasticity is added to the invasion model. To do this we consider a model with stochastic G_R, G_R and f as described in Section 5.3.1, and let the density dependent functions, ϕ and α, be given by equations (5.8) and (5.9). The model is not patch-based but the stochasticity in the matrix depends on the population size and therefore the initial conditions remain dependent on p. Therefore, similar to above we first explore the effect of p by fixing the initial conditions of the invader to be $0.01 \times p$ in the third stage class, and plot the probability of invasion for varying population inertia and Allee effect for 4 different choices of p to get Figure 5.14. Also, as before, it is important to consider the probability of survival of the resident population for varying population inertia and Allee effect for 4 values of p, which gives Figure 5.15.

As the number of patches substantially affects whether invasion occur, we consider 12 initial conditions of the invader for both $p = 20 \times 20$ and $p = 100 \times 100$ to give Figures 5.16 and 5.17, respectively.

Figure 5.14 shows, for this model with deterministic ϕ and α and stochastic G_R, G_I and f, that p has a huge affect on whether invasion occurs. Therefore we calculate the basins of attraction for $p = 20 \times 20$ and $p = 100 \times 100$, with the same choices of maximum inertia and Allee effect the previous models in Figures 5.9 and 5.13, this gives Figures 5.18 and 5.19.

Patch-based density dependent functions and stochastic demography

Next we calculate the probability of invasion for a model with patch-based models to generate ϕ and α and stochastic entries of G_I, G_R and f. First, we vary the number of patches, p, when the initial condition of the invader is $0.01 \times p$ in the third stage. Then the likelihood of invasion for a range of population inertia and Allee effects is given in Figure 5.20. We also find the probability of survival of the resident population for different numbers of patches when the initial invader population is in the third stage with density $0.01 \times p$, as shown in Figure 5.21.

Similarly to above, in the model with just stochastic vital rates, the number of patches has a large effect on the results. Therefore, we find the likelihood of invasion for 12 initial conditions of the invader when $p = 20 \times 20$ and $p = 100 \times 100$ in Figures 5.22 and 5.23, respectively.

Finally, we find the basins of attraction for the model with stochastic G_R, G_I and f values with patch-based ϕ and α. The basins of attractions are found for the same 3 choices of maximum inertia and Allee effect for $p = 20 \times 20$ and $p = 100 \times 100$ as shown in Figures 5.24 and 5.25.

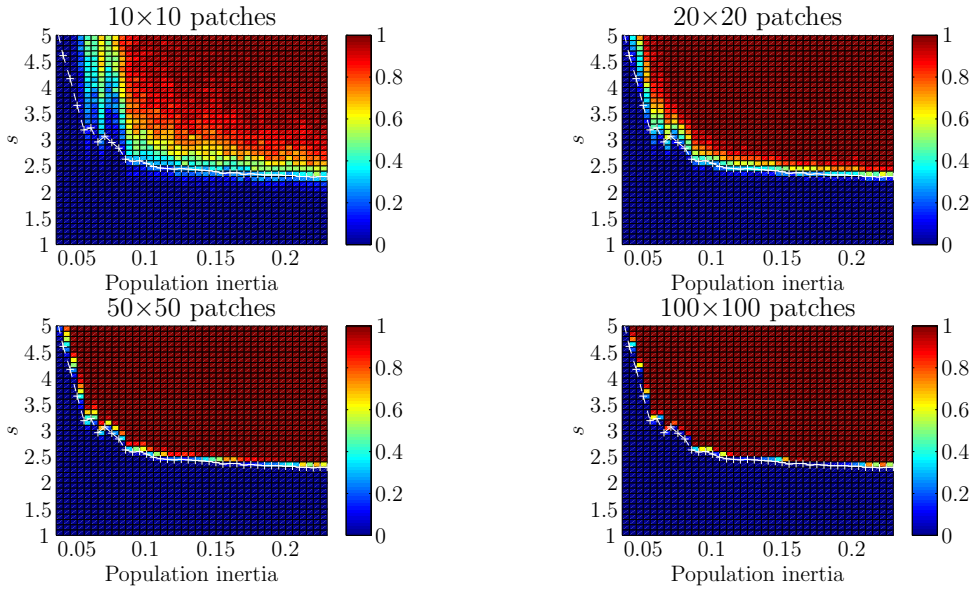

Figure 5.10: The probability of invasion for range of population inertia and s (determining the magnitude of the Allee effect) with 4 choices of p for model with patch-based ϕ and α. The white line indicates the minimum Allee effect required for invasion in the deterministic. The initial invader population is $0.01 \times p$ in the third stage class.

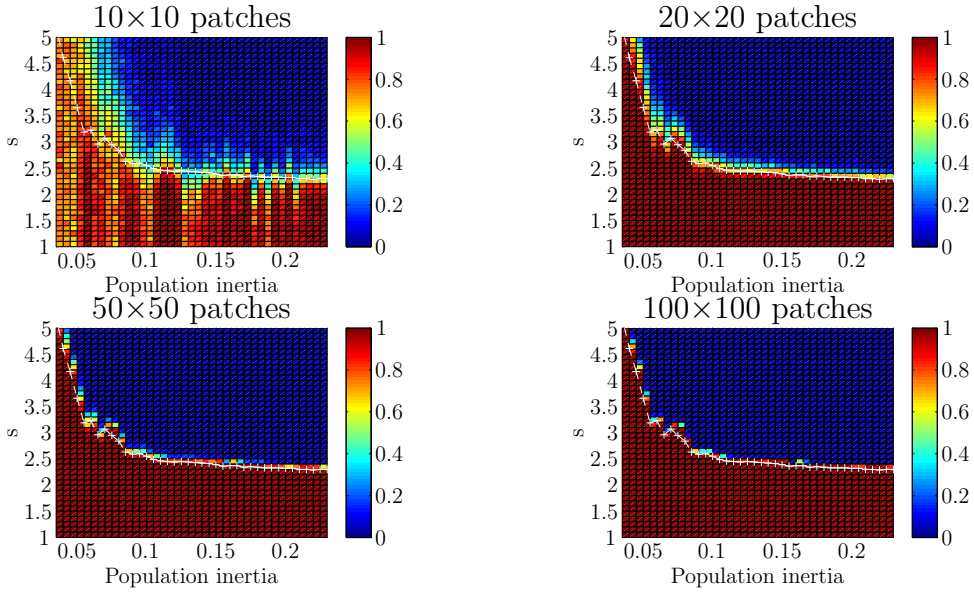

Figure 5.11: The probability the resident population survives for varying population inertia and s (determining the magnitude of the Allee effect) for 4 choices of p for model with patch-based ϕ and α. The white line gives the maximum Allee effect which gives survival of the resident in the deterministic model. The initial condition of the invader is $0.01 \times p$ in the third stage class.

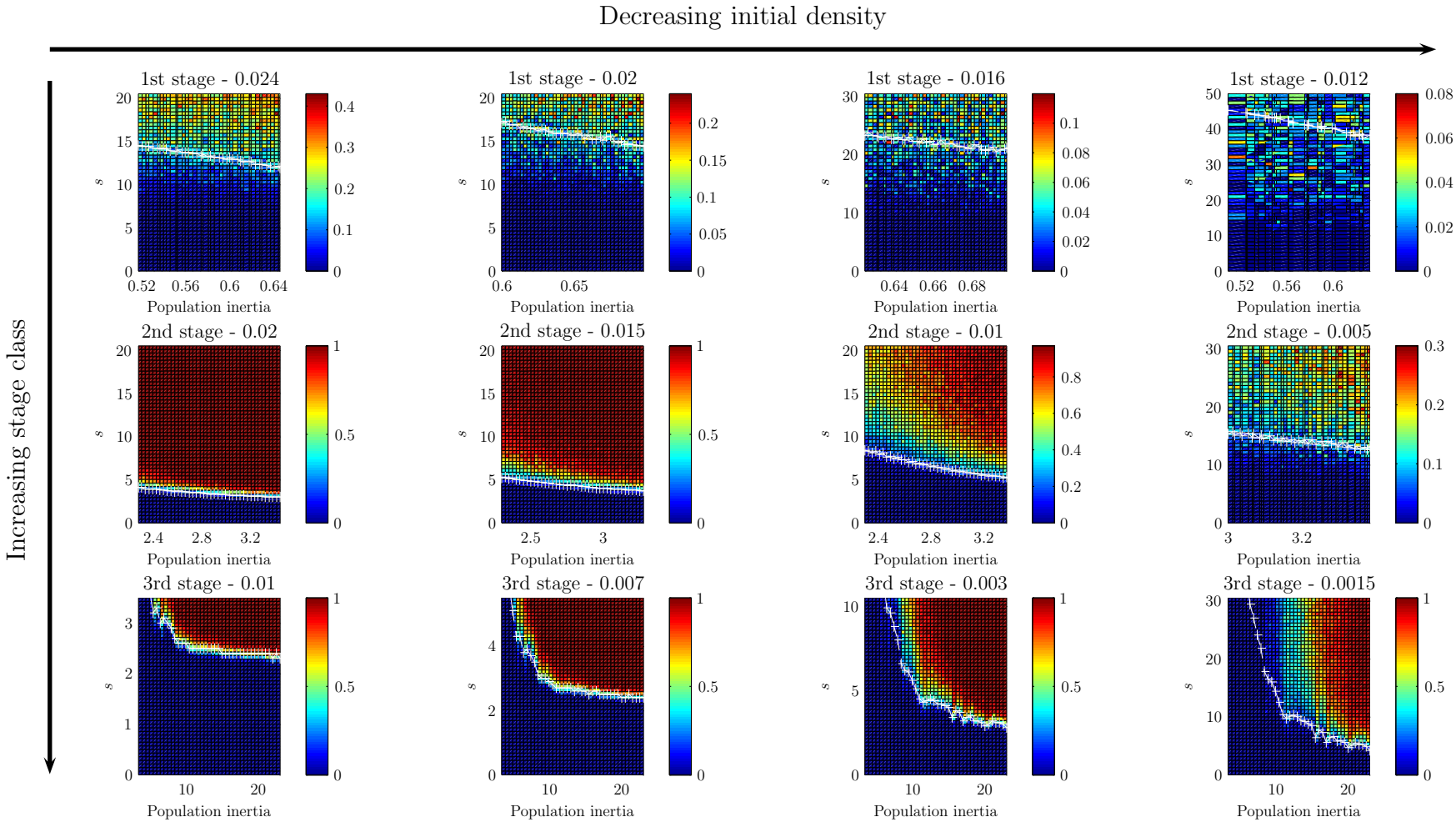

Figure 5.12: The probability of invasion for varying population inertia and s (determining the magnitude of the Allee effect) with 12 initial conditions of the invader, for the model with patch-based ϕ and α where $p = 20 \times 20$. The white line gives the minimum Allee effect required for invasion in the deterministic model.

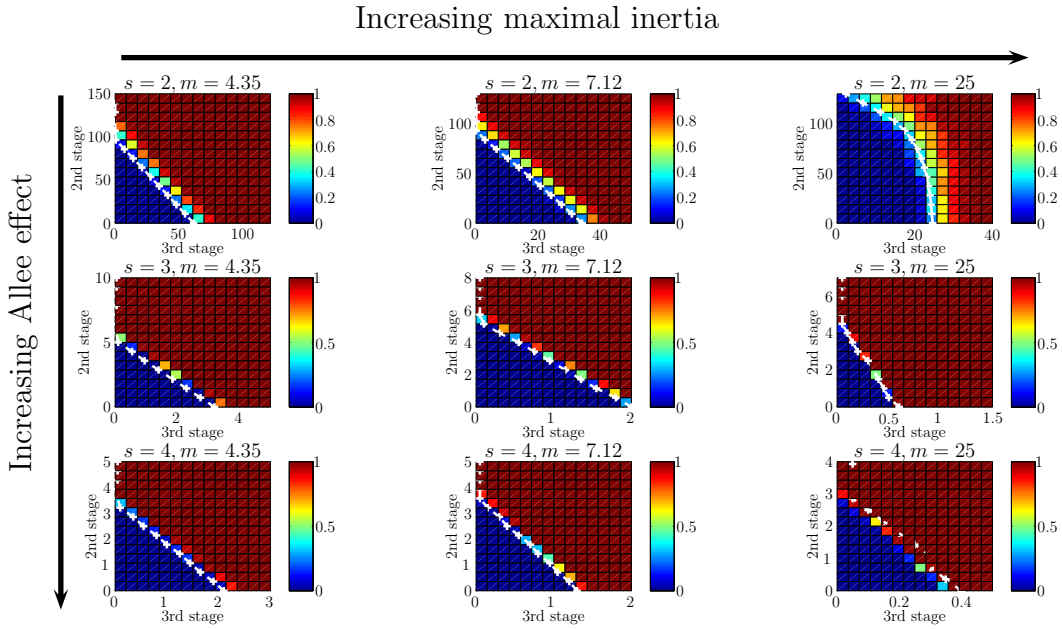

Figure 5.13: The probability of invasion for varying densities of the second and third stage of the invader initial condition, for the model with patch-based ϕ and α where $p = 20 \times 20$. The basin of attraction is found for 3 choices of maximum inertia and Allee effects.

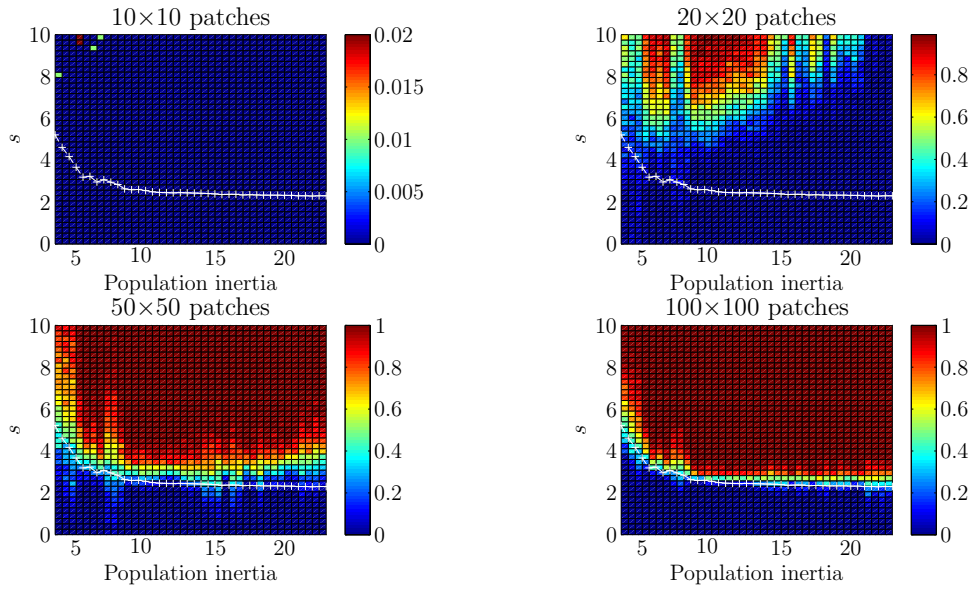

Figure 5.14: The probability of invasion for varying population inertia and s (determining the magnitude of the Allee effect) with 4 p values for the model with stochastic G_R, G_R and f entries. The invader initial condition is $0.01 \times p$ in the third stage class. The white lines gives the minimum Allee effect required for invasion in the deterministic model.

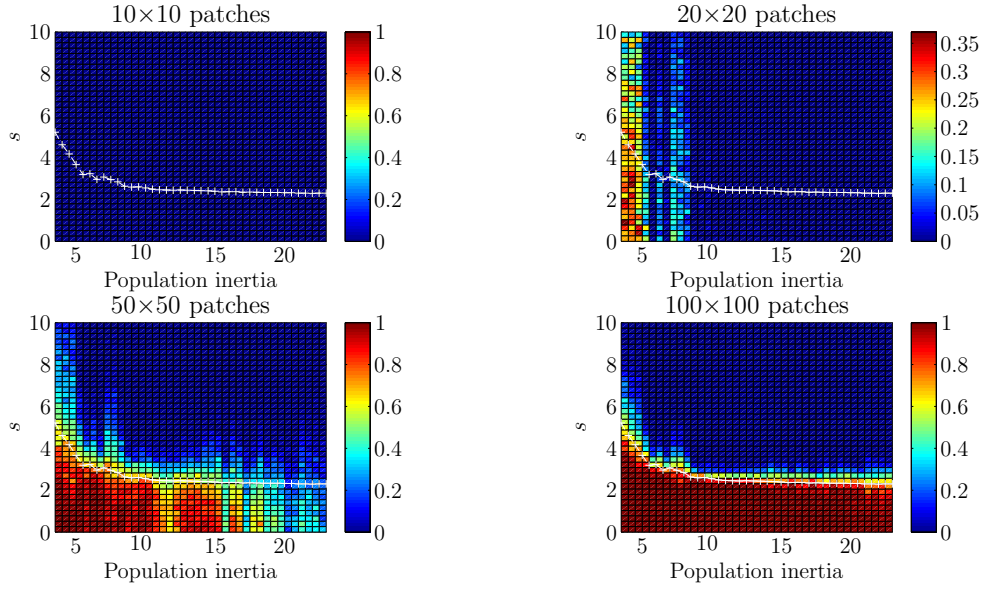

Figure 5.15: The probability of resident survival for varying population inertia and s (determining the magnitude of the Allee effect) with 4 p values for the model with stochastic G_R, G_R and f entries. The invader initial condition is $0.01 \times p$ in the third stage class. The white lines gives the maximum s which gives resident survival in the deterministic model.

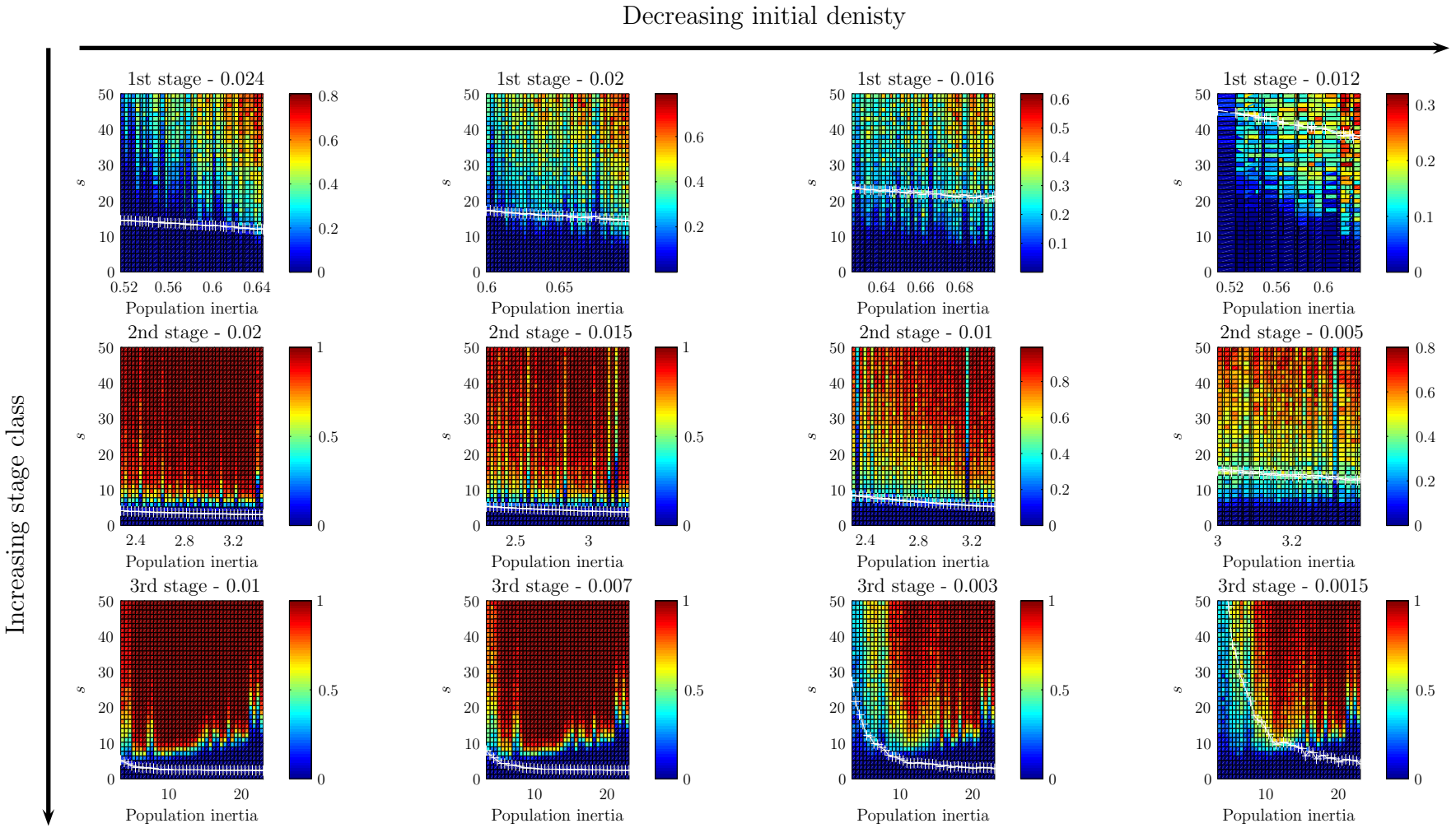

Figure 5.16: The probability of invasion for varying population inertia and s (determining the magnitude of the Allee effect) with 12 initial conditions for the model with stochastic G_R, G_R and f entries. The initial conditions given in the titles are scaled by p, and $p = 20 \times 20$. The white lines gives the minimum s required for invasion in the deterministic model.

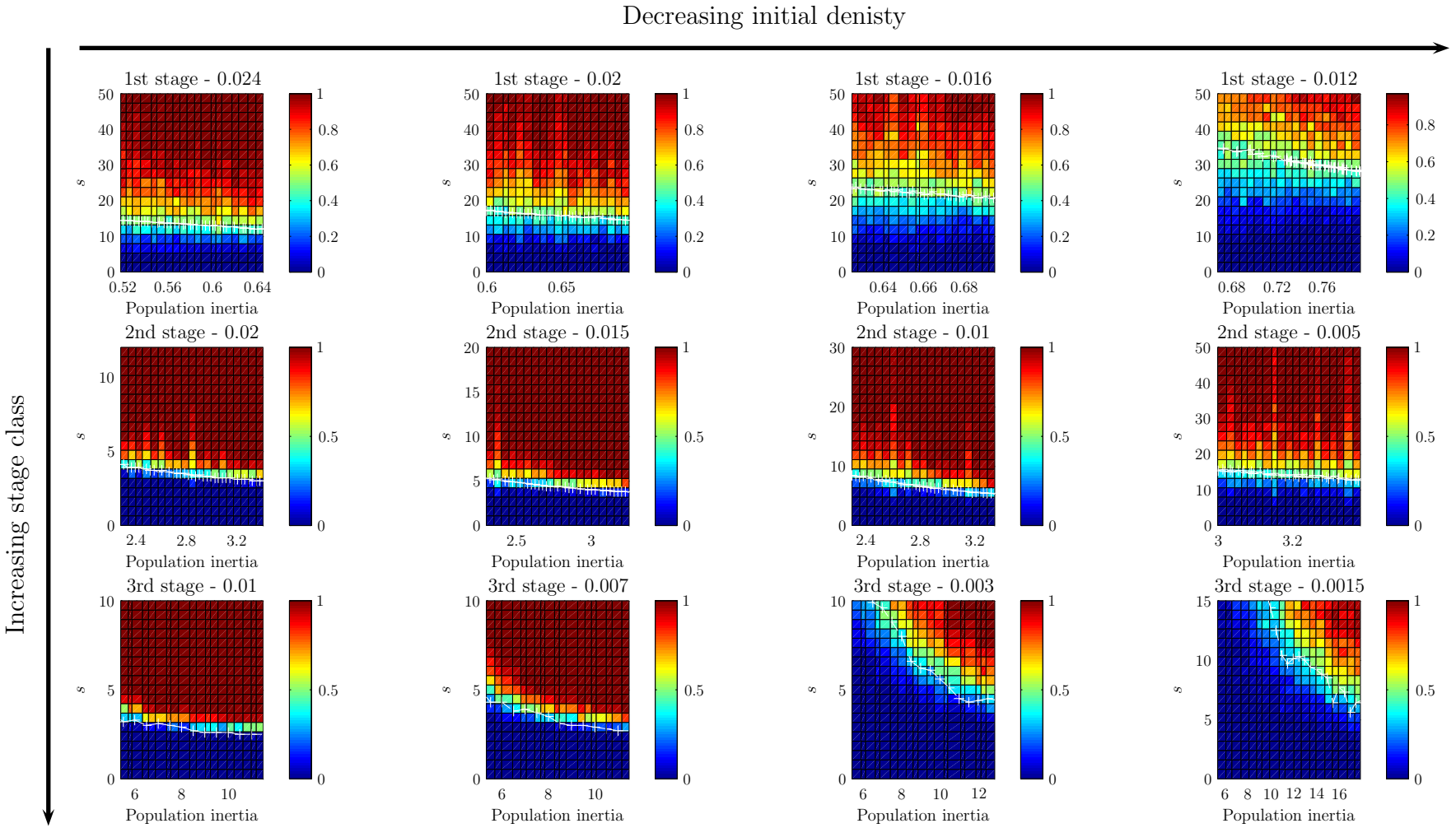

Figure 5.17: The probability of invasion for varying population inertia and s (determining the magnitude of the Allee effect) with 12 initial conditions for the model with stochastic G_R, G_R and f entries. The initial conditions given in the titles are scaled by p, and $p = 100 \times 100$. The white lines gives the minimum s required for invasion in the deterministic model.

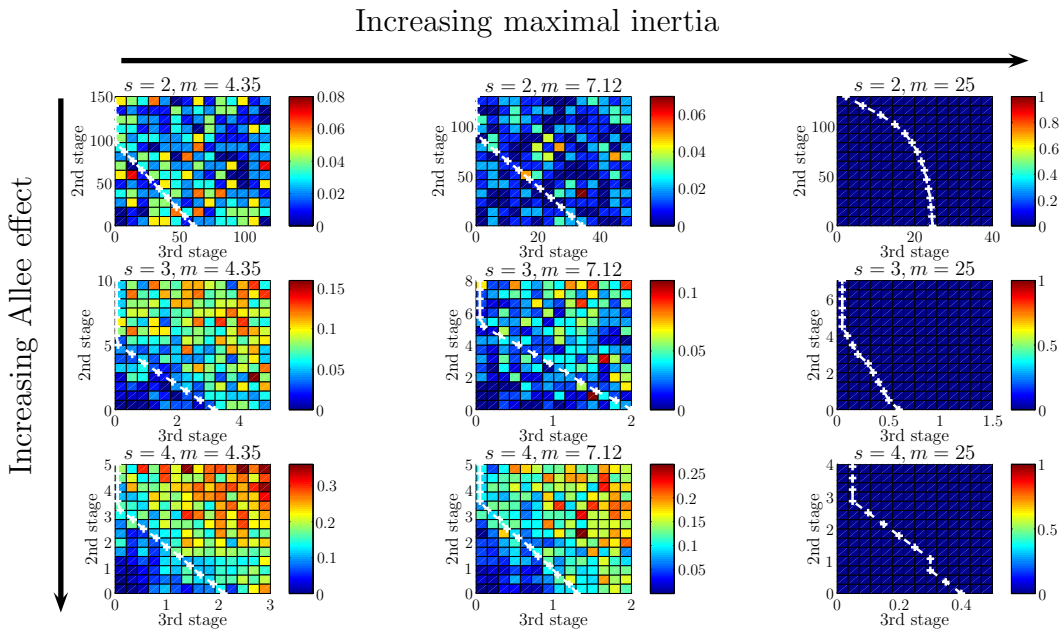

Figure 5.18: The probability of invasion for varying densities of the second and third stage of the invader initial condition, for the model with stochastic G_R, G_I and f where $p = 20 \times 20$. The basin of attraction is found for 3 choices of maximum inertia and Allee effects.

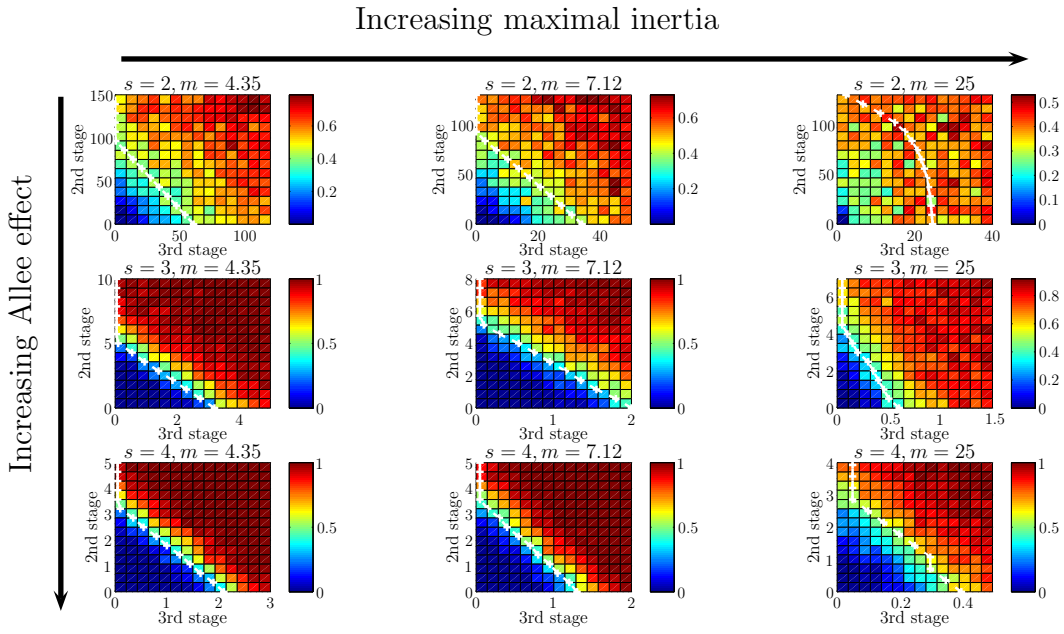

Figure 5.19: The probability of invasion for varying densities of the second and third stage of the invader initial condition, for the model with stochastic G_R, G_I and f where $p = 100 \times 100$. The basin of attraction is found for 3 choices of maximum inertia and Allee effects.

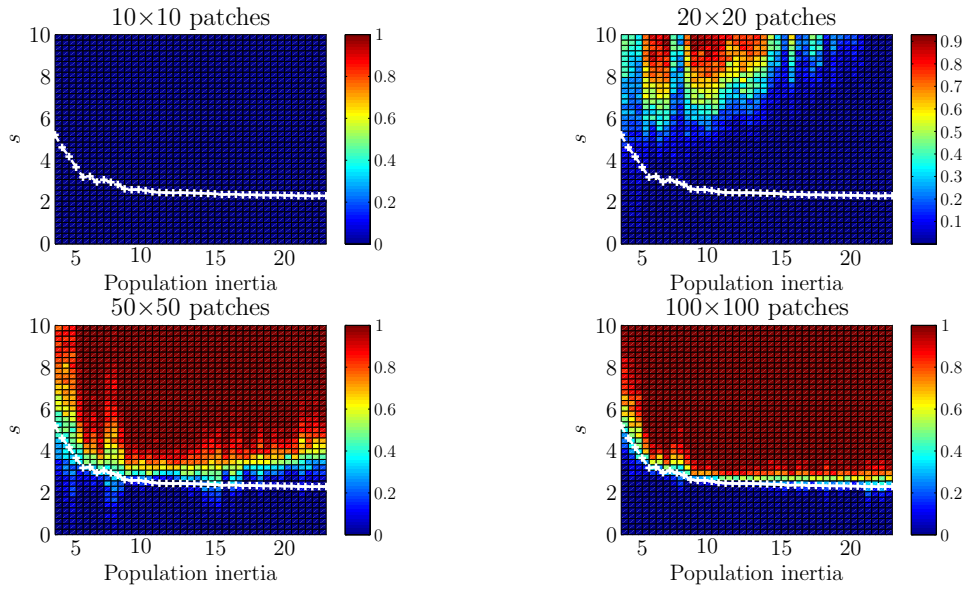

Figure 5.20: The probability of invasion for varying population inertia and s (determining the magnitude of the Allee effect) with different numbers of patches for the model with patch-based ϕ and α and stochastic G_R, G_I and f. The initial condition of the invader is $0.01 \times p$ into the third stage class. The white line gives the minimum s required for invasion in the deterministic model.

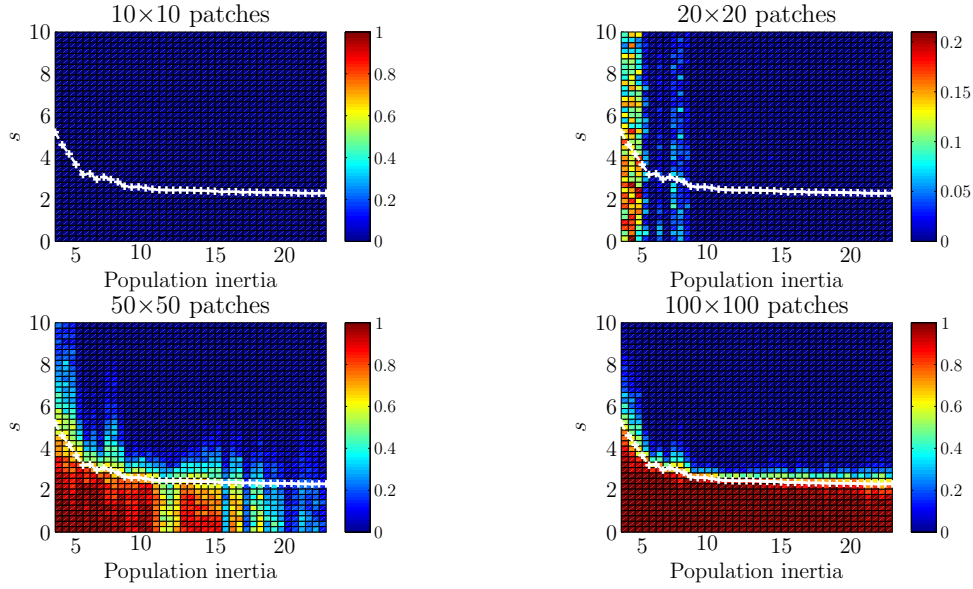

Figure 5.21: The probability of survival of the resident population for varying population inertia and s (determining the magnitude of the Allee effect) with different numbers of patches for the model with patch-based ϕ and α and stochastic G_R, G_I and f. The initial condition of the invader is $0.01 \times p$ in the third stage class. The white line shows the maximum s which gives survival of the resident population.

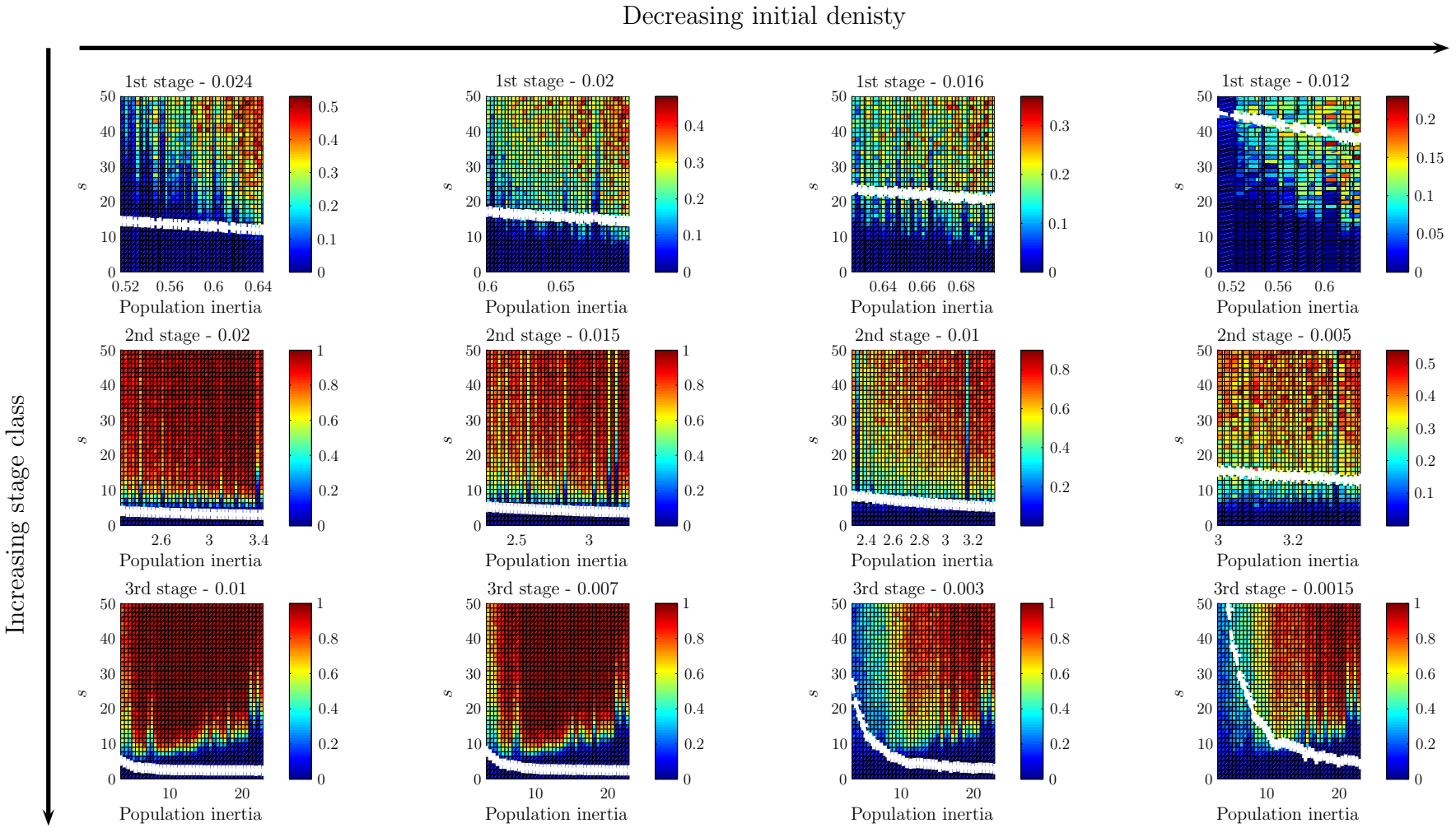

Figure 5.22: The probability of invasion for varying maximum inertia and s (determining the magnitude of the Allee effect) with 12 initial conditions of the invader, for the model with patch-based ϕ and α where $p = 20 \times 20$ and stochastic G_R, G_I and f. The white line gives the minimum s required for invasion in the deterministic model.

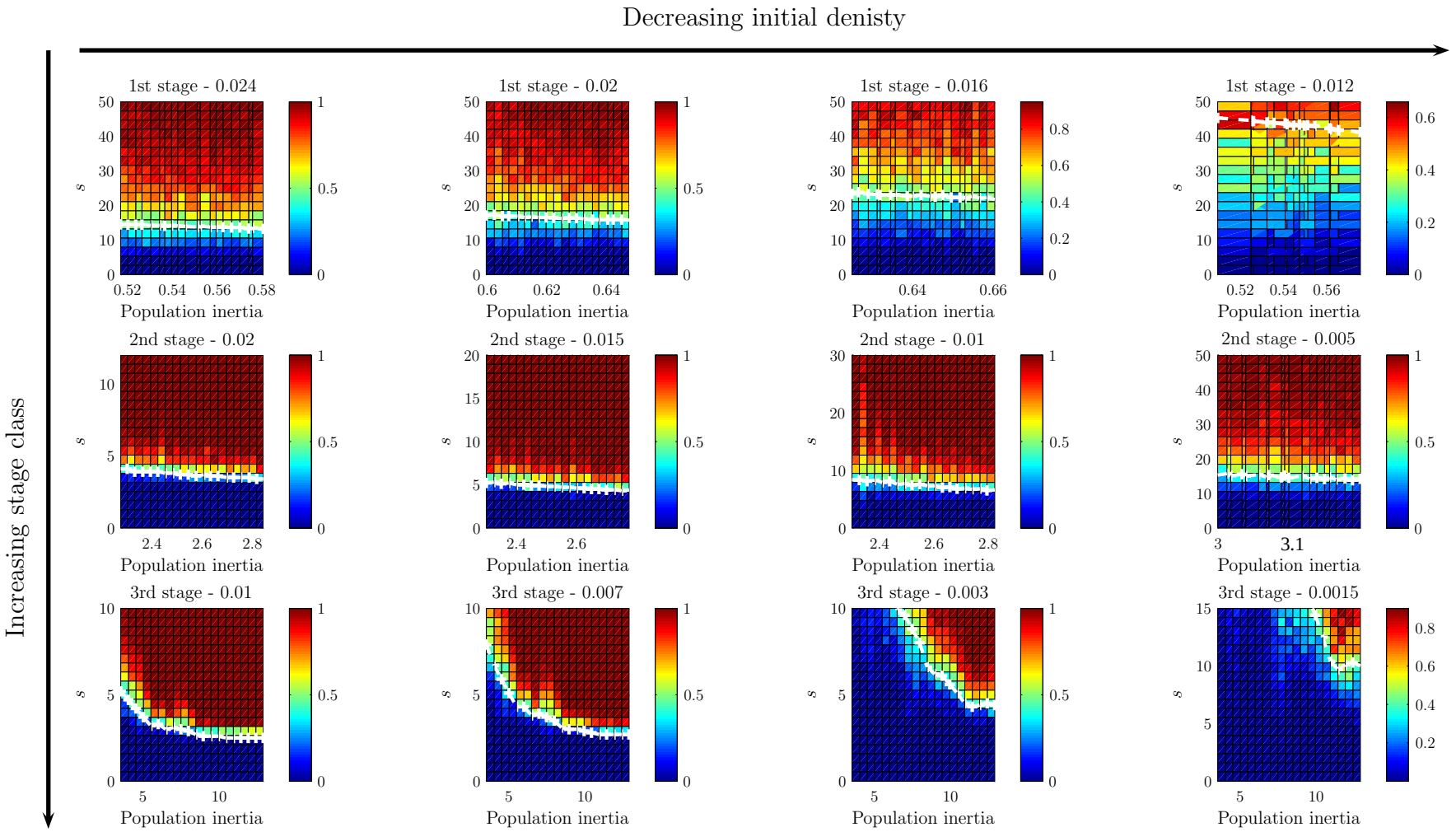

Figure 5.23: The probability of invasion for varying maximum inertia and s (determining the magnitude of the Allee effect) with 12 initial conditions of the invader, for the model with patch-based ϕ and α where $p = 100 \times 100$ and stochastic G_R, G_I and f. The white line gives the minimum s required for invasion in the deterministic model.

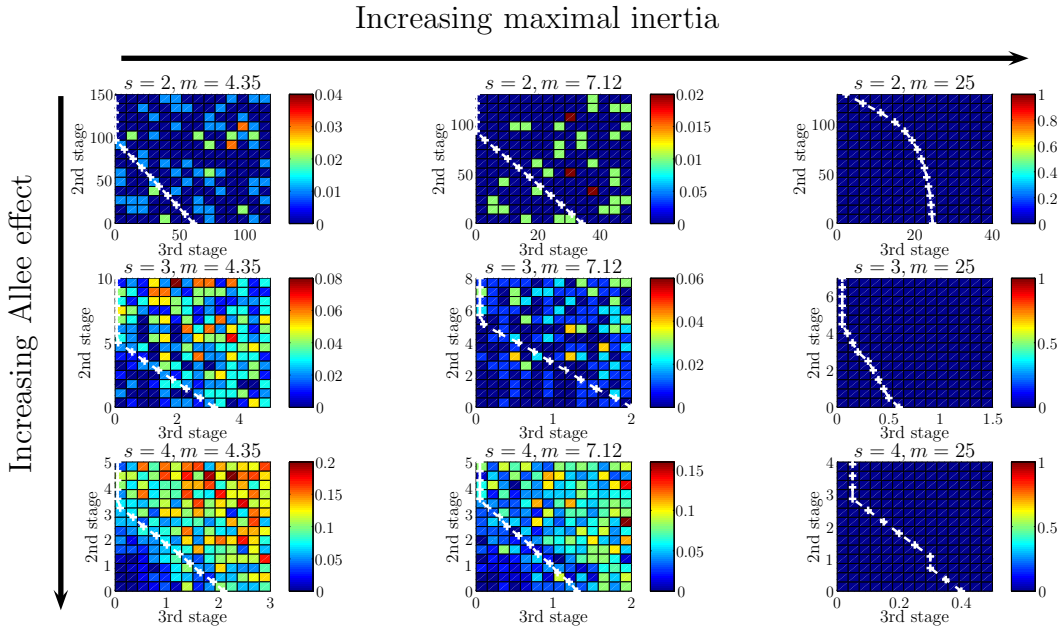

Figure 5.24: The probability of invasion for varying densities of the second and third stage of the invader initial condition, for the model with patch-based ϕ and α and stochastic G_R, G_I and f where $p = 20 \times 20$. The basin of attraction is found for 3 choices of maximum inertia and Allee effects.

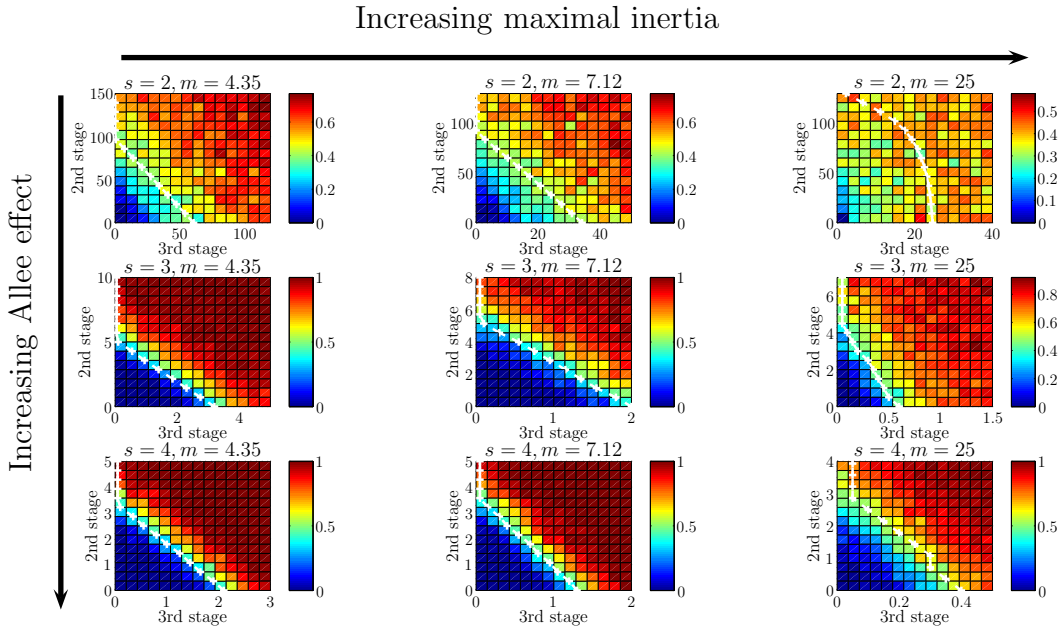

Figure 5.25: The probability of invasion for varying densities of the second and third stage of the invader initial condition, for the model with patch-based ϕ and α and stochastic G_R, G_I and f where $p = 100 \times 100$. The basin of attraction is found for 3 choices of maximum inertia and Allee effects.

5.3.3 Discussion

Deterministic Case

Figure 5.8 shows that there is an inverse relationship between the population inertia and the Allee effect required for invasion. This is consistent with the results given in [49]. This inverse relationship occurs because at higher population inertia there is greater transient dynamics which results in a larger population boost. Invasion occurs when the invader gains an advantage over the resident, which will happen when $\alpha > 1$. Equation (5.9) shows that at any time t, α depends on the Allee effect, s, and the size of the invader population, $N_z(t)$. Therefore, when the population is larger due to greater transients then less of an Allee effect is required to ensure that $\alpha > 1$. Hence, as the population inertia increases the Allee effect required for invasion to occur decreases. Also notice that the Allee effect required for invasion is much higher when the initial invader population is in the first stage class, even though the initial densities are greater. In general the fecundity vector f is skewed such that the third stage class is highest, which means when the initial invader population is in the first stage class it must reach the third stage class before it has high fecundity, and the population can increase. However, the survival and growth rates are 0.1 which means that not much of the initial population reaches the third stage class. The result is that the population inertia is much smaller than when the initial invader population is in the third stage class. So, the invader population is smaller, and the Allee effect required for invasion is greater.

Figure 5.9 shows that for most choices of maximum inertia and Allee effect a linear combination of juveniles and adults is required for invasion to occur. For example, when maximum inertia is 7.12 and the Allee effect is 4 invasion occurs when $(x_2, x_3) = (0, 1.3)$ and $(x_2, x_3) = (3.5, 0)$. The straight line between these two points creates a lower bound for a successful invasion, so if

$$\frac{x_2}{3.5} + \frac{x_3}{1.3} > 1$$

is satisfied then invasion will occur. Comparing the basins of attractions shows that for larger Allee affects then the basin of attraction is smaller, because a smaller population

is required to ensure that $\alpha > 1$. Also, as the maximum inertia increases the basins of attraction get smaller and the component required in the third stage class is much less. This is consistent with Figure 5.8 which shows as transient dynamics increase invasion is more likely to occur, and so the resident only equilibrium has a smaller basin of attraction.

Patch-based density dependent functions

To create a finite population model we used patch-based models to approximate ϕ and α. Figure 5.10 shows the probability of invasion for a range of population inertia and Allee effects for the model using patch-based approximations with 4 choices of p. It can be seen that at high numbers of patches the model with patch-based ϕ and α tends towards the deterministic model, as nearly 100% invasion occurs above the minimum Allee effect required for invasion in the deterministic model. This is because for larger numbers of patches the magnitude of the population is much greater so any affect caused by having a finite population is reduced. However, at low number of patches, Figure 5.10 shows that there are Allee effects which are above the minimum Allee effect required for invasion in the deterministic model, but the probability of invasion in the patch-based model is very low. This means that invasion is less likely to occur in the patch-based model, particularly when the population inertia is low. This may be a result of having a finite population which requires rounding of the population before applying ϕ and α. Rounding the population down is likely to have a greater effect as once the population is rounded to 0 it can not recover, but rounding the population up is unlikely to have as extreme effects on the dynamics. This suggests that having a finite population, particularly for smaller populations, is likely to decrease the survival of the invader.

Figure 5.11 shows the probability that the resident population persists in this model with patch-based density dependent functions, for a range of population inertia and Allee effect for 4 choices of p. To compare Figures 5.10 and 5.11 first consider the lines (shown in white) for the deterministic model, which shows that the minimum Allee effect required for survival of the resident is the same as the minimum Allee

effect required for invasion. This means that in the deterministic model exactly one population survives, so there is no stable equilibrium where both populations are over the thresholds given in Section 5.3.1. Comparing Figures 5.10 and 5.11 for the patch-based model shows that when $p \geq 20 \times 20$, as the Allee effect increases the probability of the resident surviving decreases and the probability of invasion increases, such that exactly one population persists. When $p = 10 \times 10$ Figure 5.11 shows that there are Allee effects, particularly at low maximum inertia, where although invasion has not occurred, the probability of the resident surviving is still low. This is because at low densities rounding down has a greater effect on the survival of both the resident and invader populations.

So far, the initial population has only been non-zero in the third stage class with a density of $0.01 \times p$. Figure 5.12 now explores the effect of varying the initial conditions of the invader for $p = 20 \times 20$. It shows that for lower invader density there is a greater difference between when invasion occurs in the patch-based and deterministic models. Also, although the initial densities in the first stage class are higher than in the third stage class the probability of invasion is much lower. This is because the rounding created by having a finite integer valued population has a larger effect on the population size. When the initial population is in the third stage class with low density the difference between when invasion occurs in the deterministic and the patch-based model is much greater at low population inertia. This is likely to be because at low inertia the fecundity if less skewed towards the third stage, so the reproduction of the initial population is lower, resulting in a smaller population density.

Lastly, Figure 5.13 shows the basins of attraction for the model with patch-based ϕ and α, with $p = 20 \times 20$. It shows that even at relatively low number of patches there is a strong agreement between the deterministic and the finite population model using patch-based density dependent functions.

Stochastic demography

Next, we explore the impact of stochastic G_R, G_I and f, and deterministic ϕ and α given by equations (5.8) and (5.9). Figure 5.14 considers 4 choices of p when the initial condition of the invader is into the third stage with density $0.01 \times p$. It shows that when $p = 10 \times 10$, the stochasticity of G_R, G_I and f has a huge affect on the probability of invasion, as the invasion rarely occurs for the chosen range of Allee effects. Also, when $p = 20 \times 20$, invasion is less likely to occur at high population inertia in the stochastic model. In fact there is an optimal population inertia which has a minimum Allee effect required for invasion. So, as we anticipated when the vital rates are stochastic the likelihood of invasion gives a different relationship to the deterministic model which has a monotonic decreasing relationship. This is due to the fecundity being highly skewed to the third stage class. However due to the stochasticity of survival and growth rates, at low number of patches the individuals are overall less likely to reach the third stage class and therefore be able to reproduce. This means that in the stochastic model with high population inertia the invader population does not get large enough for $\alpha > 1$ and therefore if invasion is to occur a greater Allee effect is required. At $p = 100 \times 100$ the stochastic results agree with the deterministic model, as with a larger overall population the stochastic entries are much closer to the average value used in the deterministic model.

Figure 5.15 shows the probability of survival of the resident population for 4 choices of p. For $p = 10 \times 10$, the resident population never survives for our choices of Allee effect. When $p = 20 \times 20$, the resident population only survives at very low population inertia. The initial resident population is at stable stage structure which is highly skewed to the first stage class. With high population inertia, fecundity is skewed towards higher stage classes and so the resident population is less likely to reach a stage with high fecundity, and be able to survive. Even at $p = 50 \times 50$ when $s = 0$, so the invader does not gain an advantage over the resident, the probability that the resident population persists is low when the population inertia is high. This suggests that stochastic vital rates have a large impact on resident survival when the population inertia is high. When $p = 100 \times 100$, the resident population agrees with the deterministic model which means that, as the Allee effect increases, there is a clear transition between the

resident population persisting and invasion occurring.

Next, Figure 5.16 shows the probability of invasion for 12 different initial condition of the invader for $p = 20 \times 20$. Similarly to Figure 5.12, for each of the stage classes, as the density of the initial condition decreases, the stochastic effect increases, reducing the chance of invasion. Also when the initial invader population is in the first stage class, the probability of invasion is much lower. This is because the stochasticity of the survival and growth rates means that the population is overall less likely to reach the second or third stage classes, where fecundity is higher. Figure 5.17 shows that in general with a larger population there is little difference between when invasion occurs in the stochastic and deterministic models. However, when the initial invader density decreases then there is a greater difference between the stochastic and deterministic models. This is due to the stochasticity having a greater affect on smaller populations.

Finally, we explore the basins of attraction for the model with stochastic G_R, G_I and f. Figure 5.18 shows that when $p = 20 \times 20$, then for our choice of initial conditions invasion is quite unlikely to occur. For higher maximum inertias, invasion does not occur at all for our choices of initial conditions. This is consistent with Figure 5.14 which shows that invasion is less likely at higher population inertia. Figure 5.19 shows the basin of attraction for $p = 100 \times 100$, where it can be seen that for low maximum inertia and high Allee effect the basin of attraction is similar to the deterministic basin of attraction. However, at low Allee effect or high maximum inertia the stochastic basin of attraction even at relatively high numbers of patches is not approximated by the deterministic model.

Patch-based density dependent functions and stochastic demography

Finally, we consider the same choice of parameters for the model with patch-based density dependent functions and stochastic demography. Figure 5.20 shows that at high numbers of patches the minimum Allee effect required for invasion in the deterministic model is approximately the Allee effect where the patch-based stochastic model changes from 0% invasion to 100% invasion. This means that the two models

give approximately the same results. This is because with more patches the population is larger, which means the ϕ and α functions are accurate approximations and overall the stochastic entries will be closer to their mean values, used in the deterministic model. Figure 5.20 also shows that when $p = 10 \times 10$, for the range of Allee effects chosen, no invasion occurs. Figure 5.14 shows the probability of invasion for the model with stochastic demography but deterministic ϕ and α for the same choice of parameters. Comparing these results for $p = 10 \times 10$ shows that the probability of invasion is slightly less in the stochastic model which has patch-based ϕ and α. This is consistent for $p = 20 \times 20$ and $p = 50 \times 50$ where the probability of invasion is slightly less likely, in Figure 5.20 compared to Figure 5.14.

For the same choice of parameters, we calculate the survival of the resident population as shown Figure 5.21. When $p = 10 \times 10$ the resident population does not survive, even when $s = 0$ which means that for any population density the growth rate from the first to second stage class is lower for the invader population. This is the same result as in Figure 5.15, which suggests that the lack of persistence of the resident population is due to the stochastic demography. Comparing Figures 5.15 and 5.21 for $p = 20 \times 20$ shows that for both models the resident only persists at low population inertia. The initial resident population is at stable stage structure which is skewed to the first stage class. However, as population inertia increases the fecundity becomes more skewed towards the third stage class. Due to the stochasticity, the population is less likely to grow from the first stage class to the third. Therefore it can only persist at low population inertia where the fecundity is less skewed. Also notice that the probability of resident survival is slightly lower in Figure 5.21 for $p = 20 \times 20$, which suggests that having patch-based ϕ and α slightly reduces the likelihood of resident persistence. Figures 5.20 and 5.21 show that at low numbers of patches there is a large range of Allee effects where neither the resident or invader persists. Whereas when $p = 100 \times 100$, there is a clear transition from when the resident survives to when invasion occurs. This is similar to the stochastic model where at high numbers of patches the population tends to the resident only or invader only equilibrium.

Figures 5.22 and 5.23 show the probability of invasion for 12 initial conditions of the invader for $p = 20 \times 20$ and $p = 100 \times 100$, respectively. For the $p = 20 \times 20$ case, comparing Figure 5.22 with Figure 5.16 shows that the results for all 12 initial conditions are very similar for the models with stochastic G_R, G_I and f and ϕ and α are either deterministic or patch-based. The slight difference, particularly at low initial densities, shows that invasion is less likely to occur in the model with patch-based ϕ and α. This agrees with the previous results, that having patch-based ϕ and α increases the stochasticity and therefore when the invader population is small the probability of invasion decreases. Figure 5.25 is very similar to Figure 5.17 which suggests that at high numbers of patches having patched based ϕ and α functions has little effect on the likelihood of invasion.

Finally, Figures 5.24 and 5.25 show the basins of attraction for the model with stochastic demography and patch-based density dependent functions. Comparing these figures with Figures 5.18 and 5.19 shows that these are consistent with the conclusion that probability of invasion is slightly smaller when the model has patch-based ϕ and α, but with larger numbers of patches there is little difference between the two models with stochastic demography.

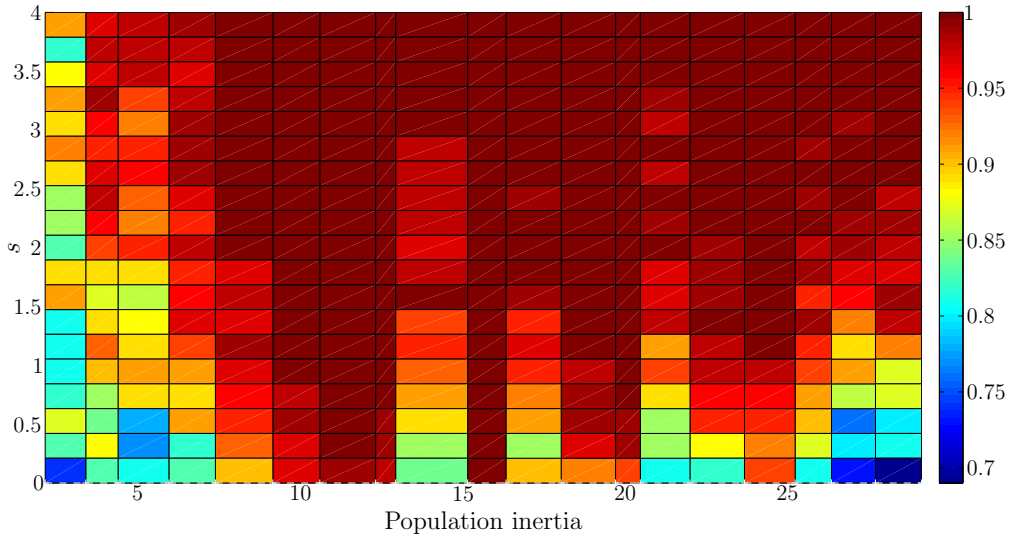

Figure 5.26: Probability of invasion for varying population inertia and s (determining the magnitude of the Allee effect) for a model with positive invasion exponent.

5.4 Conclusion

As shown in [49] the invasion exponent is not a good proxy for invasion, as invasion can take place even when the invasion exponent is negative. We also find that by considering a stochastic model where the invasion exponent is positive that invasion may not take place, as illustrated in Figure 5.26. Therefore, for our model we can not use the invasion exponent to predict if invasion will occur. Instead we use the population inertia.

Similar to the results in [49], we find for our deterministic model, that there is an inverse relationship between the population inertia and minimum Allee effect required for invasion. This is also reflected in the small subset of basins of attractions we calculated for the deterministic model, as the basins of attraction is smaller at high maximum inertia.

We then consider 3 finite population models, and find that, when the population size is large enough, all 3 models with or without stochastic demography can be approximated by the deterministic model.

We create a finite population model by using patch-based density dependent functions, and find that for low numbers of patches the model gives slightly different results to the deterministic model, due to having a finite population. Then we introduce stochastic demography which hugely affects the likelihood of invasion, particularly for small populations as shown in Figure 5.14. The inverse relationship given by the deterministic model is reversed at high population inertia, such that the relationship between s and population inertia has a minimum. This suggests that in small populations with stochastic demography then an intermediate population inertia gives the population a slight advantage, allowing it to invade with smaller Allee effect or population density. Therefore, over evolutionary time populations will tend toward intermediate population inertia, where the fecundity is only moderately skewed.

Overall, we have found that finite populations do give rise to different results and when stochastic demography is introduced the results given in [49] may be an over simplification.

Chapter 6

Conclusion and future work

In this thesis we have used several control theory approaches to explore the management of populations affected by disturbances and uncertainty. The following states our key results and discusses how our work could be expanded.

In Chapter 2 we used linear programming to find optimal translocation strategies which maximise a declining wild population. For 31 animal and 983 plant PPM's we classified these strategies depending on which stages were kept in captivity, and then compared the classification for different levels of resource. We find that when the resource is limited, so that the optimal strategy can not capture the entire wild population, then depending on the species the optimal strategy may focus on particular stages classes. Depending on the stages kept in captivity we referred to the optimal strategies as ark, headstart or zoo strategies. To expand on our results, our framework could be applied to COMADRE which is a database which has only become available within the last few months. It is an immense database containing 1625 animal PPM's, along with more data on phenologies and geographical location. This extra information could be used for extensive statistical analysis to find trends in the classification of the optimal strategies. Any trends could be used to inform conservationists of the best translocation programmes for species with unknown life cycles. Although we have not established clear trends, for the species we have considered our results could be used to indicate which stages should be kept in captivity in a translocation programme.

Chapter 3 considered the management of an invading population affected by disturbance. We used a discrete time model and linear programming to find the control strategy which minimised the final total population for different choices of disturbances. We found that for a sinusoidal disturbance, if no removal occurs then the transfer function can be used to approximate the total final population, and a feedback strategy approximates the final population if the resource available for removal is unlimited. We then considered unknown disturbance, and assumed the worse case scenario given that the disturbance is bounded. This creates a 2-player game as we minimised the total final population with respect to removal whilst maximised the effect the disturbance has on the final population. In this 2-player game no Nash equilibrium exists but instead minimax$\geq$maximin. We found that the solutions to the minimax problem were more complex than the maximin solutions due the constraint that the population must remain positive being dependent on the removal and disturbance. This work could be expanded by using ideas from Stochastic Dynamic Programming to consider the effect stochashicity in the model has in the optimal disturbance or removal. Also adaptive management could be used to examine a 2-player game where the disturbance is unknown.

Chapter 4 studies a discrete time model with management and disturbance (similar to Chapter 3), but with a quadratic cost function. We solve this problem using discrete time Riccati equations to find solutions for the control strategy and disturbance. These solutions form a Nash equilibrium where minimax=maximin. Then we introduce the disturbance attenuation problem into ecology, which to our knowledge has not been done before. It gives a measure of how a disturbance may be amplified or attenuated by the system. The framework we used does not ensure non-negativity of the population so we approximate the disturbance attenuation by choosing the removal so that the population is non-negative and using the idea of steady state gain. We find that in most cases there is little difference between the optimal disturbance attenuation and the solution obtained from the steady state gain, suggesting that the disturbance attenuation framework can be used to approximate how the disturbance is amplified by the system. Future work would require revisiting the Liner Quadratic

Dynamic Game theory with the addition of constraints to ensure non-negativity of the population. Using this framework it would be possible to calculate the attenuation of a coloured disturbance. From this it would be possible to explore how vital rates of a population would adapt if the population is continuously subjected to coloured disturbance.

In Chapter 5 we explore the effect stochasticity may have on an invading population. To do this we build on the work in [49], by considering 3 models with varying levels of stochasticity. We find that having a finite population only slightly decreases the likelihood of invasion. However, when we considered models with stochastic demography the results were very different to those found in [49]. With small population and stochastic demography the probability of invasion and survival of the resident was dramatically reduced. Furthermore, we found that with the addition of stochastic demography we no longer have a decreasing relationship between the Allee effect and the population inertia. Instead we found that for small populations the relationship between Allee effect and population inertia has a minimum, suggesting that populations with intermediate population inertia are slightly more likely to invade. This suggests that over evolutionary time, populations will tend towards intermediate population inertia, where the fecundity is only moderately skewed. We found that finite and infinite population models give rise to different results. It may be possible to quantify the difference between the models by using the results of Boland et al. [16] which use a finite correction term to establish the difference between finite and infinite models.

Appendix A1

Animal population projection matrices

The following contains the animal population projection matrices and taxa for the 31 species used in Chapter 2 to create Figures 2.2 – 2.5. As discussed in Section 2.6.1 these matrices are taken from a database and in this appendix we include the references used to create the database.

Secondly, this appendix gives the nine population projection matrices used in Chapter 4 to create Figure 4.7.

Species **(Reference)**	**Taxa**	**PPM**
Puerto Rican Vireo (Woodworth, *Conserv. Biol.*, 1999))	Bird	$\begin{pmatrix} 0.146 & 0.2482 \\ 0.4 & 0.68 \end{pmatrix}$
House sparrow (Maclean et al. *Ibis*, 2008)	Bird	$\begin{pmatrix} 0.44 & 1.57 \\ 0.13 & 0.47 \end{pmatrix}$
Coral (Hughes & Tanner, *Ecology*, 2000)	Marine invertebrate	$\begin{pmatrix} 0.29967 & 0.395 & 0.44433 \\ 0.075333 & 0.42367 & 0.33567 \\ 0 & 0.065333 & 0.669 \end{pmatrix}$
Island fox (Roemer et al., *Anim. Conserv.*, 2001)	Mammalia	$\begin{pmatrix} 0.07 & 0.21 & 0.26 \\ 0.53 & 0 & 0 \\ 0 & 0.71 & 0.69 \end{pmatrix}$
Wild boar (Bieber & Ruf, *J. Appl. Ecol.*, 2005)	Mammalia	$\begin{pmatrix} 0.13 & 0.56 & 1.64 \\ 0.25 & 0 & 0 \\ 0 & 0.31 & 0.58 \end{pmatrix}$
Spanish ibex (Escos et al., *Can. J. Zoolog.*, 1994)	Mammalia	$\begin{pmatrix} 0 & 0 & 0.244 \\ 0.38 & 0 & 0 \\ 0 & 0.87 & 0.87 \end{pmatrix}$
Sage grouse (Clark et al., *J Wildlife Manage.*, 2008)	Bird	$\begin{pmatrix} 0.181 & 0.596 & 0.598 \\ 0.33 & 0 & 0 \\ 0 & 0.731 & 0.733 \end{pmatrix}$
Northern spotted owl (Lande, *Oecologia,*, 1988)	Bird	$\begin{pmatrix} 0 & 0 & 0.22608 \\ 0.108 & 0 & 0 \\ 0 & 0.71 & 0.942 \end{pmatrix}$
Grass shrimp (Sable, *Dissertation: Louisiana State University.*, 2007)	Arthropod	$\begin{pmatrix} 0 & 0 & 0.7457 & 12 \\ 0.1381 & 0.1703 & 0 & 0 \\ 0 & 0.1166 & 0.6577 & 0 \\ 0 & 0 & 0.111 & 0.7882 \end{pmatrix}$

Mexican lizard (Zuniga-Vega et al., *Copeia*, 2007)	Reptilia	$\begin{pmatrix} 0.069 & 0 & 1.148 & 1.1027 \\ 0.2759 & 0.1875 & 0 & 0 \\ 0 & 0.625 & 0.1837 & 0 \\ 0 & 0 & 0.3265 & 0.4324 \end{pmatrix}$
Varnish clam (Dudas et al., *Ecology*, 2007)	Arthropod	$\begin{pmatrix} 0.014 & 0.022 & 0.126 & 0.496 & 0.731 \\ 0.097 & 0.274 & 0 & 0 & 0 \\ 0 & 0.233 & 0.64 & 0 & 0 \\ 0 & 0 & 0.024 & 0.836 & 0 \\ 0 & 0 & 0 & 0.005 & 0.766 \end{pmatrix}$
Bullfrog (Govindarajulu et al., *Ecol. Appl.*, 2005)	Amphibian	$\begin{pmatrix} 0 & 0 & 0 & 0 & 2080 \\ 0.07 & 0 & 0 & 0 & 0 \\ 0 & 0.078 & 0 & 0 & 0 \\ 0 & 0.016 & 0.02 & 0 & 0 \\ 0 & 0 & 0 & 0.129 & 0.318 \end{pmatrix}$
Columbian ground squirrel (Dobson & Oli, *Am. Nat.*, 2001)	Mammalia	$\begin{pmatrix} 0 & 1.382 & 1.382 & 1.382 & 1.382 \\ 0.35 & 0 & 0 & 0 & 0 \\ 0 & 0.35 & 0 & 0 & 0 \\ 0 & 0 & 0.765 & 0 & 0 \\ 0 & 0 & 0 & 0.765 & 0 \end{pmatrix}$
Asp viper (Altwegg et al., *Oikos*, 2005)	Reptilia	$\begin{pmatrix} 0 & 0 & 0 & 0 & 0.923 \\ 0.42 & 0 & 0 & 0 & 0 \\ 0 & 0.506 & 0 & 0 & 0 \\ 0 & 0 & 0.591 & 0 & 0 \\ 0 & 0 & 0 & 0.671 & 0.744 \end{pmatrix}$
Least tern (Akçakaya et al., *J Wildlife Manage*, 2003)	Bird	$\begin{pmatrix} 0 & 0 & 0.399 & 0.399 & 0.389 \\ 0.395 & 0 & 0 & 0 & 0 \\ 0 & 0.461 & 0 & 0 & 0 \\ 0 & 0 & 0.81 & 0 & 0 \\ 0 & 0 & 0 & 0.81 & 0.79 \end{pmatrix}$

Subtidal snail (Noda & Nakao, *J. Anim. Ecol.*, 1996)	Arthropod	$\begin{pmatrix} 0.0085819 & 0.069472 & 0.11034 & 0.13077 & 0.14303 & 0.1512 \\ 0.565 & 0 & 0 & 0 & 0 & 0 \\ 0 & 0.77 & 0 & 0 & 0 & 0 \\ 0 & 0 & 0.757 & 0 & 0 & 0 \\ 0 & 0 & 0 & 0.722 & 0 & 0 \\ 0 & 0 & 0 & 0 & 0.785 & 0.785 \end{pmatrix}$
European hare (Mollet, *Moss Landing Marine Labs*, 2010)	Mammalia	$\begin{pmatrix} 0 & 1.7147 & 1.7147 & 1.7147 & 1.7147 & 1.7147 \\ 0.1732 & 0 & 0 & 0 & 0 & 0 \\ 0 & 0.51 & 0 & 0 & 0 & 0 \\ 0 & 0 & 0.51 & 0 & 0 & 0 \\ 0 & 0 & 0 & 0.51 & 0 & 0 \\ 0 & 0 & 0 & 0 & 0.51 & 0 \end{pmatrix}$
Jumping mouse (Mollet, *Moss Landing Marine Labs*, 2010)	Mammalia	$\begin{pmatrix} 0.4123 & 0.4123 & 0.4123 & 0.4123 & 0.4123 & 0.4123 \\ 0.59 & 0 & 0 & 0 & 0 & 0 \\ 0 & 0.59 & 0 & 0 & 0 & 0 \\ 0 & 0 & 0.59 & 0 & 0 & 0 \\ 0 & 0 & 0 & 0.59 & 0 & 0 \\ 0 & 0 & 0 & 0 & 0.59 & 0 \end{pmatrix}$
Coypu (Mollet, *Moss Landing Marine Labs*, 2010)	Mammalia	$\begin{pmatrix} 0 & 1.159 & 1.461 & 1.461 & 1.461 & 1.461 \\ 0.4123 & 0 & 0 & 0 & 0 & 0 \\ 0 & 0.4123 & 0 & 0 & 0 & 0 \\ 0 & 0 & 0.52 & 0 & 0 & 0 \\ 0 & 0 & 0 & 0.52 & 0 & 0 \\ 0 & 0 & 0 & 0 & 0.52 & 0 \end{pmatrix}$
Red-cockaded woodpecker (MacGuire et al., *J. Wildlife Manage.*, 1995)	Bird	$\begin{pmatrix} 0 & 0.05054 & 0.7033 & 1.0149 & 0.636 & 0.93651 \\ 0.38 & 0 & 0 & 0 & 0 & 0 \\ 0 & 0.65 & 0 & 0 & 0 & 0 \\ 0 & 0 & 0.85 & 0 & 0 & 0 \\ 0 & 0 & 0 & 0.4 & 0 & 0 \\ 0 & 0 & 0 & 0 & 0.589 & 0.589 \end{pmatrix}$

Yellow bellied marmot (Mollet, *Moss Landing Marine Labs*, 2010)	Mammalia	$\begin{pmatrix} 0 & 0.5347 & 0.5347 & 0.5347 & 0.5347 & 0.5347 & 0.5347 \\ 0.469 & 0 & 0 & 0 & 0 & 0 & 0 \\ 0 & 0.75 & 0 & 0 & 0 & 0 & 0 \\ 0 & 0 & 0.75 & 0 & 0 & 0 & 0 \\ 0 & 0 & 0 & 0.75 & 0 & 0 & 0 \\ 0 & 0 & 0 & 0 & 0.75 & 0 & 0 \\ 0 & 0 & 0 & 0 & 0 & 0.75 & 0 \end{pmatrix}$
Grey squirrel (Barkalow et al., *J Wildlife Manage.*, 1970)	Mammalia	$\begin{pmatrix} 0.13 & 0.67 & 0.98 & 0.95 & 0.95 & 1.0095 & 0.826 & 0.57 \\ 0.36 & 0 & 0 & 0 & 0 & 0 & 0 & 0 \\ 0 & 0.61 & 0 & 0 & 0 & 0 & 0 & 0 \\ 0 & 0 & 0.71 & 0 & 0 & 0 & 0 & 0 \\ 0 & 0 & 0 & 0.66 & 0 & 0 & 0 & 0 \\ 0 & 0 & 0 & 0 & 0.66 & 0 & 0 & 0 \\ 0 & 0 & 0 & 0 & 0 & 0.76 & 0 & 0 \\ 0 & 0 & 0 & 0 & 0 & 0 & 0.44 & 0 \end{pmatrix}$
Cheetah (Crooks et al., *Conserv. Biol.*, 1998)	Mammalia	$\begin{pmatrix} 0 & 0 & 0 & 0 & 1.143 & 1.143 & 1.143 & 1.312 \\ 0.081 & 0 & 0 & 0 & 0 & 0 & 0 & 0 \\ 0 & 0.771 & 0 & 0 & 0 & 0 & 0 & 0 \\ 0 & 0 & 0.771 & 0 & 0 & 0 & 0 & 0 \\ 0 & 0 & 0 & 0.92 & 0 & 0 & 0 & 0 \\ 0 & 0 & 0 & 0 & 0.92 & 0 & 0 & 0 \\ 0 & 0 & 0 & 0 & 0 & 0.92 & 0 & 0 \\ 0 & 0 & 0 & 0 & 0 & 0 & 0.92 & 0.879 \end{pmatrix}$
Desert tortoise (Doak et al., *Ecol. Appl.*, 1994)	Reptilia	$\begin{pmatrix} 0 & 0 & 0 & 0 & 0 & 1.3 & 1.98 & 2.57 \\ 0.716 & 0.567 & 0 & 0 & 0 & 0 & 0 & 0 \\ 0 & 0.149 & 0.567 & 0 & 0 & 0 & 0 & 0 \\ 0 & 0 & 0.149 & 0.604 & 0 & 0 & 0 & 0 \\ 0 & 0 & 0 & 0.235 & 0.56 & 0 & 0 & 0 \\ 0 & 0 & 0 & 0 & 0.225 & 0.678 & 0 & 0 \\ 0 & 0 & 0 & 0 & 0 & 0.249 & 0.851 & 0 \\ 0 & 0 & 0 & 0 & 0 & 0 & 0.016 & 0.86 \end{pmatrix}$

Sponge (Cropper & Di Resta, *Ecol. Model.*, 1999)	Marine invertebrate	$\begin{pmatrix} 0.24 & 0 & 0 & 0.75 & 0.75 & 0.75 & 0.75 & 0.75 & 0.75 & 0.75 \\ 0.62 & 0.47 & 0.016 & 0 & 0 & 0 & 0 & 0 & 0 & 0 \\ 0 & 0.032 & 0.44 & 0 & 0.02 & 0 & 0 & 0 & 0 & 0 \\ 0 & 0 & 0.34 & 0.41 & 0 & 0 & 0 & 0 & 0 & 0 \\ 0 & 0 & 0.082 & 0.41 & 0.33 & 0.03 & 0 & 0 & 0 & 0 \\ 0 & 0 & 0 & 0.11 & 0.45 & 0.29 & 0.05 & 0 & 0.04 & 0 \\ 0 & 0 & 0 & 0 & 0.12 & 0.44 & 0.37 & 0.04 & 0 & 0 \\ 0 & 0 & 0 & 0 & 0.02 & 0.12 & 0.58 & 0.26 & 0 & 0 \\ 0 & 0 & 0 & 0 & 0 & 0 & 0 & 0.57 & 0.64 & 0.06 \\ 0 & 0 & 0 & 0 & 0 & 0 & 0 & 0 & 0.2 & 0.88 \end{pmatrix}$
Little brown bat (Mollet, *Moss Landing Marine Labs*, 2010)	Mammalia	$\begin{pmatrix} 0.155 & 0.43 & 0.43 & 0.43 & 0.43 & 0.43 & 0.43 & 0.43 & 0.43 & 0.43 & 0.43 & 0.43 \\ 0.31 & 0 & 0 & 0 & 0 & 0 & 0 & 0 & 0 & 0 & 0 & 0 \\ 0 & 0.86 & 0 & 0 & 0 & 0 & 0 & 0 & 0 & 0 & 0 & 0 \\ 0 & 0 & 0.86 & 0 & 0 & 0 & 0 & 0 & 0 & 0 & 0 & 0 \\ 0 & 0 & 0 & 0.86 & 0 & 0 & 0 & 0 & 0 & 0 & 0 & 0 \\ 0 & 0 & 0 & 0 & 0.86 & 0 & 0 & 0 & 0 & 0 & 0 & 0 \\ 0 & 0 & 0 & 0 & 0 & 0.86 & 0 & 0 & 0 & 0 & 0 & 0 \\ 0 & 0 & 0 & 0 & 0 & 0 & 0.86 & 0 & 0 & 0 & 0 & 0 \\ 0 & 0 & 0 & 0 & 0 & 0 & 0 & 0.86 & 0 & 0 & 0 & 0 \\ 0 & 0 & 0 & 0 & 0 & 0 & 0 & 0 & 0.86 & 0 & 0 & 0 \\ 0 & 0 & 0 & 0 & 0 & 0 & 0 & 0 & 0 & 0.86 & 0 & 0 \\ 0 & 0 & 0 & 0 & 0 & 0 & 0 & 0 & 0 & 0 & 0.86 & 0 \end{pmatrix}$

Warthog (Oli & Zinner, *Oikos*, 2001)	Mammalia	$\begin{pmatrix} 0 & 0.633 & 0.633 & 0.633 & 0.633 & 0.633 & 0.633 & 0.633 & 0.633 & 0.633 & 0.633 & 0.633 \\ 0.309 & 0 & 0 & 0 & 0 & 0 & 0 & 0 & 0 & 0 & 0 & 0 \\ 0 & 0.715 & 0 & 0 & 0 & 0 & 0 & 0 & 0 & 0 & 0 & 0 \\ 0 & 0 & 0.715 & 0 & 0 & 0 & 0 & 0 & 0 & 0 & 0 & 0 \\ 0 & 0 & 0 & 0.715 & 0 & 0 & 0 & 0 & 0 & 0 & 0 & 0 \\ 0 & 0 & 0 & 0 & 0.715 & 0 & 0 & 0 & 0 & 0 & 0 & 0 \\ 0 & 0 & 0 & 0 & 0 & 0.715 & 0 & 0 & 0 & 0 & 0 & 0 \\ 0 & 0 & 0 & 0 & 0 & 0 & 0.715 & 0 & 0 & 0 & 0 & 0 \\ 0 & 0 & 0 & 0 & 0 & 0 & 0 & 0.715 & 0 & 0 & 0 & 0 \\ 0 & 0 & 0 & 0 & 0 & 0 & 0 & 0 & 0.715 & 0 & 0 & 0 \\ 0 & 0 & 0 & 0 & 0 & 0 & 0 & 0 & 0 & 0.715 & 0 & 0 \\ 0 & 0 & 0 & 0 & 0 & 0 & 0 & 0 & 0 & 0 & 0.715 & 0 \end{pmatrix}$
Waterbuck (Mollet, *Moss Landing Marine Labs*, 2010)	Mammalia	$\begin{pmatrix} 0 & 0.238 & 0.279 & 0.279 & 0.279 & 0.279 & 0.279 & 0.279 & 0.279 & 0.279 & 0.279 & 0.279 \\ 0.7 & 0 & 0 & 0 & 0 & 0 & 0 & 0 & 0 & 0 & 0 & 0 \\ 0 & 0.7 & 0 & 0 & 0 & 0 & 0 & 0 & 0 & 0 & 0 & 0 \\ 0 & 0 & 0.82 & 0 & 0 & 0 & 0 & 0 & 0 & 0 & 0 & 0 \\ 0 & 0 & 0 & 0.82 & 0 & 0 & 0 & 0 & 0 & 0 & 0 & 0 \\ 0 & 0 & 0 & 0 & 0.82 & 0 & 0 & 0 & 0 & 0 & 0 & 0 \\ 0 & 0 & 0 & 0 & 0 & 0.82 & 0 & 0 & 0 & 0 & 0 & 0 \\ 0 & 0 & 0 & 0 & 0 & 0 & 0.82 & 0 & 0 & 0 & 0 & 0 \\ 0 & 0 & 0 & 0 & 0 & 0 & 0 & 0.82 & 0 & 0 & 0 & 0 \\ 0 & 0 & 0 & 0 & 0 & 0 & 0 & 0 & 0.82 & 0 & 0 & 0 \\ 0 & 0 & 0 & 0 & 0 & 0 & 0 & 0 & 0 & 0.82 & 0 & 0 \end{pmatrix}$

White-tailed deer (Mollet, *Moss Landing Marine Labs*, 2010)	Mammalia

$$\begin{pmatrix}
0 & 0.4546 & 0.497 & 0.497 & 0.497 & 0.497 & 0.497 & 0.497 & 0.497 & 0.497 & 0.497 & 0.497 & 0.497 & 0.497 & 0.497 & 0.497 \\
0.6403 & 0 & 0 & 0 & 0 & 0 & 0 & 0 & 0 & 0 & 0 & 0 & 0 & 0 & 0 & 0 \\
0 & 0.6403 & 0 & 0 & 0 & 0 & 0 & 0 & 0 & 0 & 0 & 0 & 0 & 0 & 0 & 0 \\
0 & 0 & 0.7 & 0 & 0 & 0 & 0 & 0 & 0 & 0 & 0 & 0 & 0 & 0 & 0 & 0 \\
0 & 0 & 0 & 0.7 & 0 & 0 & 0 & 0 & 0 & 0 & 0 & 0 & 0 & 0 & 0 & 0 \\
0 & 0 & 0 & 0 & 0.7 & 0 & 0 & 0 & 0 & 0 & 0 & 0 & 0 & 0 & 0 & 0 \\
0 & 0 & 0 & 0 & 0 & 0.7 & 0 & 0 & 0 & 0 & 0 & 0 & 0 & 0 & 0 & 0 \\
0 & 0 & 0 & 0 & 0 & 0 & 0.7 & 0 & 0 & 0 & 0 & 0 & 0 & 0 & 0 & 0 \\
0 & 0 & 0 & 0 & 0 & 0 & 0 & 0.7 & 0 & 0 & 0 & 0 & 0 & 0 & 0 & 0 \\
0 & 0 & 0 & 0 & 0 & 0 & 0 & 0 & 0.7 & 0 & 0 & 0 & 0 & 0 & 0 & 0 \\
0 & 0 & 0 & 0 & 0 & 0 & 0 & 0 & 0 & 0.7 & 0 & 0 & 0 & 0 & 0 & 0 \\
0 & 0 & 0 & 0 & 0 & 0 & 0 & 0 & 0 & 0 & 0.7 & 0 & 0 & 0 & 0 & 0 \\
0 & 0 & 0 & 0 & 0 & 0 & 0 & 0 & 0 & 0 & 0 & 0.7 & 0 & 0 & 0 & 0 \\
0 & 0 & 0 & 0 & 0 & 0 & 0 & 0 & 0 & 0 & 0 & 0 & 0.7 & 0 & 0 & 0 \\
0 & 0 & 0 & 0 & 0 & 0 & 0 & 0 & 0 & 0 & 0 & 0 & 0 & 0.7 & 0 & 0
\end{pmatrix}$$

Lion (Oli & Zinner, *Oikos*, 2001)	Mammalia

$$\begin{pmatrix}
0 & 0 & 0.669 & 0.669 & 0.669 & 0.669 & 0.669 & 0.669 & 0.669 & 0.669 & 0.669 & 0.669 & 0.669 & 0.669 & 0.669 & 0.669 \\
0.432 & 0 & 0 & 0 & 0 & 0 & 0 & 0 & 0 & 0 & 0 & 0 & 0 & 0 & 0 & 0 \\
0 & 0.432 & 0 & 0 & 0 & 0 & 0 & 0 & 0 & 0 & 0 & 0 & 0 & 0 & 0 & 0 \\
0 & 0 & 0.891 & 0 & 0 & 0 & 0 & 0 & 0 & 0 & 0 & 0 & 0 & 0 & 0 & 0 \\
0 & 0 & 0 & 0.891 & 0 & 0 & 0 & 0 & 0 & 0 & 0 & 0 & 0 & 0 & 0 & 0 \\
0 & 0 & 0 & 0 & 0.891 & 0 & 0 & 0 & 0 & 0 & 0 & 0 & 0 & 0 & 0 & 0 \\
0 & 0 & 0 & 0 & 0 & 0.891 & 0 & 0 & 0 & 0 & 0 & 0 & 0 & 0 & 0 & 0 \\
0 & 0 & 0 & 0 & 0 & 0 & 0.891 & 0 & 0 & 0 & 0 & 0 & 0 & 0 & 0 & 0 \\
0 & 0 & 0 & 0 & 0 & 0 & 0 & 0.891 & 0 & 0 & 0 & 0 & 0 & 0 & 0 & 0 \\
0 & 0 & 0 & 0 & 0 & 0 & 0 & 0 & 0.891 & 0 & 0 & 0 & 0 & 0 & 0 & 0 \\
0 & 0 & 0 & 0 & 0 & 0 & 0 & 0 & 0 & 0.891 & 0 & 0 & 0 & 0 & 0 & 0 \\
0 & 0 & 0 & 0 & 0 & 0 & 0 & 0 & 0 & 0 & 0.891 & 0 & 0 & 0 & 0 & 0 \\
0 & 0 & 0 & 0 & 0 & 0 & 0 & 0 & 0 & 0 & 0 & 0.891 & 0 & 0 & 0 & 0 \\
0 & 0 & 0 & 0 & 0 & 0 & 0 & 0 & 0 & 0 & 0 & 0 & 0.891 & 0 & 0 & 0 \\
0 & 0 & 0 & 0 & 0 & 0 & 0 & 0 & 0 & 0 & 0 & 0 & 0 & 0.891 & 0 & 0 \\
0 & 0 & 0 & 0 & 0 & 0 & 0 & 0 & 0 & 0 & 0 & 0 & 0 & 0 & 0.891 & 0
\end{pmatrix}$$

North American black bear (Oli & Zinner, *Oikos*, 2001)	Mammalia

$$\begin{pmatrix}
0 & 0 & 0 & 0 & 0.395 & 0.395 & 0.395 & 0.395 & 0.395 & 0.395 & 0.395 & 0.395 & 0.395 & 0.395 & 0.395 & 0.395 & 0.395 & 0.395 \\
0.663 & 0 & 0 & 0 & 0 & 0 & 0 & 0 & 0 & 0 & 0 & 0 & 0 & 0 & 0 & 0 & 0 & 0 \\
0 & 0.663 & 0 & 0 & 0 & 0 & 0 & 0 & 0 & 0 & 0 & 0 & 0 & 0 & 0 & 0 & 0 & 0 \\
0 & 0 & 0.663 & 0 & 0 & 0 & 0 & 0 & 0 & 0 & 0 & 0 & 0 & 0 & 0 & 0 & 0 & 0 \\
0 & 0 & 0 & 0.663 & 0 & 0 & 0 & 0 & 0 & 0 & 0 & 0 & 0 & 0 & 0 & 0 & 0 & 0 \\
0 & 0 & 0 & 0 & 0.824 & 0 & 0 & 0 & 0 & 0 & 0 & 0 & 0 & 0 & 0 & 0 & 0 & 0 \\
0 & 0 & 0 & 0 & 0 & 0.824 & 0 & 0 & 0 & 0 & 0 & 0 & 0 & 0 & 0 & 0 & 0 & 0 \\
0 & 0 & 0 & 0 & 0 & 0 & 0.824 & 0 & 0 & 0 & 0 & 0 & 0 & 0 & 0 & 0 & 0 & 0 \\
0 & 0 & 0 & 0 & 0 & 0 & 0 & 0.824 & 0 & 0 & 0 & 0 & 0 & 0 & 0 & 0 & 0 & 0 \\
0 & 0 & 0 & 0 & 0 & 0 & 0 & 0 & 0.824 & 0 & 0 & 0 & 0 & 0 & 0 & 0 & 0 & 0 \\
0 & 0 & 0 & 0 & 0 & 0 & 0 & 0 & 0 & 0.824 & 0 & 0 & 0 & 0 & 0 & 0 & 0 & 0 \\
0 & 0 & 0 & 0 & 0 & 0 & 0 & 0 & 0 & 0 & 0.824 & 0 & 0 & 0 & 0 & 0 & 0 & 0 \\
0 & 0 & 0 & 0 & 0 & 0 & 0 & 0 & 0 & 0 & 0 & 0.824 & 0 & 0 & 0 & 0 & 0 & 0 \\
0 & 0 & 0 & 0 & 0 & 0 & 0 & 0 & 0 & 0 & 0 & 0 & 0.824 & 0 & 0 & 0 & 0 & 0 \\
0 & 0 & 0 & 0 & 0 & 0 & 0 & 0 & 0 & 0 & 0 & 0 & 0 & 0.824 & 0 & 0 & 0 & 0 \\
0 & 0 & 0 & 0 & 0 & 0 & 0 & 0 & 0 & 0 & 0 & 0 & 0 & 0 & 0.824 & 0 & 0 & 0 \\
0 & 0 & 0 & 0 & 0 & 0 & 0 & 0 & 0 & 0 & 0 & 0 & 0 & 0 & 0 & 0.824 & 0 & 0 \\
0 & 0 & 0 & 0 & 0 & 0 & 0 & 0 & 0 & 0 & 0 & 0 & 0 & 0 & 0 & 0 & 0.824 & 0
\end{pmatrix}$$

Species **(Reference)**	**PPM**
White alabone (Rogers-Bennett & Leaf, *Ecol. Appl.*, 2006)	$\begin{pmatrix} 0.071 & 0.252 & 0.874 & 2.298 \\ 0.354 & 0.226 & 0 & 0 \\ 0 & 0.301 & 0 & 0 \\ 0 & 0 & 0.626 & 0.717 \end{pmatrix}$
Wallaby (Fisher et al., *Ecol. Appl.*, 2000)	$\begin{pmatrix} 0 & 0 & 0 & 3.1 \\ 0.93 & 0 & 0 & 0 \\ 0 & 0.82 & 0 & 0 \\ 0 & 0 & 0.47 & 0.8 \end{pmatrix}$
Grass shrimp (Sable, *Dissertation: Louisiana State University.*, 2007)	$\begin{pmatrix} 0 & 0 & 0.7457 & 12 \\ 0.1381 & 0.1703 & 0 & 0 \\ 0 & 0.1166 & 0.6577 & 0 \\ 0 & 0 & 0.111 & 0.7882 \end{pmatrix}$
Columbian ground squirrel (Dobson & Oli, *Am. Nat.*, 2001)	$\begin{pmatrix} 0 & 1.382 & 1.382 & 1.382 & 1.382 \\ 0.35 & 0 & 0 & 0 & 0 \\ 0 & 0.35 & 0 & 0 & 0 \\ 0 & 0 & 0.765 & 0 & 0 \\ 0 & 0 & 0 & 0.765 & 0 \end{pmatrix}$
Red fox (Nelson et al, *PlosOne*, 2010)	$\begin{pmatrix} 0.55 & 0.63 & 1.63 & 0.65 \\ 0.38 & 0 & 0 & 0 \\ 0 & 0.32 & 0 & 0 \\ 0 & 0 & 0.79 & 0.28 \end{pmatrix}$
Pronghorn (Berger & Conner, *Ecol. Appl.*, 2008)	$\begin{pmatrix} 0 & 0 & 0.829 & 0 \\ 0.059 & 0 & 0 & 0 \\ 0 & 0.872 & 0.872 & 0 \\ 0 & 0 & 0.022 & 0 \end{pmatrix}$
Northern right whale (Fujiwara & Caswell, *Nature*, 2001)	$\begin{pmatrix} 0 & 0.009 & 0.087 & 0 \\ 0.92 & 0.86 & 0 & 0 \\ 0 & 0.08 & 0.8 & 0.83 \\ 0 & 0.02 & 0.19 & 0 \end{pmatrix}$
Mexican lizard (Zuniga-Vega et al., *Copeia*, 2007)	$\begin{pmatrix} 0.069 & 0 & 1.148 & 1.1027 \\ 0.2759 & 0.1875 & 0 & 0 \\ 0 & 0.625 & 0.1837 & 0 \\ 0 & 0 & 0.3265 & 0.4324 \end{pmatrix}$
Kemp's ridly sea turtle (Heppell et al., *Ecol. Appl.*, 1996)	$\begin{pmatrix} 0 & 0 & 3.14 & 86.08 \\ 0.33 & 0.57 & 0 & 0 \\ 0 & 0.054 & 0.74 & 0 \\ 0 & 0 & 0.03 & 0.82 \end{pmatrix}$

Appendix A2

Plant population projection matrices

This appendix contains population projection matrices and growth type for 122 plant species, which are used in Chapter 2 to create Figure 2.7. This data is taken from COMPADRE III [83], and in this appendix we show the references used to create the data in [83].

Species **(Reference)**	**Growth type**	**PPM**
Arenaria serpyllifolia (Dostal, *J Veg Sci*, 2007)	Annual	$\begin{pmatrix} 0.83416 & 0.00703 \\ 0.7475 & 0.0063 \end{pmatrix}$
Phacelia insularis insularis (Levine; McEachern; Cowan, *J Ecol*, 2008)	Annual	$\begin{pmatrix} 0.75 & 14.6064 \\ 0.016208 & 0 \end{pmatrix}$
Dorycnium spectabile (Iriondo; Albert; Gimenez; Lozano; Escudero, *Book*, 2009)	Herbaceous perennial	$\begin{pmatrix} 0.357 & 0.857 \\ 0.071 & 0.857 \end{pmatrix}$
Physaria ovalifolia (Dalgleish; Koons; Adler, *J Ecol*, 2010)	Herbaceous perennial	$\begin{pmatrix} 0.4 & 0.4 \\ 0.28 & 0.5 \end{pmatrix}$
Lobelia boykinii (Lacey; Royo; Bates; Herr, *Cast*, 2001)	Herbaceous perennial	$\begin{pmatrix} 0 & 0.08 \\ 0.29 & 0.8325 \end{pmatrix}$
Aechmea nudicaulis (Sampaio; Pico; Scarano, *Am J Bot*, 2005)	Herbaceous perennial	$\begin{pmatrix} 0.37 & 0.24 & 0.04 \\ 0.89 & 0.53 & 0 \\ 0 & 0.2 & 0.19 \end{pmatrix}$
Alliaria petiolata (Evans; Davis; Raghu; Ragavendran; Landis; Schemske, *Ecol Appl*, 2012)	Herbaceous perennial	$\begin{pmatrix} 0.9624 & 0 & 16.1411 \\ 0.011339 & 0 & 3.3899 \\ 0 & 0.10735 & 0 \end{pmatrix}$
Cirsium perplexans (Dodge, *PhD thesis*, 2005)	Herbaceous perennial	$\begin{pmatrix} 0 & 0 & 9.16 \\ 0.205 & 0.429 & 0.236 \\ 0 & 0.101 & 0.028 \end{pmatrix}$
Corallorhiza trifida (Iriondo; Albert; Gimenez; Lozano; Escudero, *Book*, 2009)	Herbaceous perennial	$\begin{pmatrix} 0.86 & 0 & 0.148 \\ 0 & 0 & 0.05 \\ 0.14 & 1 & 0.05 \end{pmatrix}$
Limonium erectum (Iriondo; Albert; Gimenez; Lozano; Escudero, *Book*, 2009)	Herbaceous perennial	$\begin{pmatrix} 0.493 & 0.457 & 1.996 \\ 0.045 & 0.462 & 0.182 \\ 0 & 0.053 & 0.545 \end{pmatrix}$

Linum tenuifolium (Munzbergova, *Plant Biology*, 2013)	Herbaceous perennial	$\begin{pmatrix} 0.19 & 0 & 1.33 \\ 0.24 & 0.48 & 0.31 \\ 0.05 & 0.21 & 0.2 \end{pmatrix}$
Plantago coronopus (Waite, *J Ecol*, 1984)	Herbaceous perennial	$\begin{pmatrix} 0 & 0 & 0.999 \\ 0 & 0 & 0.01054 \\ 0.213 & 0.285 & 0.427 \end{pmatrix}$
Ranunculus peltatus (Idestam-Almquist, *PhD thesis*, 1998)	Herbaceous perennial	$\begin{pmatrix} 0 & 0 & 4.4 \\ 0.094 & 0.096 & 0.205 \\ 0.136 & 0.1 & 0.152 \end{pmatrix}$
Sarcocapnos pulcherrima (Salinas; Suarez; Blanca, *Can J Bot*, 2002)	Herbaceous perennial	$\begin{pmatrix} 0.217 & 0 & 0.17 \\ 0.136 & 0.5 & 0 \\ 0 & 0.25 & 0.915 \end{pmatrix}$
Vella pseudocytisus pseudocytisus (Iriondo; Albert; Gimenez; Lozano; Escudero, *Book*, 2009)	Shrub	$\begin{pmatrix} 0.77475 & 0.022 & 0.0935 \\ 0.11675 & 0.962 & 0.25 \\ 0 & 0.002 & 0 \end{pmatrix}$
Cypripedium fasciculatum (Thorpe; Stanley; Kayne; Latham, *IAE*, 2011)	Herbaceous perennial	$\begin{pmatrix} 0.476 & 0.061 & 0.35 & 0 \\ 0.095 & 0.576 & 0.075 & 0.355 \\ 0 & 0.152 & 0.875 & 0.161 \\ 0.092 & 0.08 & 0.046 & 0.258 \end{pmatrix}$
Eryngium alpinum (Andrello; Bizoux; Barbet-Massin; Gaudeul; Nicole; Till-Bottraud, *Biol Cons*, 2012	Herbaceous perennial	$\begin{pmatrix} 0 & 0 & 0 & 15.53 \\ 0.02 & 0.8 & 0 & 0 \\ 0 & 0 & 0.62 & 0.84 \\ 0 & 0.05 & 0.28 & 0.13 \end{pmatrix}$
Pyrrocoma radiata (Kaye; Pyke, *Ecol*, 2003)	Herbaceous perennial	$\begin{pmatrix} 0 & 0 & 0 & 2.125 \\ 0.217 & 0.513 & 0.6 & 0 \\ 0 & 0.282 & 0.133 & 0.75 \\ 0 & 0 & 0.2 & 0.25 \end{pmatrix}$
Heracleum mantegazzianum (Nehrbass; Winkler; Pergl; Perglova; Pysek, *Pers Plant Ecol Evol Syst*, 2006	Herbaceous perennial	$\begin{pmatrix} 0.27 & 0.18 & 0.05 & 1.85 \\ 0.19 & 0.32 & 0.12 & 0.5 \\ 0.04 & 0.2 & 0.32 & 0 \\ 0 & 0.06 & 0.42 & 0 \end{pmatrix}$

Heteropogon contortus (O'Connor, *J Appl Ecol*, 1993)	Herbaceous perennial	$\begin{pmatrix} 0.6425 & 0.62 & 0.92 & 1.69 \\ 0.1125 & 0.455 & 0.1175 & 0.145 \\ 0.005 & 0.14 & 0.35 & 0.16 \\ 0 & 0 & 0.1725 & 0.5 \end{pmatrix}$
Hieracium floribundum (Thomas; Dale, *Can J Bot*, 1975)	Herbaceous perennial	$\begin{pmatrix} 0.239 & 0 & 0.597 & 0 \\ 0.263 & 0 & 0.213 & 0 \\ 0 & 0.008 & 0.93 & 0.93 \\ 0 & 0 & 0.07 & 0 \end{pmatrix}$
Hilaria mutica (Vega; Montana, *Plant Ecol*, 2004)	Herbaceous perennial	$\begin{pmatrix} 0.0773 & 0.1713 & 0.3145 & 0.6527 \\ 0.1362 & 0.3906 & 0.5256 & 0.069 \\ 0.0245 & 0.0781 & 0.359 & 0.5862 \\ 0 & 0.0078 & 0.0128 & 0.3448 \end{pmatrix}$
Limonium geronense (Iriondo; Albert; Gimenez; Lozano; Escudero, *Book*, 2009)	Herbaceous perennial	$\begin{pmatrix} 0 & 0 & 0.447 & 0.856 \\ 0.5 & 0.186 & 0.08 & 0 \\ 0.038 & 0.419 & 0.659 & 0.375 \\ 0 & 0.07 & 0.043 & 0.188 \end{pmatrix}$
Lotus arinagensis (Iriondo; Albert; Gimenez; Lozano; Escudero, *Book*, 2009)	Herbaceous perennial	$\begin{pmatrix} 0 & 0.019667 & 2.3953 & 6.0757 \\ 0 & 0 & 0.0023333 & 0.0046667 \\ 0 & 0.0063333 & 0.022 & 0.0043333 \\ 0.037 & 0.18167 & 0.44533 & 0.59367 \end{pmatrix}$
Mimulus cardinalis (Angert, *Ecol*, 2006)	Herbaceous perennial	$\begin{pmatrix} 0.184 & 376 & 720 & 1340 \\ 2.14e-05 & 0.0345 & 0.0104 & 0 \\ 2.14e-05 & 0.2759 & 0.3229 & 0.2632 \\ 0 & 0.1034 & 0.1979 & 0.3684 \end{pmatrix}$
Mimulus lewisii (Angert, *Ecol*, 2006)	Herbaceous perennial	$\begin{pmatrix} 0.0353 & 719 & 2810 & 13588 \\ 4.32e-05 & 0.0909 & 0.0263 & 0 \\ 1.05e-05 & 0.2727 & 0.5132 & 0.3248 \\ 3.08e-07 & 0.0303 & 0.1184 & 0.5726 \end{pmatrix}$

Anogra deltoidea (Thomson, *Cons Biol*, 2005)	Herbaceous perennial	$\begin{pmatrix} 0.81797 & 0 & 0.59 & 0.44 \\ 0.0967 & 0 & 0.0967 & 0.0967 \\ 0 & 0.36 & 0.3403 & 0.0784 \\ 0 & 0 & 0.0697 & 0.4816 \end{pmatrix}$
Pityopsis aspera (Gornish, *AoB Plants*, 2013)	Herbaceous perennial	$\begin{pmatrix} 0 & 0.166 & 0 & 0.622 \\ 0 & 0.05 & 0 & 0.189 \\ 0.302 & 0.474 & 0.61 & 0.705 \\ 0.038 & 0 & 0.051 & 0.106 \end{pmatrix}$
Plantago coronopus (http://www.hear.org/gcw/species/plantago_coronopus/)	NA	$\begin{pmatrix} 0 & 0.01696 & 0.13614 & 0.5194 \\ 0.3529 & 0 & 0 & 0.0476 \\ 0.3235 & 0.11111 & 0 & 0 \\ 0.3235 & 0.33333 & 0.5 & 0.2857 \end{pmatrix}$
Primula farinosa (Lindborg; Ehrlen, *Cons Biol*, 2002)	Herbaceous perennial	$\begin{pmatrix} 0 & 0 & 0 & 0.316 \\ 0.46 & 0.471 & 0.107 & 0.061 \\ 0 & 0.412 & 0.592 & 0.276 \\ 0 & 0.059 & 0.165 & 0.551 \end{pmatrix}$
Rubus saxatilis (Eriksson, *Ecol Res*, 1994)	Herbaceous perennial	$\begin{pmatrix} 0 & 0 & 0 & 0.4 \\ 0.59 & 0.51 & 0.12 & 0 \\ 0 & 0.36 & 0.75 & 0.78 \\ 0 & 0.04 & 0.08 & 0.09 \end{pmatrix}$
Rumex rupestris (Iriondo; Albert; Gimenez; Lozano; Escudero, *Book*, 2009)	Herbaceous perennial	$\begin{pmatrix} 0 & 0 & 0.2 & 0.353 \\ 0.333 & 0.426 & 0.276 & 0.59 \\ 0.333 & 0.213 & 0.213 & 0.103 \\ 0 & 0.191 & 0.191 & 0.282 \end{pmatrix}$
Saponaria bellidifolia (Csergo; Molnar; Garcia, *Popul Ecol*, 2011)	Herbaceous perennial	$\begin{pmatrix} 0.5 & 0 & 0 & 0.015 \\ 0.5 & 0.375 & 0 & 0.197 \\ 0 & 0.063 & 0.333 & 0.288 \\ 0 & 0.25 & 0.667 & 0.515 \end{pmatrix}$

Taraxacum officinale (Vavrek; McGraw; Yang, *J Ecol*, 1997)	Herbaceous perennial	$\begin{pmatrix} 0.1719 & 0.2155 & 0.0536 & 0.1429 \\ 0.0912 & 0.25 & 0.1607 & 0.0952 \\ 0.0363 & 0.2457 & 0.3036 & 0.2381 \\ 0.0058 & 0.0905 & 0.3214 & 0.4286 \end{pmatrix}$
Zea diploperennis (Sanchez-Velazquez; Ezcurra; Martinez-Ramos; Alvarez-Buylla; Lorente, *J Ecol*, 2002)	Herbaceous perennial	$\begin{pmatrix} 0.258 & 0 & 44.155 & 373.3974 \\ 0.0002445 & 0.3684 & 0.04 & 0.99 \\ 0 & 0.3684 & 0.6 & 0 \\ 0 & 0.2104 & 0.32 & 0 \end{pmatrix}$
Betula nana (Ebert; Ebert, *Vegetatio*, 1989)	Shrub	$\begin{pmatrix} 0.059 & 0 & 0.111 & 0.091 \\ 0.176 & 0.4 & 0.111 & 0 \\ 0.118 & 0.4 & 0.556 & 0.091 \\ 0 & 0.1 & 0.22 & 0.818 \end{pmatrix}$
Dodonaea viscosa angustifolia (Bekele, *PhD thesis*, 2000)	Shrub	$\begin{pmatrix} 0.13245 & 0.04645 & 0.0828 & 1.5629 \\ 0.22795 & 0.2137 & 0.03595 & 0.57645 \\ 0.02085 & 0.38325 & 0.35595 & 0.1 \\ 0 & 0 & 0.0937 & 0.3255 \end{pmatrix}$
Miconia prasina (Pascarella; Alde; Zimmerman, *Biotrop*, 2007)	Shrub	$\begin{pmatrix} 0.5825 & 0.6675 & 0.4225 & 0.325 \\ 0.05 & 0.7625 & 0.14 & 0.025 \\ 0 & 0.1425 & 0.7325 & 0.2825 \\ 0 & 0 & 0.0825 & 0.6725 \end{pmatrix}$
Coryphanta robbinsorum (Schmalzel; Reichenbacher; Rutman, *Madrono*, 1995)	Succulent	$\begin{pmatrix} 0 & 0 & 0 & 33 \\ 0.003 & 0.333 & 0 & 0 \\ 0 & 0.222 & 0.75 & 0 \\ 0 & 0 & 0.188 & 0.941 \end{pmatrix}$
Rhododendron ponticum (Salguero-Gomez, *MSc thesis*, 2004)	Tree	$\begin{pmatrix} 0 & 0 & 0.05 & 0.1 \\ 0.0195 & 0.25 & 0 & 0.01 \\ 0 & 0.59 & 0.89 & 0 \\ 0 & 0 & 0.15 & 0.91 \end{pmatrix}$

Laminaria digitata (Chapman, *Hydrobiol*, 1993)	Algae	$\begin{pmatrix} 0.341 & 0.338 & 0.255 & 0.06 & 0.024 \\ 0.123 & 0.254 & 0 & 0 & 0 \\ 0.004 & 0.218 & 0.444 & 0.333 & 0 \\ 0 & 0.056 & 0.221 & 0.444 & 0 \\ 0 & 0 & 0 & 0.111 & 0 \end{pmatrix}$
Aeschynomene virginica (Griffith; Forseth, *Ecol Appl*, 2005)	Annual	$\begin{pmatrix} 0 & 0 & 1.3256 & 1.3256 & 1.3256 \\ 0.014781 & 0 & 0 & 0 & 0 \\ 0 & 0 & 0.81527 & 0.81527 & 0.81527 \\ 0.023986 & 0 & 0 & 0 & 0 \\ 0 & 0.023986 & 0 & 0 & 0 \end{pmatrix}$
Catopsis compacta (del Castillo et al., *Ecol & Evol*, 2013)	Epiphyte	$\begin{pmatrix} 0.5 & 0 & 0 & 0 & 0.33 \\ 0.25 & 0.392 & 0.061 & 0 & 0 \\ 0 & 0.459 & 0.696 & 0.167 & 0 \\ 0 & 0 & 0.101 & 0.528 & 0.133 \\ 0 & 0 & 0.027 & 0.139 & 0.8 \end{pmatrix}$
Tillandsia multicaulis (Winkler; Hulber; Hietz, *Bas & Appl Ecol*, 2007)	Epiphyte	$\begin{pmatrix} 0.123 & 0.009 & 0 & 0.007 & 16.041 \\ 0.221 & 0.704 & 0.039 & 0.007 & 0 \\ 0 & 0.031 & 0.39 & 0.029 & 0.082 \\ 0 & 0 & 0.284 & 0.73 & 0.673 \\ 0 & 0 & 0 & 0.182 & 0.102 \end{pmatrix}$
Asplenium scolopendrium americanum (Bremer; Jongejans, *Popul Ecol*, 2010)	Fern	$\begin{pmatrix} 0.29091 & 0.030303 & 0.05346 & 3.1188 & 0 \\ 0.39887 & 0.4258 & 0.10959 & 0.1232 & 0 \\ 0.011216 & 0.30148 & 0.16751 & 0 & 0 \\ 0 & 0.019425 & 0.26819 & 0.41084 & 0.07254 \\ 0 & 0 & 0 & 0.34716 & 0.73346 \end{pmatrix}$
Cochlearia pyrenaica (Abs, *Fol Geobot*, 1999)	Herbaceous perennial	$\begin{pmatrix} 0 & 0 & 0 & 0 & 24 \\ 0.2 & 0 & 0 & 0 & 0 \\ 0 & 0.2 & 0.13 & 0 & 0.07 \\ 0 & 0 & 0.22 & 0.08 & 0.05 \\ 0 & 0 & 0.16 & 0.86 & 0.18 \end{pmatrix}$

Echinacea angustifolia (Hurlburt, *PhD thesis*, 1999)	Herbaceous perennial	$\begin{pmatrix} 0 & 0 & 0.213 & 0.502 & 0 \\ 0.3333 & 0.6029 & 0.0595 & 0 & 0.7273 \\ 0 & 0.0574 & 0.5714 & 0.0536 & 0.2273 \\ 0 & 0 & 0.2381 & 0.875 & 0.0455 \\ 0.0667 & 0.0435 & 0.0465 & 0.0196 & 0 \end{pmatrix}$
Eriogonum longifolium (Satterthwaite; Menges; Quintana-Ascencio, *Ecol Appl*, 2002)	Herbaceous perennial	$\begin{pmatrix} 0 & 0 & 0 & 0.287 & 0 \\ 0.601 & 0.091 & 0 & 0.019 & 0 \\ 0 & 0.636 & 0.708 & 0.767 & 0.4 \\ 0.021 & 0.091 & 0.167 & 0.157 & 0 \\ 0.025 & 0.045 & 0 & 0.013 & 0.6 \end{pmatrix}$
Eupatorium perfoliatum (Byers; Meagher, *Ecol Appl*, 1997)	Herbaceous perennial	$\begin{pmatrix} 0 & 0 & 0.088 & 0 & 0.069667 \\ 0.10333 & 0.17067 & 0.092667 & 0.143 & 0.23933 \\ 0.037 & 0 & 0.089333 & 0.068667 & 0.24133 \\ 0.13467 & 0.157 & 0.24767 & 0.141 & 0.15433 \\ 0.247 & 0.078333 & 0.402 & 0.12533 & 0.55133 \end{pmatrix}$
Gaura neomexicana coloradensis (Floyd; Ranker, *Int J Plant Sci*, 1998)	Herbaceous perennial	$\begin{pmatrix} 0 & 0 & 0 & 0 & 0.4359 \\ 0.5833 & 0.1333 & 0.0588 & 0 & 0 \\ 0 & 0.5333 & 0.2647 & 0 & 0.0256 \\ 0 & 0.1333 & 0.0294 & 0 & 0 \\ 0.0833 & 0.1333 & 0.5 & 0.9 & 0 \end{pmatrix}$
Lepanthes rubripetala (Tremblay; Ackerman, *Biol J Linn Soc*, 2001)	Herbaceous perennial	$\begin{pmatrix} 0 & 0 & 0 & 0.159 & 0 \\ 0.667 & 0.667 & 0 & 0 & 0 \\ 0 & 0.37 & 0.812 & 0 & 0 \\ 0 & 0 & 0.01 & 0.784 & 0.131 \\ 0 & 0 & 0 & 0.179 & 0.801 \end{pmatrix}$
Liatris scariosa (Ellis, *Ecol*, 2012)	Herbaceous perennial	$\begin{pmatrix} 0 & 0 & 10.4545 & 0 & 0 \\ 0.28814 & 0.43125 & 0 & 0 & 0.5 \\ 0 & 0.00625 & 0.090909 & 0.055556 & 0 \\ 0 & 0 & 0.36364 & 0.5 & 0.16667 \\ 0.0067797 & 0.10625 & 0.18182 & 0.055556 & 0.33333 \end{pmatrix}$

Lupinus tidestromii (Dangremond; Knight, *Ecol*, 2010)	Herbaceous perennial	$\begin{pmatrix} 0 & 0 & 0 & 0 & 0.5051 \\ 1 & 0 & 0 & 0 & 1.1234 \\ 0 & 1 & 0 & 0 & 0.3704 \\ 0 & 0 & 0.2 & 0.2817 & 0.2 \\ 0 & 0 & 0 & 0.3714 & 0.48 \end{pmatrix}$
Oxalis acetosella (Berg, *Ecog*, 2002)	Herbaceous perennial	$\begin{pmatrix} 0 & 0 & 0.35 & 0 & 0.35 \\ 0 & 0.161 & 0.161 & 0.161 & 0.161 \\ 0 & 0.037 & 0.037 & 0.037 & 0.037 \\ 0.25 & 0.5125 & 0.237 & 0.5605 & 0.2295 \\ 0 & 0.197 & 0.6705 & 0.151 & 0.5715 \end{pmatrix}$
Panax quinquefolius (Van de Voort; McGraw, *Biol Cons*, 2006)	Herbaceous perennial	$\begin{pmatrix} 0.4518 & 0 & 0.1809 & 0.5935 & 2.4135 \\ 0.0963 & 0.5848 & 0.0753 & 0 & 0 \\ 0 & 0.192 & 0.5858 & 0.1775 & 0.021 \\ 0 & 0 & 0.1841 & 0.4901 & 0.0659 \\ 0 & 0 & 0.0879 & 0.1649 & 0.7403 \end{pmatrix}$
Plantago media (Eriksson; Eriksson, *J Veg Sci*, 2000)	Herbaceous perennial	$\begin{pmatrix} 0 & 0 & 0 & 0 & 0.67 \\ 0.06 & 0 & 0 & 0 & 0 \\ 0 & 0.06 & 0.65 & 0.05 & 0.05 \\ 0 & 0 & 0.29 & 0.49 & 0.15 \\ 0 & 0 & 0 & 0.43 & 0.8 \end{pmatrix}$
Primula elatior (Jacquemyn; Brys, *Ecol*, 2008)	Herbaceous perennial	$\begin{pmatrix} 0 & 0 & 0 & 1.375 & 1.9412 \\ 0.06 & 0 & 0 & 0 & 0 \\ 0 & 0.625 & 0.2 & 0.125 & 0.058824 \\ 0 & 0 & 0.4 & 0.625 & 0 \\ 0 & 0 & 0 & 0.25 & 0.88235 \end{pmatrix}$
Ramonda myconi (Pico; Riba, *Plant Ecol*, 2002)	Herbaceous perennial	$\begin{pmatrix} 0.5714 & 0 & 0 & 0.0142 & 0.0875 \\ 0.0714 & 0.6667 & 0.125 & 0.0833 & 0.04 \\ 0 & 0.1111 & 0.625 & 0.0833 & 0 \\ 0 & 0 & 0.25 & 0.4167 & 0.04 \\ 0 & 0 & 0 & 0.4167 & 0.92 \end{pmatrix}$

Sanicula elata (Gustafsson; Ehrlen, *Oikos*, 2003)	Herbaceous perennial	$\begin{pmatrix} 0 & 0 & 0 & 0 & 0.762 \\ 0.125 & 0.348 & 0.216 & 0.077 & 0 \\ 0.031 & 0.304 & 0.49 & 0.077 & 0.4 \\ 0 & 0.101 & 0.078 & 0.231 & 0.35 \\ 0 & 0 & 0.118 & 0.462 & 0.2 \end{pmatrix}$
Succisa pratensis (Milden, *Phd thesis*, 2005)	Herbaceous perennial	$\begin{pmatrix} 0.08 & 0 & 0 & 0 & 3.151 \\ 0.003467 & 0 & 0 & 0 & 0.13656 \\ 0 & 0.13391 & 0.15385 & 0.028249 & 0.041667 \\ 0 & 0 & 0.53846 & 0.69492 & 0.35417 \\ 0 & 0 & 0.076923 & 0.18644 & 0.5625 \end{pmatrix}$
Trollius laxus (Scanga; Leopold, *Biol Cons*, 2012)	Herbaceous perennial	$\begin{pmatrix} 0 & 0.009 & 0.1888 & 0.424 & 0.4159 \\ 0.1305 & 0.4135 & 0.1852 & 0.115 & 0.0159 \\ 0.0062 & 0.0709 & 0.3786 & 0.1947 & 0.0398 \\ 0 & 0.0138 & 0.2181 & 0.3894 & 0.1155 \\ 0 & 0.0035 & 0.0412 & 0.2124 & 0.7371 \end{pmatrix}$
Viola montana (Eckstein; Otte, *Flora*, 2004)	Herbaceous perennial	$\begin{pmatrix} 0 & 0 & 0 & 0.689 & 0.589 \\ 0.4 & 0.481 & 0 & 0.117 & 0 \\ 0 & 0.079 & 0.15 & 0.383 & 0.333 \\ 0 & 0.267 & 0.2 & 0.283 & 0 \\ 0 & 0 & 0.05 & 0.217 & 0 \end{pmatrix}$
Viola pumila (Eckstein; Danihelka; Otte, *Biol*, 2009)	Herbaceous perennial	$\begin{pmatrix} 0 & 0 & 0 & 1.532 & 1.532 \\ 0.491 & 0.272 & 0.094 & 0.113 & 0.099 \\ 0.008 & 0.21 & 0.386 & 0.336 & 0.37 \\ 0 & 0.046 & 0.114 & 0.189 & 0.065 \\ 0 & 0 & 0.179 & 0.09 & 0.345 \end{pmatrix}$
Viola stagnina (Eckstein; Danihelka; Otte, *Biol*, 2009)	Herbaceous perennial	$\begin{pmatrix} 0 & 0 & 0 & 0.042 & 0.042 \\ 0.667 & 0.443 & 0.084 & 0.325 & 0 \\ 0 & 0.172 & 0.392 & 0.23 & 0.291 \\ 0 & 0.093 & 0.269 & 0 & 0.067 \\ 0 & 0.026 & 0.238 & 0.397 & 0.456 \end{pmatrix}$

Chamaedorea radicalis (Endress; Gorchov; Robert; Noble, *Ecol Appl*, 2004)	Palm	$\begin{pmatrix} 0.06 & 0 & 0 & 0.02 & 1.24 \\ 0.16 & 0.58 & 0.08 & 0 & 0 \\ 0 & 0.2 & 0.44 & 0 & 0 \\ 0 & 0 & 0.2 & 0.53 & 0.09 \\ 0 & 0 & 0 & 0.27 & 0.86 \end{pmatrix}$
Purshia subintegra (Maschinski; Baggs; Quintano-Ascencio; Menges, *Cons Biol*, 2006)	Shrub	$\begin{pmatrix} 0.057 & 0 & 0 & 0 & 3.6 \\ 1e-09 & 0 & 0 & 0 & 0.136 \\ 0 & 0.041 & 0.5 & 0 & 0 \\ 0 & 0 & 0.001 & 0.255 & 0.327 \\ 0 & 0 & 0 & 0.553 & 0.668 \end{pmatrix}$
Mammillaria pectinifera (Valverde; Zavala-Hurtado, *J Arid Env*, 2006)	Succulent	$\begin{pmatrix} 0.25 & 0 & 0 & 1 & 3.971 \\ 0.051 & 0.16 & 0 & 0.206 & 0.817 \\ 0 & 0.04 & 0.528 & 0.074 & 0.059 \\ 0 & 0 & 0.085 & 0.667 & 0.176 \\ 0 & 0 & 0 & 0.056 & 0.412 \end{pmatrix}$
Abies magnifica (van Mantgem; Stepheson, *J Ecol*, 2005)	Tree	$\begin{pmatrix} 0.784 & 0 & 0 & 0 & 0.094 \\ 0.082 & 0.777 & 0 & 0 & 0 \\ 0 & 0.092 & 0.906 & 0 & 0 \\ 0 & 0 & 0.044 & 0.911 & 0 \\ 0 & 0 & 0 & 0.024 & 0.939 \end{pmatrix}$
Guettarda viburnoides (Loayza; Knight, *Ecol*, 2010)	Tree	$\begin{pmatrix} 0.05 & 0 & 0 & 0 & 1.99 \\ 0.05 & 0.316 & 0.444 & 0 & 0 \\ 0.05 & 0.105 & 0.111 & 0.223 & 0.07 \\ 0 & 0.053 & 0.111 & 0.777 & 0 \\ 0 & 0 & 0 & 0.01 & 0.923 \end{pmatrix}$
Pinus ponderosa (van Mantgem; Stepheson, *Ecol*, 2005)	Tree	$\begin{pmatrix} 0.73 & 0 & 0 & 0 & 0.052 \\ 0.108 & 0.656 & 0 & 0 & 0 \\ 0 & 0.063 & 0.756 & 0 & 0 \\ 0 & 0 & 0.049 & 0.8 & 0 \\ 0 & 0 & 0 & 0.091 & 0.99 \end{pmatrix}$

Tillandsia violacea (Mondragon; Ticktin, *Cons Biol*, 2011)	Epiphyte	$\begin{pmatrix} 0.143 & 0 & 0 & 0 & 0 & 0.568 \\ 0.571 & 0.2 & 0.035 & 0 & 0.05 & 0.193 \\ 0 & 0.55 & 0.556 & 0.069 & 0 & 0 \\ 0 & 0 & 0.268 & 0.725 & 0.178 & 0 \\ 0 & 0 & 0 & 0.041 & 0.589 & 0.261 \\ 0 & 0 & 0 & 0 & 0.022 & 0.545 \end{pmatrix}$
Actaea spicata (Froborg; Eriksson, *Can J Bot*, 2003)	Herbaceous perennial	$\begin{pmatrix} 0.41 & 0 & 0 & 0 & 0 & 107.8 \\ 0.003 & 0 & 0 & 0 & 0 & 0 \\ 0 & 0.30167 & 0.33 & 0 & 0 & 0 \\ 0 & 0 & 0.35 & 0.56 & 0.11 & 0.07 \\ 0 & 0 & 0 & 0.15 & 0.39667 & 0.22 \\ 0 & 0 & 0 & 0.13 & 0.4 & 0.64 \end{pmatrix}$
Euterpe edulis (Freckleton et al, *NA*, 2003)	Palm	$\begin{pmatrix} 0.41 & 0 & 0 & 0 & 0 & 73.7 \\ 0.002 & 0 & 0 & 0 & 0 & 0 \\ 0 & 0.54 & 0.59 & 0 & 0 & 0 \\ 0 & 0 & 0.3 & 0.62 & 0.18 & 0.2 \\ 0 & 0 & 0 & 0.17 & 0.28 & 0.12 \\ 0 & 0 & 0 & 0.14 & 0.46 & 0.63 \end{pmatrix}$
Actaea spicata (Froborg; Eriksson, *Can J Bot*, 2003)	Herbaceous perennial	$\begin{pmatrix} 0.41 & 0 & 0 & 0 & 0 & 135 \\ 0.001 & 0 & 0 & 0 & 0 & 0 \\ 0 & 0.2 & 0.43 & 0 & 0 & 0 \\ 0 & 0 & 0.143 & 0.44 & 0.1 & 0.03 \\ 0 & 0 & 0 & 0.16 & 0.39 & 0.22 \\ 0 & 0 & 0 & 0.04 & 0.24 & 0.59 \end{pmatrix}$
Cirsium dissectum (Jongejans; de Vere; de Kroon, *Plant Ecol*, 2008)	Herbaceous perennial	$\begin{pmatrix} 0.3 & 0 & 0 & 0.005 & 0 & 0.005 \\ 0.15 & 0.27 & 0.18 & 0.0095 & 0.23 & 0.0095 \\ 0 & 0.32 & 0.306 & 0 & 0.24 & 0 \\ 0 & 0.024 & 0.095 & 0 & 0.065 & 0 \\ 0 & 0.412 & 0.41 & 1.718 & 0.04 & 2.05 \\ 0 & 0.04 & 0.03 & 0.14 & 0.017 & 0.07 \end{pmatrix}$

Cirsium palustre (Ramula, *Acta Oeco*, 2008)	Herbaceous perennial	$\begin{pmatrix} 0.005 & 0 & 0 & 0 & 4.342 & 6.283 \\ 0.02 & 0 & 0 & 0 & 17.101 & 24.747 \\ 0 & 0.25 & 0 & 0 & 0 & 0 \\ 0 & 0 & 0.075 & 0.083 & 0 & 0 \\ 0 & 0 & 0.118 & 0 & 0 & 0 \\ 0 & 0 & 0 & 0.019 & 0 & 0 \end{pmatrix}$
Dicerandra frutescens (Menges; Quintano-Ascencio; Weekley; Gaoue, *Biol Cons*, 2006)	Herbaceous perennial	$\begin{pmatrix} 0.1 & 0 & 0 & 4.0503 & 18.631 & 66.62 \\ 0.001 & 0 & 0 & 0.086 & 0.398 & 1.422 \\ 0 & 0.167 & 0.2 & 0.25 & 0.25 & 0 \\ 0 & 0 & 0 & 0.25 & 0.083 & 0 \\ 0 & 0 & 0.4 & 0.25 & 0.416 & 0.333 \\ 0 & 0 & 0 & 0 & 0.083 & 0.667 \end{pmatrix}$
Digitalis purpurea (Sletvold; Rydgren, *J Ecol*, 2007)	Herbaceous perennial	$\begin{pmatrix} 0.67 & 0 & 0 & 0 & 0 & 30.5 \\ 0.0871 & 0.00424 & 0.0385 & 0.00911 & 0 & 3.41 \\ 0.0165 & 0.0127 & 0.0315 & 0.0478 & 0 & 0.646 \\ 0.00261 & 0.00847 & 0.0175 & 0.164 & 0.0313 & 0.102 \\ 0 & 0 & 0 & 0.0387 & 0.121 & 0 \\ 0 & 0 & 0 & 0.00911 & 0.383 & 0 \end{pmatrix}$
Eryngium cuneifolium (Menges; Quintano-Ascencio, *Ecol Monog*, 2004)	Herbaceous perennial	$\begin{pmatrix} 0.5 & 0 & 0 & 58.47 & 115.8 & 128.3 \\ 0.0025 & 0 & 0 & 0 & 0 & 0 \\ 0 & 0.67 & 0.56 & 0.38 & 0.04 & 0 \\ 0 & 0.11111 & 0.074 & 0.13 & 0.16 & 0.08 \\ 0 & 0 & 0.037 & 0.083 & 0.36 & 0.16 \\ 0 & 0 & 0.074 & 0 & 0.2 & 0.32 \end{pmatrix}$
Gentianella campestris (Lennartsson; Oostermeijer, *J Ecol*, 2001)	Herbaceous perennial	$\begin{pmatrix} 0 & 0 & 0 & 0 & 417 & 737 \\ 0.66 & 0 & 0 & 0 & 0 & 0 \\ 0.00011 & 1.7e-05 & 0 & 0 & 0.26 & 0.46 \\ 5.2e-05 & 8e-06 & 0 & 0 & 0.13 & 0.23 \\ 0 & 0 & 0.60 & 0.23 & 0 & 0 \\ 0 & 0 & 0.0045 & 0.64 & 0 & 0 \end{pmatrix}$

Potentilla congesta (Kaye; Benfield, *Report*, 2004)	Herbaceous perennial	$\begin{pmatrix} 0 & 0 & 0 & 0.088 & 0.177 & 0.356 \\ 0.59 & 0.5 & 0.16 & 0.1 & 0.077 & 0 \\ 0.077 & 0.14 & 0.23 & 0.0698 & 0.058 & 0.03 \\ 0 & 0.06 & 0.13 & 0.21 & 0.1538 & 0.03 \\ 0 & 0.06 & 0.19 & 0.2 & 0.29 & 0.09 \\ 0 & 0.02 & 0.10 & 0.19 & 0.29 & 0.76 \end{pmatrix}$
Hypericum cumulicola (Ellis et al., *Ecol*, 2012)	Herbaceous perennial	$\begin{pmatrix} 0.824 & 0 & 0 & 170.6 & 468.4 & 576 \\ 0.0002 & 0 & 0 & 0 & 0 & 0 \\ 0 & 0.082 & 0 & 0.03 & 0 & 0 \\ 0 & 0.46 & 0.29 & 0.3 & 0.1 & 0 \\ 0 & 0.13 & 0 & 0.39 & 0.4 & 0 \\ 0 & 0 & 0.14 & 0.03 & 0.067 & 0.2 \end{pmatrix}$
Hypochaeris radicata (Jongejans; de Kroon, *J Ecol*, 2005)	Herbaceous perennial	$\begin{pmatrix} 0.375 & 0.033 & 0 & 1.743 & 0 & 1.743 \\ 0.163 & 0.26 & 0.111 & 0.572 & 0.184 & 0.334 \\ 0 & 0.282 & 0.479 & 0.349 & 0.107 & 0.111 \\ 0 & 0.033 & 0.135 & 0.19 & 0 & 0.111 \\ 0 & 0.015 & 0.011 & 0.025 & 0 & 0 \\ 0 & 0 & 0.005 & 0.007 & 0 & 0 \end{pmatrix}$
Lomatium bradshawii (Kaye; Pendergrass; Finley; Kauffman, *Ecol Appl*, 2001)	Herbaceous perennial	$\begin{pmatrix} 0 & 0 & 0 & 0.078 & 0.892 & 3.356 \\ 0.286 & 0.328 & 0.106 & 0.06 & 0.018 & 0 \\ 0.17 & 0.262 & 0.362 & 0.168 & 0.09 & 0 \\ 0.006 & 0.07 & 0.18 & 0.278 & 0.22 & 0.04 \\ 0 & 0.018 & 0.12 & 0.298 & 0.394 & 0.146 \\ 0 & 0 & 0.004 & 0.022 & 0.102 & 0.68 \end{pmatrix}$
Lomatium cookii (Kaye; Pyke, *Ecol*, 2003)	Herbaceous perennial	$\begin{pmatrix} 0 & 0 & 0 & 0 & 0.252 & 1.567 \\ 0.426 & 0.405 & 0.2 & 0 & 0 & 0 \\ 0.115 & 0.23 & 0.54 & 0.154 & 0.231 & 0 \\ 0 & 0.014 & 0.04 & 0 & 0.077 & 0.083 \\ 0 & 0 & 0.04 & 0.385 & 0.231 & 0.167 \\ 0 & 0 & 0.02 & 0 & 0.154 & 0.333 \end{pmatrix}$

Orchis purpurea (Jacquemyns; Brys; Jongejans, *Ecol*, 2010)	Herbaceous perennial	$\begin{pmatrix} 0 & 0 & 0 & 0 & 0 & 142.29 \\ 0.015 & 0 & 0 & 0 & 0 & 0 \\ 0 & 0.026 & 0 & 0 & 0 & 0 \\ 0 & 0 & 1 & 0.667 & 0 & 0 \\ 0 & 0 & 0 & 0.333 & 0.80808 & 0.571 \\ 0 & 0 & 0 & 0 & 0.15392 & 0.429 \end{pmatrix}$
Potentilla anserina (Eriksson, *J Ecol*, 1988)	Herbaceous perennial	$\begin{pmatrix} 0 & 0.13 & 0 & 1.05 & 1.05 & 0 \\ 0 & 0.04 & 0 & 0 & 0.47 & 0.47 \\ 0.1 & 0.75 & 0.56 & 0.51 & 0.42 & 0.43 \\ 0 & 0.13 & 0.02 & 0.11 & 0.03 & 0 \\ 0 & 0.04 & 0.01 & 0.03 & 0.08 & 0.07 \\ 0 & 0.02 & 0.03 & 0.04 & 0.13 & 0.07 \end{pmatrix}$
Primula vulgaris (Endels; Jacquemyn; Brys; Hermy, *J Ecol*, 2007)	Herbaceous perennial	$\begin{pmatrix} 0 & 0 & 0 & 0.0335 & 0.0727 & 0.2429 \\ 0.0107 & 0.0232 & 0 & 0.028 & 0.0607 & 0.2028 \\ 0.023 & 0.0498 & 0.0747 & 0.0601 & 0.1302 & 0 \\ 0.0242 & 0.0524 & 0.0786 & 0.0631 & 0 & 0 \\ 0 & 0 & 0.0919 & 0.0739 & 0.1602 & 0.5355 \\ 0 & 0 & 0.1143 & 0.0919 & 0.1992 & 0.6658 \end{pmatrix}$
Euterpe edulis (Freckleton et al, *NA*, 2003)	Palm	$\begin{pmatrix} 0.41 & 0 & 0 & 0 & 0 & 73.7 \\ 0.002 & 0 & 0 & 0 & 0 & 0 \\ 0 & 0.54 & 0.59 & 0 & 0 & 0 \\ 0 & 0 & 0.3 & 0.62 & 0.18 & 0.2 \\ 0 & 0 & 0 & 0.17 & 0.28 & 0.12 \\ 0 & 0 & 0 & 0.14 & 0.46 & 0.63 \end{pmatrix}$
Euterpe oleracea (Arango; Duque; Munoz, *Int J Trop Biol*, 2010)	Palm	$\begin{pmatrix} 0.443 & 0.1702 & 0.3355 & 0.5813 & 0.9009 & 1.6158 \\ 0.051 & 0.4 & 0 & 0 & 0 & 0 \\ 0 & 0.4 & 0.519 & 0 & 0 & 0 \\ 0 & 0 & 0.296 & 0.425 & 0 & 0 \\ 0 & 0 & 0.019 & 0.5 & 0.447 & 0 \\ 0 & 0 & 0 & 0.025 & 0.447 & 0.89 \end{pmatrix}$

Iriartea deltoidea (Pinard, *Biotrop*, 1993)	Palm	$\begin{pmatrix} 0.7943 & 0 & 0 & 0.1951 & 1.5605 & 2.6314 \\ 0.0402 & 0.8142 & 0 & 0 & 0 & 0 \\ 0 & 0.0372 & 0.8958 & 0 & 0 & 0 \\ 0 & 0 & 0.0335 & 0.95 & 0 & 0 \\ 0 & 0 & 0 & 0.05 & 0.9399 & 0 \\ 0 & 0 & 0 & 0 & 0.0451 & 0.8284 \end{pmatrix}$
Ambrosia deltoidea (Goldberg; Turner, *Ecol*, 1986)	Shrub	$\begin{pmatrix} 0.18903 & 0.18393 & 0.1605 & 0.11658 & 0.27573 & 0.5204 \\ 0.032775 & 0.041725 & 0.045775 & 0.00265 & 0.001125 & 0 \\ 0.10595 & 0.31145 & 0.44085 & 0.039712 & 0.0089875 & 0.0047125 \\ 0.00345 & 0.03725 & 0.1724 & 0.31649 & 0.1193 & 0.02655 \\ 0 & 0 & 0.009675 & 0.095437 & 0.27455 & 0.14779 \\ 0.00025 & 0 & 0.00195 & 0.0123 & 0.079812 & 0.29424 \end{pmatrix}$
Pinus lambertiana (Maloney; Vogler; Eckert; Jensen; Neale, *Ecol & Manag*, 2011)	Tree	$\begin{pmatrix} 0.8662 & 0 & 0 & 0.0091 & 0.0705 & 0.964 \\ 0.0385 & 0.7692 & 0 & 0 & 0 & 0 \\ 0 & 0.0336 & 0.9567 & 0 & 0 & 0 \\ 0 & 0 & 0.0431 & 0.7779 & 0 & 0 \\ 0 & 0 & 0 & 0.0392 & 0.9362 & 0 \\ 0 & 0 & 0 & 0 & 0.0374 & 0.9762 \end{pmatrix}$
Collinsia verna (Kalisz; McPeek, *Ecol*, 1992)	Annual	$\begin{pmatrix} 0 & 0 & 0 & 4.305 & 4.305 & 4.305 & 4.305 \\ 0.15 & 0 & 0 & 0 & 0 & 0 & 0 \\ 0 & 0.19 & 0.095 & 0 & 0 & 0 & 0 \\ 0 & 0 & 0 & 0.514 & 0.514 & 0.514 & 0.514 \\ 0.029 & 0 & 0 & 0 & 0 & 0 & 0 \\ 0 & 0.0145 & 0 & 0 & 0 & 0 & 0 \\ 0 & 0 & 0.0145 & 0 & 0 & 0 & 0 \end{pmatrix}$

Aspasia principissa (Zotz; Schmidt, *Biol Cons*, 2006)	Epiphyte	$\begin{pmatrix} 0.5 & 0.13 & 0.02 & 0 & 0 & 0.11 & 0.19 \\ 0.24 & 0.39 & 0.2 & 0 & 0 & 0 & 0 \\ 0.02 & 0.32 & 0.47 & 0.06 & 0.02 & 0 & 0 \\ 0 & 0.02 & 0.3 & 0.55 & 0.1 & 0.01 & 0 \\ 0 & 0 & 0 & 0.24 & 0.47 & 0.1 & 0.05 \\ 0 & 0 & 0 & 0.03 & 0.31 & 0.57 & 0.29 \\ 0 & 0 & 0 & 0 & 0.03 & 0.2 & 0.59 \end{pmatrix}$
Cryptantha flava (Lucas; Casper; Forseth, *J Ecol*, 2008)	Herbaceous perennial	$\begin{pmatrix} 0 & 0.0019 & 0.0095 & 0.0261 & 0.0504 & 0.085 & 0.2942 \\ 0.43 & 0.2059 & 0.057 & 0.0068 & 0 & 0 & 0 \\ 0.31 & 0.3382 & 0.3377 & 0.068 & 0.0476 & 0 & 0 \\ 0 & 0.0515 & 0.2632 & 0.381 & 0.1048 & 0.1053 & 0 \\ 0 & 0.0147 & 0.0746 & 0.3401 & 0.4 & 0.2632 & 0 \\ 0 & 0 & 0.0044 & 0.0476 & 0.2857 & 0.2632 & 0.1429 \\ 0 & 0 & 0.0044 & 0.0136 & 0.0571 & 0.2632 & 0.7143 \end{pmatrix}$
Dipsacus fullonum (Werner; Caswell, *Ecol*, 1977)	Herbaceous perennial	$\begin{pmatrix} 0 & 0 & 0 & 0 & 0 & 0 & 476 \\ 0.423 & 0 & 0 & 0 & 0 & 0 & 0 \\ 0 & 0.987 & 0 & 0 & 0 & 0 & 0 \\ 0.024 & 0.009 & 0.006 & 0.007 & 0 & 0 & 0 \\ 0.044 & 0 & 0 & 0.05 & 0.158 & 0 & 0 \\ 0.001 & 0 & 0 & 0.002 & 0.008 & 0 & 0 \\ 0 & 0 & 0 & 0 & 0 & 0.25 & 0 \end{pmatrix}$
Hydrastis canadensis (Sinclair, *PhD thesis*, 2002)	Herbaceous perennial	$\begin{pmatrix} 0 & 0 & 0 & 6.8 & 0 & 0 & 0.54 \\ 0.024 & 0.4 & 0.12 & 0.049 & 0.016 & 0 & 0 \\ 0.0016 & 0.3 & 0.5 & 0.19 & 0 & 0 & 0 \\ 0.0025 & 0.089 & 0.17 & 0.58 & 0 & 0 & 0 \\ 0 & 0.15 & 0.265 & 0.26 & 0.436 & 0.15 & 0.07 \\ 0 & 0.027 & 0.04 & 0.09 & 0.11 & 0.08 & 0.07 \\ 0 & 0.007 & 0.016 & 0 & 0.009 & 0 & 0.036 \end{pmatrix}$

Lathyrus vernus (Ehrlen, *J Ecol 287-295*, 1995)	Herbaceous perennial	$\begin{pmatrix} 0.22 & 0 & 0 & 0 & 0.126 & 0.518 & 0 \\ 0.08 & 0 & 0 & 0 & 0.045 & 0.185 & 0 \\ 0 & 1e-20 & 0.59 & 0.071 & 0 & 0 & 0 \\ 0 & 0 & 0.22 & 0.64 & 0.19 & 0.069 & 0.56 \\ 0 & 0 & 0 & 0 & 0.3 & 0.1 & 0.22 \\ 0 & 0 & 0 & 0 & 0.5 & 0.79 & 0 \\ 0 & 0 & 0 & 0.07 & 0 & 0.034 & 0 \end{pmatrix}$
Trillium grandiflorum (Rooney; Gross, *Plant Ecol*, 2003)	Herbaceous perennial	$\begin{pmatrix} 0 & 0 & 0 & 0 & 18.7 & 0 & 0 \\ 0.025 & 0 & 0 & 0 & 0 & 0 & 0 \\ 0 & 0.709 & 0.894 & 0 & 0 & 0 & 0 \\ 0 & 0 & 0.035 & 0.73 & 0.216 & 0.458 & 0.928 \\ 0 & 0 & 0 & 0.047 & 0.463 & 0.068 & 0.027 \\ 0 & 0 & 0 & 0.07 & 0.154 & 0.22 & 0.045 \\ 0 & 0 & 0 & 0.1 & 0.117 & 0.17 & 0 \end{pmatrix}$
Cytisus scoparius (Neubert; Parker, *Risk Anal*, 2004)	Shrub	$\begin{pmatrix} 0.45 & 0 & 0 & 9.1 & 52.8 & 159.6 & 605.7 \\ 0.0086 & 0.19 & 0 & 0 & 0 & 0 & 0 \\ 0 & 0.032 & 0.2 & 0 & 0 & 0 & 0 \\ 0 & 0 & 0.13 & 0.2 & 0 & 0 & 0 \\ 0 & 0 & 0 & 0.067 & 0.3 & 0.095 & 0 \\ 0 & 0 & 0 & 0 & 0.25 & 0.43 & 0.067 \\ 0 & 0 & 0 & 0 & 0 & 0.19 & 0.9 \end{pmatrix}$
Eremosparton songoricum (Zhang; Wang; Shi, *Chin J Plant Ecol*, 2009)	Shrub	$\begin{pmatrix} 0.431 & 0.319 & 0.23 & 0.168 & 0.112 & 0.073 & 0.035 \\ 0.824 & 0 & 0 & 0 & 0 & 0 & 0 \\ 0 & 0.668 & 0 & 0 & 0 & 0 & 0 \\ 0 & 0 & 0.498 & 0 & 0 & 0 & 0 \\ 0 & 0 & 0 & 0.434 & 0 & 0 & 0 \\ 0 & 0 & 0 & 0 & 0.467 & 0 & 0 \\ 0 & 0 & 0 & 0 & 0 & 0.297 & 0 \end{pmatrix}$

Mammillaria magnimamma (Valverde; Quijas; Lopez-Villavicencio; Castillo, *Plant Ecol*, 2004)	Succulent	$\begin{pmatrix} 0 & 0.07 & 0.38 & 0.55 & 0.34 & 0.63 & 1.13 \\ 0.001 & 0.27 & 0.01 & 0 & 0 & 0 & 0 \\ 0 & 0.55 & 0.29 & 0.03 & 0 & 0 & 0 \\ 0 & 0.1 & 0.56 & 0.24 & 0 & 0 & 0 \\ 0 & 0 & 0.09 & 0.36 & 0.15 & 0 & 0 \\ 0 & 0 & 0.04 & 0.27 & 0.85 & 0.54 & 0 \\ 0 & 0 & 0 & 0.06 & 0 & 0.46 & 0.967 \end{pmatrix}$
Phyllanthus emblica (Ellis et al., *Ecology*, 2012)	Tree	$\begin{pmatrix} 0.205 & 0 & 0 & 0 & 0 & 0 & 98.62 \\ 0.0077 & 0 & 0 & 0 & 0 & 0 & 0.928 \\ 0 & 0.3 & 0.5 & 0.22 & 0 & 0 & 0 \\ 0 & 0.28 & 0.27 & 0.56 & 0 & 0 & 0 \\ 0 & 0 & 0 & 0.018349 & 0.86 & 0 & 0 \\ 0 & 0 & 0 & 0 & 0.005 & 0.8 & 0 \\ 0 & 0 & 0 & 0 & 0 & 0.038 & 0.9 \end{pmatrix}$
Phyllanthus indofischeri (Ticktin; Ganesan; Paramesha; Setty, *J Appl Ecol*, 2012	Tree	$\begin{pmatrix} 0.586 & 0 & 0 & 0 & 0 & 37.9 & 74.9 \\ 0.015 & 0 & 0 & 0 & 0 & 0.64 & 0.97 \\ 0 & 0.4 & 0.7 & 0.23 & 0.019 & 0 & 0 \\ 0 & 0.20257 & 0.19 & 0.62 & 0.085 & 0 & 0 \\ 0 & 0 & 0 & 0.037 & 0.78 & 0.012 & 0 \\ 0 & 0 & 0 & 0 & 0.018 & 0.91 & 0 \\ 0 & 0 & 0 & 0 & 0 & 0.029 & 0.97 \end{pmatrix}$
Agropyron cristatum (Hansen; Wilson, *J Appl Ecol*, 2006)	Herbaceous perennial	$\begin{pmatrix} 0 & 0 & 0 & 0 & 1 & 0.26 & 0.635 & 1.58 \\ 0.49 & 0 & 0 & 0 & 0 & 0 & 0 & 0 \\ 0 & 0.49 & 0 & 0 & 0 & 0 & 0 & 0 \\ 0.11 & 0.11 & 0.11 & 0 & 0.07 & 0.02 & 0.165 & 0.405 \\ 0 & 0 & 0 & 0.13 & 0.805 & 0.61 & 0.345 & 0 \\ 0 & 0 & 0 & 0 & 0.145 & 0.205 & 0.255 & 0.28 \\ 0 & 0 & 0 & 0 & 0 & 0.18 & 0.25 & 0.315 \\ 0 & 0 & 0 & 0 & 0 & 0 & 0.165 & 0.39 \end{pmatrix}$

Cynoglossum virginianum (Cipollini; Whigham; O'Neill, *Plant Spp Biol*, 1993)	Herbaceous perennial	$\begin{pmatrix} 0 & 0 & 0 & 0.15 & 1.4 & 1.5 & 1.47 & 0.24 \\ 0.771 & 0.23 & 0 & 0 & 0 & 0 & 0 & 0 \\ 0.229 & 0.05 & 0 & 0 & 0 & 0 & 0 & 0 \\ 0 & 0 & 0.63 & 0.68 & 0.3 & 0.66 & 0.26 & 0.67 \\ 0 & 0 & 0 & 0.13 & 0.51 & 0.19 & 0.56 & 0.11 \\ 0 & 0 & 0 & 0.0038 & 0.0082 & 0 & 0 & 0 \\ 0 & 0 & 0 & 0.011 & 0.13 & 0.15 & 0.14 & 0.02 \\ 0 & 0 & 0.04657 & 0.025 & 0.013 & 0 & 0 & 0.2 \end{pmatrix}$
Ardisia elliptica (Koop; Horvitz, *Ecol*, 2005)	Shrub	$\begin{pmatrix} 0 & 0 & 0 & 0 & 0 & 0.131 & 3.04 & 25.333 \\ 0.018 & 0.535 & 0.015 & 0 & 0.017 & 0 & 0 & 0 \\ 0 & 0.093 & 0.859 & 0.074 & 0.052 & 0 & 0 & 0 \\ 0 & 0 & 0.052 & 0.809 & 0.052 & 0.024 & 0 & 0 \\ 0 & 0 & 0 & 0.059 & 0.81 & 0.167 & 0.014 & 0 \\ 0 & 0 & 0 & 0.015 & 0.069 & 0.762 & 0 & 0 \\ 0 & 0 & 0 & 0 & 0 & 0.048 & 0.972 & 0.017 \\ 0 & 0 & 0 & 0 & 0 & 0 & 0.014 & 0.978 \end{pmatrix}$
Mammillaria crucigera (Contreras; Valverde, *J Arid Env*, 2002)	Succulent	$\begin{pmatrix} 0 & 0.261 & 1.291 & 1.242 & 1.758 & 1.5 & 2.788 & 3.19 \\ 0.001 & 0.425 & 0.03 & 0 & 0 & 0 & 0 & 0 \\ 0 & 0.391 & 0.455 & 0 & 0 & 0 & 0 & 0 \\ 0 & 0.087 & 0.424 & 0.563 & 0 & 0 & 0 & 0 \\ 0 & 0 & 0 & 0.33 & 0.485 & 0 & 0 & 0 \\ 0 & 0 & 0 & 0.042 & 0.242 & 0.455 & 0 & 0 \\ 0 & 0 & 0 & 0 & 0.152 & 0.364 & 0.333 & 0 \\ 0 & 0 & 0 & 0 & 0.091 & 0.136 & 0.667 & 0.975 \end{pmatrix}$

Fucus vesiculosus (Ang; de Wreede, *Mar Ecol Prog Ser*, 1993)	Algae	$\begin{pmatrix} 0.0751 & 0.066 & 0.22 & 0.3 & 1.3 & 6.89 & 11.1 & 14.15 & 15.96 \\ 0.0072 & 0.01 & 0.04 & 0.06 & 0.28 & 1.1 & 1.43 & 1.57 & 1.6 \\ 0.072 & 0.14 & 0.64 & 0.99 & 4.9 & 18.29 & 21.44 & 21.1 & 19.55 \\ 0.0032 & 0.0037 & 0.018 & 0.028 & 0.15 & 0.7 & 0.1 & 1.1 & 1.1 \\ 0.005 & 0.0023 & 0.0058 & 0.0072 & 0.03 & 0.39 & 0.76 & 1.046 & 1.231 \\ 0.002 & 0.001 & 0.0024 & 0.0027 & 0.0093 & 0.11 & 0.236 & 0.3 & 0.39 \\ 0.0008 & 0.0006 & 0.002 & 0.0025 & 0.0095 & 0.06 & 0.11 & 0.15 & 0.18 \\ 0.0002 & 0.0002 & 0.0007 & 0.001 & 0.0044 & 0.018 & 0.03 & 0.03 & 0.03 \\ 0 & 0 & 0.0002 & 0.0004 & 0.0019 & 0.0079 & 0.0092 & 0.0088 & 0.008 \end{pmatrix}$
Machaerium cuspidatum (Nabe-Nielsen, *J Trop Ecol*, 2004)	Liana	$\begin{pmatrix} 0.72 & 0 & 0.046 & 0 & 0 & 0 & 0 & 1.941 & 16 \\ 0 & 0.588 & 0.033 & 0.049 & 0 & 0.026 & 0 & 0 & 0 \\ 0.065 & 0 & 0.761 & 0 & 0.088 & 0 & 0 & 0 & 0.125 \\ 0 & 0.176 & 0 & 0.899 & 0.071 & 0.348 & 0.053 & 0.059 & 0 \\ 0 & 0 & 0.055 & 0 & 0.882 & 0 & 0 & 0 & 0 \\ 0 & 0 & 0 & 0.022 & 0 & 0.679 & 0.035 & 0 & 0 \\ 0 & 0 & 0 & 0 & 0.005 & 0.038 & 0.933 & 0 & 0 \\ 0 & 0 & 0 & 0 & 0 & 0 & 0.013 & 0.98 & 0 \\ 0 & 0 & 0 & 0 & 0 & 0 & 0 & 0.005 & 0.98 \end{pmatrix}$
Ceratozamia mirandae (Perez-Farrera et al., *Plant Ecol*, 2006)	Palm	$\begin{pmatrix} 0 & 0 & 0.41305 & 0.42365 & 0.19495 & 0.30105 & 0.12495 & 0 & 0.3422 \\ 0.4153 & 0 & 0 & 0 & 0 & 0 & 0 & 0 & 0 \\ 0 & 1 & 0.3223 & 0 & 0 & 0 & 0 & 0 & 0 \\ 0 & 0 & 0.87095 & 0 & 0 & 0 & 0 & 0 & 0 \\ 0 & 0 & 0 & 0.69695 & 0.0278 & 0 & 0 & 0 & 0 \\ 0 & 0 & 0 & 0 & 0.81835 & 0 & 0 & 0 & 0 \\ 0 & 0 & 0 & 0 & 0 & 0.37255 & 0 & 0 & 0 \\ 0 & 0 & 0 & 0 & 0 & 0 & 0.54765 & 0 & 0 \\ 0 & 0 & 0 & 0 & 0 & 0 & 0 & 0.75 & 0.2 \end{pmatrix}$

Hymenanthes maxima (McGraw, *Am J Bot*, 1989)	Shrub	$\begin{pmatrix} 0.012 & 0.032 & 0 & 0.115 & 0.037 & 0.046 & 0 & 0 & 0.077 \\ 1 & 0 & 0 & 0 & 0 & 0 & 0 & 0 & 0 \\ 0 & 0.984 & 0 & 0 & 0 & 0 & 0 & 0 & 0 \\ 0 & 0 & 1 & 0 & 0 & 0 & 0 & 0 & 0 \\ 0 & 0 & 0 & 0.923 & 0 & 0 & 0 & 0 & 0 \\ 0 & 0 & 0 & 0 & 0.796 & 0 & 0 & 0 & 0 \\ 0 & 0 & 0 & 0 & 0 & 0.523 & 0 & 0 & 0 \\ 0 & 0 & 0 & 0 & 0 & 0 & 0.286 & 0 & 0 \\ 0 & 0 & 0 & 0 & 0 & 0 & 0 & 0.118 & 0.154 \end{pmatrix}$
Mammillaria gaumeri (Ferrer; Duran; Mendez; Dorantes; Dzib, *Bol Soc Bot Mex*, 2011)	Succulent	$\begin{pmatrix} 0 & 0 & 0 & 0.238 & 1.701 & 2.97 & 0 & 0 & 0.233 & 1.716 \\ 0.016 & 0.1 & 0 & 0 & 0 & 0 & 0 & 0 & 0 & 0 \\ 0 & 0.1 & 0.5 & 0 & 0 & 0 & 0 & 0 & 0 & 0 \\ 0 & 0 & 0.083 & 0.85 & 0 & 0 & 0 & 0 & 0 & 0 \\ 0 & 0 & 0 & 0.05 & 0.556 & 0.125 & 0 & 0 & 0 & 0 \\ 0 & 0 & 0 & 0 & 0.037 & 0.75 & 0 & 0 & 0 & 0 \\ 0 & 0 & 0 & 0 & 0.111 & 0 & 0.1 & 0 & 0 & 0 \\ 0 & 0 & 0 & 0 & 0 & 0 & 0.9 & 0.667 & 0.059 & 0 \\ 0 & 0 & 0 & 0 & 0 & 0 & 0 & 0.167 & 0.471 & 0 \\ 0 & 0 & 0 & 0 & 0 & 0 & 0 & 0 & 0.059 & 0.667 \end{pmatrix}$
Neobuxbaumia mezcalaensis (Esparza-Olguin; Valverde; Mandujano, *Popul Ecol*, 2005)	Succulent	$\begin{pmatrix} 0 & 0 & 0 & 0 & 0 & 0 & 0 & 5.226 & 42.552 & 41.461 \\ 0.05 & 0.8 & 0.016 & 0 & 0 & 0 & 0 & 0 & 0 & 0 \\ 0 & 0.1 & 0.875 & 0 & 0 & 0 & 0 & 0 & 0 & 0 \\ 0 & 0 & 0.016 & 0.818 & 0.017 & 0 & 0 & 0 & 0 & 0 \\ 0 & 0 & 0 & 0.091 & 0.914 & 0 & 0 & 0 & 0 & 0 \\ 0 & 0 & 0 & 0 & 0.034 & 0.941 & 0 & 0 & 0 & 0 \\ 0 & 0 & 0 & 0 & 0 & 0.059 & 0.947 & 0 & 0 & 0 \\ 0 & 0 & 0 & 0 & 0 & 0 & 0.053 & 0.895 & 0 & 0 \\ 0 & 0 & 0 & 0 & 0 & 0 & 0 & 0.105 & 0.882 & 0.077 \\ 0 & 0 & 0 & 0 & 0 & 0 & 0 & 0 & 0.059 & 0.846 \end{pmatrix}$

Neobuxbaumia tetetzo (Esparza-Olguin; Valverde; Mandujano, *Popul Ecol*, 2005)	Succulent	$\begin{pmatrix} 0 & 0 & 0 & 0 & 0 & 0 & 0 & 0.748 & 10.325 & 47.322 \\ 0.06 & 0.76 & 0.037 & 0 & 0 & 0 & 0 & 0 & 0 & 0 \\ 0 & 0.02 & 0.9 & 0 & 0 & 0 & 0 & 0 & 0 & 0 \\ 0 & 0 & 0.037 & 0.964 & 0 & 0 & 0 & 0 & 0 & 0 \\ 0 & 0 & 0 & 0.036 & 0.938 & 0 & 0 & 0 & 0 & 0 \\ 0 & 0 & 0 & 0 & 0.063 & 0.882 & 0 & 0 & 0 & 0 \\ 0 & 0 & 0 & 0 & 0 & 0.059 & 0.943 & 0.042 & 0 & 0 \\ 0 & 0 & 0 & 0 & 0 & 0 & 0.029 & 0.875 & 0.048 & 0 \\ 0 & 0 & 0 & 0 & 0 & 0 & 0 & 0.083 & 0.81 & 0 \\ 0 & 0 & 0 & 0 & 0 & 0 & 0 & 0 & 0.095 & 0.95 \end{pmatrix}$
Euterpe precatoria (Zuidema, *Ecol Bolivia*, 2000)	Palm	$\begin{pmatrix} 0.677 & 0.125 & 0 & 0 & 0 & 0 & 0 & 0 & 0.15 & 3.88 & 5.65 \\ 0.044 & 0.724 & 0 & 0 & 0 & 0 & 0 & 0 & 0 & 0 & 0 \\ 0 & 0.093 & 0.896 & 0 & 0 & 0 & 0 & 0 & 0 & 0 & 0 \\ 0 & 0 & 0.044 & 0.919 & 0 & 0 & 0 & 0 & 0 & 0 & 0 \\ 0 & 0 & 0 & 0.022 & 0.909 & 0 & 0 & 0 & 0 & 0 & 0 \\ 0 & 0 & 0 & 0 & 0.048 & 0.875 & 0 & 0 & 0 & 0 & 0 \\ 0 & 0 & 0 & 0 & 0 & 0.082 & 0.836 & 0 & 0 & 0 & 0 \\ 0 & 0 & 0 & 0 & 0 & 0 & 0.121 & 0.847 & 0 & 0 & 0 \\ 0 & 0 & 0 & 0 & 0 & 0 & 0 & 0.11 & 0.885 & 0 & 0 \\ 0 & 0 & 0 & 0 & 0 & 0 & 0 & 0 & 0.073 & 0.923 & 0 \\ 0 & 0 & 0 & 0 & 0 & 0 & 0 & 0 & 0 & 0.034 & 0.957 \end{pmatrix}$

Agave marmorata (Jimenez-Valdes; Godinez-Alvarez; Caballero; Lira, *Econ Bot*, 2010)	Succulent	$\begin{pmatrix} 0.263 & 0 & 0 & 0 & 0 & 0 & 0 & 0 & 0 & 0 & 0 & 84 \\ 0.001 & 0.24 & 0 & 0 & 0 & 0 & 0 & 0 & 0 & 0 & 0 & 0 \\ 0 & 0.18 & 0.58 & 0 & 0 & 0 & 0 & 0 & 0 & 0 & 0 & 0 \\ 0 & 0.05 & 0.18 & 0.9 & 0 & 0 & 0 & 0 & 0 & 0 & 0 & 0 \\ 0 & 0 & 0.24 & 0.1 & 0.88 & 0 & 0 & 0 & 0 & 0 & 0 & 0 \\ 0 & 0 & 0 & 0 & 0.001 & 0.53 & 0 & 0 & 0 & 0 & 0 & 0 \\ 0 & 0 & 0 & 0 & 0 & 0.29 & 0.78 & 0 & 0 & 0 & 0 & 0 \\ 0 & 0 & 0 & 0 & 0 & 0 & 0.2 & 0.56 & 0 & 0 & 0 & 0 \\ 0 & 0 & 0 & 0 & 0 & 0 & 0 & 0.19 & 0.833 & 0 & 0 & 0 \\ 0 & 0 & 0 & 0 & 0 & 0 & 0 & 0 & 0.056 & 0.823 & 0 & 0 \\ 0 & 0 & 0 & 0 & 0 & 0 & 0 & 0 & 0.05 & 0.2 & 0.7 & 0 \\ 0 & 0 & 0 & 0 & 0 & 0 & 0 & 0 & 0 & 0 & 0.3 & 0.6 \end{pmatrix}$
Calocedrus macrolepis (Chien; Zuidema; Nghia, *Popul Ecol*, 2008)	Tree	$\begin{pmatrix} 0.7 & 0 & 0 & 0 & 0 & 0 & 1.38 & 2.7 & 3.8 & 4.3 & 4.5 & 4.5 & 4.5 & 4.5 \\ 0.09 & 0.7 & 0 & 0 & 0 & 0 & 0 & 0 & 0 & 0 & 0 & 0 & 0 & 0 \\ 0 & 0.1 & 0.77 & 0 & 0 & 0 & 0 & 0 & 0 & 0 & 0 & 0 & 0 & 0 \\ 0 & 0 & 0.07 & 0.8 & 0 & 0 & 0 & 0 & 0 & 0 & 0 & 0 & 0 & 0 \\ 0 & 0 & 0 & 0.07 & 0.9 & 0 & 0 & 0 & 0 & 0 & 0 & 0 & 0 & 0 \\ 0 & 0 & 0 & 0 & 0.02 & 0.9 & 0 & 0 & 0 & 0 & 0 & 0 & 0 & 0 \\ 0 & 0 & 0 & 0 & 0 & 0.03 & 0.9 & 0 & 0 & 0 & 0 & 0 & 0 & 0 \\ 0 & 0 & 0 & 0 & 0 & 0 & 0.04 & 0.9 & 0 & 0 & 0 & 0 & 0 & 0 \\ 0 & 0 & 0 & 0 & 0 & 0 & 0 & 0.05 & 0.9 & 0 & 0 & 0 & 0 & 0 \\ 0 & 0 & 0 & 0 & 0 & 0 & 0 & 0 & 0.06 & 0.9 & 0 & 0 & 0 & 0 \\ 0 & 0 & 0 & 0 & 0 & 0 & 0 & 0 & 0 & 0.07 & 0.9 & 0 & 0 & 0 \\ 0 & 0 & 0 & 0 & 0 & 0 & 0 & 0 & 0 & 0 & 0.03 & 0.9 & 0 & 0 \\ 0 & 0 & 0 & 0 & 0 & 0 & 0 & 0 & 0 & 0 & 0 & 0.03 & 0.9 & 0 \\ 0 & 0 & 0 & 0 & 0 & 0 & 0 & 0 & 0 & 0 & 0 & 0 & 0.03 & 0.95 \end{pmatrix}$

Magnolia fordiana (Chien; Zuidema; Nghia, *Popul Ecol*, 2008)	Tree	$\begin{pmatrix} 0.609 & 0 & 0 & 0 & 0 & 0 & 0.16 & 0.27 & 0.42 & 0.56 & 0.67 & 0.74 & 0.77 & 0.76 \\ 0.135 & 0.598 & 0 & 0 & 0 & 0 & 0 & 0 & 0 & 0 & 0 & 0 & 0 & 0 \\ 0 & 0.184 & 0.653 & 0 & 0 & 0 & 0 & 0 & 0 & 0 & 0 & 0 & 0 & 0 \\ 0 & 0 & 0.187 & 0.726 & 0 & 0 & 0 & 0 & 0 & 0 & 0 & 0 & 0 & 0 \\ 0 & 0 & 0 & 0.014 & 0.896 & 0 & 0 & 0 & 0 & 0 & 0 & 0 & 0 & 0 \\ 0 & 0 & 0 & 0 & 0.014 & 0.913 & 0 & 0 & 0 & 0 & 0 & 0 & 0 & 0 \\ 0 & 0 & 0 & 0 & 0 & 0.037 & 0.916 & 0 & 0 & 0 & 0 & 0 & 0 & 0 \\ 0 & 0 & 0 & 0 & 0 & 0 & 0.067 & 0.891 & 0 & 0 & 0 & 0 & 0 & 0 \\ 0 & 0 & 0 & 0 & 0 & 0 & 0 & 0.092 & 0.874 & 0 & 0 & 0 & 0 & 0 \\ 0 & 0 & 0 & 0 & 0 & 0 & 0 & 0 & 0.11 & 0.865 & 0 & 0 & 0 & 0 \\ 0 & 0 & 0 & 0 & 0 & 0 & 0 & 0 & 0 & 0.119 & 0.863 & 0 & 0 & 0 \\ 0 & 0 & 0 & 0 & 0 & 0 & 0 & 0 & 0 & 0 & 0.121 & 0.867 & 0 & 0 \\ 0 & 0 & 0 & 0 & 0 & 0 & 0 & 0 & 0 & 0 & 0 & 0.116 & 0.879 & 0 \\ 0 & 0 & 0 & 0 & 0 & 0 & 0 & 0 & 0 & 0 & 0 & 0 & 0.101 & 0.94 \end{pmatrix}$
Parashorea chinensis (Chien; Zuidema; Nghia, *Popul Ecol*, 2008)	Tree	$\begin{pmatrix} 0.7 & 0 & 0 & 0 & 0 & 0 & 0.78 & 1.17 & 1.64 & 2.13 & 2.58 & 2.94 & 3.28 & 3.5 & 3.57 \\ 0.101 & 0.704 & 0 & 0 & 0 & 0 & 0 & 0 & 0 & 0 & 0 & 0 & 0 & 0 & 0 \\ 0 & 0.136 & 0.793 & 0 & 0 & 0 & 0 & 0 & 0 & 0 & 0 & 0 & 0 & 0 & 0 \\ 0 & 0 & 0.096 & 0.819 & 0 & 0 & 0 & 0 & 0 & 0 & 0 & 0 & 0 & 0 & 0 \\ 0 & 0 & 0 & 0.118 & 0.901 & 0 & 0 & 0 & 0 & 0 & 0 & 0 & 0 & 0 & 0 \\ 0 & 0 & 0 & 0 & 0.019 & 0.922 & 0 & 0 & 0 & 0 & 0 & 0 & 0 & 0 & 0 \\ 0 & 0 & 0 & 0 & 0 & 0.039 & 0.946 & 0 & 0 & 0 & 0 & 0 & 0 & 0 & 0 \\ 0 & 0 & 0 & 0 & 0 & 0 & 0.037 & 0.93 & 0 & 0 & 0 & 0 & 0 & 0 & 0 \\ 0 & 0 & 0 & 0 & 0 & 0 & 0 & 0.0527 & 0.9238 & 0 & 0 & 0 & 0 & 0 & 0 \\ 0 & 0 & 0 & 0 & 0 & 0 & 0 & 0 & 0.0594 & 0.924 & 0 & 0 & 0 & 0 & 0 \\ 0 & 0 & 0 & 0 & 0 & 0 & 0 & 0 & 0 & 0.059 & 0.929 & 0 & 0 & 0 & 0 \\ 0 & 0 & 0 & 0 & 0 & 0 & 0 & 0 & 0 & 0 & 0.055 & 0.935 & 0 & 0 & 0 \\ 0 & 0 & 0 & 0 & 0 & 0 & 0 & 0 & 0 & 0 & 0 & 0.048 & 0.964 & 0 & 0 \\ 0 & 0 & 0 & 0 & 0 & 0 & 0 & 0 & 0 & 0 & 0 & 0 & 0.019 & 0.97 & 0 \\ 0 & 0 & 0 & 0 & 0 & 0 & 0 & 0 & 0 & 0 & 0 & 0 & 0 & 0.014 & 0.983 \end{pmatrix}$

Bertholletia excelsa (Zuidema; Boot, *J Trop Ecol*, 2002)	Tree

$$\begin{pmatrix}
0.411 & 0 & 0 & 0 & 0 & 0 & 0 & 0 & 0 & 0 & 0 & 3.2 & 3.8 & 4.4 & 5 & 5.8 & 6.9 \\
0.028 & 0.56 & 0 & 0 & 0 & 0 & 0 & 0 & 0 & 0 & 0 & 0 & 0 & 0 & 0 & 0 & 0 \\
0 & 0.057 & 0.772 & 0 & 0 & 0 & 0 & 0 & 0 & 0 & 0 & 0 & 0 & 0 & 0 & 0 & 0 \\
0 & 0 & 0.065 & 0.873 & 0 & 0 & 0 & 0 & 0 & 0 & 0 & 0 & 0 & 0 & 0 & 0 & 0 \\
0 & 0 & 0 & 0.095 & 0.941 & 0 & 0 & 0 & 0 & 0 & 0 & 0 & 0 & 0 & 0 & 0 & 0 \\
0 & 0 & 0 & 0 & 0.044 & 0.938 & 0 & 0 & 0 & 0 & 0 & 0 & 0 & 0 & 0 & 0 & 0 \\
0 & 0 & 0 & 0 & 0 & 0.047 & 0.961 & 0 & 0 & 0 & 0 & 0 & 0 & 0 & 0 & 0 & 0 \\
0 & 0 & 0 & 0 & 0 & 0 & 0.034 & 0.946 & 0 & 0 & 0 & 0 & 0 & 0 & 0 & 0 & 0 \\
0 & 0 & 0 & 0 & 0 & 0 & 0 & 0.049 & 0.94 & 0 & 0 & 0 & 0 & 0 & 0 & 0 & 0 \\
0 & 0 & 0 & 0 & 0 & 0 & 0 & 0 & 0.055 & 0.937 & 0 & 0 & 0 & 0 & 0 & 0 & 0 \\
0 & 0 & 0 & 0 & 0 & 0 & 0 & 0 & 0 & 0.058 & 0.936 & 0 & 0 & 0 & 0 & 0 & 0 \\
0 & 0 & 0 & 0 & 0 & 0 & 0 & 0 & 0 & 0 & 0.059 & 0.966 & 0 & 0 & 0 & 0 & 0 \\
0 & 0 & 0 & 0 & 0 & 0 & 0 & 0 & 0 & 0 & 0 & 0.029 & 0.968 & 0 & 0 & 0 & 0 \\
0 & 0 & 0 & 0 & 0 & 0 & 0 & 0 & 0 & 0 & 0 & 0 & 0.027 & 0.971 & 0 & 0 & 0 \\
0 & 0 & 0 & 0 & 0 & 0 & 0 & 0 & 0 & 0 & 0 & 0 & 0 & 0.024 & 0.965 & 0 & 0 \\
0 & 0 & 0 & 0 & 0 & 0 & 0 & 0 & 0 & 0 & 0 & 0 & 0 & 0 & 0.02 & 0.967 & 0 \\
0 & 0 & 0 & 0 & 0 & 0 & 0 & 0 & 0 & 0 & 0 & 0 & 0 & 0 & 0 & 0.018 & 0.985
\end{pmatrix}$$

Appendix A3

The upper and lower bounds on maximal inertia

Here we show for our invasion model in Chapter 5, that the maximal inertia is bounded above and below.

From equation (5.10), the maximal inertia is given by

$$\frac{\|v\|_\infty}{v^T w},$$

where v and w are the left and right eigenvectors of $A_{inv} = G_I + \phi(0.1 \times p) df^T + \alpha(0) bc^T$. So to show that the maximal inertia is bounded, we must show that both $\|v\|_\infty$ and $v^T w$ are bounded above and below. We choose the parameters for the model given by equations (5.3) and (5.4) so that the total population of the resident at the resident only equilibrium is 1000. To do this we scale f such that

$$\phi(1000) f^T (I - G_R)^{-1} d = 1. \tag{A3.1}$$

Also we choose f so that the invasion exponent is negative, which means the largest eigenvalue of A_{inv} must be less than one. So we consider f such that the dominant eigenvalue of A_{inv} is between 0.64 and 0.94 which we denote by $\underline{\lambda}$ and $\overline{\lambda}$, respectively.

First, we calculate v for A_{inv}. Let $G = G_I + \alpha(0) bc^T$ so that $A_{inv} = G + \phi(0.1 \times p) df^T$. So

$$v^T (A_{inv}) = v^T (G + \phi(0.1 \times p) df^T) = \lambda v^T.$$

Then

$$v^T (\lambda I - G) = \phi(0.1 \times p) v^T df^T$$

so that

$$v^T = \phi(0.1 \times p) v^T df^T (\lambda I - G)^{-1}.$$

But $\phi(0.1 \times p) v^T d$ is a scalar. Therefore

$$v^T = f^T (\lambda I - G)^{-1}. \tag{A3.2}$$

In a similar way, the right eigenvector w of A_{inv} satisfies

$$A_{inv}w = (G + \phi(0.1 \times p)df^T)w = \lambda w.$$

Then

$$(\lambda I - G)w = \phi(0.1 \times p)df^T w$$

so that

$$w = \phi(0.1 \times p)(\lambda I - G)^{-1}df^T w.$$

As $\phi(0.1 \times p)$ and $f^T w$ are scalars, we have

$$w = (\lambda I - G)^{-1}d. \tag{A3.3}$$

Using that $\underline{\lambda} \leq \lambda \leq \overline{\lambda}$ and $v^T = f^T(\lambda I - G)^{-1}$, then the upper and lower bounds on the left eigenvector v are given by

$$f^T(\overline{\lambda}I - G)^{-1} \leq v^T \leq f^T(\underline{\lambda}I - G)^{-1}.$$

So $\|v\|_\infty$ is bounded above and below by

$$||f^T(\overline{\lambda}I - G)^{-1}||_\infty \leq ||v||_\infty \leq ||f^T(\underline{\lambda}I - G)^{-1}||_\infty. \tag{A3.4}$$

We can make these upper and lower bounds on $\|v\|_\infty$ independent of f in the following way. Let $u = (I - G_R)^{-1}d$ then equation (A3.1) gives that

$$\min_i(u_i)\sum_i f_i \leq \sum_i f_i u_i = \exp(-1000) \leq \max_i(u_i)\sum_i f_i.$$

Also let $\underline{u} = \min_i(u_i)$ and $\overline{u} = \max_i(u_i)$. Then

$$\sum_i f_i \leq \frac{\exp(-1000)}{\underline{u}} \text{ and } \sum_i f_i \geq \frac{\exp(-1000)}{\overline{u}}.$$

But f is a non-negative vector. So $\|f^T\|_1 = \sum_i f_i$ and the upper bound on $\|v\|_\infty$ becomes

$$\begin{aligned}\|v\|_\infty \leq \|f^T(\underline{\lambda}I - G)^{-1}\|_\infty &\leq \|f^T\|_1\|(\underline{\lambda}I - G)^{-1}\| \\ &= \sum_i f_i\|(\underline{\lambda}I - G)^{-1}\| \leq \frac{\exp(-1000)}{\underline{u}}\|(\underline{\lambda}I - G)^{-1}\|.\end{aligned}$$

Now $m := (\overline{\lambda}I - G)^{-1}$ is a positive matrix so that

$$m \geq q\begin{pmatrix} 1 & \cdots & 1 \\ \vdots & \ddots & \vdots \\ 1 & \cdots & 1 \end{pmatrix}$$

where q is the minimum entry of m. Then

$$f^T m \geq q f^T \begin{pmatrix} 1 & \cdots & 1 \\ \vdots & \ddots & \vdots \\ 1 & \cdots & 1 \end{pmatrix} = q \left[\sum_i f_i, \ldots, \sum_i f_i \right] \geq q \left[\frac{\exp(-1000)}{\overline{u}}, \ldots, \frac{\exp(-1000)}{\overline{u}} \right].$$

Therefore the lower bound on $\|v\|_\infty$ is given by

$$\|v\|_\infty \geq \|f^T(\overline{\lambda} I - G)^{-1}\|_\infty = \|f^T m\|_\infty \geq q \frac{\exp(-1000)}{\overline{u}}.$$

Having shown that the numerator of the maximal population inertia is bounded, next we explore the denominator $v^T w$. Using equations (A3.2) and (A3.3) then $v^T w = f^T(\lambda I - G)^{-2} d$, which using that $\underline{\lambda} \leq \lambda \leq \overline{\lambda}$ gives

$$f^T(\overline{\lambda} I - G)^{-2} d \leq v^T w \leq f^T(\underline{\lambda} I - G)^{-2} d. \tag{A3.5}$$

Let $\overline{z} = (\overline{\lambda} I - G)^{-2} d$. $\overline{z}$ is positive. Then equation (A3.5) gives that

$$v^T w \geq f^T(\overline{\lambda} I - G)^{-2} d = \sum_i f_i \overline{z}_i = \sum_i f_i u_i \frac{\overline{z}_i}{u_i} \geq \min_i \left(\frac{\overline{z}_i}{u_i} \right) \sum_i f_i u_i = \min_i \left(\frac{\overline{z}_i}{u_i} \right) \exp(-1000).$$

Therefore $v^T w$ has a lower bound. In a similar way, we calculate the upper bound for $v^T w$. First let $\underline{z} = (\underline{\lambda} I - G)^{-2} d$. $\underline{z}$ is positive. Then

$$\begin{aligned} v^T w \leq f^T(\underline{\lambda} I - G)^{-2} d = \sum_i f_i \underline{z}_i = \sum_i f_i u_i \frac{\underline{z}_i}{u_i} &\leq \sum_i f_i u_i \max_i \left(\frac{\underline{z}_i}{u_i} \right) \\ &= \max_i \left(\frac{\underline{z}_i}{u_i} \right) \sum_i f_i u_i = \max_i \left(\frac{\underline{z}_i}{u_i} \right) \frac{1}{\exp(1000)}. \end{aligned}$$

Therefore we have found upper and lower bounds for $\|v\|_\infty$ and $v^T w$ which are independent of f. Then the upper and lower bounds on the maximal inertia are given by

$$\frac{q}{\overline{u} \max_i \left(\frac{\underline{z}_i}{u_i} \right)} \leq \frac{\|v\|_\infty}{v^T w} \leq \frac{\|\underline{\lambda} I - G)^{-1}\|_\infty}{\underline{u} \min_i \left(\frac{\overline{z}_i}{u_i} \right)}.$$

Bibliography

[1] Peter B Adler and Janneke Hille Ris Lambers. The influence of climate and species composition on the population dynamics of ten prairie forbs. *Ecology*, 89(11):3049–3060, 2008.

[2] Walter G Aiello and H I Freedman. A time-delay model of single-species growth with stage structure. *Mathematical biosciences*, 101(2):139–153, 1990.

[3] Linda JS Allen. Persistence and extinction in single-species reaction-diffusion models. *Bulletin of Mathematical Biology*, 45(2):209–227, 1983.

[4] Fred W Allendorf and Laura L Lundquist. Introduction: population biology, evolution, and control of invasive species. *Conservation Biology*, 17(1):24–30, 2003.

[5] Brian DO Anderson and John B Moore. *Optimal control: linear quadratic methods*. Courier Corporation, 2007.

[6] Paul R Armsworth. Recruitment limitation, population regulation, and larval connectivity in reef fish metapopulations. *Ecology*, 83(4):1092–1104, 2002.

[7] Anthony D Barnosky, Nicholas Matzke, Susumu Tomiya, Guinevere OU Wogan, Brian Swartz, Tiago B Quental, Charles Marshall, Jenny L McGuire, Emily L Lindsey, Kaitlin C Maguire, et al. Has the earth's sixth mass extinction already arrived? *Nature*, 471(7336):51–57, 2011.

[8] Tamer Başar and Pierre Bernhard. *H-infinity optimal control and related minimax design problems: a dynamic game approach*. Springer Science & Business Media, 2008.

[9] Benjamin B Beck, Lisa G Rapaport, MR Stanley Price, and Alison C Wilson. Reintroduction of captive-born animals. In *Creative conservation*, pages 265–286. Springer, 1994.

[10] Benjamin B Beck, Lisa G Rapaport, MR Stanley Price, and Alison C Wilson. Reintroduction of captive-born animals. In *Creative conservation*, pages 265–286. Springer, 1994.

[11] John R Beddington and Robert M May. Time delays are not necessarily destabilizing. *Mathematical Biosciences*, 27(1):109–117, 1975.

[12] Tim G Benton and Alastair Grant. Elasticity analysis as an important tool in evolutionary and population ecology. *Trends in Ecology & Evolution*, 14(12):467–471, 1999.

[13] Edoardo Beretta and Yang Kuang. Global analyses in some delayed ratio-dependent predator-prey systems. *Nonlinear Analysis: Theory, Methods & Applications*, 32(3):381–408, 1998.

[14] Julie Blackwood, Alan Hastings, and Christopher Costello. Cost-effective management of invasive species using linear-quadratic control. *Ecological Economics*, 69(3):519–527, 2010.

[15] Tiffany Bogich and Katriona Shea. A state-dependent model for the optimal management of an invasive metapopulation. *Ecological Applications*, 18(3):748–761, 2008.

[16] Richard P Boland, Tobias Galla, and Alan J McKane. How limit cycles and quasi-cycles are related in systems with intrinsic noise. *Journal of Statistical Mechanics: Theory and Experiment*, 2008(09):P09001, 2008.

[17] Joseph Briggs, Kathryn Dabbs, Michael Holm, Joan Lubben, Richard Rebarber, Brigitte Tenhumberg, and Daniel Riser-Espinoza. Structured population dynamics: An introduction to integral modeling. *Mathematics Magazine*, 83(4):243–257, 2010.

[18] RE Brockie, Lloyd L Loope, Michael B Usher, and Ole Hamann. Biological invasions of island nature reserves. *Biological Conservation*, 44(1):9–36, 1988.

[19] Robert Stephen Cantrell and Chris Cosner. *Spatial ecology via reaction-diffusion equations*. John Wiley & Sons, 2004.

[20] James Carlton. *Invasive species: vectors and management strategies*. Island Press, 2003.

[21] Marco Castellani, Mikko Heino, John Gilbey, Hitoshi Araki, Terje Svåsand, and Kevin A Glover. Ibsem: An individual-based atlantic salmon population model. *PloS one*, 10(9):e0138444, 2015.

[22] Hal Caswell. Stable population structure and reproductive value for populations with complex life cycles. *Ecology*, pages 1223–1231, 1982.

[23] Hal Caswell. *Matrix population models*. Wiley Online Library, 1989.

[24] Hal Caswell. Sensitivity analysis of transient population dynamics. *Ecology Letters*, 10(1):1–15, 2007.

[25] Hal Caswell. Stage, age and individual stochasticity in demography. *Oikos*, 118(12):1763–1782, 2009.

[26] Hal Caswell and Takenori Takada. Elasticity analysis of density-dependent matrix population models: the invasion exponent and its substitutes. *Theoretical population biology*, 65(4):401–411, 2004.

[27] F Stuart Chapin III, Erika S Zavaleta, Valerie T Eviner, Rosamond L Naylor, Peter M Vitousek, Heather L Reynolds, David U Hooper, Sandra Lavorel, Osvaldo E Sala, Sarah E Hobbie, et al. Consequences of changing biodiversity. *Nature*, 405(6783):234–242, 2000.

[28] Matthew K Chew and Andrew L Hamilton. *The rise and fall of biotic nativeness: a historical perspective*. Wiley-Blackwell: Chichester, UK, 2011.

[29] Miguel Clavero and Emili Garcia-Berthou. Invasive species are a leading cause of animal extinctions. *TRENDS in Ecology and Evolution*, 20(3):110–110, 2005.

[30] Michael Norman Clout and Peter A Williams. *Invasive species management: a handbook of techniques*. Oxford Universuty Press, 2009.

[31] Thierry Dauxois, Francesca Di Patti, Duccio Fanelli, and Alan J McKane. Enhanced stochastic oscillations in autocatalytic reactions. *Physical Review E*, 79(3):036112, 2009.

[32] Mark A Davis, Matthew K Chew, Richard J Hobbs, Ariel E Lugo, John J Ewel, Geerat J Vermeij, James H Brown, Michael L Rosenzweig, Mark R Gardener, Scott P Carroll, et al. Don't judge species on their origins. *Nature*, 474(7350):153–154, 2011.

[33] DL DeAngelis, JC Waterhouse, WM Post, and RV O'Neill. Ecological modelling and disturbance evaluation. *Ecological Modelling*, 29(1):399–419, 1985.

[34] John M Drake. Allee effects and the risk of biological invasion. *Risk Analysis*, 24(4):795–802, 2004.

[35] William F Fagan, Robert Stephen Cantrell, and Chris Cosner. How habitat edges change species interactions. *The American Naturalist*, 153(2):165–182, 1999.

[36] Lenore Fahrig and Gray Merriam. Habitat patch connectivity and population survival. *Ecology*, pages 1762–1768, 1985.

[37] Meng Fan, Ke Wang, and Daqing Jiang. Existence and global attractivity of positive periodic solutions of periodic n-species lotka–volterra competition systems with several deviating arguments. *Mathematical Biosciences*, 160(1):47–61, 1999.

[38] Michael F Fay. Conservation of rare and endangered plants using in vitro methods. *In Vitro Cellular & Developmental Biology-Plant*, 28(1):1–4, 1992.

[39] John Fieberg and Stephen P Ellner. Stochastic matrix models for conservation and management: a comparative review of methods. *Ecology Letters*, 4(3):244–266, 2001.

[40] Jennifer Firn, Tracy Rout, Hugh Possingham, and Yvonne M Buckley. Managing beyond the invader: manipulating disturbance of natives simplifies control efforts. *Journal of Applied Ecology*, 45(4):1143–1151, 2008.

[41] Richard Frankham. Genetics and extinction. *Biological conservation*, 126(2):131–140, 2005.

[42] B Frapard and C Champetier. H techniques: From research to industrial applications. In *Spacecraft Guidance, Navigation and Control Systems*, volume 381, page 231, 1997.

[43] Drew Fudenberg and Jean Tirole. Game theory, 1991. *Cambridge, Massachusetts*, 393, 1991.

[44] Wayne M Getz and Andrew P Gutierrez. A perspective on systems analysis in crop production and insect pest management. *Annual review of entomology*, 27(1):447–466, 1982.

[45] Jennifer A Gill, William J Sutherland, and Andrew R Watkinson. A method to quantify the effects of human disturbance on animal populations. *Journal of applied Ecology*, pages 786–792, 1996.

[46] Kondalsamy Gopalsamy. *Stability and oscillations in delay differential equations of population dynamics*, volume 74. Springer Science & Business Media, 2013.

[47] JV Greenman and TG Benton. The frequency spectrum of structured discrete time population models: its properties and their ecological implications. *Oikos*, 110(2):369–389, 2005.

[48] Volker Grimm. Ten years of individual-based modelling in ecology: what have we learned and what could we learn in the future? *Ecological modelling*, 115(2):129–148, 1999.

[49] Chris Guiver, Hanan Dreiwi, Donna-Maria Filannino, Dave Hodgson, Stephanie Lloyd, and Stuart Townley. The role of population inertia in predicting the outcome of stage-structured biological invasions. *Mathematical biosciences*, 265:1–11, 2015.

[50] Robert G Haight and Stephen Polasky. Optimal control of an invasive species with imperfect information about the level of infestation. *Resource and Energy Economics*, 32(4):519–533, 2010.

[51] Deborah R Hart and Robert H Gardner. A spatial model for the spread of invading organisms subject to competition. *Journal of Mathematical Biology*, 35(8):935–948, 1997.

[52] Alan Hastings, Kim Cuddington, Kendi F Davies, Christopher J Dugaw, Sarah Elmendorf, Amy Freestone, Susan Harrison, Matthew Holland, John Lambrinos, Urmila Malvadkar, et al. The spatial spread of invasions: new developments in theory and evidence. *Ecology Letters*, 8(1):91–101, 2005.

[53] Alan Hastings, Richard Hall, and Caz Taylor. A simple approach to optimal control of invasive species. *Theoretical Population Biology*, (70):431–435, 2006.

[54] Selina S Heppell, Larry B Crowder, and Deborah T Crouse. Models to evaluate headstarting as a management tool for long-lived turtles. *Ecological applications*, 6(2):556–565, 1996.

[55] Steven I Higgins, David M Richardson, and Richard M Cowling. Modeling invasive plant spread: the role of plant-environment interactions and model structure. *Ecology*, 77(7):2043–2054, 1996.

[56] Alexandre H Hirzel, Bertrand Posse, Pierre-Alain OGggier, Yvon Crettenand, Christian Glenz, and Raphaël Arlettaz. Ecological requirements of reintroduced species and the implications for release policy: the case of the bearded vulture. *Journal of Applied Ecology*, 41(6):1103–1116, 2004.

[57] Dave Hodgson, Stuart Townley, and Dominic McCarthy. Robustness: predicting the effects of life history perturbations on stage-structured population dynamics. *Theoretical Population Biology*, 70(2):214–224, 2006.

[58] David J Hodgson and Stuart Townley. Methodological insight: linking management changes to population dynamic responses: the transfer function of a projection matrix perturbation. *Journal of Applied Ecology*, 41(6):1155–1161, 2004.

[59] EE Holmes, MA Lewis, JE Banks, and RR Veit. Partial differential equations in ecology: spatial interactions and population dynamics. *Ecology*, pages 17–29, 1994.

[60] William F Hyde. Marginal costs of managing endangered species: the case of the red-cockaded woodpecker. *Journal of Agricultural Economics Research*, 41(2):12–19, 1989.

[61] Vincent AA Jansen and Jin Yoshimura. Populations can persist in an environment consisting of sink habitats only. *Proceedings of the National Academy of Sciences*, 95(7):3696–3698, 1998.

[62] Alberto Jiménez-Valverde, Andrew Townsend Peterson, Jorge Soberón, JM Overton, P Aragón, and Jorge M Lobo. Use of niche models in invasive species risk assessments. *Biological Invasions*, 13(12):2785–2797, 2011.

[63] Edward O Jones, Andrew White, and Michael Boots. The evolution of host protection by vertically transmitted parasites. *Proceedings of the Royal Society of London B: Biological Sciences*, 278(1707):863–870, 2011.

[64] Chudamani Joshi, Jan de Leeuw, and Iris C van Duren. Remote sensing and gis applications for mapping and spatial modelling of invasive species. In *Proceedings of ISPRS*, volume 35, page B7, 2004.

[65] Kenneth L Judd. *Numerical methods in economics*. MIT press, 1998.

[66] John OS Kennedy et al. *Applications of dynamic programming to agriculture, forestry and fisheries: Review and prognosis*. La Trobe University, 1981.

[67] Nathan Keyfitz, Hal Caswell, Hal Caswell, and Nathan Keyfitz. *Applied mathematical demography*, volume 47. Springer, 2005.

[68] Mark Kot. Discrete-time travelling waves: ecological examples. *Journal of mathematical biology*, 30(4):413–436, 1992.

[69] Mark Kot, Mark A Lewis, and Pauline van den Driessche. Dispersal data and the spread of invading organisms. *Ecology*, 77(7):2027–2042, 1996.

[70] Yang Kuang. *Delay differential equations: with applications in population dynamics*. Academic Press, 1993.

[71] Lawrence A Kuznar. Herd composition in an aymara community of the peruvian altiplano: A linear programming problem. *Human Ecology*, 19(3):369–387, 1991.

[72] Russell Lande, Steinar Engen, and Bernt-Erik Saether. *Stochastic population dynamics in ecology and conservation*. Oxford University Press, 2003.

[73] B. Larson, C. Kueffer, and the ZiF working Group on Ecological Novelty. Managing invasive species admist high uncertainty and novelty. *TREE*, 2013.

[74] Benjamin H Letcher, Jeffery A Priddy, Jeffrey R Walters, and Larry B Crowder. An individual-based, spatially-explicit simulation model of the population dynamics of the endangered red-cockaded woodpecker, picoides borealis. *Biological Conservation*, 86(1):1–14, 1998.

[75] Brian Leung, David M Lodge, David Finnoff, Jason F Shogren, Mark A Lewis, and Gary Lamberti. An ounce of prevention or a pound of cure: bioeconomic risk analysis of invasive species. *Proceedings of the Royal Society of London B: Biological Sciences*, 269(1508):2407–2413, 2002.

[76] MA Lewis. Spread rate for a nonlinear stochastic invasion. *Journal of Mathematical Biology*, 41(5):430–454, 2000.

[77] MA Lewis and S Pacala. Modeling and analysis of stochastic invasion processes. *Journal of Mathematical Biology*, 41(5):387–429, 2000.

[78] Alfred J Lotka. On an integral equation in population analysis. *The Annals of Mathematical Statistics*, 10(2):144–161, 1939.

[79] Bruce C Lubow. Optimal translocation strategies for enhancing stochastic metapopulation viability. *Ecological Applications*, pages 1268–1280, 1996.

[80] Ariel E Lugo. Estimating reductions in the diversity of tropical forest species. *Biodiversity*, pages 58–70, 1988.

[81] I Macdonald and G Frame. The invasion of introduced species into nature reserves in tropical savannas and dry woodlands. *Biological Conservation*, 44(1):67–93, 1988.

[82] Lynn A Maguire, Ulysses S Seal, and Peter F Brussard. Managing critically endangered species: the sumatran rhino as a case study. *Viable populations for conservation*, pages 141–158, 1987.

[83] Max Planck Institute for Demographic Research. Compadre plant matrix database. `http://www.compadre-db.org/`, 2015. [Online; accessed 12-November-2015].

[84] Jane M Maxwell and Ian G Jamieson. Survival and recruitment of captive-reared and wild-reared takahe in fiordland, new zealand. *Conservation Biology*, pages 683–691, 1997.

[85] Rebecca J McLain and Robert G Lee. Adaptive management: promises and pitfalls. *Environmental management*, 20(4):437–448, 1996.

[86] Shefali V Mehta, Robert G Haight, Frances R Homans, Stephen Polasky, and Robert C Venette. Optimal detection and control strategies for invasive species management. *Ecological Economics*, 61(2):237–245, 2007.

[87] Elliott Mendelson. *Introducing game theory and its applications*. CRC Press, 2004.

[88] Jennifer L Molnar, Rebecca L Gamboa, Carmen Revenga, and Mark D Spalding. Assessing the global threat of invasive species to marine biodiversity. *Frontiers in Ecology and the Environment*, 6(9):485–492, 2008.

[89] Harold A Mooney and Elsa E Cleland. The evolutionary impact of invasive species. *Proceedings of the National Academy of Sciences*, 98(10):5446–5451, 2001.

[90] A Mukhopadhyay, J Chattopadhyay, and PK Tapaswi. A delay differential equations model of plankton allelopathy. *Mathematical biosciences*, 149(2):167–189, 1998.

[91] Roger B Myerson. *Game theory*. Harvard university press, 2013.

[92] Masahiro Nakaoka. Dynamics of age-and size-structured populations in fluctuating environments: applications of stochastic matrix models to natural populations. *Researches on Population Ecology*, 38(2):141–152, 1996.

[93] Michael G Neubert, Mark Kot, and Mark A Lewis. Dispersal and pattern formation in a discrete-time predator-prey model. *Theoretical Population Biology*, 48(1):7–43, 1995.

[94] Stephen J O'Brien and James F Evermann. Interactive influence of infectious disease and genetic diversity in natural populations. *Trends in Ecology & Evolution*, 3(10):254–259, 1988.

[95] Lars J Olson et al. The economics of terrestrial invasive species: a review of the literature. *Agricultural and Resource Economics Review*, 35(1):178, 2006.

[96] Martin J Osborne and Ariel Rubinstein. *A course in game theory*. MIT press, 1994.

[97] Camille Parmesan and Gary Yohe. A globally coherent fingerprint of climate change impacts across natural systems. *Nature*, 421(6918):37–42, 2003.

[98] Henrique M Pereira, Paul W Leadley, Vânia Proença, Rob Alkemade, Jörn PW Scharlemann, Juan F Fernandez-Manjarrés, Miguel B Araújo, Patricia Balvanera, Reinette Biggs, William WL Cheung, et al. Scenarios for global biodiversity in the 21st century. *Science*, 330(6010):1496–1501, 2010.

[99] Sandra L Postel, Gretchen C Daily, Paul R Ehrlich, et al. Human appropriation of renewable fresh water. *Science-AAAS-Weekly Paper Edition*, 271(5250):785–787, 1996.

[100] Carsten Rahbek. Captive breeding-a useful tool in the preservation of biodiversity? *Biodiversity & Conservation*, 2(4):426–437, 1993.

[101] DA Rand, HB Wilson, and JM McGlade. Dynamics and evolution: evolutionarily stable attractors, invasion exponents and phenotype dynamics. *Philosophical Transactions of the Royal Society B: Biological Sciences*, 343(1305):261–283, 1994.

[102] David M Richardson. Invasion science: the roads travelled and the roads ahead. *Fifty years of invasion ecology: The legacy of Charles Elton*, pages 397–401, 2011.

[103] Jorgen Ripa and Per Lundberg. Noise colour and the risk of population extinctions. *Proceedings: Biological Sciences*, pages 1751–1753, 1996.

[104] DA Roff. Spatial heterogeneity and the persistence of populations. *Oecologia*, 15(3):245–258, 1974.

[105] TM Rout, CE Hauser, and HP Possingham. Minimise long-term loss or maximise short-term gain?: Optimal translocation strategies for threatened species. *Ecological Modelling*, 201(1):67–74, 2007.

[106] Helen E Roy, Jodey Peyton, David C Aldridge, Tristan Bantock, Tim M Blackburn, Robert Britton, Paul Clark, Elizabeth Cook, Katharina Dehnen-Schmutz, Trevor Dines, et al. Horizon scanning for invasive alien species with the potential to threaten biodiversity in great britain. *Global change biology*, 20(12):3859–3871, 2014.

[107] D. Ruscio. Discrete time linear quadratic optimal control. `http://home.hit.no/~hansha/documents/control/theory/lq$\_$control.pdf`, 2008.

[108] Robin E Russell, J Andrew Royle, Victoria A Saab, John F Lehmkuhl, William M Block, and John R Sauer. Modeling the effects of environmental disturbance on wildlife communities: avian responses to prescribed fire. *Ecological Applications*, 19(5):1253–1263, 2009.

[109] Osvaldo E Sala, F Stuart Chapin, Juan J Armesto, Eric Berlow, Janine Bloomfield, Rodolfo Dirzo, Elisabeth Huber-Sanwald, Laura F Huenneke, Robert B Jackson, Ann Kinzig, et al. Global biodiversity scenarios for the year 2100. *science*, 287(5459):1770–1774, 2000.

[110] Monika Schwager, Karin Johst, and Florian Jeltsch. Does red noise increase or decrease extinction risk? single extreme events versus series of unfavorable conditions. *The American Naturalist*, 167(6):879–888, 2006.

[111] Rupert Seidl, Paulo M Fernandes, Teresa F Fonseca, François Gillet, Anna Maria Jönsson, Katarína Merganičová, Sigrid Netherer, Alexander Arpaci, Jean-Daniel Bontemps, Harald Bugmann, et al. Modelling natural disturbances in forest ecosystems: a review. *Ecological Modelling*, 222(4):903–924, 2011.

[112] K Shea and Hugh Philip Possingham. Optimal release strategies for biological control agents: an application of stochastic dynamic programming to population management. *Journal of Applied Ecology*, 37(1):77–86, 2000.

[113] D Shepherdson. The role of environmental enrichment in the captive breeding and reintroduction of endangered species. In *Creative Conservation*, pages 167–177. Springer, 1994.

[114] Christine Shoemaker et al. Applications of dynamic programming and other optimization methods in pest management. *Automatic Control, IEEE Transactions on*, 26(5):1125–1132, 1981.

[115] Daniel Simberloff. Non-native invasive species and novel ecosystems. *F1000prime reports*, 7, 2015.

[116] Daniel Simberloff, Jean-Louis Martin, Piero Genovesi, Virginie Maris, David A Wardle, James Aronson, Franck Courchamp, Bella Galil, Emili García-Berthou, Michel Pascal, et al. Impacts of biological invasions: what's what and the way forward. *Trends in Ecology & Evolution*, 28(1):58–66, 2013.

[117] Elisabeth Slooten, Stephen Dawson, William Rayment, and Simon Childerhouse. A new abundance estimate for maui's dolphin: What does it mean for managing this critically endangered species? *Biological Conservation*, 128(4):576–581, 2006.

[118] Noel FR Snyder, Scott R Derrickson, Steven R Beissinger, James W Wiley, Thomas B Smith, William D Toone, and Brian Miller. Limitations of captive breeding in endangered species recovery. *Conservation Biology*, pages 338–348, 1996.

[119] Michael G Sorice, C Scott Shafer, and Robert B Ditton. Managing endangered species within the use–preservation paradox: The florida manatee (trichechus

manatus latirostris) as a tourism attraction. *Environmental Management*, 37(1):69–83, 2006.

[120] Clifford Stein, T Cormen, R Rivest, and C Leiserson. *Introduction to algorithms*, volume 3. MIT Press Cambridge, MA, 2001.

[121] Iain Stott, David James Hodgson, and Stuart Townley. Beyond sensitivity: nonlinear perturbation analysis of transient dynamics. *Methods in Ecology and Evolution*, 3(4):673–684, 2012.

[122] Iain Stott, Stuart Townley, and David James Hodgson. A framework for studying transient dynamics of population projection matrix models. *Ecology Letters*, 14(9):959–970, 2011.

[123] RW Sutherst and AS Bourne. Modelling non-equilibrium distributions of invasive species: a tale of two modelling paradigms. *Biological Invasions*, 11(6):1231–1237, 2009.

[124] Zenas M Sykes. Some stochastic versions of the matrix model for population dynamics. *Journal of the American Statistical Association*, 64(325):111–130, 1969.

[125] Yasuhiro Takeuchi. *Global dynamical properties of Lotka-Volterra systems*. World Scientific, 1996.

[126] Caz M Taylor and Alan Hastings. Finding optimal control strategies for invasive species: a density-structured model for spartina alterniflora. *Journal of Applied Ecology*, 41(6):1049–1057, 2004.

[127] Caz M Taylor and Alan Hastings. Allee effects in biological invasions. *Ecology Letters*, 8(8):895–908, 2005.

[128] Brigitte Tenhumberg, Andrew J Tyre, Katriona Shea, and Hugh P Possingham. Linking wild and captive populations to maximize species persistence: optimal translocation strategies. *Conservation Biology*, 18(5):1304–1314, 2004.

[129] Stuart Townley, David Carslake, Owen Kellie-Smith, Dominic McCarthy, and David Hodgson. Predicting transient amplification in perturbed ecological systems. *Journal of Applied Ecology*, 44(6):1243–1251, 2007.

[130] Stuart Townley, Richard Rebarber, and Brigitte Tenhumberg. Feedback control systems analysis of density dependent population dynamics. *Systems & Control Letters*, 61(2):309–315, 2012.

[131] Michael B Usher, Hans Kornberg, JW Horwood, Richard Southwood, and PD Moore. Invasibility and wildlife conservation: invasive species on nature reserves [and discussion]. *Philosophical Transactions of the Royal Society B: Biological Sciences*, 314(1167):695–710, 1986.

[132] Teresa Valverde and Rocío Bernal. ¿ hay asincronía demográfica entre poblaciones locales de tillandsia recurvata?: Evidencias de su funcionamiento metapoblacional. *Boletín de la Sociedad Botánica de México*, (86):23–36, 2010.

[133] Peter M Vitousek, Carla M D'Antonio, Lloyd L Loope, Randy Westbrooks, et al. Biological invasions as global environmental change. *American Scientist*, 84(5):468–478, 1996.

[134] Peter M Vitousek, Harold A Mooney, Jane Lubchenco, and Jerry M Melillo. Human domination of earth's ecosystems. *Science*, 277(5325):494–499, 1997.

[135] Carl J Walters and Ray Hilborn. Adaptive control of fishing systems. *Journal of the Fisheries Board of Canada*, 33(1):145–159, 1976.

[136] Carl J Walters and Ray Hilborn. Ecological optimization and adaptive management. *Annual review of Ecology and Systematics*, pages 157–188, 1978.

[137] Andrew Whittle, Suzanne Lenhart, and KAJ White. Optimal control of gypsy moth populations. *Bulletin of mathematical biology*, 70(2):398–411, 2008.

[138] Jianguo Wu and Simon A Levin. A patch-based spatial modeling approach: conceptual framework and simulation scheme. *Ecological Modelling*, 101(2):325–346, 1997.

[139] Muhittin Yilmaz, Salman Mujeeb, and Naren Reddy Dhansri. A h-infinity control approach for oil drilling processes. *Procedia Computer Science*, 20:134–139, 2013.

[140] Kemin Zhou and John Comstock Doyle. *Essentials of robust control*, volume 180. Prentice hall Upper Saddle River, NJ, 1998.

[141] Chao Zhu and G Yin. On competitive lotka–volterra model in random environments. *Journal of Mathematical Analysis and Applications*, 357(1):154–170, 2009.